

Health &  
Medicine

Lancaster  
University



**Ph.D. Thesis in Biomedical and Life Sciences**

By

**JULIANNE ALBEZO VILELA**

**Title**

**Development of CRISPR/Cas9-Based Novel Vaccines Against  
Poultry Viruses**

Under supervision of

**Prof. Muhammad Munir**

**Division of Biomedical and Life Sciences, Lancaster University,  
Lancaster, United Kingdom**

**Dr. Leonie Unterholzner**

**Division of Biomedical and Life Sciences, Lancaster University,  
Lancaster, United Kingdom**

**December 2023**

## **Declaration of originality**

I declare that the content of this thesis is my own work and has not been submitted by myself in substantially the same form for the award of a higher degree elsewhere. Any sections of the thesis which have been published have been clearly identified.

Julianne A. Vilela



## **List of Contents**

<b>LIST OF CONTENTS</b>	<b>3</b>
<b>LIST OF TABLES</b>	<b>11</b>
<b>LIST OF FIGURES</b>	<b>13</b>
<b>LIST OF ABBREVIATIONS</b>	<b>20</b>
<b>ACKNOWLEDGMENT</b>	<b>26</b>
<b>ABSTRACT</b>	<b>27</b>
<b>Chapter 1. General Introduction</b>	<b>29</b>
1.1. Vaccine Development	31
1.1.1. Vaccine Approach	33
1.1.1.1. Inactivated Whole-Pathogen	33
1.1.1.2. Live Attenuated Pathogens	34
1.1.1.3. Protein Subunit Vaccines	36
1.1.1.4. Recombinant Viral Vector	37
1.1.1.4.1. Herpesviridae as a Recombinant Viral Vector	38
1.1.1.4.2. Structure and Genomic Organisation	44
1.1.1.4.3. ILTV as a Viral Vector	48
1.1.2. Antigen	52
1.1.2.1. Economically Important Poultry Viruses	52
1.1.2.1.1. NDV	53
1.1.2.1.1.1. Immunogenic proteins of NDV: F and HN proteins	54
1.1.2.1.2. IBV	56
1.1.2.1.2.1. IBV Infectivity: S protein	58
1.1.2.1.3. AIV	59
1.1.2.1.3.1. AIV Infectivity: HA protein	61

1.1.3. Vaccine Adjuvants	64
1.1.3.1. Chicken IgY Fc	65
1.1.3.2. Foldon-based Multimerisation	66
1.2. CRISPR-based Genome Editing System	67
1.2.1. CRISPR/Cas9 in Vaccine Development for Poultry	69
1.2.2. CRISPR/Cas9 Workflow for Vaccine Development	71
1.2.2.1. Selection of Viral Vector and Target Insertion Site	73
1.2.2.2. Choosing a Target Insertion Site	73
1.2.2.3. Choosing Viral Antigen	74
1.2.2.4. Selection of Host Cell Lines	74
1.2.2.5. Construction of sgRNAs, Donor Plasmids, and Cas9/gRNA Expression Plasmids	75
1.3. Project Aims	80
<b>Chapter 2. Materials and Methods</b>	<b>81</b>
2.1. Materials	81
2.2. Methods	86
2.2.1. Cell Culture Techniques	86
2.2.1.1. Cell Types and Culture Medium	86
2.2.1.2. Cell Subculture	87
2.2.1.3. Cell Cryopreservation and Recovery	87
2.2.1.4. Transfection	88
2.2.1.4.1. ViaFect™ Transfection	88
2.2.2. Microbiology Techniques	89
2.2.2.1. Cloning Techniques using <i>E. coli</i>	89
2.2.2.1.1. Agar Plate Preparation	89

2.2.2.1.2.	Transformation	89
2.2.2.1.3.	Cell Plating and Colony Picking	89
2.2.3.	Virology Techniques	90
2.2.3.1.	Viral Strain and Culture Medium	90
2.2.3.2.	Viral Infection	90
2.2.3.3.	Plaque Assay	91
2.2.3.4.	Immunofluorescence	93
2.2.3.4.1.	Immunofluorescent Assay	93
2.2.3.4.2.	Flow Cytometry Analysis	94
2.2.4.	Molecular Biology Techniques	95
2.2.4.1.	DNA Techniques	95
2.2.4.1.1.	Plasmid DNA Extraction	95
2.2.4.1.1.1.	Medium-scale of Plasmid DNA (midi-prep)	95
2.2.4.1.2.	Genomic DNA Extraction	96
2.2.4.2.	DNA Amplification	97
2.2.4.2.1.	Routine PCR with Q5 DNA Polymerase	99
2.2.4.3.	DNA Visualisation and Quantification	100
2.2.4.4.	DNA Purification	101
2.2.4.4.1.	Gel Bands Isolation and Purification	101
2.2.4.5.	DNA Digestion	102
2.2.4.6.	DNA Sequencing	102
2.2.4.7.	Quantitative PCR	102
2.2.4.7.1.	Generation of Plasmid Standard	104
2.2.5.	Protein Techniques	106
2.2.5.1.	Western Blot	106

2.2.6. Assembly of CRISPR/Cas9 Reagents	108
2.2.6.1. sgRNA Design and Synthesis	108
2.2.6.2. Assembly of CRISPR/Cas9 Reagents	112
2.2.7. <i>In silico</i> -based Techniques	114
2.2.7.1. Sequencing of Philippine Endemic Viral Poultry Strains	114
2.2.7.2. Reference Sequence Data Acquisition	115
2.2.7.3. Evolutionary Analysis	115
2.2.7.4. Protein Analysis	116
2.2.8. Statistical Analysis	117
<b>Chapter 3. Genetic Characterisation of Field Strains of Important Viral Diseases in Commercial Poultry</b>	<b>118</b>
3.1. Introduction	118
3.1.1. Aims	120
3.2. Results	121
3.2.1. <i>In silico</i> Characterisation of Antigenic Proteins and Epitopes of NDV, IBV, and AIV	122
3.2.2. Phylogenetic Analysis	143
3.2.2.1. NDV-F Gene	143
3.2.2.2. IBV-S Gene	148
3.2.2.3. AIV-HA (H9N2) Gene	152
3.3. Chapter Discussion	156
<b>Chapter 4. Establishment of CRISPR/Cas9 Approach for the Generation of Recombinant ILTV</b>	<b>161</b>
4.1. Introduction	161
4.1.1. Aims	165

4.2.	General Workflow	166
4.3.	Results	167
4.3.1.	Propagation of Recombinant ILTV + GFP	167
4.3.2.	Assembly of Donor Plasmid	169
4.3.2.1.	Assembly and Cloning of the Fluorescent Marker Into the Multiple Cloning Site 2 (MCS2)	173
4.3.2.2.	Assembly and Cloning of the Target Antigen NDV-F Into the Multiple Cloning Site 1 (MCS1)	176
4.3.2.3.	Functional Validation of the Donor Plasmid pcDNA-NDVF-mRFP	179
4.3.3.	Knock-in Experiments	181
4.3.3.1.	Design, Assembly, and Cloning of sgRNAs	181
4.3.3.2.	Generation of Recombinant ILTV with NDV-F Knock-in	187
4.3.3.3.	Characterisation of the Recombinant ILTV with NDV-F Knock-in	189
4.3.3.3.1.	Validation of NDV-F Knock-in	189
4.3.3.3.2.	Functional Validation of the Recombinant ILTVs	190
4.3.4.	Knockout Experiments	196
4.3.4.1.	Assembly and Construction of the ICP4 sgRNAs	196
4.3.4.2.	Generation of ICP4 Knockout Recombinant ILTV	197
4.3.4.3.	Validation of the ICP4 Knockout Recombinant ILTV	202
4.4.	Chapter Discussion	204
<b>Chapter 5. Construction of Recombinant ILTV-expressing NDV-F Gene Variants</b>		<b>211</b>
5.1.	Introduction	211
5.1.1.	Aims	214

5.2.	Results	215
5.2.1.	<i>In silico</i> Characterisation of NDV-F Gene Variants	215
5.2.2.	Cloning and Validation of Gene Cassettes	218
5.2.3.	Generation of Recombinant ILTV Variants	223
5.2.3.1.	Characterisation of the Recombinant ILTV-GFP-NDVF Variants	229
5.3.	Chapter Discussion	236
<b>Chapter 6.</b>	<b>Construction and Evaluation of Herpesvirus as a Multivalent Vaccine Vector using Two Surface Glycoproteins of NDV (F and HN)</b>	<b>242</b>
6.1.	Introduction	242
6.1.1.	Aims	245
6.2.	Results	246
6.2.1.	Cloning and Validation of Gene Cassettes	246
6.2.2.	Generation of Recombinant ILTV with the NDV-HN Gene	249
6.2.2.1.	Characterisation of the Recombinant ILTV-GFP-NDV-HN	252
6.2.3.	Generation of a Recombinant Multivalent ILTV Viral Vector with F and HN Gene	258
6.2.3.1.	Characterisation of the Recombinant Multivalent ILTV-GFP-NDV-F-HN Viral Vector	259
6.2.4.	Immunogenicity and Protective Efficacy of the Recombinant ILTV Vaccines Against the NDV Challenge	269
6.2.4.1.	General Workflow	270
6.2.4.2.	Serological Assays	271
6.3.	Chapter Discussion	277

<b>Chapter 7. Construction of a Herpesvirus-based Vaccine Against Economically Important Poultry Viruses (Infectious Bronchitis Virus and Avian Influenza)</b>	<b>283</b>
7.1. Introduction	283
7.1.1. Aims	286
7.2. Results	287
7.2.1. Spike Gene of the Infectious Bronchitis Virus	287
7.2.1.1. Cloning and Validation of Gene Cassettes	287
7.2.1.2. Generation of Recombinant ILTV Strains	290
7.2.1.2.1. Characterisation of the Recombinant ILTV-GFP-IBVS	293
7.2.2. HA (H9N2) Gene of the Avian Influenza Virus	299
7.2.2.1. Cloning and Validation of Gene Cassettes	299
7.2.2.2. Generation of Recombinant ILTV Strains	301
7.2.2.2.1. Characterisation of the Recombinant ILTV-GFP-HAH9N2	304
7.3. Chapter Discussion	311
<b>CHAPTER 8. General Discussion</b>	<b>316</b>
8.1. Overview of Thesis Findings	318
8.2. CRISPR/Cas9 Gene Editing Technology as a Tool in the Development of Novel Avian Recombinant Vaccine Vectors	320
8.3. ILTV as a Candidate Viral Vector in the Development of Novel Avian Recombinant Vaccine Vectors	321
8.4. Immunoenhancement of the Recombinant Viral Vector through the Addition of Enhancers/Adjuvants	322
8.5. ILTV as a Potential Multivalent or Polyvalent Broad-Spectrum	

Recombinant Viral Vector	323
8.6. ILTV as a Potential Multivalent or Polyvalent Recombinant Viral Vector Against Economically Important Avian Diseases	323
8.7. Future Work	324
<b>Chapter 9. Appendices</b>	<b>325</b>
Annex 1. NDV, IBV, and AIV reference sequence and genotypes	325
Annex 2. Stability testing	339
Annex 3: qPCR standard curve	341
<b>Chapter 10. References</b>	<b>343</b>



## **List of Tables**

Table 1.1:	Animal herpesviruses carrying several foreign immunogenic genes to protect against several important diseases	40
Table 1.2:	Advantage and disadvantage of current techniques used for generating recombinant herpesviruses.	70
Table 1.3:	List of existing free online tools and open-source local software for sgRNA design.	77
Table 2.1:	List of chemicals, enzymes, and solutions used in this study.	81
Table 2.2:	Primers for DNA amplification.	98
Table 2.3:	PCR components and conditions using Q5 DNA Polymerase.	99
Table 2.4:	Summary of the components used for restriction enzyme digestion.	102
Table 2.5:	qPCR primers used for the detection of ILTV gB gene.	103
Table 2.6:	qPCR reaction setup and real-time cycler conditions.	103
Table 2.7:	Summary of the components and conditions used for the amplification of ILTV gB using Taq polymerase.	105
Table 2.8:	pTOPO cloning components.	105
Table 2.9:	List of antibodies.	106
Table 2.10:	List of components utilised for the SDS-PAGE stacking and resolving gels.	107
Table 2.11:	List of the sgRNA oligo sequences as designed and predicted by CHOPCHOP.	111
Table 2.12:	The conditions of CRISPR/Cas9 construct assembly.	113
Table 2.13:	List of primers for antigen amplification.	115
Table 3.1:	Physico-chemical parameter results predicted by the ExpASyProtParam.	124

Table 3.2:	Secondary structures results predicted by GOR IV.	127
Table 3.3:	Transmembrane helices, localisation, and antigenicity results predicted by TMHMM, Virus-mPLoc and Vaxijen, respectively.	133
Table 3.4:	B cell epitopes predicted by both Bcepred and IEDB and antigenicity value predicted by Vaxijen v2.0.	135
Table 3.5:	Epitopes specific to selected MHC-I alleles.	139
Table 3.6:	Epitopes specific to selected MHC-II alleles.	142
Table 4.1:	Summary of the components and purpose of the MCS1-MCS2 gene fragment.	172
Table 4.2:	Guide RNAs designed to target the UL0/UL50/US4 region of the ILTV genome.	183
Table 5.1:	Summary of the physico-chemical and antigenic properties deduced from the NDV-F variant protein sequences as well as the NDF wild type.	218
Annex 1:	NDV, IBV, and AIV reference sequence and genotypes.	325

## **List of Figures**

### **Chapter 1: General Introduction**

Figure 1.1:	Comparison of the human and chicken immune systems.	30
Figure 1.2:	Elements of vaccine design.	32
Figure 1.3:	Illustrative overview of the various types of herpesvirus genomes and the structural characteristics of the virion.	47
Figure 1.4:	Replication of the ILT virus.	49
Figure 1.5:	AOAV-1/NDV mRNA synthesis.	55
Figure 1.6:	Genomic representation of the avian infectious bronchitis virus.	57
Figure 1.7:	Influenza A virus structural organisation.	60
Figure 1.8:	Different influenza vaccines produce various immune responses.	63
Figure 1.9:	Comparison of the structure of avian IgY to mammalian IgG.	66
Figure 1.10:	Illustrative representation of the CRISPR/Cas9 workflow for vaccine development.	72
Figure 1.11:	Overview of steps in the construction of CRISPR/Cas9 and donor plasmids.	78
Figure 1.12:	Illustrative representation of the Cas9 plasmid.	79

### **Chapter 2: Materials and Methods**

Figure 2.1:	Plaque Assay.	92
Figure 2.2:	Example workflow usage of CHOPCHOP web tool.	109

### **Chapter 3: Genetic Characterisation of Field Strains of Important Viral Diseases in Commercial Poultry**

Figure 3.1:	Phylogenetic analysis of the NDV-F complete gene shows the lineage of the Philippine isolates.	145
Figure 3.2:	Multiple sequence analysis of the Philippine NDV-F gene.	146

Figure 3.3:	Representative NDV-F protein cleavage site.	147
Figure 3.4:	Phylogenetic analysis of the IBV-S gene showing lineage of the Philippine isolates (PH 1 IBV S Gene).	149
Figure 3.5:	Multiple sequence analysis of the Philippine IBV-S gene.	150
Figure 3.6:	Representative furin recognition consensus motif of the IBV-S protein.	151
Figure 3.7:	Phylogenetic analysis of the AIV-HA complete gene showing lineage of the Philippine isolates (PH_HAH9N2).	153
Figure 3.8:	Comprehensive analyses of the amino acid residue of the Philippine AIV-HA (H9N2) gene.	154
Figure 3.9:	Representative AIV-HA protein cleavage site.	155
<b>Chapter 4:</b>	<b>Establishment of CRISPR/Cas9 Approach for the Generation of Recombinant ILTV</b>	
Figure 4.1:	Schematic representation of the workflow used in this chapter.	166
Figure 4.2:	Propagation and validation of the attenuated recombinant ILTV expressing the GFP fluorescence marker.	168
Figure 4.3:	Construct map illustrating of the assembly of the donor plasmid.	171
Figure 4.4:	Assembly and validation of the recombinant donor plasmid pCDNA-MCS1-mRFP.	175
Figure 4.5:	Assembly and sequence validation of the recombinant donor plasmid pCDNA-NDVF-mRFP.	178
Figure 4.6:	GFP protein expressed at the protein level in plasmid pcDNA-NDVF-mRFP.	180
Figure 4.7:	Diagram illustrating the positioning of the guide RNA inside the genome of ILTV.	184

Figure 4.8:	Diagrammatic representation of the assembly of the sgRNAs into the CRISPR/Cas9 plasmid (pX459v2).	185
Figure 4.9:	Molecular and sequence validation of pX459v2-sgRNAs.	186
Figure 4.10:	Illustrative representation of the workflow used for the generation of recombinant ILTV with NDV-F-mRFP knock-in.	188
Figure 4.11:	NDV-F gene is expressed at the molecular and protein levels in LMH cells post-infection of recombinant ILTV strains.	191
Figure 4.12:	NDV-F protein localised expression in the cellular cytoplasm of LMH cells post-infection of recombinant ILTV strains.	192
Figure 4.13:	Viral infectivity of the recombinant ILTV strains is not significantly different from that of ILTV-WT.	194
Figure 4.14:	Comparison of the replication kinetics of the ILTV-WT and recombinant ILTV strains.	194
Figure 4.15:	Trend towards an increase in GFP positivity in LMH cells post-viral infection.	195
Figure 4.16:	Diagram illustrating the positioning of the guide RNA inside the ILTV ICP4 genomic region.	198
Figure 4.17:	Diagram of the assembly of the ICP4 sgRNAs into the CRISPR/Cas9 plasmid (pX459v2).	199
Figure 4.18:	Molecular and sequence validation of pX459v2-sgRNAs.	200
Figure 4.19:	Illustrative representation of the workflow used to generate recombinant ILTV with ICP4 knockout.	201
Figure 4.20:	Viral infectivity significantly decreased in recombinant ILTV strains with ICP4 gene knockout.	203

## **Chapter 5: Construction of Recombinant ILTV-expressing NDV-F**

### **Gene Variants**

- Figure 5.1: Illustrative depiction of the *in silico*-based design of the NDV-F gene cassette fused with enhancers. 217
- Figure 5.2: A schematic representation illustrating the structural organisation of the donor plasmid construct map for the Newcastle Disease Virus (NDV) F variants. 220
- Figure 5.3: NDV-F variant expression assessed at the molecular and protein levels. 221
- Figure 5.4: Illustrative representation of the workflow used for the generation of recombinant ILTV-GFP-NDVF variants. 225
- Figure 5.5: Illustrative representation of the CRISPR/Cas9 – Cre/Lox system used to create the recombinant ILTV-GFP-NDVF-Fd. 226
- Figure 5.6: Illustrative representation of the CRISPR/Cas9 – Cre/Lox system used to create the recombinant ILTV-GFP-NDVF-Fc. 227
- Figure 5.7: Illustrative representation of the CRISPR/Cas9 – Cre/Lox system used to create the recombinant ILTV-GFP-NDVF-FcTail. 228
- Figure 5.8: NDV-F variants expressed at the molecular and protein-levels in LMH cells post-infection with recombinant ILTV-GFP-NDVF variants. 232
- Figure 5.9: The viral infectivity of the recombinant ILTV-NDVF variant strains is not significantly different from that of ILTV-WT. 234
- Figure 5.10: Comparison of the replication kinetics of the ILTV-WT

and recombinant ILTV-GFP-NDVF variant strains.	234
Figure 5.11: Trend towards an increase in GFP positivity in LMH cells post-viral infection.	235
<b>Chapter 6: Construction and Evaluation of Herpesvirus as a Multivalent Vaccine Vector using Two Surface Glycoproteins of NDV (F and HN).</b>	
Figure 6.1: Assembly and sequence validation of the recombinant donor plasmid pCDNA-NDVHN-mRFP.	248
Figure 6.2: Illustrative representation of the workflow used for the generation of recombinant ILTV-GFP-NDV-HN.	251
Figure 6.3: NDV-HN is expressed at the molecular and protein-levels in LMH cells post infection with the recombinant ILTV-GFP-NDV-HN strain.	255
Figure 6.4: Viral infectivity of the recombinant ILTV-NDV-HN strain is significantly different from that of ILTV-WT.	256
Figure 6.5: Comparison of the replication kinetics of the ILTV-WT and recombinant ILTV-GFP-NDV-HN strains.	256
Figure 6.6: Trend towards the increase in GFP positivity in LMH cells post-viral infection.	257
Figure 6.7: Illustrative representation of the workflow used for the generation of a recombinant multivalent ILTV-GFP-NDV-FHN viral vector.	260
Figure 6.8: NDV-F and -HN expressed at the molecular and protein-levels in LMH cells post-infection with the recombinant multivalent ILTV-GFP-NDV-FHN viral vector.	264

Figure 6.9:	The viral infectivity of the recombinant multivalent ILTV-NDV-FHN strain is not significantly different from that of ILTV-WT.	266
Figure 6.10:	Comparison of the replication kinetics of the ILTV-WT and recombinant multivalent ILTV-GFP-NDV-FHN strains.	266
Figure 6.11:	Trend towards an increase in GFP positivity in LMH cells Post-viral infection.	267
Figure 6.12:	Stable integration of the NDV-F and -HN gene into the recombinant multivalent ILTV-GFP-NDV-FHN.	268
Figure 6.13:	Illustrative representation of the methods used to validate the effectivity of the recombinant ILTV vaccines.	270
Figure 6.14:	Increasing trend in antibody production over time post recombinant ILTV vaccination.	273
Figure 6.15:	Observed upward trend in antibody production after the administration of recombinant ILTV vaccine strains.	275
<b>Chapter 7:</b>	<b>Construction of a Herpesvirus-Based Vaccine Against Economically Important Poultry Viruses (Infectious Bronchitis Virus and Avian Influenza)</b>	
Figure 7.1:	Assembly and sequence validation of the recombinant donor plasmid pCDNA-IBVS-mRFP.	289
Figure 7.2:	Illustrative representation of the workflow used for the generation of recombinant ILTV-GFP-IBVS.	292
Figure 7.3:	IBV-S expressed at the molecular and protein-levels in LMH cells post-infection with the recombinant ILTV-GFP-IBVS strain.	296
Figure 7.4:	Viral infectivity of the recombinant ILTV-GFP-IBVS strain	



	is significantly different from that of ILTV-WT.	297
Figure 7.5:	Comparison of the replication kinetics of the ILTV-WT and recombinant ILTV-GFP-IBVS strains.	297
Figure 7.6:	Trend towards the increase in GFP positivity in LMH cells post-viral infection.	298
Figure 7.7:	Assembly and sequence validation of the recombinant donor plasmid pCDNA-HAH9N2-mRFP.	300
Figure 7.8:	Illustrative representation of the workflow used for the generation of recombinant ILTV-GFP-HAH9N2.	303
Figure 7.9:	AIV-HA expressed at the molecular and protein-levels in LMH cells post-infection with the recombinant ILTV-GFP-HAH9N2 strain.	307
Figure 7.10:	The viral infectivity of the recombinant ILTV-GFP-HAH9N2 strain is significantly different from that of ILTV-WT.	308
Figure 7.11:	Comparison of the replication kinetics of the ILTV-WT and recombinant ILTV-GFP-HAH9N2 strains.	308
Figure 7.12:	Trend towards an increase in GFP positivity in LMH cells post-viral infection.	309
Figure 7.13:	The cytopathogenicity of Leghorn Male Hepatoma (LMH) Cells.	310
<b>Chapter 9: Appendices</b>		
Annex 2:	Stability testing.	339
Annex 3:	qPCR standard curve.	341

## **List of Abbreviations**

---

3D	Three-dimensional
a.a.	Amino acid
AIV	Avian influenza virus
ANOVA	One-way analysis of variance
APC	Antigen-presenting cells
APS	Ammonium persulphate
BHV-1	Bovine herpesvirus type 1
bp	base pairs
BSA	Bovine serum albumin
BVD	Bovine Viral Diarrhoea
BVDV	Bovine viral diarrhoea virus
cDNA	Complementary deoxyribonucleic acid
CDV	Canine distemper virus
CEF	Chicken embryo fibroblasts
CHV	Canine herpesvirus
CIV	Canine influenza virus
CMV	Cytomegalovirus
CpHV-1	Bovine herpesvirus 4 against Caprine herpesvirus type 1
CRISPR	Clustered Regularly Interspaced Short Palindromic Repeats
cRNA	Complementary RNA
DAPI	4',6-diamidino-2-phenylindole
DIVA	Differentiate between infected and vaccinated individuals
DMSO	Dimethyl sulphoxide

DNA	Deoxyribonucleic acid
dNTPs	Deoxynucleotide triphosphates
E	Envelope
<i>E. coli</i>	<i>Escherichia coli</i>
EBOV	Ebola virus
EBV	Epstein - Barr Virus
EDTA	Ethylene diamine tetra acetic acid
ELISA	Enzyme-linked immune-sorbent assay
ER	Endoplasmic reticulum
F	Fusion
FACS	Fluorescence-activated cell sorting
FAO	Food and agricultural organization
Fc	Fragment crystallizable
FcR	Fc receptors
FCV	Feline calicivirus
Fd	Foldon of fibrin
FeLV	Feline leukemia virus
FFU	Foci-forming unit
FHV-1	Feline Herpesvirus 1
FIV	Feline immunodeficiency virus
FMDV	Foot and mouth disease virus
gB	glycoprotein B
gC	glycoprotein C
gD	glycoprotein D

gE	glycoprotein E
GE	gene-end
GFP	Green fluorescent protein
gG	glycoprotein G
gI	glycoprotein I
GS	Gene-start
HA	Hemagglutinin
HI	Hemagglutination inhibition
HIV-1	Human immunodeficiency virus type 1
HN	Hemagglutinin-neuraminidase protein
HPAIV	Highly Pathogenic Avian Influenza Virus
HSV-1	Herpes simplex virus type 1
HVT	Herpesvirus of turkeys
IB	Infectious Bronchitis
IBV	Infectious Bronchitis Virus
IFA	Immunofluorescence assay
IgG	Immunoglobulin G
IGS	intergenic sequences
IgY	Immunoglobulin Y
ILT	Infectious Laryngotracheitis
ILTV	Infectious Laryngotracheitis Virus
IR	Internal inverted repeats
kb	kilobase
kDa	Kilo Dalton

L	Large polymerase protein
LMH	Leghorn male hepatoma
LPAIVs	Low pathogenic avian influenza viruses
M	matrix protein
MCMC	Bayesian Markov chain Monte Carlo
MDV	Marek's disease virus
ML	Maximum likelihood
MOI	Multiplicity of infection
MPXV	Monkeypox virus
mRFP	Monomeric Red Fluorescent Protein
mRNA	Messenger RNA
MSA	Multiple sequence alignments
MWs	Molecular weights
N	Nucleocapsid
NDV	Newcastle disease virus
NFDM	Non-fat dry milk
NFW	Nuclease free water
NK	Natural killer
nm	nanometres
NP	Neuraminidase or nucleoprotein
nsp	non-structural proteins
ORF	Open reading Frame
P	Phosphoprotein
PAGE	Polyacrylamide gel electrophoresis

PAM	protospacer adjacent motif
PBS	Phosphate buffered saline
PBST	Phosphate buffered saline-tween 20
PCR	Polymerase chain reaction
PCV	Pig circovirus
PDB	Protein database
PFU	Plaque forming unit
PH	Philippines
PK	Protein Kinase
PPV	Porcine parvovirus
PRRS	Porcine Reproductive and Respiratory Syndrome
PVDF	polyvinylidene fluoride
RNA	Ribonucleic acid
RNP	Ribonucleoprotein
rpm	Revolution per minute
RVF	Rift Valley fever
S	Spike
SARS-CoV-2	Severe Acute Respiratory Syndrome Coronavirus-2
SDS	Sodium dodecyl sulfate
sgRNA	single guide RNA
TAE	Tris Acetate EDTA
TALENs	Transcription activator-like effector nucleases
TE	Tris-EDTA
TEMED	Tetramethylethylenediamine

TK	Thymidine kinase
TM	Transmembrane
TR	Terminal Repeat
TIR	Terminal inverted repeats
U	Unique region
UL	Unique large
US	Unique small
UTR	Untranslated regions
UV	Ultraviolet
WHO	World Health Organization
WT	Wildtype
ZFNs	Zinc-finger nucleases
µg	Microgram
µl	Microliter
µM	Micromolar

---

## **Acknowledgements**

I would like to thank my esteemed supervisors, Prof. Muhammad Munir and Dr. Leonie Unterholzner, for their invaluable supervision, support, and tutelage during the course of my PhD degree. My gratitude extends to the British Council and the Philippine Department of Science and Technology (SEI) for the funding opportunity to undertake my studies at the Department of Biomedical and Life Sciences, Lancaster University. Additionally, I would also like to thank Dr. Mohammed Rohaim and Dr. Mustafa Atasoy for their support, which was really influential in shaping my experimental methods and critiquing my results. I would like to thank my friends, labmates, colleagues, and research team—Dr. Manar Khalifa, Dr. Sheila Macharia, Nadia Iqbal, Dr. Mahmoud Bayumi, Dr. Rebecca Barker, Louise Brennan, Dr. Lucy Balderstone, and Hejan Bozkurt—for a cherished time spent together in the lab and in social settings. I would like to thank all the members of the Department of Biomedical and Life Sciences. It is their kind help and support that have made my study and life in the UK a wonderful time.

I would like to express my gratitude to my family and friends: Tin, Mafe, Reli, Kane, and Ami, for their unwavering encouragement and support during the duration of my academic pursuits. I would like to express my utmost appreciation to the Lancaster Filipino community, which has served as my support system during the duration of my studies over the last three years. In particular, I extend my heartfelt thanks to Zy, Yanna, Baby Z, Lean, Cherry, Nadine, Jayson, and Mariel for their unwavering companionship and assistance. Throughout the course of my doctoral studies, I have had the privilege of meeting several individuals who have greatly enriched my academic journey. I am very grateful to each and every one of them for their invaluable contributions, which have not only facilitated the successful completion of my research but have also made this entire PhD experience really remarkable.

*Soli Deo gloria.*



## **Abstract**

The poultry industry significantly depends on the use of vaccinations as a primary strategy for disease control. Consequently, there exists a critical need for further research and development of novel vaccines to effectively address the challenges posed by the emergence and re-emergence of novel virus strains. The utilisation of recombinant viral vaccine vectors has played a crucial role in the advancement of novel vaccines, presenting several advantages in comparison to traditional approaches. These advantages include enhanced precision and efficacy in cell targeting, as well as the capacity to elicit robust immune responses and augment cellular immunity. Recent developments in the fields of pathogen biology and recombinant DNA technologies have opened up new avenues for addressing challenges associated with traditional vaccination creation. In recent times, the application of CRISPR/Cas9 genome editing technology has facilitated the creation of innovative recombinant viral vectors, thereby facilitating progress in the field of vaccine development.

The primary objective of this PhD thesis is to create recombinant viral vectors derived from herpesvirus, employing the CRISPR/Cas9 genome editing approach. These vectors will be specifically designed to combat economically significant poultry viruses, including NDV, IBV, and AIV. The findings of this study successfully facilitated the identification of prospective antigenic proteins and epitopes that may be utilised in the development of vaccines. Additionally, the genotypic profiling of the primary antigens, namely F and HN for NDV, S for IBV, and HA for AIV H9N2, was conducted on circulating field strains in the Philippines. The findings of this study demonstrate the efficacy of the CRISPR/Cas9 genome editing method in accurately targeting sections

of the ILTV genome and inducing the necessary cleavage, hence enabling the successful integration of foreign gene cassettes into the ILTV genome. As a consequence, a total of ten recombinant viral vectors were generated, specifically referred to as ILTV-NDV-F (-UL0, -UL50, and -US4), ILTV-NDV-HN, ILTV-NDVFHN, ILTV-NDVF-Variants (-Fd, -Fc, and -FcTail), ILTV-IBV-S, and ILTV-HAH9N2. Following molecular and protein investigations, it was shown that these recombinant ILTV strains demonstrate stability and comparable functionality to the wild-type ILTV.

The results presented in this study offer evidence to support the concept that ILTV might potentially serve as a tool for developing recombinant viral vectors, particularly for the creation of a multivalent viral vector. Moreover, it underscores the efficacy of CRISPR/Cas9 genome editing technology as the preferred technique for the advancement of novel vaccines.

# CHAPTER 1

## General Introduction

Poultry represents a vital global food source and exhibits continuous growth to meet the increasing demands of the world's population (Speedy, 2003). However, the industrialisation of poultry production, along with high expectations, has laid the foundation for an increased disease burden among poultry birds (Swayne et al., 2013; Imran et al., 2020). Among the diverse array of infectious diseases affecting poultry, viral infections have been identified as the most significant and arguably the foremost contributors to the decline in poultry production (Marín-López & Ortego, 2016; Habiba et al., 2020). To date, vaccinations continue to serve as the predominant method for disease prevention in the poultry industry through the implementation of immunisation regimens (Pollard & Bijker, 2021; Thomas, 2000; Vilela et al., 2020).

Chickens and mammals share comparable overall organisation and functions of the immune system. The chicken possesses a unique organ called the bursa of Fabricius, where B lymphocytes originate from immature progenitors, unlike mammals (Arstila et al., 1994; Glick et al., 1956). While, T cell development occurs in the thymus, a characteristic shared with mammals. Chickens and mammals share both innate and acquired immunological responses (Garcia et al., 2021) (**Figure 1.1**). Birds respond to vaccines by producing both humoral and cellular immune responses. The Bursa of Fabricius and the thymus are the main lymphoid organs of the immune system. B cells utilise surface immunoglobulins as antigen receptors and undergo differentiation into plasma cells to produce antibodies. Three kinds of antibodies are generated: IgM, IgG

(sometimes known as IgY), and IgA (Karlsson et al., 2004; Sharma, 1999). Effective vaccination response in a group of animals is often assessed by observing an increase in antibody levels shortly after vaccination. ELISA is primarily utilised for serological surveillance. T cells are the primary effector cells of targeted cellular immunity (Ferreira Júnior et al., 2018; Sharma, 1999).

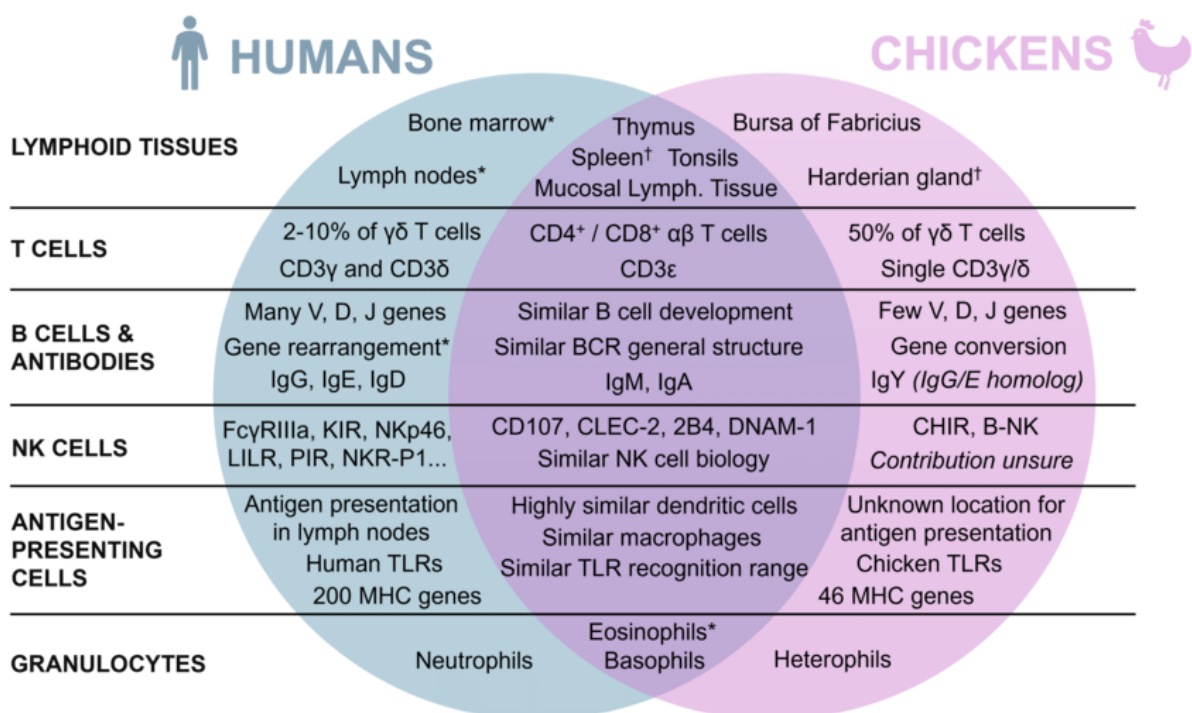


**Figure 1.1. Comparison of the human and chicken immune systems.** \*Found in both species, with a lesser impact in chickens. † Found in both species, but with a lesser impact in humans (Garcia et al., 2021).

Given the ongoing arms race against rapidly changing viruses, there is an urgent need for novel advancements in vaccine research to effectively combat the emergence and re-emergence of new viral strains (S. Khan et al., 2016; Nadeem et al., 2020; Vilela et al., 2020). Advances in pathogen biology and recombinant DNA technology are laying the foundations for providing novel approaches to overcome the problems

encountered with conventional vaccine design (Khan et al., 2016; Nadeem et al., 2020), such as reverse genetic systems, which permit the manipulation and rescue of infectious RNA viruses (Lauring et al., 2010), and genome editing technologies (i.e., CRISPR/Cas9), which allow precise manipulation of the viral genome. This research aims to develop a novel immunogenic platform that is safe and induces long-term immunity through the use of the CRISPR/Cas9 genome editing technology.

This chapter aims to present a preliminary overview of the study, beginning with an analysis of the background and context. Following this, the research problem will be further elaborated, followed by an explanation of the study's aims, objectives, and questions. The study's relevance will subsequently be expounded.

## **1.1. Vaccine Development**

Infectious diseases triggered by existing and evolving viruses continue to endanger our safety and economy (Josefsberg & Buckland, 2012). Vaccination is the most successful method of avoiding emerging infectious infections, protecting millions of lives per year, but the ongoing lengthy and complicated path to create antiviral vaccines is rather ineffective (Josefsberg & Buckland, 2012). Even more difficult, the virus evolves quickly to get around the previous immunity the vaccine had induced (Devaux, 2012). With the ongoing arms race with the rapidly changing virus, innovative developments to promote and improve vaccine production against novel emerging and re-emerging viruses are therefore urgently needed.

The following figure (**Figure 1.2**) presents a framework that describes the different elements that may be considered when developing vaccines for poultry. Careful

consideration of the key elements of viral vaccine design includes choosing the appropriate vaccine approach, the antigen to use, and, lastly, adding specific adjuvants to enhance protection.

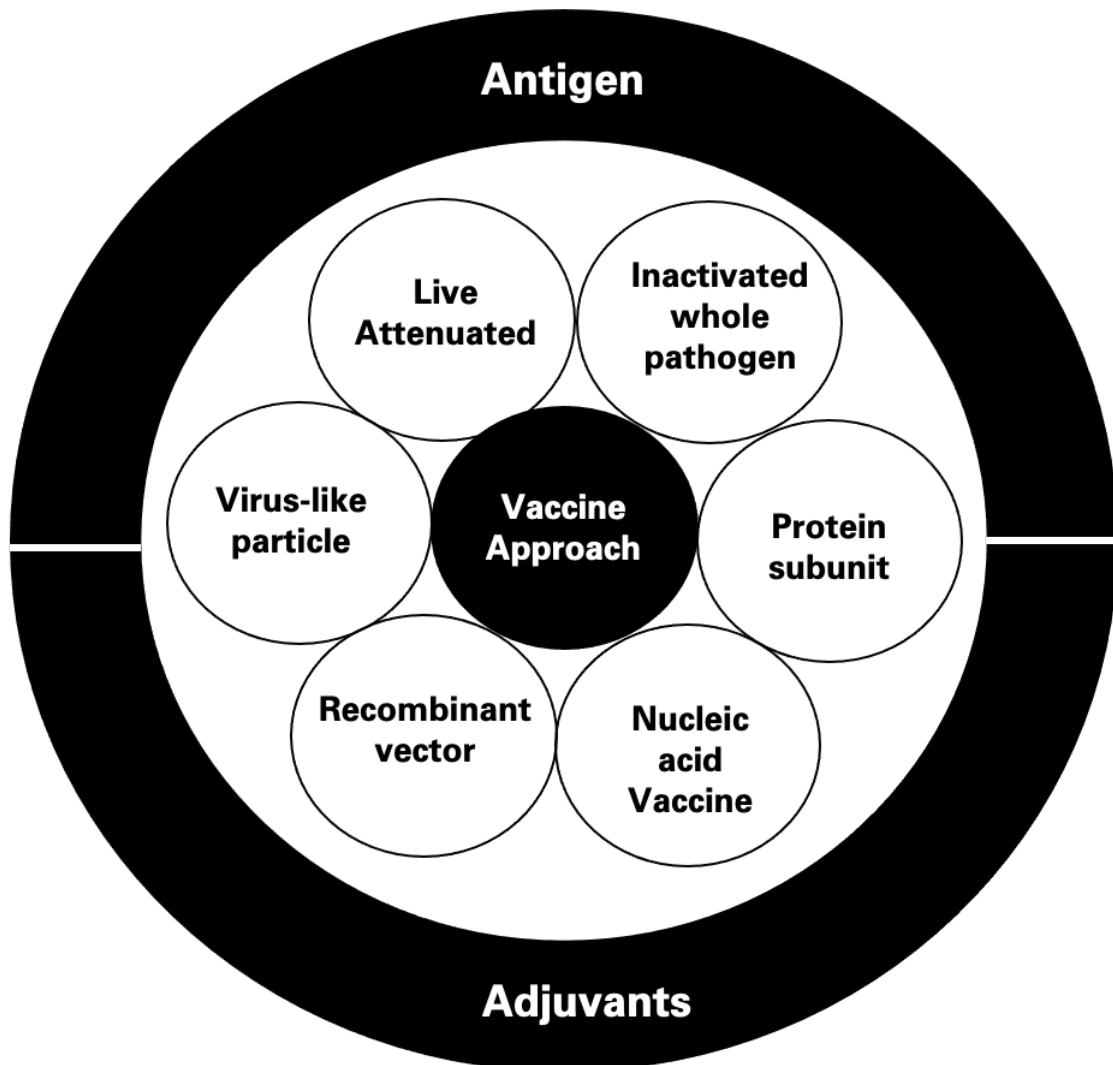


**Figure 1.2. Elements of vaccine design.** Different elements are considered when developing vaccines. Foremost is the choice of vaccine approach, which will then dictate the choice of antigens and possible adjuvants.

### **1.1.1. Vaccine Approach**

Vaccines are commonly categorised as either live or non-live, with the latter frequently informally referred to as "inactivated." This classification is used to differentiate vaccines that include weakened strains of the specific pathogenic organism from those that just consist of pathogen components or dead complete organisms (Chambers et al., 2016; Thomas, 2000). In addition to conventional live and non-live vaccinations, other alternative platforms have emerged in recent decades, such as viral vectors, nucleic acid-based RNA and DNA vaccines, and virus-like particles (Pollard & Bijker, 2021).

#### **1.1.1.1. Inactivated Whole-Pathogen**

For several decades, veterinary vaccinations have effectively used inactivated whole-pathogens, encompassing viruses, parasites, and bacteria. Inactivation is commonly accomplished by employing thermal, chemical, or irradiation-based methods. The stability of these vaccines allows for the preservation of a significant proportion of the live pathogen's antigens (Sanders et al., 2014). Nevertheless, these pathogens are incapable of infecting or reproducing within the host organism, hence necessitating the administration of booster immunisations and adjuvants to ensure sufficient protection (Vetter et al., 2018). Booster immunisations frequently require the use of inactivated whole-pathogen vaccines (Chambers et al., 2016).

Inactivated whole-virus vaccines may not elicit cross-protection across different viral geno/sero-types. This lack of cross-protection observed in diseases such as FMDV (Lu et al., 2022) could potentially be attributed to the mechanism of action of inactivated whole-pathogen vaccines. These vaccines primarily stimulate antibody-

mediated immunity rather than cell-mediated immune responses, which are typically more broadly cross-reactive. However, this limitation can potentially be overcome by incorporating multiple inactivated types within the same vaccine formulation (Chambers et al., 2016; Vetter et al., 2018).

#### **1.1.1.2. Live Attenuated Pathogens**

Live-attenuated vaccines are modified forms of the target pathogen that have reduced virulence. These vaccines are capable of undergoing limited reproduction within the host, therefore stimulating immune responses that provide protection against the fully virulent form of the organism (Minor, 2015). These vaccines seldom need the use of an adjuvant and can be delivered in a manner that replicates the natural route of infection (Chambers et al., 2016). Lifelong immunity may be conferred by vaccines, as exemplified by the successful eradication of the Rinderpest virus, which stands as the second disease to be exterminated via deliberate human intervention (Roeder et al., 2013).

Live vaccines are of great importance in the development of vaccinations against protozoa and helminth parasites (Solana et al., 2022). This is because live vaccines have the ability to express a broader spectrum of pathogen antigens, including those that necessitate active metabolism. The variation of antigens throughout different life cycle phases of these parasites further underscores the significance of using live vaccines in their prevention and control (Minor, 2015; Solana et al., 2022).



The use of inactivated whole-pathogen or live attenuated vaccines has several challenges, notably the potential for immune responses that closely resemble those elicited by natural infection. This similarity in immune responses may hinder their efficacy in disease eradication endeavours, hence reducing their suitability for such purposes (Suarez, 2012). Some examples of diseases are foot-and-mouth disease, leptospirosis, brucellosis, and bovine tuberculosis (Chambers et al., 2016). Vaccines have the potential to disrupt surveillance techniques by causing difficulties in differentiating between wild-type pathogens and vaccination strains in diagnostic samples, as well as potentially leading to false positive results in immunodiagnostic testing (Erdem & Sareyyupoglu, 2022).

The efficacy of attenuated viral vaccines surpasses that of inactivated whole-virus vaccinations owing to their heightened T cell responses, elevated levels of virus-neutralising antibodies, and extended duration of protection (Chambers et al., 2016; Minor, 2015). Nevertheless, there exists a potential hazard wherein the vaccine virus may undergo a reversion to a highly pathogenic state or engage in genetic recombination with naturally occurring viruses, as exemplified by the attenuated vaccines employed for Bovine Viral Diarrhoea (BVD) (Antos et al., 2021) and Porcine Reproductive and Respiratory Syndrome (PRRS) (X. J. Meng, 2000).

The use of attenuated vaccines for avian influenza (AI) carries the potential for gene reassortment with wild-type viruses, hence giving rise to the development of harmful variants (Wu et al., 2013). Infectious laryngotracheitis (ILT) is a substantial concern within the poultry sector. The use of attenuated vaccines generated from chicken embryos has been associated with adverse consequences, including residual

virulence, transmission to susceptible birds, latent infection, and reversion to virulence subsequent to *in vivo* passage (Coppo et al., 2013). In recent years, the occurrence of recombination events among attenuated infectious laryngotracheitis (ILT) vaccinations has resulted in the creation of novel virulent viral strains, leading to a significant increase in the prevalence of the associated diseases (Coppo et al., 2013).

The administration of live attenuated virus vaccinations in pregnant animals carries the possibility of vertical transmission, which may result in adverse pregnancy outcomes or the establishment of chronic infection (Ficken et al., 2006; Tizard, 2021). Therefore, certain vaccinations have not obtained approval in certain countries. Taken together, these possible adverse effects highlight the need for the creation of safer vaccination alternatives that are similarly efficacious.

#### **1.1.1.3. Protein Subunit Vaccines**

The significant benefit associated with subunit vaccines is their inherent safety. Nonetheless, the creation of recombinant proteins necessitates a comprehensive understanding of the protective antigen (Moyle & Toth, 2013). This is frequently either unclear or mediated by a variety of antigens (Hansson et al., 2000). The potential concern mentioned earlier may not be a significant problem, as demonstrated by the existence of commercial vaccines for porcine contagious pleuropneumonia (L. Zhang et al., 2022). These vaccines effectively protect against all known serotypes of the causative organism, *Actinobacillus pleuropneumoniae*, by combining four or five recombinant proteins (Loera-Muro & Angulo, 2018). However, another constraint is that the recombinant variant of the antigen could not elicit an immune response of the same nature or magnitude as the native antigen due to its inability to maintain its

original shape. The matter at hand pertains specifically to vaccinations designed to combat parasites and viruses, wherein the intended target for immunisation frequently manifests as a glycoprotein (Cid & Bolívar, 2021; Heidary et al., 2022).

Moreover, subunit protein vaccines frequently exhibit suboptimal immunogenicity and need further immunisations and adjuvants to achieve sufficient protective efficacy (Cid & Bolívar, 2021). The elevated costs associated with their manufacture render them less economically appealing. Nevertheless, there are commercially accessible subunit vaccines, such as the Porcilis PCV vaccine (MSD Animal Health), which are derived from recombinant proteins. The vaccine under consideration utilises the baculovirus-vectored expression technique to produce the recombinant ORF2 protein derived from pig circovirus type 2, which is the etiological agent responsible for swine circoviral disease (Sno et al., 2016).

#### **1.1.1.4. Recombinant Viral Vector**

Over the past few decades, the development of recombinant vaccines has emerged as a prominent area of study, characterised by its revolutionary nature. It has become one of the most exciting aspects of the discipline of molecular virology. Recombinant viral vaccine vectors have been essential in the advancement of novel vaccine development (Kamel & El-Sayed, 2019). Several types of viruses, including poxviruses, adenoviruses, parvoviruses, flaviviruses, alphaviruses, NDV, and herpesviruses, have been employed as viral vector vaccines (Dutta & Langenburg, 2023; Kamel & El-Sayed, 2019; Kim & Samal, 2016; Lundstrom, 2014; Palmer et al., 2004; Pastoret & Vanderplasschen, 2003; Tatsis & Ertl, 2004; Vilela et al., 2022). These viral vectors can express genes from external sources targeting different

diseases. In general, the use of viral vectors offers several benefits. These advantages encompass not only the ability to transport foreign genes to target cells with a higher degree of specificity and efficiency, but also the capacity to induce strong immune responses and enhance cellular immunity (Ewer et al., 2016; Kamel & El-Sayed, 2019; Schultz & Chamberlain, 2008).

#### **1.1.1.4.1. Herpesviridae as a Recombinant Viral Vector**

Herpesviruses can infect a wide range of organisms, including both vertebrates and non-vertebrates. Thus far, scientists have identified and partially characterised over two hundred different herpesviruses (Rechenchoski et al., 2017; Santos et al., 2012).

A variety of vaccine types have been developed through different vaccine approaches, including inactivated vaccines, live attenuated vaccines, DNA vaccines, peptide vaccines, and vector vaccines (Kamel & El-Sayed, 2019). Throughout the past decade, Herpesviruses have been one of the most successful recombinant viral vector platform available for carrying foreign immunogenic genes to protect various veterinary species (**Table 1.1**).

Herpesvirus-based viral vectors are regarded as a type of vaccine that possesses several advantages for application in the manufacturing of recombinant vaccines. The herpesviruses pose a lower safety risk as a result of their restricted host range and widely established attenuation, supported by multiple studies showing continued viral growth and replication in TK-defective mutants (Field & Wildy, 1978; S. Kit et al., 1985; Slater et al., 1993; Tenser et al., 1983). Numerous infections have significant socioeconomic implications for the livestock and poultry sectors and may possess

zoonotic significance. Examples include foot and mouth disease, avian influenza virus, bovine viral diarrhoea, and blue tongue, among others. Herpesvirus-based viral vectors effectively deliver immunogenic viral structural proteins, eliciting a robust cell-mediated and humoral immune response in vaccinated animals by expressing these proteins within infected cells (M Bublot et al., 2007; Yang Chen et al., 2011; Darteil et al., 1995; Donofrio et al., 2013; Esaki, Godoy, et al., 2013; Franceschi et al., 2015; Yongqing Li et al., 2011; C. T. Rosas et al., 2008; Y. Wang et al., 2015; Yokoyama et al., 1998). Among the most merited characteristics of the herpesvirus as a viral vector are its diverse genomic regions that allow for the integration of foreign genes, resulting in high efficacy and no adverse impact on viral replication (Borchers et al., 1994; Fuchs et al., 2007; Kamel & El-Sayed, 2019; S.-W. Lee et al., 2011). This leads to a strong immunological response in vaccinated animals, including cell-mediated and humoral components (T. Chen et al., 2019; M. Kit et al., 1991; S. Liu et al., 2015; Macchi et al., 2018; Taylor et al., 1998; Tian et al., 2006; Xuan et al., 1998). Furthermore, herpesviruses as a viral vector can be used to differentiate between infected and vaccinated individuals (DIVA), which is vital in controlling and eradicating infections (Murr et al., 2020). The relative ease of mass production contributes to the economic advantage of herpesvirus use in vaccine development. Overall, herpesviruses manifest characteristics that are considered vaccination-friendly, efficiently expressing foreign genes, and exhibit mass production stability, eliminating the need for cold chain conditions (Kamel & El-Sayed, 2019).

**Table 1.1.** Animal herpesviruses carrying several foreign immunogenic genes to protect against several important diseases.

Viral Vector	Disease	Target Gene	Reference
<i>Herpesviruses of dogs, cats, and pigs</i>			
Canine herpesvirus (CHV)	Neospora caninum	NcSRS2	(Nishikawa et al., 2000)
	Rabies virus	G protein	(Xuan et al., 1998)
Feline herpesvirus (FHV-1)	Rabies virus	Glycoprotein (G) of rabies virus	(T. Chen et al., 2019)
	Toxoplasma gondii	Glycoprotein (G) of rabies virus	(Mishima et al., 2002)
	Feline leukemia virus (FeLV)	Envelope glycoprotein gene	(Willemse et al., 1996)
	Feline immunodeficiency virus (FIV)	Gag protein	(Sato et al., 2001)
	Feline calicivirus (FCV)	Precursor capsid gene	(Yokoyama et al., 1998)
Pseudorabies virus	PRRS	GP5-M	(Y. Jiang et al., 2007)
		P1 gene	(X. Li et al., 2008)
	Foot and mouth disease virus (FMDV)	P1 and multiepitope gene "FHG" consisting of 6 B cell epitopes and two T cell epitopes of FMDV	(Y. He et al., 2008)
		VP1	(Qian et al., 2004)
		FMDV and PPV	(Hong et al., 2007)
		ORF2	(Song et al., 2007; Zheng et al., 2015)

	Porcine circovirus type 2	ORF1 and partial ORF2 gene	(Ju et al., 2005)
	Hog cholera virus	Glycoprotein E1 NS1 gene	(Qian et al., 2015; G. Xu et al., 2004)
	Japanese encephalitis virus	Premembrane (prM) and envelope (E) proteins SX09S- 01 strain	(G. Xu et al., 2004)
	CSFV	E2 gene	(Y. Wang et al., 2015)
	Schistosoma japonicum	Sj26GST and SjFABP	(F. Wei et al., 2010)
	H3N2 subtype swine influenza virus (SIV)	Haemagglutinin (HA)	(Tian et al., 2006)
	Swine-origin H1N1 influenza A	HA gene	(Klingbeil et al., 2014, 2015)
	Porcine parvovirus (PPV)	VP2	(Yang Chen et al., 2011)
	Transmissible gastroenteritis virus	S gene	(Yin et al., 2007)
	T. gondii	TgSAG1	(Q. Liu et al., 2008)
	Rabies virus	rgp	(Z. Yuan et al., 2008)
<hr/>			
<i>Herpesviruses of ruminants and equine</i>			
Bovine herpesvirus type 1 (BHV-1)	FMDV	Capsid protein (VPI) epitope	(M. Kit et al., 1991)
	FMDV	VP1 gene	(Ren et al., 2009)
	Bovine respiratory syncytial virus	Synthetic G gene	(Taylor et al., 1998)
	Bovine viral diarrhea virus	Glycoprotein E2	(Schmitt et al., 1999)

	Mannheimia haemolytica	The viral Glycoprotein C gene with a leukotoxin-plpE chimeric gene	(Batra et al., 2017)
	Caprine herpesvirus type 1 (CpHV-1)	gD	(Donofrio et al., 2013)
	Peste des Petits Ruminants Virus	H glycoprotein	(Macchi et al., 2018)
	Bluetongue virus	VP2 provided by a heterologous signal peptide to its N terminus and a transmembrane domain to its c-terminus	(Franceschi et al., 2011)
Bovine herpesvirus 4	Bovine viral diarrhea virus (BVDV)	The (gE2-14) putative transmembrane domain was removed and a 14 amino acids peptide was added to its c-terminus and an Ig K signal peptide to N terminus	(Donofrio et al., 2007)
	Monkeypox virus (MPXV)	MPXV glycoproteins, A29 L, M1R and B6R	(Franceschi et al., 2015)
	Ebola virus (EBOV)	Synthetic EBOV glycoprotein (GP) gene	(Rosamilia et al., 2016)
Equine herpes virus	Equine herpes virus Swine influenza virus (H1N1)	H1	(Said et al., 2013)
	Bluetongue virus	VP5 & VP2	(G. Ma et al., 2012)



	Bovine viral diarrhea virus (BVDV)	Structural proteins (E1, E2, C, Erns)	(C. T. Rosas, König, et al., 2007)
	West Nile virus	E & prM proteins	(C. T. Rosas, Tischer, et al., 2007)
	Venezuelan equine encephalitis virus	Structural proteins	(C. T. Rosas et al., 2008)
	Canine influenza virus (CIV)	H3	(C. Rosas et al., 2008)
	Canine distemper virus (CDV)	H & N protein	(Z. Pan et al., 2017)
	Rift Valley fever (RVF) virus	Gc & Gn	(Said et al., 2017)
	Empty Cell Schmallenberg virus (SBV)	Gc domain of the SBV	(Wernike et al., 2018)
<hr/> <i>Poultry herpesviruses (HVT and MDV)</i> <hr/>			
	Coccidiosis	Ea1A gene	(Vermeulen, 1998)
	H7N1 avian influenza virus	HA	(Yongqing Li et al., 2011)
	Chlamydia psittaci	pmpD-N	(S. Liu et al., 2015)
HVT	A clade 2.2 H5N1 strain (A/swan/Hungary/4999/2006)	HA gene	(Kapczynski et al., 2015)
	Newcastle disease	F gene	(Esaki, Noland, et al., 2013)
	Infectious bursal disease	VP2	(M Bublot et al., 2007; Darteil et al., 1995)
	Laryngotracheitis virus	Glycoprotein B	(Godoy et al., 2013)
MDV	Low pathogenic avian influenza virus (LPAIV) H9N2	HA and neuraminidase gene (NA)	(Z. Zhang et al., 2014)

#### **1.1.1.4.2. Structure and Genomic Organisation**

Herpesviruses are composed of four primary components, namely a core, capsid, tegument, and envelope (Kamel & El-Sayed, 2019) (**Figure 1.3.A**). The characteristics of the virion structure of viruses within the family Herpesviridae primarily determine their classification. The viruses under consideration possess double-stranded DNA that is situated within the central core. The exact configuration of DNA within the nucleus remains uncertain. The molecular weight of herpesvirus DNA ranges from around 80 to 150 million, or 120 to 250 kilobase pairs, depending on the specific virus (Hones, 1984). The DNA core is enveloped by a capsid composed of 162 capsomers, organised in a symmetrical icosapentahedral arrangement. The diameter of the capsid is estimated to be around 100 to 110 nanometres. The tegument, which is observed to be composed of amorphous material, has close adherence to the capsid (Hones et al., 1980). The lipid bilayer envelope, which is generated from host cell membranes, is loosely encircling the capsid and tegument. The composition of the envelope includes polyamines, lipids, and glycoproteins. The glycoproteins impart specific characteristics to each virus and provide exclusive antigens that elicit an immune response from the host (Connolly et al., 2011).

The size, structure, and organisation of herpesvirus genomes exhibit distinct variations, which align with the intricate taxonomic classification of this particular viral family. The genomes of organisms are partitioned into distinct regions known as unique small (US) and unique large (UL), which are separated by repetitive sequences. These repetitive sequences are often found at the ends of the genomes, and in certain viruses, they may also occur inside (Borchers et al., 1994; Pellett &

Roizman, 2013) (**Figure 1.3.B**). During the process of replication, when the repeated sequences undergo oriented inversion, both the UL and US components exhibit the same inversion pattern. This results in the generation of either two or four distinct genome isomers. Importantly, these isomers exist in equimolar amounts (Roizman et al., 1981).

Approximately 75 proteins that exhibit variable expression are encoded inside the herpesvirus genome. Initially, the productive cycle begins with the synthesis of immediate-early (IE) genes in order to initiate the transcription process of early and late genes. These genes encode for viral regulatory proteins involved in transcriptional control of the early (also referred to as E or  $\beta$ ) genes. The replication of DNA is mostly facilitated by early genes, whereas late genes (L) predominantly encode structural proteins (Gruffat et al., 2016).

TK, gl, PK, gG, gE, UL 45/46, HVT 065/066, and US (1, 2, 3, and 10) genes constitute the herpesvirus insertion sites targeted for the development of herpesvirus-based recombinant viral vectors; these genes are proven to not be essential for viral replication (Klupp et al., 2004; S.-W. Lee et al., 2011; Olsen et al., 2006; Schnitzlein et al., 1995; N. Tang et al., 2020).

Herpesviruses can be categorised into three distinct groups based on their characteristics. The first group, known as alphaherpesviruses, includes the ILTV (Ou & Giambrone, 2012) and Marek's disease virus (Afonso et al., 2001). These viruses exhibit a short replicative cycle, causing cytopathology in monolayer cell cultures, and have a wide range of hosts they can infect. The second group, referred to as  $\beta$

herpesviruses, consists of cytomegaloviruses and human herpesviruses 6 and 7 (Salameh et al., 2012). These viruses have a longer replicative cycle and a more limited host range compared to the alphaherpesviruses. Lastly, the third group,  $\gamma$  herpesviruses, includes the Epstein-Barr virus and human herpesvirus 8. These viruses have a highly restricted host range (Whitley, 1996).

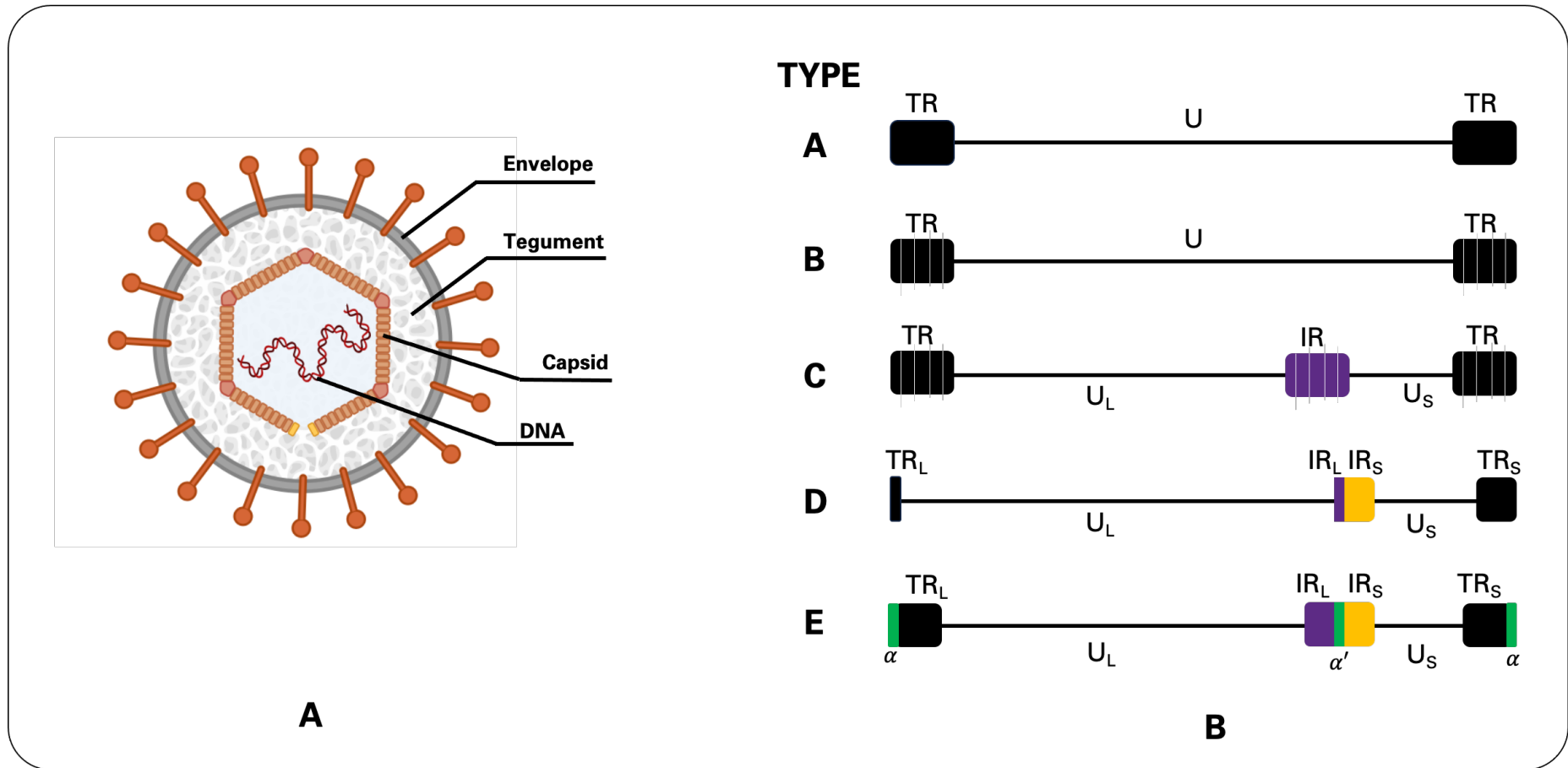


**Figure 1.3. Illustrative overview of the various types of herpesvirus genomes and the structural characteristics of the virion.** (A) The viral structure is composed of four distinct components: (1) a central region composed of the double-stranded DNA of the virus; (2) a capsid with an icosahedral shape and a T=16 symmetry that encapsulates the central region; (3) a protein layer known as the tegument, which lacks a defined structure and surrounds the capsid; and (4) an outer envelope composed of lipids. (B) The genomes of type A, such as EHV-2, are characterised by the presence of a unique (U) region that is bordered by a direct terminal repeat (TR). The type B structure, including Kaposi's sarcoma-associated herpesvirus, is characterised by the presence of a U region that is surrounded by varying quantities of TRs. The genomes of type C, such as the Epstein-Barr virus, has varying quantities

of terminal sequences and an internal direct repeat. This direct repeat is not associated with the TR and divides the U region into two distinct sections known as U<sub>L</sub> and U<sub>S</sub>. The genomes of type D viruses, such as PRV, and type E viruses, such as HSV-1, consist of U<sub>L</sub> and U<sub>S</sub> sections. These regions are characterised by the presence of terminal and internal inverted repeats, specifically known as TR<sub>L</sub>/IR<sub>L</sub> and IR<sub>S</sub>/TR<sub>S</sub>, respectively. Most of the viruses relevant to animal diseases belong to the D or E type. The type E structure is characterised by the presence of a terminal direct repeat, referred to as the “α sequence,” which spans several hundred base pairs. Additionally, an internally existent inverted copy, referred to as the α' sequence, can be observed. (Adapted from You et al., 2017).

#### **1.1.1.4.3. ILTV as a Viral Vector**

The causal pathogen of infectious laryngotracheitis is the ILTV. ILTV is an alphaherpesvirus that infects the trachea and upper respiratory system of chickens, resulting in a sickness with a high morbidity and a variable fatality rate depending on the strain (Kirkpatrick et al., 2006; S.-W. Lee et al., 2015; Vagnozzi et al., 2015).

The replication cycle of ILTV appears to exhibit similarities with those of other alphaherpesviruses (**Figure 1.4**). Envelope glycoproteins, particularly gC, are primarily responsible for facilitating the attachment of the viral envelope to host cell receptors. This process is believed to be crucial for mediating the fusion between the viral envelope and the host cell membrane (Kingsley et al., 1994; Kingsley & Keeler, 1999). According to Kingsley and Keeler (1999), the entry of ILTV is not dependent on heparin sulphate, in contrast to HSV-1 (herpes simplex virus type 1). Following attachment, the viral tegument and nucleocapsid are carried into the cytoplasm. Subsequently, the viral DNA, which has been freed from the nucleocapsid, enters the nucleus via nuclear pores (Cardone et al., 2007; Trus et al., 2004). The transcription and replication of ILTV DNA are tightly controlled processes that take place within the

nucleus, making use of the cellular machinery of the host cell (Guo et al., 1993; Prideaux et al., 1992).

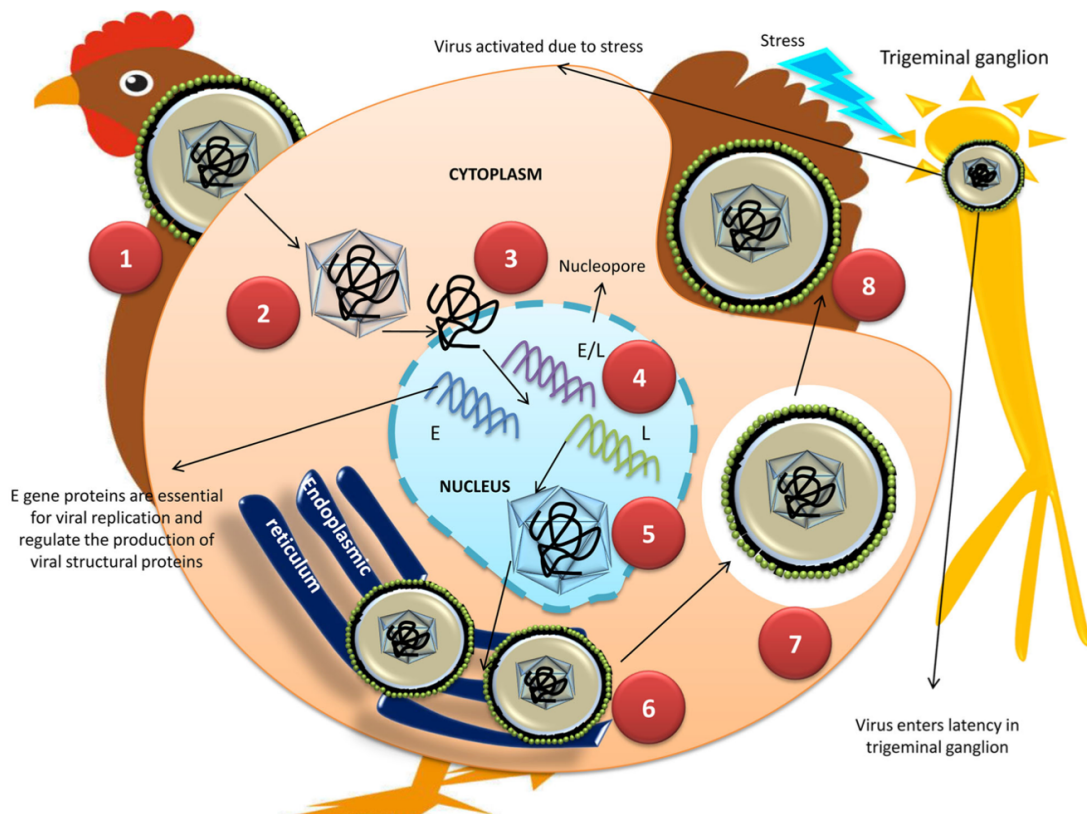


**Figure 1.4. Replication of the ILT virus.** Illustrates the process of replication of the Infectious Laryngotracheitis (ILT) virus. **(1)** Attachment of the virus. **(2)** The tegument and nucleocapsid are transferred into the cytoplasm. **(3)** The viral DNA is liberated from the nucleocapsid and then enters the nucleus by traversing through nuclear pores. **(4)** There are three distinct categories of ILTV genes, specifically early (E), early/late (E/L), and late (L), that are activated during the process of viral transcription and translation, depending on their respective expression levels. **(5)** Nucleocapsids that carry DNA undergo the process of acquiring an envelope when they bud out from the inner lamellae of the nuclear membrane. **(6)** Virions are carried into the lumen of the endoplasmic reticulum to get a second envelope and subsequently aggregate within the cytoplasmic vacuoles. **(7 and 8)** The vacuoles that hold the virions are expelled from the cell by either exocytosis or cell lysis (Gowthaman et al., 2020).

ILTV is composed of a double-stranded DNA molecule enclosed in an icosahedral capsid with a proteinaceous tegument layer and an outer envelope containing viral glycoproteins (Cruickshank et al., 1963; Watrach et al., 1963). ILTV's genomic DNA is roughly 155 kb in length and is composed of distinct long and short segments (UL and US) separated by inverted repeats (Johnson et al., 1991; Leib et al., 1987). The envelope includes significant immunogenic glycoproteins, including gB, gC, gD, gE, gG, gH, gI, gJ, gK, gL, and gM, which are encoded by UL27, UL44, US6, US8, US4, UL22, US7, US5, UL53, UL1, and UL10, respectively (York et al., 1987, 1990). Herpesviruses utilise the envelope glycoproteins for viral entrance, cell-to-cell fusion, and virus outflow (Pereira, 1994; Spear et al., 2000). The gB protein of herpesviruses is involved in membrane fusion and virus penetration (Connolly et al., 2011; Dunaevskaia, 1988). On the contrary, the gD protein of the majority of herpesviruses functions as a receptor for viral binding to susceptible cells (Di Giovine et al., 2011; Eisenberg et al., 2012). Both gB and gD proteins produce neutralising antibodies upon virus infection (Lazear et al., 2012; Rouse & Kaistha, 2006). In addition, both gB and gD proteins of herpesvirus have been shown to be the target antigens for recombinant vaccine production (Lazear et al., 2012; Rouse & Kaistha, 2006; Stanberry et al., 2002; W. Zhao et al., 2014). The gB and gD proteins are highly conserved herpesvirus structural glycoproteins. Additionally, it is suggested that the gD protein of ILTV is a superior antigen for the development of ELISAs than the gB protein (Kanabagatte Basavarajappa et al., 2014). Immunisation with gD elicits a stronger neutralising antibody response than treatment with gB alone or in combination with other ILTV glycoproteins (Kanabagatte Basavarajappa et al., 2014).



Due to the simplicity with which ILTV vaccines may be administered in large quantities by aerosol or drinking water, ILTV vaccines are also excellent vectors for immunogenic proteins from other chicken diseases. Apart from the NDV-F protein and MDV gB, the H5 and H7 HA genes of highly pathogenic avian influenza viruses (HPAIV) were efficiently expressed in ILTV recombinants (Fuchs et al., 2006; Lüschow et al., 2001; Veits et al., 2003). Animal experiments with the latter constructs generated ILTV and HA-specific antibodies and demonstrated that inoculated chickens were protected against challenge infections with virulent ILTV and HPAIV serotypes. Protection against fowl plague was equivalent to that achieved with inactivated AIV formulations, which must be administered subcutaneously or intramuscularly. Additionally, epidemiological management of avian influenza in the field by serology is more challenging following full AIV vaccination. In comparison, the use of vector-based or subunit vaccines containing only HA as the AIV component would allow for the differentiation of vaccinated from naturally infected animals using serological tests that detect antibodies to other influenza virus proteins such as neuraminidase or nucleoprotein (NP) (Capua et al., 2003; Shafer et al., 1998; Veits et al., 2006).

These findings clearly illustrate the potential of attenuated ILTV mutants as viral vectors for the expression of immunogenic proteins from other chicken diseases such as infectious bronchitis virus, bursal disease virus, or fowlpox virus, as well as bacteria or parasites.

### **1.1.2. Antigen**

The careful consideration of vaccine antigens is of utmost importance, as it dictates the potential for achieving sufficient protective immunity via the utilisation of either a single antigen or a combination of several antigens. The precise characteristics and mechanisms of protective antigens are still not fully understood, which may impede the ability to effectively detect and assess them. Vaccine development is subject to several issues that impact its efficacy, including the intrinsic diversity of antigens and the requirement to preserve their original conformation to ensure an adequate immune response upon immunisation. Various elements and restrictions exert an impact on the formulation and assessment of methods pertaining to antigen identification and evaluation (Chambers et al., 2016).

#### **1.1.2.1. Economically Important Poultry Viruses**

The economic significance of the disease or the likelihood of transmission are frequently factors that influence the choice of a host species for the purpose of vaccine development. However, additional considerations may also come into play, such as the significance of protecting certain species that have value, such as companion animals or those that are rare or endangered species (Chambers et al., 2016; Gerdtz et al., 2015; Ravikumar et al., 2022). Economically important poultry viruses include NDV, IBV, and AIV.

#### 1.1.2.1.1. NDV

NDV, or avian paramyxovirus 1, is one of the most significant avian viral diseases, responsible for severe economic losses globally (Alexander, 2001). NDV is taxonomically classified as a member of the order *Mononegavirales*, family *Paramyxoviridae*, and sub-family *Paramoxivirinae* under the genus *Avulavirus* (Alexander, 2001; Ganar et al., 2014). The NDV virion structure is pleomorphic but mostly roughly spherical, with diameters around 100 – 500 nm (Ganar et al., 2014; Yusoff & Wen Siang Tan, 2001). The NDV genome is around 15 kb of linear single-stranded, negative-sense RNA with six essential genes from 3' to 5' direction: nucleocapsid (N), phosphoprotein (P), matrix protein (M), fusion protein (F), haemagglutinin-neuraminidase protein (HN), and large polymerase protein (L) (Acheson, 2011). Each gene is identified by the presence of signal sequences at the start (GS = gene-start) and at the end of the gene (GE = gene-end). Additionally, the presence of intergenic sequences (IGS) separates the genes from each other (Ganar et al., 2014). All the NDV genes code for a single major protein; however, transcriptional editing or differential initiation of gene P mRNA may result in the formation of a non-structural protein V (Acheson, 2011). The viral RNA polymerase (L protein) initiates the transcription of the viral genome at the 3' terminal nucleotide, sequentially terminating and reinitiating at multiple start/stop gene sites. At the end of each gene, a fraction of RNA polymerase dissociates from the genome and is unable to restart transcription to the next downstream gene, thus resulting in diminished quantities of mRNAs of genes located further from the 3' end of the genome. This mechanism enables the balance in synthesising proteins that are needed in high concentrations, such as N and M, and proteins needed in smaller amounts (i.e., HN and L) (Acheson, 2011) (**Figure 1.5**).

#### **1.1.2.1.1 Immunogenic proteins of NDV: F and HN proteins**

Virulence and infectivity of NDV depend on F and HN proteins (Iorio & Mahon, 2008; Panda et al., 2004). The co-expression and interaction of homologous HN and F proteins are required for virus fusion. The HN protein is involved in virus-specific membrane fusion. Through hemagglutination (HA) and neuraminidase (NA) activities, HN protein facilitates the interaction of host receptors and viruses. This allows the host membrane and viral membrane to be closer together, allowing F protein to come into contact with the host cell. As a result, the virus is able to penetrate the cell surface (Yusoff & Wen Siang Tan, 2001). F proteins mediate the fusion of the NDV with the host cell membrane. When the virion binds to the cell surface receptor, it undergoes a conformational change, allowing the cleavage of the protein precursor F to F1/F2 subunits, which also brings the viral envelope closer to the cell membrane, leading to the fusion of the two membranes (Acheson, 2011). Thus, the amino acid sequence of the cleavage site of the F protein is theorised to be a major determinant of infection (Ganar et al., 2014; Panda et al., 2004; Samal et al., 2011).

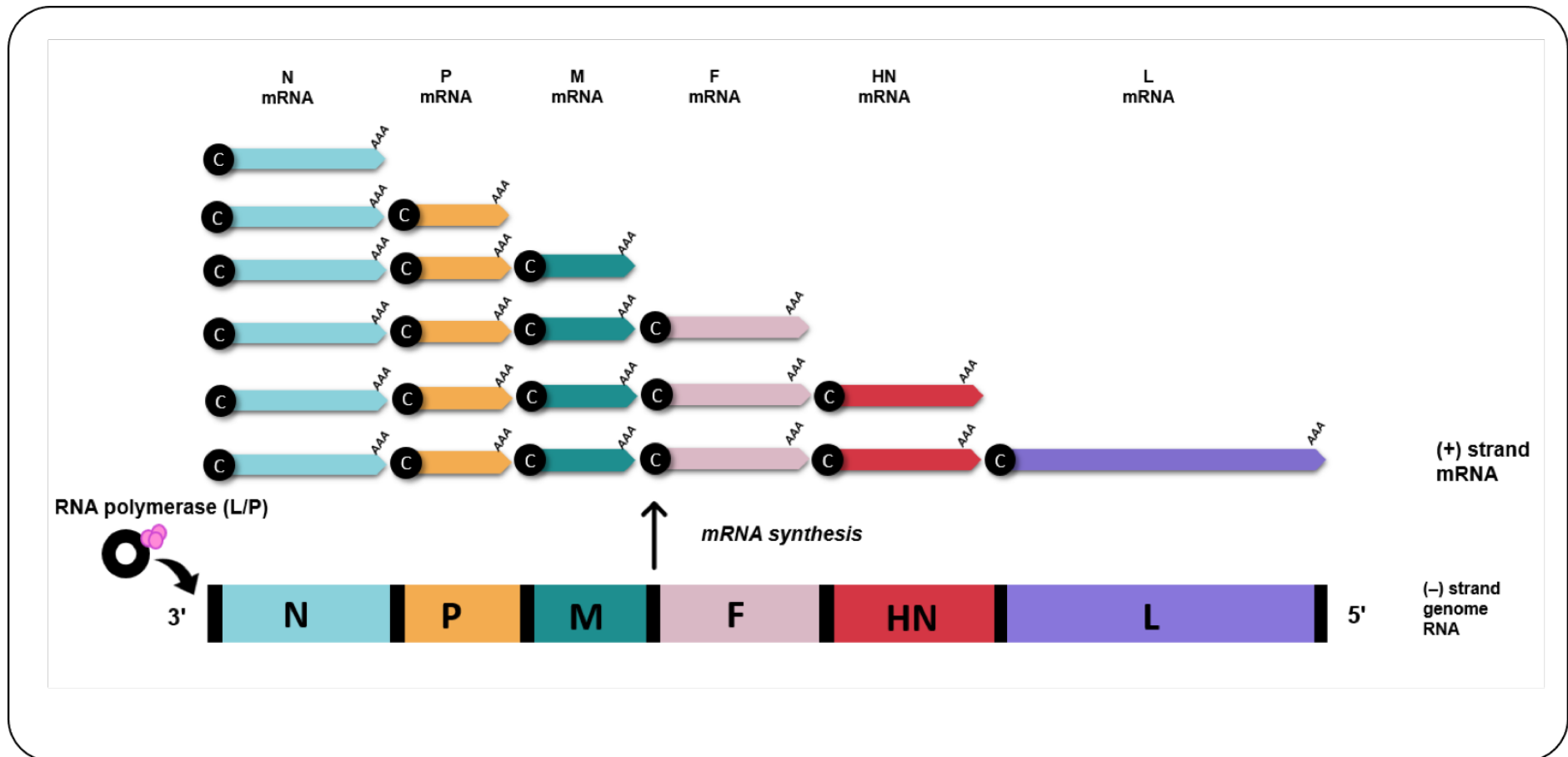


**Figure 1.5. AOAV-1/NDV mRNA synthesis.** Viral (-) strand genomes serve as templates for the generation of subgenomic mRNAs. The RNA polymerase (L/P) initiates mRNA synthesis at the beginning of the N gene, near the 3' end of the viral genome. Small red spheres denote 5' caps; AAA denotes poly(A) tails (Vilela et al., 2022). The viral genome consists of a non-segmented, negative-stranded RNA molecule of approximately 15.2 kilobases (kb) in length. It encompasses six genes responsible for generating several proteins, including nucleoprotein (N), phosphoprotein (P), matrix protein (M), fusion protein (F), hemagglutinin-neuraminidase protein (HN), and large protein (L) (Vilela et al., 2022).

#### 1.1.2.1.2. IBV

Infectious Bronchitis (IB) is a highly contagious viral respiratory disease of chickens, causing significant economic losses to the poultry industry worldwide (Houta et al., 2021). Control of IB is primarily achieved using live attenuated and inactivated vaccines that can elicit effective humoral and cellular immunity; however, their preparation is time-consuming, expensive, and complicated (R. Zhao et al., 2017).

IBV is currently classified within the species Avian coronavirus, genus Gammacoronavirus, family Coronaviridae, and order Nidovirales. IBV is an enveloped virus with a single-stranded positive-sense RNA genome of approximately 27 kb, which displays the following gene organisation: 5'UTR-1a/1ab-S-3a-3b-E-M-5a-5b-N-3'UTR (**Figure 1.6**). The RNA molecule has a 5' cap and a 3' poly(A) tail and acts as mRNA for translation of the replicase polyproteins, whose coding regions occupy the 5' two-thirds of the viral genome. The two untranslated regions (UTR) play a key role in virus replication by interacting with viral replicases and potentially other host proteins (L. Li et al., 2008; Yang & Leibowitz, 2015). Non-structural proteins (nsp) are encoded by two open reading frames (ORFs) (ORF1a and ORF1ab), which are translated into two polyproteins (pp1a and pp1ab) through a -1 ribosomal frameshift.

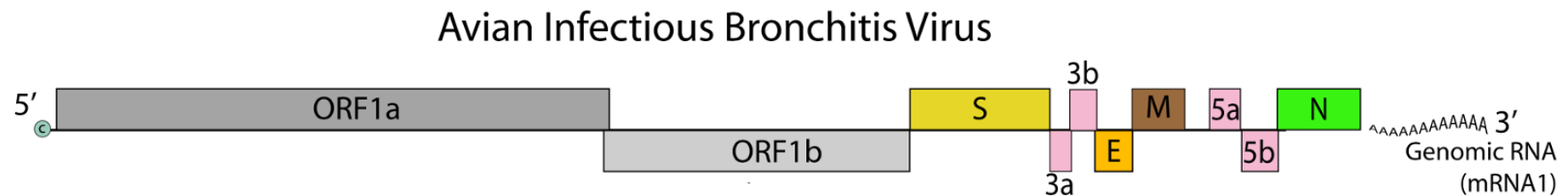


**Figure 1.6. Genomic representation of the avian IBV.** Monopartite, linear ssRNA(+) genome of 27 - 32 kb in size (the largest of all RNA virus genomes), capped, and polyadenylated. The majority of the genome is characterised by the presence of two overlapping open reading frames (ORFs) that can be translated into massive polyproteins 1a and 1b through the utilisation of a ribosomal frameshift mechanism. The coding regions include the remaining portion of the genome, whereas the primary protein structures consist of the spike (S), envelope (E), membrane (M), and nucleocapsid (N). Nevertheless, the presence of two supplementary genes, namely ORF3 and ORF5, results in the production of accessory proteins 3a and 3b, as well as 5a and 5b, respectively (Hulo et al., 2011).

#### **1.1.2.1.2.1. IBV Infectivity: S Protein**

The S protein is the most described IBV structural protein. This transmembrane protein, organised in trimers, determines the typical crown-like aspect of coronaviruses, observable at electron microscopy (Wickramasinghe et al., 2014). It is post-translationally cleaved into two sub-units, S1 and S2. The S1 contains at least 2 domains potentially involved in host receptor binding (Shang et al., 2018) and is therefore considered the main determinant of host and tissue tropism (Promkuntod et al., 2014; Wickramasinghe et al., 2014). For the same reason, the most relevant epitopes are located on this protein, including neutralising ones. The high intensity of the selective pressures driven by the host immune response acting on this region is believed to be responsible for its remarkable genetic heterogeneity, both among coronaviruses and within IBV (Franzo et al., 2019; Jackwood et al., 2012; Shang et al., 2018). Because of strain heterogeneity and linkage with biological features, the spike-coding gene has been used to classify IBV variants into genotypes for a long time. However, the absence of common classification and nomenclature criteria complicated the understanding of IBV molecular epidemiology until recent years (Valastro et al., 2016). The more conserved S2 sub-unit contains the transmembrane domain anchoring the S protein to the envelope (Li, 2016) and is fundamental for viral fusion (Belouzard et al., 2012). The interplay between S1 and S2 subunits might determine the overall avidity and specificity of virus attachment and thus viral tissue and host range (Promkuntod et al., 2013).



Due to its high antigenicity and propensity to elicit powerful immune responses, S glycoprotein has been an excellent target for vaccine development on several platforms. (Martínez-Flores et al., 2021). While the S glycoprotein is crucial for the virus's entry into host cells, from which it spreads, the immune system can also detect it and mount a protective response, which is the main goal of vaccinations (Salvatori et al., 2020; Walls et al., 2020).

#### **1.1.2.1.3. AIV**

The extensive spread of highly pathogenic avian influenza viruses (AIVs) results in significant economic losses for the poultry industry, while the infrequent transfer of these viruses to humans poses a continuous pandemic threat (Peiris et al., 2007). Influenza A viruses are encapsulated negative-sense RNA viruses with an eight-segmented, single-stranded genome. They are members of the family Orthomyxoviridae. Each year, influenza virus types A and B create repeated epidemics, resulting in considerable human morbidity and mortality. Only influenza A virus, on the other hand, is connected with influenza virus pandemics, in which an antigenically unique influenza virus spreads fast around the world in an immunologically naive population (Crosby, 1976; Webster et al., 1992). The current vaccination strategies for AIVs serve as a preventive measure against virus infection in birds rather than eradication (Swayne et al., 2013; Irshad et al., 2020). However, despite the current effectiveness of these vaccination strategies, birds are susceptible to influenza A viruses (Swayne et al., 2013).

The eight gene segments of influenza A virus encodes 11 proteins: hemagglutinin (HA), neuraminidase (NA), matrix proteins M2 and M1, non-structural (NS) proteins NS1 and NS2, the nucleocapsid, and the three polymerases PB1 (polymerase basic 1), PB2, and PA (polymerase acidic) proteins (Webster et al., 1992) (**Figure 1.7**).

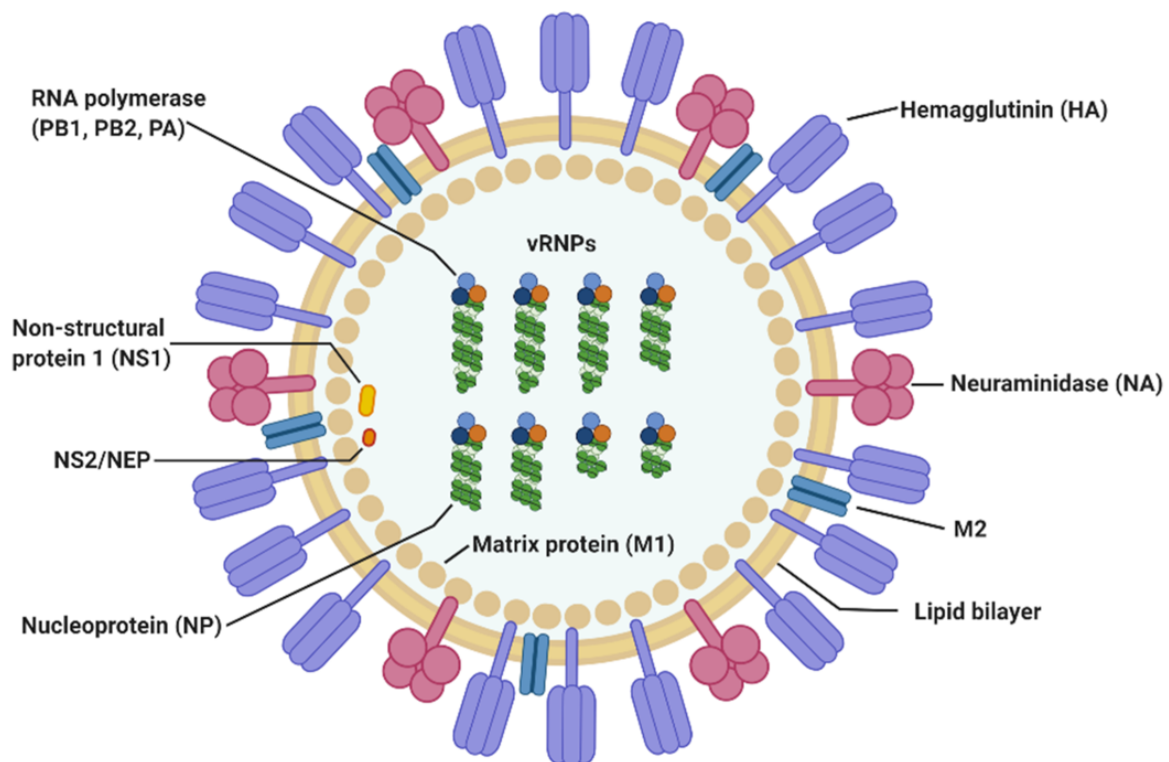


**Figure 1.7. Influenza A virus structural organisation.** A viral pathogen. IAV is classified as a negative-stranded RNA virus of the Orthomyxoviridae family. The genome of the Influenza A virus (IAV) is comprised of eight segments, each of which is responsible for encoding a total of 11 viral proteins. These proteins include Hemagglutinin (HA), Neuraminidase (NA), Matrix protein 1 (M1), Matrix protein 2 (M2), Nucleoprotein (NP), Non-structural protein 1 (NS1), Non-structural protein 2 (NS2), Polymerase acidic protein (PA), Polymerase basic protein 1 (PB1), Polymerase basic protein 2 (PB2), and PB1-F2 protein. The influenza A virus (IAV) possesses a viral envelope that comprises transmembrane proteins, including hemagglutinin (HA), neuraminidase (NA), and matrix protein 2 (M2) (H. E. Jung & Lee, 2020).

#### **1.1.2.1.3.1. AIV Infectivity: HA Protein**

Hemagglutinin (HA) is a glycoprotein of type I, and it is the most common transmembrane protein on the surface of influenza virus particles. The influenza virus's surface HA protein has two structural components (head and stalk) that have varying potential value as vaccine targets. Antibodies that give protective immunity against influenza viruses primarily target the head of the HA protein (Aamir et al., 2007; Stech et al., 2015).

HA, a polypeptide chain-encoded protein, is generated from the HA1 and HA2 domains and translocated into the endoplasmic reticulum's lumen and surface (Klenk et al., 1975). It undergoes the cleavage required for infection, allowing it to undergo an irreversible conformational shift in acidic endosomes (J. Chen et al., 1998). This cleavage is catalysed by cellular proteases, forming two disulfide-linked subunits, HA1 and HA2. HA is expressed as a trimeric protein on the virion. Two areas comprise the HA ectodomain: a stem region and a globular head region (Skehel & Wiley, 2000).

The targeting of antibodies towards the globular head of the HA protein is of utmost importance in the prevention and treatment of viral infections (Fleury et al., 1999). The viral pathogenicity is greatly influenced by the amino acid sequence of the HA0 cleavage site (Horimoto & Kawaoka, 1994; Webster & Rott, 1987). The Furin cellular protease is responsible for the cleavage of HA proteins derived from highly pathogenic avian influenza viruses (HPAIVs). In contrast, low-pathogenic avian influenza viruses (LPAIVs) exhibit a tissue-selective HA cleavage mechanism, leading to comparatively milder clinical manifestations in chickens. The identification of a polybasic cleavage site on the HA protein is a notable indicator of the pathogenicity of H5 viruses.

However, it should be noted that the mere insertion of polybasic sequences does not inevitably result in a lethal phenotype (Bogs et al., 2010). Additional proteins found in the influenza virus, namely PB2, PB1, and NP, have the potential to play a role in the virus's pathogenicity (Stech et al., 2015).

Vaccines, either inactivated or live-attenuated, are the most efficacious and economically viable approach to protecting against AIV. Antibodies that target the HA protein—with a focus on the globular head domain—provoke the majority of protective responses (Rajão & Pérez, 2018).

Novel strategies for a universal influenza vaccine are now being developed in response to the dynamic characteristics of influenza viruses. The aforementioned strategies aim to specifically target conserved epitopes found on the HA, NA, or M2 protein in order to elicit the production of cross-reactive antibodies or internal proteins that can generate a T-cell response with cross-protective capabilities (Rajão & Pérez, 2018). (**Figure 1.8**).

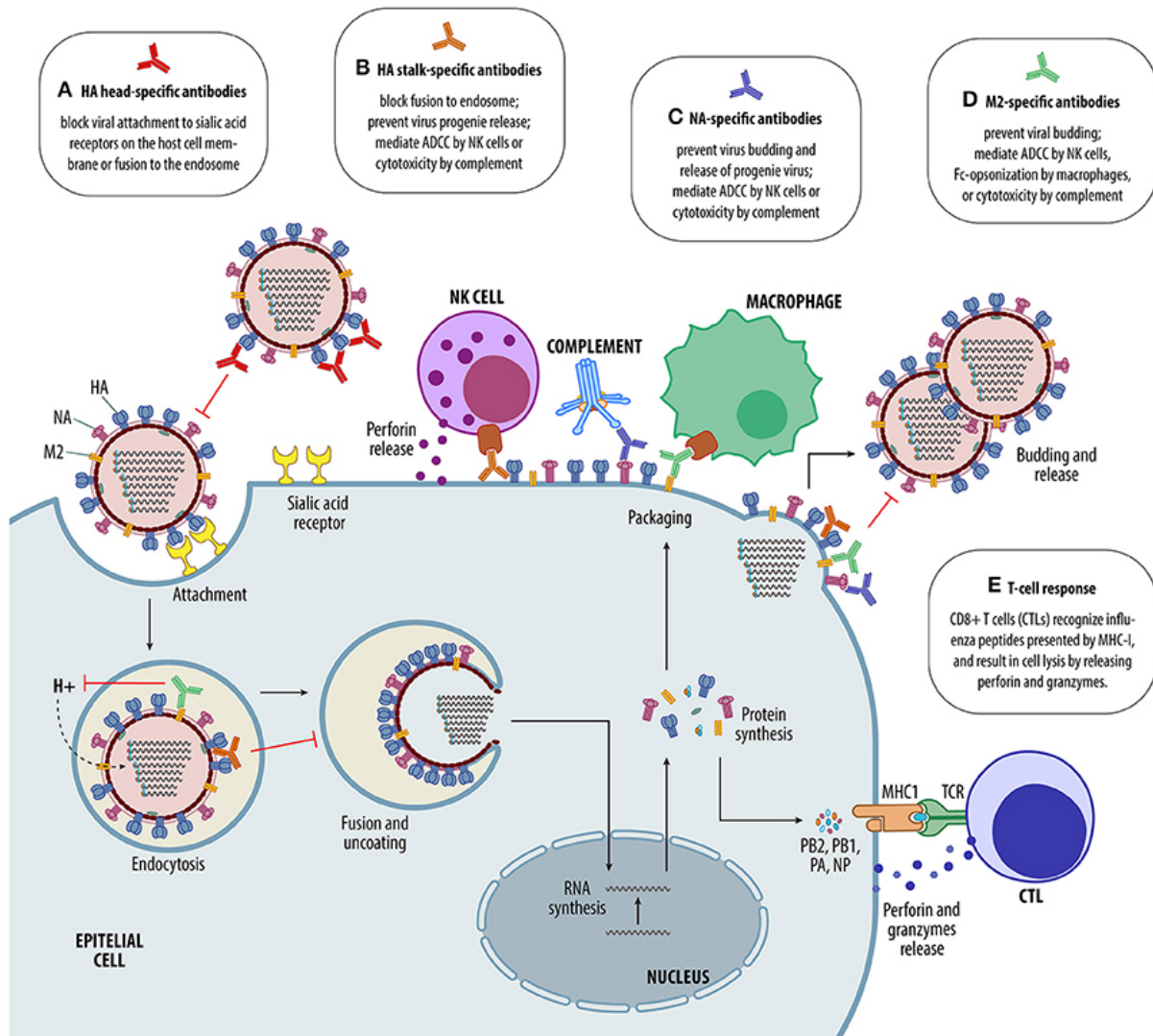


**Figure 1.8. Different influenza vaccines produce various immune responses. (A)** Antibodies that are specifically targeted towards the HA-head region of the virus hinder or obstruct the binding of the virus to sialic acid receptors located on the surface of host cells. As a result, this prevents the virus from entering the host cells. **(B)** Antibodies that are specifically targeted towards the HA-stalk region of the virus inhibit the fusion of the virus with the endosome. Additionally, these antibodies restrict the process of virus budding and release. Moreover, they induce antibody-dependent cell-mediated cytotoxicity (ADCC) through the activation of natural killer (NK) cells or complement activation. **(C)** Antibodies that are specifically targeted towards the NA protein effectively inhibit the process of viral budding and release. Additionally, these antibodies have the ability to cause antibody-dependent cellular cytotoxicity (ADCC) through the activation of natural killer (NK) cells or the complement system. **(D)** Antibodies that exhibit specificity towards M2 effectively impede the process of viral budding and release. Additionally, they facilitate antibody-dependent cellular cytotoxicity (ADCC) through the involvement of natural killer cells. Furthermore, these antibodies promote Fc-opsonization by macrophages and activate the complement system. **(E)** CD8+ T cells, also known as cytotoxic T lymphocytes (CTLs), recognise influenza peptides that are displayed on the surface of infected cells through their T cell receptor (TCR). Subsequently, they release cytotoxic granules containing perforin and granzymes, leading to the lysis of the infected cells. (Rajão & Pérez, 2018).

### **1.1.3. Vaccine Adjuvants**

Adjuvants are defined in the context of vaccinations as components that can enhance and/or shape antigen-specific immune responses. Modern vaccines are based on engineered recombinant antigens that have highly purified components with favourable safety characteristics (Reed et al., 2013). In comparison to vaccines composed of live attenuated or inactivated pathogen, the immunogenicity of such well-defined vaccine antigens may be minimal. Natural adjuvants may be inherent in live attenuated or inactivated vaccines due to their heterogeneous compositions, which may include particulate forms of proteins, lipids, and oligonucleotides (McKee et al., 2007). Aluminium salts, oil-in-water emulsions (MF59, AS03, and AF03), virosomes, and AS04 (monophosphoryl lipid A preparation (MPL) with aluminium salt) are being used as adjuvants in human vaccines licenced for use in the United States and/or Europe. Adjuvant and formulation selection may be influenced by a variety of factors, including the physical and chemical properties of the vaccine antigen, the desired type of immune response, the target population's age, and the route of vaccination. The desired features of each vaccine may entail the use of adjuvants with unique properties. Furthermore, the incorrect adjuvant can render a vaccination antigen ineffective. Thus, vaccine antigen selection must take adjuvant selection into account to avoid excluding potentially efficacious vaccination antigen candidates (Awate et al., 2013; Reed et al., 2013).

### 1.1.3.1. Chicken IgY Fc

The Fc of IgG is a crucial fusion tag for co-expression with a variety of viral proteins (**Figure 1.9**). For example, it has been demonstrated that fusing Fc to HIV-1 protein increases the immunogenicity of F proteins and elicits neutralising antibody responses (Qi et al., 2010). This is explained by Fc's ability to promote proper folding of F proteins following expression, as well as the likelihood that IgG Fc may contribute to enhancing binding to antigen-presenting cells (APCs) and cell lines expressing Fc receptors (FcR) (Martyn et al., 2009).

The mammalian IgG molecule is composed of two Fab regions that bind to highly varied antigens and an Fc region that recruits and activates immunological effector leukocytes. The interaction of Fc with the activating Fc receptor (FcR) enhances these antigen-presenting cells' ability to eliminate antigens and activates effector functions for the removal of damaged cells (Jefferis, 2009; Schwab & Nimmerjahn, 2013). Moreover, the antigen-antibody complex can avoid degradation in lysosomes by interacting with FcR, resulting in its prolonged half-life *in vivo* (Mancardi & Daëron, 2014).

In avian species, although the Fc segments between IgG and immunoglobulin Y (IgY) demonstrate different structures, IgY is similar to mammalian IgG in terms of functionality (Linden & Roth, 1978; Tressler & Roth, 1987) (**Figure 1.8**). Previous research has established that the Fc component of chicken IgY promotes macrophage activation and increases antigen processing efficiency, hence boosting the immunological response elicited by the antigen (W. Dong et al., 2016). Hence, it was postulated that the fusion of chicken IgY Fc to specific antigens have the capacity to

enhance the immunological efficacy of recombinant vaccines against NDV, IBV, and AIV.

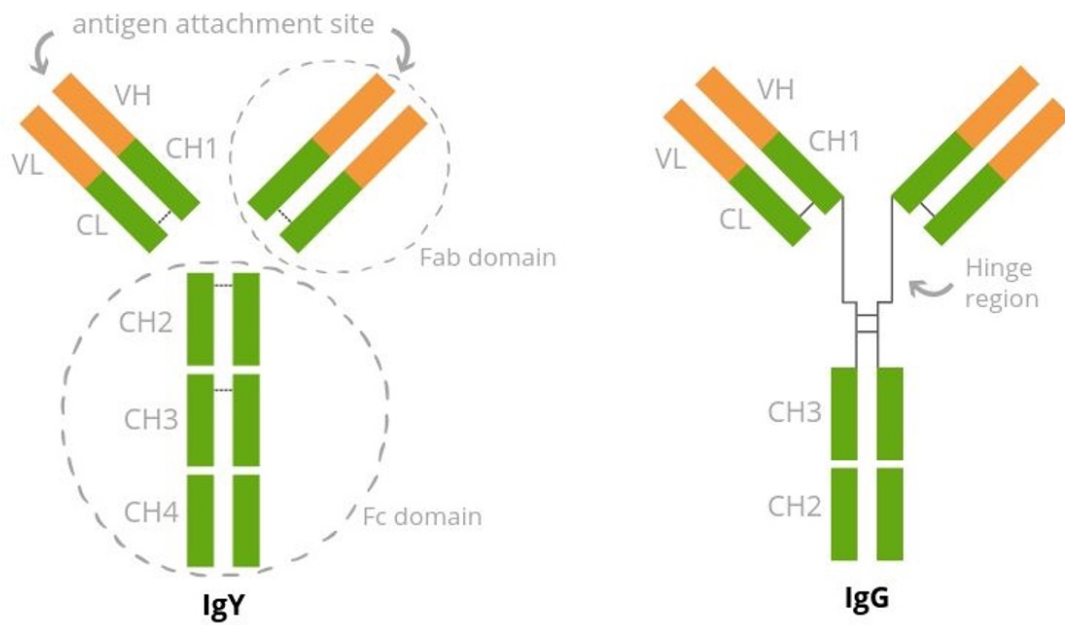


**Figure 1.9. Comparison of the structure of avian IgY to mammalian IgG.** Both have two heavy chains and two light chains, each with a variable domain (VH and VL) and four constant domains (CH1, CH2, CH3, and CH4). IgG has a longer hinge region than avian IgY, which makes it more flexible (Lee et al., 2017; Zhang et al., 2017).

### 1.1.3.2. Foldon-based Multimerisation

The foldon (Fd) sequence generated from native T4 phage fibrin has often been inserted at the C-terminus of protein molecules to assist trimer or oligomer stability, implying that the C-terminal Fd is required for proper trimerization and folding of the protein (Du et al., 2011; Elias et al., 2023). Many reports have shown the usefulness of trimerization domains—such as the foldon of fibrin from bacteriophage T4 and the isoleucine zipper of the GCN4 transcriptional activator from *Saccharomyces cerevisiae*—in the generation of recombinant HA proteins (Bosch et al., 2010; C.-J.



Wei et al., 2008; Weldon et al., 2010). Successful fusion of foldon to the antigenic S protein created a recombinant viral vector vaccine candidate against severe acute respiratory syndrome (SARS)-associated coronavirus (SARS-CoV) (J. Li et al., 2013). This observation suggests that the fusion of Fd with specific avian antigens may potentially enhance immune responses.

## **1.2. CRISPR-based Genome Editing System**

Before the discovery of the RNA-guided endonuclease CRISPR/Cas9, genome editing in animals was carried out utilising mutagenesis using chemicals and UV, nuclease-mediated using zinc-finger nucleases (ZFNs) and transcription activator-like effector nucleases (TALENs), and recombinase-mediated site-specific gene substitution using Cre recombinase (Rocha-Martins et al., 2015). In 2007, CRISPR was first described and defined as an unintended method of protection used by bacteria to suppress viruses (Travis, 2015). In 2012, the mode of action of the Cas9 protein was first demonstrated *in vitro*, demonstrating its capability of cleaving different DNA sequences through small synthetic RNA sections (Gasiunas et al., 2012). Subsequently, *in vivo* experiments started in 2013, wherein multiple laboratories demonstrated rapidly the strength of CRISPR-mediated genome alteration in mammalian cells (Cong et al., 2013; Jinek et al., 2013; Mali et al., 2013).

Through its simplicity and effectivity, the CRISPR/Cas9 technology has paved the way for transforming the world of genome editing and allowed improvements that created possibilities that were difficult or not feasible using previous technologies (Doudna & Charpentier, 2014; Hsu et al., 2014; Mali, Esvelt, et al., 2013; Sander & Joung, 2014).

The CRISPR/Cas9 system provides heritable adaptive immunity to prokaryotes to counter invading foreign genetic elements (i.e., viruses and plasmids) (Barrangou & Marraffini, 2014). The naturally occurring CRISPR system is composed of the following genomic components: (1) trans-activating crRNA (tracrRNA), (2) the Cas operon, (3) a leader sequence, and (4) arrays of short direct repeats (Bayat et al., 2018). In the CRISPR system, these short direct repeats are interspaced by non-repetitive spacer sequences, which are primarily DNA fragments from previous invading viruses or bacteriophages (Bayat et al., 2018). The organism's resistance to foreign invading elements is conferred by the processing of the transcripts from the spacer sequences to generate 20-base-length small RNAs, or CRISPR RNA (crRNA), which facilitate the binding and cutting of the Cas9 endonuclease enzyme at a precise location in the double-stranded DNA of the foreign virus or bacteriophage. This process is followed by the deletion or addition of the DNA fragments to the CRISPR spacer array (Jinek et al., 2012). To be able to introduce a site-specific double-stranded break in the DNA, the Cas9 endonuclease enzyme forms a complex with an RNA duplex, crRNA:tracrRNA. These crRNA-tracrRNA complexes were synthetically engineered as a single guide RNA (sgRNA), retaining its two critical features: a sequence that recognises the DNA target site (crRNA) and a duplex RNA that binds to Cas9 (tracrRNA) (Doudna & Charpentier, 2014). The sgRNA directs Cas9 to a specific genomic region where Cas9 creates a double-stranded break (DSB) (Gasiunas et al., 2012; Jinek et al., 2012), triggering DNA repair through intrinsic cellular mechanisms such as nonhomologous end joining (NHEJ) or homology-directed repair (HDR) (P Rouet et al., 1994; Philippe Rouet et al., 1994; Rudin et al., 1989). The development of simplified components for the CRISPR/Cas9 system allows a precise, cost-

effective, and easy-to-use technology to edit and modify genomic loci for a wide array of applications across multiple disciplines, including virology.

### **1.2.1. CRISPR/Cas9 in Vaccine Development for Poultry**

Several approaches have been applied to edit viral vectors for the construction of recombinant vaccine candidates against viral poultry viruses (Baron et al., 2018). The current available methods for modification of viral vectored vaccines are inefficient, time-consuming, and labour-intensive, especially for purification procedures (Zou et al., 2017). **Table 1.2.** highlights the advantages and disadvantages of the current techniques used for generating recombinant herpesviruses (Y. Liao et al., 2021). Thus, a more efficient and straightforward genome editing technology for constructing viral vectored vaccines is urgently needed. The CRISPR/Cas9 genome editing approach is the best choice, as it not only provides an alternative and simple approach compared to traditional approaches, but it also gives an opportunity to generate multivalent recombinant vaccines that confer simultaneous protection against major avian diseases.

To date, CRISPR/Cas9 have been successfully utilised in targeted mutagenesis of various viral vectors, including the Herpesvirus of Turkey (HVT) (Chang et al., 2019; N. Tang et al., 2018, 2020), the ILTV (Atasoy et al., 2019), and the Duck Enteritis Virus (DEV) (Chang et al., 2018; Zou et al., 2017). These recombinant viral vector genomes were edited to harbour and express specific antigens as potential viral vectored vaccines against multiple diseases such as ND (Atasoy et al., 2019), AI (Chang et al., 2019; Zou et al., 2017), MD (N. Tang et al., 2018, 2020), and ILT (N. Tang et al., 2020). Likewise, the efficacy and stability of these recombinant vaccines have been

demonstrated through multiple passages compared to classical methods, wherein transgene instability might result from the high pressure of multiple passages. So, these studies showed the potential of CRISPR/Ca9 as an effective, fast, and simple tool for the development of avian vaccines.

**Table 1.2.** Advantage and disadvantage of current techniques used for generating recombinant herpesviruses.

	<b>Marker Assisted Site-Directed Mutagenesis</b>	<b>Overlapping Cosmid Clones</b>	<b>Bacterial artificial chromosomes (BACs)</b>
<b>Advantage</b>	1. Site-specific manipulation capabilities	1. Site-specific manipulation capabilities 2. No selection or purification stages required	1. Capable of accommodating large DNA fragments 2. Simple manipulation technique due to bacteria genetics 3. Random and site-specific mutation capabilities 4. Easy to generate revertant BAC
<b>Disadvantage</b>	1. Minimal recombination efficiency 2. Plaque purification 3. The foreign gene may influence the phenotype of the recombinant virus.	1. Difficult to handle large DNA fragments 2. Introduction of unwanted mutations due to multiple recombination events 3. Difficult to construct revertant virus	1. Shearing of large BAC DNA during the manipulation process 2. Unwanted recombination events or random mutations may occur

### **1.2.2. CRISPR/Cas9 Workflow for Vaccine Development**

The application of CRISPR/Cas9 technology in the development of recombinant viral vectors constitutes a very important platform for vaccine design and experimental vaccination approaches across different species. CRISPR/Cas9 provides an alternative method to conventional approaches that is fast, efficient, and straightforward and has been applied for genetic modification in animal models (Ma et al., 2014) and genomic manipulation of several DNA viruses such as herpes simplex virus type I, adenovirus, pseudorabies virus, vaccinia virus, Epstein-Barr virus, guinea pig cytomegalovirus, herpesvirus of turkey, and duck enteritis virus (Atasoy et al., 2019; Bi et al., 2014; Bierle et al., 2016; Chang et al., 2018; Peng et al., 2016; Suenaga et al., 2014; Y. D. Tang et al., 2016; A. Xu et al., 2015; M. Yuan et al., 2015; Zou et al., 2017).

Understanding the components of CRISPR/Cas9 technology in viral vector vaccine development is essential for the success of recombinant vaccine production (**Figure 1.10**).

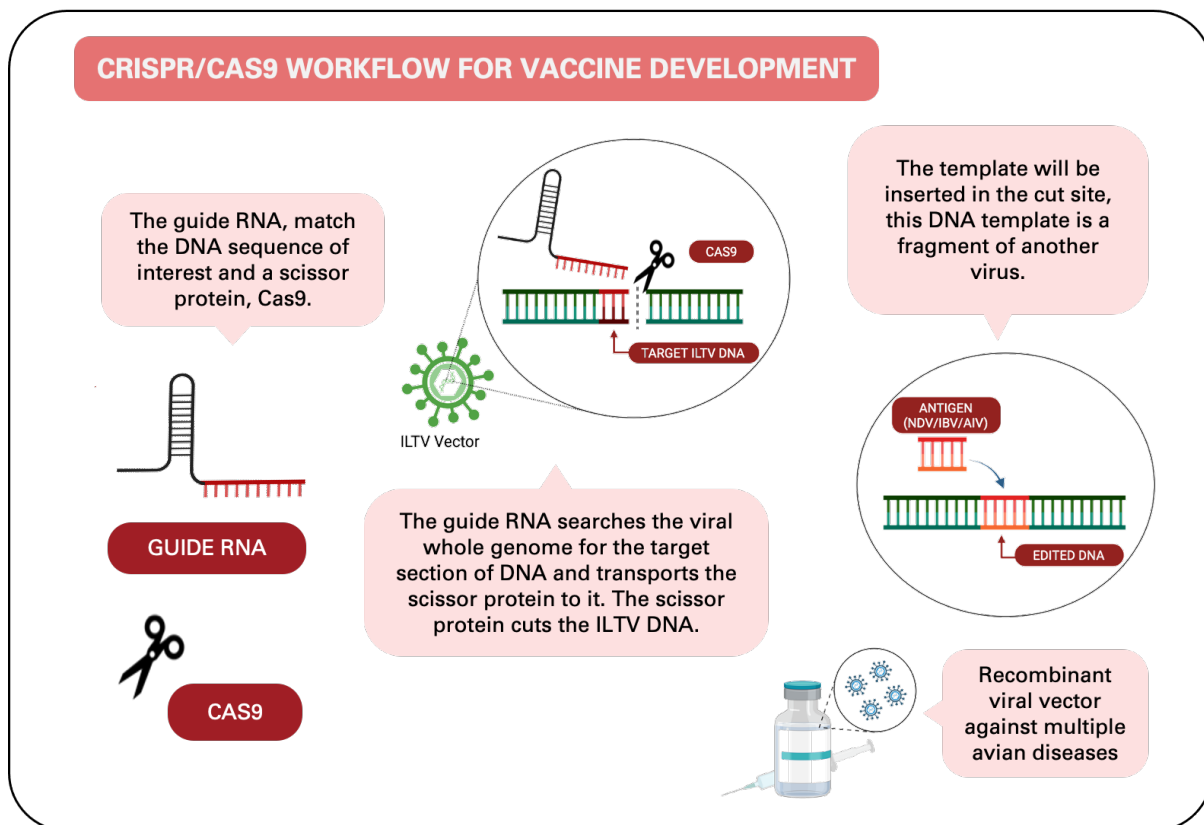


**Figure 1.10. Illustrative representation of the CRISPR/Cas9 workflow for vaccine development.** The workflow starts with the assembly of fundamental components, including the guide RNA and Cas9, which is a protein with scissor-like activity. The guide RNA will initiate a search within the viral genome for the specific target DNA sequence. Subsequently, it will facilitate the transport of the Cas9 protein to the targeted area. This process ultimately leads to the introduction of incisions inside the genome of the virus, namely the ILTV. Following this, the exogenous gene is introduced into the cleavage site, therefore generating a recombinant virus harbouring a segment of a foreign gene (antigen). The present approach also possesses the capability to introduce several exogenous genes into the genetic material of the viral vector, therefore generating a recombinant viral vector that can effectively combat various avian diseases.

**1.2.2.1. Selection of Viral Vector and Target Insertion Site.** Recombinant viral vectors are a very powerful tool for developing vaccines and addressing experimental vaccination. Generally, viruses can be used as vectors to express foreign genes. The most widely used DNA viruses for the delivery of vaccine antigens are Poxvirus (from both orthopoxvirus and parapoxvirus genus), Herpesvirus, Adenovirus, and Baculovirus (Marín-López & Ortego, 2016). For RNA viruses, several viruses from different families have been used: Alphavirus, Bunyavirus, Coronavirus, Flavivirus, Paramyxovirus, Retroviruses, and Rhabdovirus (Brun et al., 2008). The introduction of reverse genetics technologies enables us to rescue the infectious virus from a copy of its genome. The key benefit of DNA viruses rather than RNA viruses is their DNA genomic stability, multiple insertion sites, and the availability of BAC-DNA clones for engineering and rescuing recombinant viruses in the laboratory. Generally, the ideal viral vector should be: (1) safe and enable efficient antigen expression; (2) exhibit low intrinsic immunogenicity to allow for re-administration and booster vaccination; and (3) meet criteria that enable production on a large-scale basis (Haut et al., 2005). The use of CRISPR/Cas9 in generating viral vectors has been widely implemented in viral vectors such as adenovirus, herpesvirus, and poxvirus (Marín-López & Ortego, 2016; Vilela et al., 2020).

**1.2.2.2. Choosing a Target Insertion Site.** Advances in next-generation sequencing platforms have enabled the sequencing of a species entire genome and that of a virus's genome. The National Centre for Biotechnology Information (NCBI) dedicated a web-based portal for the

collection of virus sequences and datasets (Hatcher et al., 2017). The primary consideration in choosing a target region for CRISPR/Cas9 knock-in is maintaining the ability of virus vector replication (Yajima et al., 2018); thus, potential transgene insertion sites must be well characterised and verified to have a minimal effect on viral function (Vilela et al., 2020).

**1.2.2.3. Choosing Viral Antigens.** It is important to understand the mechanisms of viral infection and pathogenicity. Many of the points relating to the inserted vaccine antigen have already been described, while an essential consideration is whether a single antigen can produce sufficient protective immunity or whether multiple antigens are required (Matunis, 2016; Vilela et al., 2020).

**1.2.2.4. Selection of Host Cell Lines.** Cultured cell lines are excellent hosts for the propagation of many types of viruses. Since viruses are obligate intracellular parasites, they depend on hosts for survival. For the use of CRISPR technology, the viral vector needs to be grown in a living host to support viral replication in order to target its genome. Established animal cells, such as Vero, MDCK, or chicken embryo fibroblasts (CEFs), are still the main cell lines used for viral vaccine production (Genzel, 2015). On the other hand, the immortalised avian cell line Leghorn male hepatoma (LMH) has been widely used for the propagation of avian infectious viruses, including avian influenza, avian infectious bronchitis virus, Marek's disease virus serotype 1 (MDV-1), avian metapneumovirus (AMPV), and ILTV (Schnitzlein et al., 1994).



#### 1.2.2.5. Construction of sgRNAs, Donor Plasmids, and Cas9/gRNA Expression

**Plasmids.** Using CRISPR/Cas9 technology in the development of recombinant viral vectors requires understanding the following: (1) *in silico* design for the gRNA to target the viral genome; (2) construction of the Cas9/sgRNA expression plasmid; and (3) construction of the donor plasmid carrying the antigen and selectable markers. The specificity of the Cas9 endonuclease is dependent on a 20-nt sequence of the single guide RNA (sgRNA). **Figure 1.11.** provides an overview of the steps in the design of sgRNA and the construction of CRISPR/Cas and donor plasmids. For designing the sgRNA, the primary considerations are the 5'-NGG PAM for Cas9 recognition and the off-target activity. Various web-based and local software has been developed to locate potential PAM and target sequences and rank the associated gRNAs based on predicted off-target activity as shown in **Table 1.3.** It is also important to validate the off-target activity of sgRNA in the host cell genome (i.e., chicken) (Doudna & Charpentier, 2014; Labun et al., 2016; Vilela et al., 2020).

Cas9 enzyme and gRNA need to be expressed in the cells for the efficient CRISPR/Cas9 genome editing. Various plasmid expression systems are available to use CRISPR in mammalian cells. To select the plasmid expression system, some precautions should be considered, such as promoter species, expression of promoter for Cas enzyme and gRNA, selectable marker (drug or fluorophore), and delivery method. Addgene (<https://www.addgene.org/crispr/>) provides a wide array of CRISPR plasmids and resources (Ran et al., 2013) (**Figure 1.12**).

Meanwhile, it is essential to have a donor plasmid that carries the antigen gene and selectable marker cassettes for efficient CRISPR/Cas9 technology to develop a recombinant viral vaccine vector. This will allow homology-independent targeted integrations directed to a single cut site by providing donor DNA that is independently targeted for cutting (Pickar-Oliver & Gersbach, 2019). Donor plasmids are constructed following traditional cloning techniques; specific fragments such as promoters, terminators, selectable markers, and antigens are either PCR-amplified or synthetically generated. These fragments are then incorporated into a plasmid backbone through a digestion-ligation reaction (Doudna & Charpentier, 2014; Pickar-Oliver & Gersbach, 2019; Vilela et al., 2020).

**Table 1.3.** List of existing free online tools and open-source local software for sgRNA design.

Name	Graphical user interface	Searches whole genome for targets	Input	Output	Predicts gRNA activity	Ranked list	Reference
CHOPCHOP	Yes	Yes	Target transcript ID or sequence (raw or chromosomal position); also allows gene input	Candidate guide sequences and off-target loci	No	Yes	(Montague et al., 2014)
CHOPCHOP v2	Yes	Yes (over 200)	Target transcript ID or sequence (raw or chromosomal position); also allows gene input	Candidate guide sequences and off-target loci	Yes	Yes	(Labun et al., 2016)
Cas-OFFFinder	Yes	Yes (over 400)	Guide sequence	Off-target loci for guide sequences	No	No	(Bae et al., 2014)
CasOT	No (Perl script)	User input	Guide sequence	Off-target loci and additional guide sequences	No	No	(Xiao et al., 2014)
Benchling	Yes	Yes	DNA sequence or gene name	Candidate guide sequences and off-target loci	No	Yes	<a href="https://www.benchling.com">https://www.benchling.com</a>
CRISPOR	Yes	Yes (over 200 genomes)	DNA sequence	Candidate guide sequences and off-target loci	Yes	Yes	(Haeussler et al., 2016)

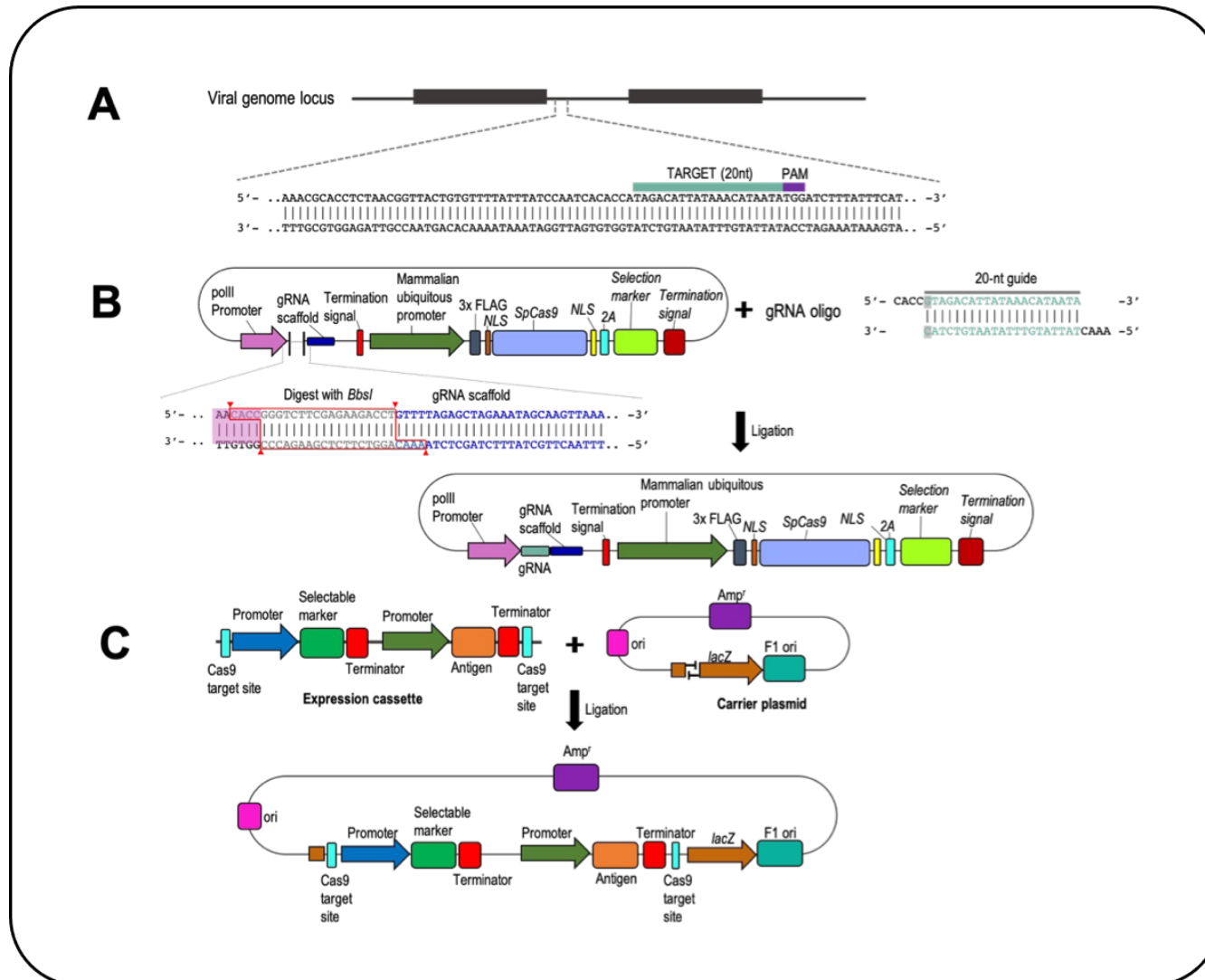


**Figure 1.11. Overview of steps in the construction of CRISPR/Cas9 and donor plasmids. (A)** Sequences of the specific target region in the ILTV genome were used to design the sgRNAs through the online platform CHOPCHOP. The 20-nucleotides viral genome target (highlighted in teal) is followed by the PAM recognition site (highlighted in purple), 5'-NGG. **(B)** Schematic of the construction and assembly of the Cas9/gRNA expression plasmid. Digestion of the plasmid containing Cas9 and gRNA scaffold with *BbsI* allows the insertion of the annealed gRNA oligos (teal) through replacing the type II restriction site (outlined in red). **(C)** Schematic of the construction of the donor plasmid harbouring the antigen and selectable marker. The T overhangs on the carrier plasmid are complementary to the overhangs in the expression cassette to facilitate ligation (Vilela et al., 2020).

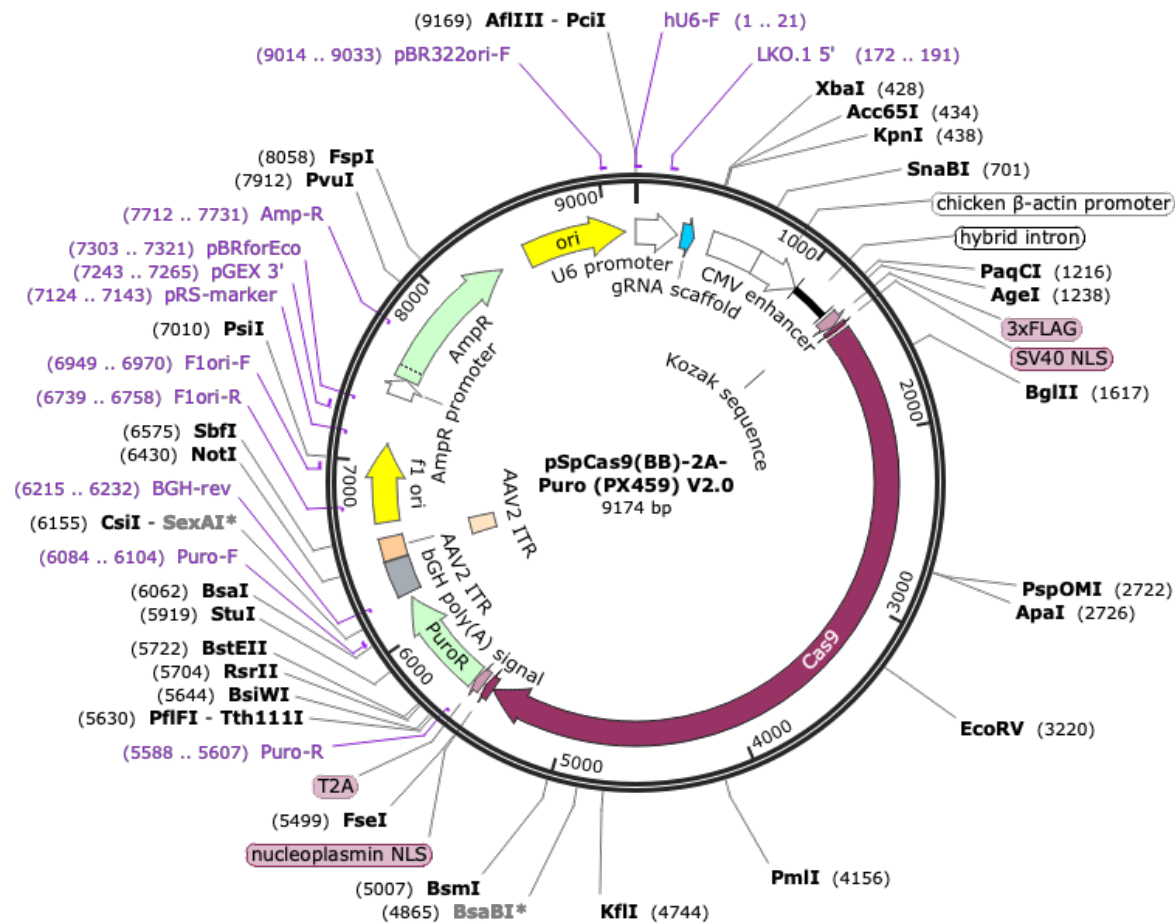


**Figure 1.12. Illustrative representation of the Cas9 plasmid.** Cas9 from *S. pyogenes* with 2A-Puro, and cloning backbone for sgRNA (Addgene, Plasmid #62988). The plasmid map shows the important features of pX459v2 including Cas9 sequence, specific restriction enzyme sites, promoters, primers, gRNA scaffold, FLAG TAG, and selectable markers. The guide sequence is cloned into this plasmid using *BbsI* sites. The hU6-F primer (5'-GAGGGCCTATTTCCCATGATT-3') can be used to confirm the gRNA sequence after cloning into the plasmid. Plasmid map created using SnapGene.

### 1.3. Project Aims

This project aims to develop a recombinant herpesvirus-based viral vector using the CRISPR/Cas9 genome editing technology.

Specifically:

1. *In silico*-based profiling of the existing field strains of NDV, IBV, and AIV in the Philippines.
2. Comprehensive characterisation of the herpesvirus-based viral vector (ILTV) and proof-of-concept validation of the suitability of CRISPR/Cas9 genome editing technology through knock-in and knockout experiments.
3. Demonstrate the effectiveness of CRISPR/Cas9 genome editing technology to create a herpesvirus-based viral vector carrying foreign genes fused with adjuvants.
4. Demonstrate the effectiveness of CRISPR/Cas9 genome editing technology to create a herpesvirus-based multivalent viral vector.
5. Demonstrate the effectiveness and flexibility of the CRISPR/Cas9 gene editing system in combination with a herpesvirus-based viral vector for the development of candidate vaccines against various poultry diseases that hold significant economic importance.

# CHAPTER 2

## Materials and Methods

### 2.1. Materials

All chemicals, enzymes, solutions, and buffers used in this study are listed in **Table 2.1** unless otherwise stated.

**Table 2.1.** List of chemicals, enzymes, and solutions used in this study.

<b>Chemicals</b>		
<b>Chemical</b>	<b>Catalogue number</b>	<b>Manufacturer</b>
Acetic acid	A6283	Sigma-Aldrich, St. Louis, USA
Acrylamide/Bis Solution (30%)	1610158	Bio-Rad, China
Ammonium persulfate (APS)	1610700	Bio-Rad, Japan
Antibiotic-Antimycotic (100X)	15240062	Gibco, Life Technologies, UK
BSA (Albumin Bovine Fraction V)	05482	Sigma-Aldrich, St. Louis, USA
Calcium chloride dihydrate	C7982	Sigma-Aldrich, St. Louis, USA
Chloroform	C14960115	Fisher Scientific, UK
Coomassie Brilliant Blue G250	27815	Fluka, Switzerland

D (+) Sucrose	62248	Sigma-Aldrich, St. Louis, USA
DAPI	62247	Thermo Scientific, USA
EDTA	324503	Millipore, USA
Ethanol	2107463	Fisher Scientific, UK
Glycerol	G5516	Sigma-Aldrich, St. Louis, USA
Glycine	G8898	Sigma-Aldrich, St. Louis, USA
HEPES buffer	15630080	Gibco, life technologies, UK
Hexadimethrine bromide (polybrene)	H9265	Sigma-Aldrich, St. Louis, USA
L-glutamine (200mM)	25030-081	Gibco, life technologies, UK
Magnesium chloride	M8266	Sigma-Aldrich, St. Louis, USA
MEM (10X)	21430-020	Gibco, life technologies, UK
Methanol	2196137	Fisher Scientific, UK
Methylene blue	M9140	Sigma-Aldrich, St. Louis, USA
NP40-50ml	85124	Thermo Scientific, USA
Nuclease free water	10977-035	Thermo Scientific, USA
NuPAGE (transfer buffer)	2270643	Novex, Life Technologies, USA
Permeabilization buffer (10X)	00833356	Thermo Scientific, USA
Pierce Protease inhibitor tablet	A32963	Thermo Scientific, USA
Potassium chloride	P5405	Sigma-Aldrich, St. Louis, USA
Potassium phosphate dibasic	P0662	Sigma-Aldrich, St. Louis, USA



Potassium phosphate monobasic	P5655	Sigma-Aldrich, St. Louis, USA
Puromycin Dihydrochloride	A1113803	Gibco, China
SDS-sample buffer	1597380	Life Technologies, USA
SDS-solution 10%	1610416	Bio-Rad, USA
Skimmed milk powder	70166	Millipore, Switzerland
Sodium bicarbonate	S5761	Sigma-Aldrich, St. Louis, USA
Sodium chloride	S5886	Sigma-Aldrich, St. Louis, USA
Sodium dodecyl sulphate (SDS)	L3771	Sigma-Aldrich, St. Louis, USA
Sodium hydroxide	221465	Sigma-Aldrich, St. Louis, USA
Sodium phosphate dibasic	S5136	Sigma-Aldrich, St. Louis, USA
TEMED	1610801	Bio-Rad, USA
TPCK-treated trypsin	T1426	Sigma-Aldrich, St. Louis, USA
Tris-base	252859	Sigma-Aldrich, St. Louis, USA
Tris-EDTA 1X	BP2473	Fisher scientific, USA
Triton X-100	T8787	Sigma-Aldrich, St. Louis, USA
Trizma hydrochloride	RDD009	Sigma-Aldrich, St. Louis, USA
Tween -20	P2287	Sigma-Aldrich, St. Louis, USA
VECTASHIELD antifade mounting buffer	ZH1108	Vector Laboratories, USA
Versene 1:5000 (1X)	15040-033	Gibco, Thermo Fisher, UK
$\beta$ -mercaptoethanol	1610710	Bio-Rad, China

## Enzymes

<b>Enzyme/marker</b>	<b>Catalogue number</b>	<b>Manufacturer</b>
<i>BbsI</i> -HF	R3539S	New England Biolabs, UK
<i>EcoRI</i> -HF	R3101S	New England Biolabs, UK
<i>KpnI</i> -HF	R3142S	New England Biolabs, UK
<i>NheI</i> -HF	R3131S	New England Biolabs, UK
<i>HindIII</i> -HF	R3104S	New England Biolabs, UK
<i>MheI</i> -HF	R3589S	New England Biolabs, UK
<i>ClaI</i>	R0197S	New England Biolabs, UK
<i>XbaI</i>	R0145S	New England Biolabs, UK
<i>BsmBI</i>	R0739S	New England Biolabs, UK
GeneRuler 1 kb DNA Ladder	SM0311	Thermo Scientific, UK
Prestained Protein Ladder (10-180 kDa)	ab116027	Abcam, UK
Q5-high fidelity DNA polymerase	M0491S	New England Biolabs, UK
OneTaq 2X Master Mix	M0482	New England Biolabs, UK
T4 DNA ligase	M0202	New England Biolabs, UK

### **Solutions/Buffer**

<b>Name</b>	<b>Purpose</b>	<b>Composition</b>
Blocking buffer	IFA blocking	5% BSA in PBS
Blocking buffer	WB	5% skimmed milk powder in PBST

Fixative	Cell fixation	4% paraformaldehyde (PFA) in PBS
Lysis buffer	WB/IP	10%NP-40, 1mM EDTA, 150mM NaCl, 20mM Tris-HCl (pH.7.4)
PBS	Washing and dilution	0.8% (w/v) NaCl, 0.02% (w/v) KCl, 0.02% (w/v) KH <sub>2</sub> PO <sub>4</sub> , 0.135% (w/v), Na <sub>2</sub> HPO <sub>4</sub> ·2H <sub>2</sub> O
PBST	WB washing buffer	0.1% tween-20 in PBS
Permeabilization buffer	Permeabilization for IFA	0.1% Triton X100 in H <sub>2</sub> O
Overlay media	Plaque assay	6 g carboxymethylcellulose, 200 mL distilled water, 500 mL MEM (2×), 40 mL FBS, 10 mL 200 mM l-glutamine, 10 mL 100× nonessential amino acids, 7.5 mL 100× sodium bicarbonate
TAE (10x)	Gel electrophoresis	48.4 g of Tris base, 11.4 mL of glacial acetic acid (17.4 M), 3.7 g of EDTA, di-sodium salt in distilled water
Crystal violet, 1% (w/v)	Plaque assay	1 g crystal violet, 20 ml absolute ethanol, 80 mL distilled water

---

## **2.2. Methods**

### **2.2.1. Cell Culture Techniques**

#### **2.2.1.1. Cell Types and Culture Medium**

There are two types of cell lines used in this study, including a primary hepatocellular carcinoma epithelial cell line (LMH) and a continuous cell line of chicken embryo fibroblasts (DF-1).

- (1) LMH cell line: Tomoyuki Kitagawa established LMH in 1981 as a primary hepatocellular carcinoma epithelial cell line at the Cancer Institute in Kami-Ikebukuro, Toshima-ku, Tokyo, Japan (Kawaguchi et al., 1987). In this study, LHM cells were used for the propagation of the wild-type and recombinant ILTV.
- (2) DF-1 cell line: primary chicken embryonic fibroblasts were dissociated and grown in culture; the fibroblasts were passaged until they began to senesce; the cells were concentrated during cell senescence to maintain about 30% to about 60% culture confluence. The cells are useful as substrates for virus propagation, recombinant protein expression, and recombinant virus production. In this study, DF-1 cells were used for expression analysis of different proteins.

There were three types of cell culture media used in this study, including complete medium, serum-free medium (SFM), and freezing medium. LMH and DF1 cells were cultured in complete medium. All cells were cultured at 37 °C in a humidified and sterile atmosphere of 5% CO<sub>2</sub>. All media were pre-warmed in a 37 °C water bath, unless otherwise stated.

- (1) Complete medium (culture medium): Dulbecco's Modified Eagle Medium (DMEM, GlutaMAx, and sodium pyruvate, Life Technologies, Cat no. 31966-

021) supplemented with 10% Fetal bovine serum (FBS, Cat no. 12657029, Gibco™), 100 U/mL Penicillin, and 100 µg/mL Streptomycin (10% pen/strep, stabilised solution, P4333, Life Technologies).

(2) Serum-free medium (SFM): D-MEM-only medium, used for transfection.

(3) Freezing medium: 90% FBS plus 10% DMSO (Dimethyl sulfoxide, Cat no. 175462, Fisher Scientific).

#### **2.2.1.2. Cell Subculture**

All adherent cells were grown in cell culture standard vessels (e.g., flasks, petri dishes, or multi-well plates) with appropriate culture medium. When the cell confluence reached 80-90% of the surface area, the cells were subcultured. Cells were washed twice with phosphate buffered saline (PBS, pH = 7.2), followed by dissociation from the surfaces of culture vessels using trypsin 2.5% (Cat no. 15090-046, Gibco, Thermo Fisher Scientific). Once the cells were detached, the trypsin was inactivated by adding at least a double volume of fresh culture medium. The mixture was then transferred into a 15-mL falcon tube, centrifuged at 300 x g for 5 minutes at room temperature, and the supernatant was removed. The cells were then passaged by gently re-suspending the pellet in fresh culture medium before seeding in the new culture vessel. All cells were grown in a 37 °C and 5% CO<sub>2</sub> incubator and were regularly inspected under a microscope to examine health status and contamination.

#### **2.2.1.3. Cell Cryopreservation and Recovery**

To freeze cells, 10<sup>6</sup> cells were harvested, re-suspended in 1.5 mL freezing medium, and transferred to 1.5-mL cryo-tube vials. The tubes were placed at -80 °C for storage. To recover cells, frozen cells were rapidly transferred to a 37 °C water bath. The

thawed cells were diluted with culture medium, followed by centrifugation in a 15-mL centrifuge tube at 200 x g for 5 min. The supernatant was aspirated, and the cell pellet was gently re-suspended in fresh culture medium before being transferred to a culture vessel.

#### **2.2.1.4. Transfection**

##### **2.2.1.4.1. ViaFect™ Transfection**

ViaFect™ transfection reagent (Cat no. E4981, Promega) was used to transfect donor and/or sgRNA plasmids into the LMH cells. LMH cells were washed, dissociated, and inoculated with  $5 \times 10^5$  cells in 6-well plates prior to transfection. On the day of transfection, at approximately 80% confluence, cells were washed, the wells were filled with culture medium, and they were prepared for transfection. Briefly, 3  $\mu$ l of ViaFect™ transfection reagent was diluted with 100  $\mu$ l of Opti-MEM Medium (Cat no. 31985062, Thermo Fisher Scientific), 1  $\mu$ g of plasmid was added, and tubes were incubated at room temperature for 20 min. The plasmid-lipid complex was evenly dropwise on the cells and incubated at 37 °C and 5 % CO<sub>2</sub> for 36 h.

In all transfection experiments, appropriate negative and positive controls were included, where the same number of cells were transfected with PBS and a 1  $\mu$ g empty vector, respectively. Successful transfection was assessed by the expression of GFP. Fluorescence-expressing cells were visualised using a Zoe™ Fluorescent Cell Imager (Cat no. 1450031EDU, Biorad) at 24- and 48-hours post-transfection (h.p.t.).

## **2.2.2. Microbiology Techniques**

### **2.2.2.1. Cloning Techniques using *E. coli***

#### **2.2.2.1.1. Agar Plate Preparation**

Ampicillin (Cat no. A9518, Sigma-Aldrich) was diluted to 50 mg/mL in nuclease-free water (NFW). Luria broth (LB) (Cat no. 12780, Invitrogen) liquid medium and agar (Cat no. 22700, Invitrogen) were prepared and sterilized. The final concentration of antibiotic-containing medium or agar used was 100 µg/mL. The melted antibiotic-containing LB agar was evenly distributed on 100-mm Petri dishes (Sarstedt), which were then stored at 4 °C for up to two weeks.

#### **2.2.2.1.2. Transformation**

DH5a *E. coli* competent cells (prepared in-house) were used in transformation experiments. They were kept at -80 °C before thawing on ice for transformation. 1-10 ng of DNA (2 µl) was added to a vial of competent cells (50 µl). The reaction was mixed gently and incubated on ice for 30 minutes. The tube had a heat shock at 42 °C for 30 seconds and was then incubated over ice for another 2 minutes.

#### **2.2.2.1.3. Cell Plating and Colony Picking**

Each transformation reaction was spread onto antibiotic-containing LB agar plates. The plates were incubated overnight at 37 °C. The following day, a number of discrete colonies were picked up by a sterile tip and dipped into a colony PCR reaction for amplifications or stored in an antibiotic-containing LB liquid at 4 °C. Positive colonies were propagated through overnight incubation (with shaking) at 37 °C for plasmid isolation.

### **2.2.3. Virology Techniques**

#### **2.2.3.1. Viral Strain and Culture Medium**

A lab-adapted attenuated ILTV virus was generated using the CRISPR/Cas9 approach, generally using the procedures described previously (Atasoy et al., 2019). There were two viral culture mediums used in this study. Overlay medium: culture medium containing 3% (w/v) Carboxymethylcellulose (Cat no. C4888-500G, Sigma-Aldrich), and this was used for the plaque assay. Viral infection medium: culture medium without serum and antibiotics.

#### **2.2.3.2. Viral Infection**

Cells were seeded on 6-well plates and cultured to achieve 80-90% confluence. Prior to viral infection, cells were transfected with the necessary donor plasmids and CRISPR-sgRNA plasmids. At 36 hours post-transfection, the culture medium was removed from the cells. Cells were then rinsed with PBS. Viral stock was quickly thawed at 37 °C and diluted in an appropriate volume of viral infection medium. The diluted virus was then inoculated in cells to provide a desirable multiplicity of infection (M.O.I.), followed by incubation at 37 °C for three hours with shaking every 20 min. Note that a negative control was included; one was not inoculated with the virus.

For a single-cycle infection, any non-internalised and inactivated absorbed virus was removed from cells by aspirating the inoculum. The cells were then overlaid with overlay medium. The protein expression and localisation were characterised by western blot and immunofluorescence (IF) analysis, respectively. For a multiple-cycle infection, cells were overlaid with culture medium directly and cultured at 37 °C. The



supernatant was harvested at the desired time points post-infection. The samples were stored at -80 °C for plaque assay.

### **2.2.3.3. Plaque Assay**

The plaque assay for wild-type ILTV and recombinant ILTV viruses was performed using LMH cells. Briefly, for each virus to be titrated, 2-mL microcentrifuge tubes were labelled as follows: Neg,  $10^{-1}$ ,  $10^{-2}$ ,  $10^{-3}$ ,  $10^{-4}$ ,  $10^{-5}$ , and  $10^{-6}$ . A total of 900  $\mu$ l of viral infection medium was added to each tube. Specimens were serially diluted 10-fold by transferring 100  $\mu$ l of each specimen to the appropriate tube labelled  $10^{-2}$ , vortexing, and then transferring 100  $\mu$ l to the subsequent tube, down to  $10^{-6}$ . Incubate at 37 °C for 3 h, with an agitation every 20 min. After 3 h, the cell monolayers were overlaid with 4 mL of overlay medium, supplemented with 3% (w/v) CMC. Cells were then maintained in a 37 °C incubator for 72 h.

For fixing and staining, the overlay medium was aspirated, and cells were incubated with 1 mL of 4% (v/v) paraformaldehyde (Cat no. J19943-k2, Thermo Scientific) at room temperature for 1 h. Fixatives were aspirated from wells and discarded into a waste bottle. Then, 1 mL of 0.5% crystal violet (Cat no. C581-25, Thermo Fisher Scientific) was added to each well and incubated at room temperature for 5-15 minutes. Then, cells were washed 2-4 times with distilled water and blot dried. The viral titre was determined according to the number of plaque-forming units (PFU) per mL:

$$\text{PFU/mL} = \text{Number of plaques} / (\text{dilution factor} \times \text{volume of diluted virus})$$

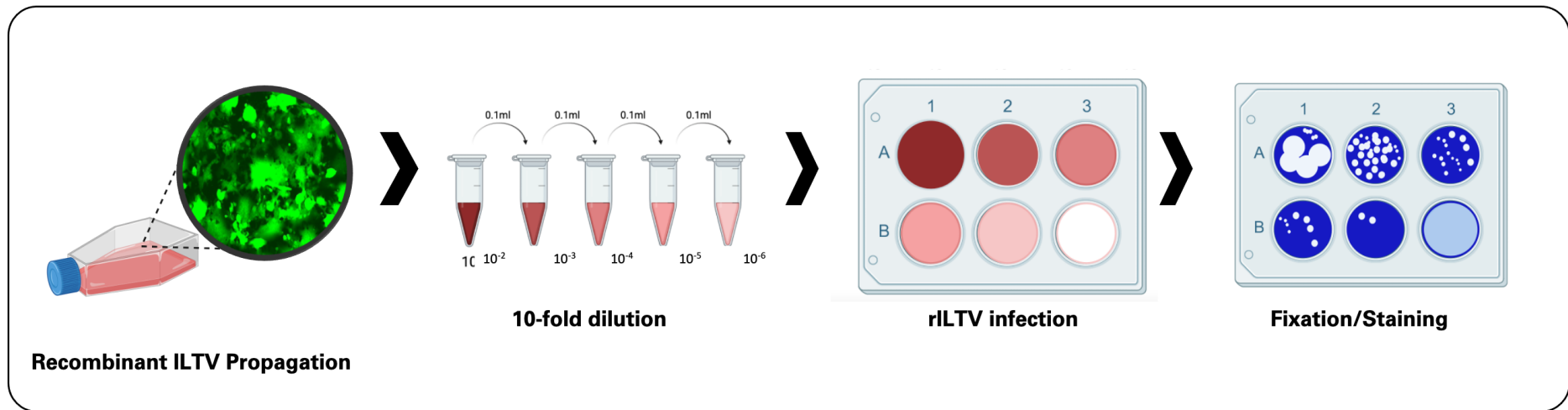


**Figure 2.1. Plaque Assay.** Illustration of the important steps in a plaque assay. Recombinant ILTVs are first propagated in LMH cells. At 36 hours post-infection, supernatant was harvested and used to perform a 10-fold dilution. Subsequent infection of the diluted recombinant and wild-type ILTVs was performed; overlay medium was added after 3 hours of infection, and at 36 hours post-infection, cells were fixed, stained with crystal violet, and washed. Plaques appeared as clear circles on a blue monolayer of cells. The negative control has a uniform monolayer, which was used as a reference. The number of plaques observed per well at each virus dilution was recorded.

#### **2.2.3.4. Immunofluorescence**

##### **2.2.3.4.1. Immunofluorescent Assay**

Following the single-cycle infection, cells on the coverslips were washed gently and fixed using PBS / 4% (v/v) paraformaldehyde for 45 min. The negative control was the one not inoculated with the virus. After fixation, samples were washed in PBS and permeabilized in 200  $\mu$ l PBS / 0.1% (v/v) Triton X-100 (Cat no. T8787, Sigma-Aldrich) for 10 min. Followed by three washes with PBS, each sample was blocked in 200  $\mu$ l of PBS / 5% BSA (Cat no. 05482, Sigma-Aldrich) for 60 min. For the primary antibody incubation, each well was incubated with 200  $\mu$ l of primary antibody containing PBS / 5% BSA (Anti-FLAG antibody, 1:2000 dilution, Cat no. F7425, Sigma-Aldrich) for 1 h at room temperature or overnight in a cold room. Cells were then washed with PBS three times. For the secondary antibody incubation, cells were then incubated for 2 h with 200  $\mu$ l secondary antibody containing PBS / 5% BSA (Goat Anti-Rabbit IgG H&L Alexa Fluor® 488, 1:3000 dilution, Cat no. A11008), washed three times with PBS, and then added with 200  $\mu$ l DAPI (1:10,000 dilution, Invitrogen). Coverslips were mounted on a microscope slide with VECTASHIELD Antifade reagent (Cat no. ZH1108, Vector Laboratories). All the mounted slides were covered with foil and kept overnight at 4 °C. On the second day, the fluorescent cells were visualised on an upright Zeiss LSM800 confocal microscope. The image size was set at 1024  $\times$  1024 pixels. To eliminate inter-channel cross talk, multitrack sequential acquisition settings were used. A 568 nm diode-pumped solid-state laser and an argon ion laser's 488 nm line were used for excitation. Zeiss Zen control software, which provides numerous viewing features for the observation and creation of high-quality confocal images, was used to establish optimized emission detection bandwidths.

#### **2.2.3.4.2. Flow Cytometry Analysis**

A flow cytometer was used to determine the number of labelled virus-infected cells (infected or transduced). After 24 hours of infection, cells were trypsinised according to Section 2.2.1.2, pelleted, and washed once with PBS. The cells were centrifuged again at 1000 x g for 5 min. The pellet was resuspended in a live/dead marker according to the manufacturer's protocol for 30 minutes. The cells were washed and then fixed with 4% paraformaldehyde for 30 min. Then, the cells were washed and resuspended in 1x permeabilization buffer for 15 min. Cells were washed and resuspended in 0.25% BSA for 30 min. The cells were washed and resuspended in 1x PBS before being analysed by flow cytometry. Live and singlet cells were gated based on forward and side scatters. Analysis was carried out using FlowJo V10.8 software, applying the same gating and analysis for all samples.

## **2.2.4. Molecular Biology Techniques**

### **2.2.4.1. DNA Techniques**

Please note that in this section, all procedures were performed at room temperature unless otherwise stated.

#### **2.2.4.1.1. Plasmid DNA Extraction**

##### **2.2.4.1.1.1. Medium-scale Plasmid DNA (midi-prep)**

Small-scale plasmid DNA extraction was performed using the Qiagen® Plasmid Plus Midi Kit (Cat no. 12943, QIAGEN Group) according to the high-yield protocol. Briefly, the overnight bacteria culture was pelleted at 6,000 x g for 10 min, and the supernatant was removed. Pellets were re-suspended in 4 mL of RNase A (100 µg/mL) containing Buffer P1. 4 mL of lysis buffer (P2) was added to the cell pellet, and the tube was gently inverted five times until the solution colour was uniformly blue. The lysis reaction was then incubated for 5 minutes, before adding 4 mL of chilled Precipitation buffer (P3) to neutralise the reaction. The tube was then inverted gently until the solution became homogenous, followed by 15 minutes of incubation on ice and then centrifugation at 20,000 x g for 30 min at 4 °C to separate the cell debris. Centrifuge the supernatant again at 20,000 x g for 15 min at 4 °C to remove residual suspended or particulate material that can clog the QIAGEN-tip. Equilibrate a QIAGEN-tip 100 by applying 4 mL buffer QBT and allowing the column to empty by gravity flow. To bind the plasmid DNA on the QIAGEN column, the supernatant was allowed to enter the resin by gravity flow. The bound DNA was washed two times with wash buffer (QC) and centrifuged again at 12,000 x g for 1 min. The DNA was eluted by adding 5 mL of Buffer QF, followed by DNA precipitation by adding 3.5 mL (0.7 volumes) of room-temperature isopropanol to the eluted DNA. The DNA pellet was washed with 2 mL of

room-temperature 70% ethanol, followed by centrifugation at 15,000 x g for 10 min. The air-dried DNA pellet was resuspended with 100 µl of nuclease-free water.

The concentration of plasmid DNA was quantified using a Nanodrop spectrophotometer (NanoDrop™ 1000, Thermo Scientific). Plasmid DNA was stored at -20°C for downstream experiments.

#### **2.2.4.1.2. Genomic DNA Extraction**

Small-scale genomic DNA extraction was performed using the DNeasy Blood and Tissue Kit (Cat no. 69504, Qiagen Group) according to the standard protocol. Briefly, cell pellets harvested from  $1.2 \times 10^6$  cells cultured cells were disrupted in 200 µl PBS, which contained 20 µl proteinase K. 200 µl of Buffer AL was gently added to the reaction, and the reaction was incubated for 10 minutes in a 56 °C water bath. 200 µl of absolute ethanol was then added to the sample and mixed by pipetting. The mixture was transferred into a DNeasy Minispin column, and the flow-through liquid was discarded after the centrifugation at 6,000 x g for 1 min. The column was inserted into a new collection tube, and 500 µl of Buffer AW1 was added, followed by centrifugation and the removal of the flow-through liquid. Next, Buffer AW2 was added to the tube, followed by another centrifugation and a flow-through step. Finally, the column harbouring the genomic DNA of interest on the membrane was inserted into a clean 1.5-mL Eppendorf tube, and 100 µl of elution buffer AE was carefully added to the membrane of the column. The tube was then incubated for 1 minute and centrifuged at 12,000 x g for 1 minute. A second elution was highly recommended to improve yields. The DNA can be directly used for the PCR procedure.

#### **2.2.4.2. DNA Amplification**

PCR primers were designed using the online tools Primer 3 Input (<http://primer3.ut.ee/>) and NCBI Blast (<https://blast.ncbi.nlm.nih.gov/Blast.cgi>), unless otherwise stated. With some design criteria of primers for PCR, the general suggestion of GC content ranged from 40 to 60%; annealing temperature was identified by a gradient PCR, with a range of temperatures setting from 60 °C to 72 °C; the optimum length ranged from 15 bp to 38 bp. After receiving the stock of lyophilized oligonucleotides, they were dissolved at 100 µM (stock concentration) and diluted to 10 µM (working concentration). All primers were kept at -20°C for long-term storage.

All the primers for PCRs are listed below:

**Table 2.2. Primers for DNA amplification.** Detailed information of primers is described in the corresponding results chapters.

Primer	Sequence (5' - 3')	Purpose
FClon1F	CTAGCTAGCTCCACCATGGGCTCCAAACTTTCTA	NDV-F gene amplification
FClon1R	GCCGGTACCTGCTCTTGTAGTGGCTCT	
mRFP-F	CCGGAATTCTCCACCATGGCCTCCTCCGAGGACG	mRFP gene amplification
mRFP-R	GTACTCTAGAGGCGCCGGTGGAGTGGC	
NDV-HN-NheI-F	CTAGCTAGCTCACCACCATGGACCGCGCGGTAAACAG	NDV-HN gene amplification
NDV-HN-KpnI-R	GCCGGTACCCAAACTCTATCATCCTTGAGGAT	
IBV-S-MCS1-NheI-F	CTAGCT AGCCCACCATGCTGGGCAAGAGCCTG	IBV-S gene amplification
IBV-S-MCS1-KpnI-R	GGTACCGGTGCTGTCCAGGCCAGCAGG	
H9N2-HA-MCS1-NheI-F	CTAGCTAGCTCCACCATGGAGATTATCCCCCTGATGGC	AIV-HA gene amplification
H9N2-HA-MCS1-KpnI-R	GGTACCGGTGCTATCCAGTCCCAGCAGTGG	
CMV-MCS1-F	AGAACCCACTGCTTACTGGCTT	Donor Plasmid internal primers
CMV-MCS1-R	AACTAGAAGGCACAGTCGAGGC	
hU6 seq primer	GACTATCATATGCTTACCGT	Sequencing forward primer



### 2.2.4.2.1. Routine PCR with Q5 DNA Polymerase

In this study, the reaction of routine PCRs was performed in a final volume of 25  $\mu$ l. The PCR components included 0.25  $\mu$ l Q5 high-fidelity DNA polymerase (Cat no. M0491S, NEB), 0.5  $\mu$ l dNTPs, 1.25  $\mu$ l volume of 10  $\mu$ M forward and reverse primer, 1  $\mu$ l of 100 ng DNA, and 15.75 NF water, and the final concentration of them, as well as the reaction protocol, are shown in **Table 2.3**.

**Table 2.3. PCR components and conditions using Q5 DNA Polymerase.** All PCR reaction components were prepared on ice and quickly transferred to the preheated thermocycler machine (98 °C). Negative control with no templates was included.

Component	Initial Concentration	Final Concentration
Reaction Buffer	5x	1x
dNTPs	10 mM	200 $\mu$ M
Forward Primer	10 $\mu$ M	0.5 $\mu$ M
Reverse Primer	10 $\mu$ M	0.5 $\mu$ M
Template DNA	-	100 ng
Q5 DNA Pol	-	0.02 U/ $\mu$ l
NF water		up to 25 $\mu$ l

PCR Profile			
Step	Temperature	Time	Cycle
Initial Denaturation	98 °C	30 sec	
Denaturation	98 °C	10 sec	
Annealing	72 °C	30 sec	30
Extension	72 °C	30 sec	
Final extension	72 °C	2 min	
Hold	4 °C	forever	

If required, colony PCRs were performed with the resuspended cell pellet of the bacteria culture as templates. Bacterial cultures were centrifuged briefly, and the cell pellet was resuspended, followed by 10 min. of boiling at 99 °C. Briefly, after the plasmid transformation (Section 2.2.2.1.2), cell plating, and overnight incubation of bacteria (Section 2.2.2.1.3), 1 µl of the resuspended lysed bacteria was added to a 25 µl volume of PCR reaction containing the components introduced above (**Table 2.3**). A negative control without any transformation was included. The PCR reactions were performed with the conditions shown above, followed by the band visualisation on a 1% agarose gel (Section 2.2.4.4).

#### **2.2.4.3. DNA Visualisation and Quantification**

UltraPure™ Agarose powder (Cat no. 17852, ThermoFisher Scientific) was added to a 1x TAE solution (40 mM Tris, 20 mM acetic acid, and 1 mM EDTA) to make agarose gels with certain percentages. The mixture was boiled in a microwave for approximately 3 minutes to dissolve the agarose completely. 10% total volume of GelRed® Nuclear Acid Stain (Cat no. SCT123, Merck) was added to the agarose solution just before pouring the solution into a casting tray. Each restriction enzyme-digested product or PCR product of interest was mixed with 6 x blue load dye (Cat no. R0611, ThermoFisher Scientific) (the final concentration was 1 x) and loaded into each well of a gel. GeneRuler 1 kb DNA ladder™ (Cat no. SM0312, ThermoFisher Scientific) was used as a size marker unless otherwise stated. Run the gel at 80-100 volts (V) for 1 hour until the marker is clearly distinguished so that the approximate sizes of the products can be determined. Subsequently, the gels were visualised under a UV light released by an ultraviolet (UV) transilluminator (256 nm).

DNA quantification was carried out using a Nanodrop ND-100 spectrometer (Nanodrop Technologies, Inc.). After cleaning the sensor of the machine with water and a lint-free cloth, 1  $\mu$ l of dilution buffer was loaded as a blank. Then 1  $\mu$ l of the DNA sample was loaded onto the clean sensor. The final concentration was reported in ng/ $\mu$ l.

#### **2.2.4.4. DNA Purification**

##### **2.2.4.4.1. Gel Bands Isolation and Purification**

PCR products excised from agarose gels were purified using the GeneJET Gel Extraction Kit (250, Cat no. K0692, ThermoFisher Scientific) according to the manufacturer's instructions. Briefly, a gel slice was weighed in a 1.5-mL Eppendorf tube before adding a 1:1 volume of binding buffer for each gel weight (100 mg-100  $\mu$ l). The sample was then incubated for 10 minutes in a 50°C water bath until the gel slice was completely dissolved. The tube was gently vortexed to solubilize the gel. After that, 800  $\mu$ l of the solubilized gel solution was transferred to a GeneJET purification column. The column was centrifuged at 12,000 x g for 1 minute, and the flow-through liquid was discarded. The column was washed with the addition of 700  $\mu$ l of wash buffer with ethanol, followed by centrifugation at 12,000 x g for 1 min. The empty GeneJet purification column was centrifuged for another minute to ensure the complete removal of residual buffer. To elute the DNA, the column was transferred to a clean Eppendorf before loading 50  $\mu$ l of elution buffer on the membrane of the column. The eluted DNA was quantified by the Nanodrop (Section 2.2.4.4) and stored at -20 °C.

#### 2.2.4.5. DNA Digestion

NEB supplied all restriction endonucleases, unless otherwise stated. 20 units of enzyme (no more than 10% of the total reaction volume) were applied in a proper reaction volume. The reaction was incubated at 37 °C for 30 minutes for routine gDNA digestion.

**Table 2.4.** Summary of the components used for restriction enzyme digestion.

COMPONENT	50 µl REACTION
DNA	1 µg
10X rCutSmart Buffer	5 µl (1X)
Restriction enzyme	1.0 µl (20 units)
Nuclease-free Water	to 50 µl

#### 2.2.4.6. DNA Sequencing

DNA sequencing was performed by Source BioScience (Cambridge, UK). PCR products were purified (Section 2.2.4.3.1) and then diluted to the final concentration according to the standard requirements. Briefly, 1.5 - 3 ng of DNA were required for a fragment of 100 - 200 bp product: 4.5 - 10 ng for the 200 bp - 500 bp product and 7.5 - 20 ng for the 500-1000 bp product. All sequencing data was obtained as ABI files and analysed using SnapGene version 7.0.2 software.

#### 2.2.4.7. Quantitative PCR

Quantitative PCR (qPCR) was used to compare the viral genomic copy number of recombinant ILTVs and ILTV wild-type at different time points. To this end, qPCR was performed in a CFX96™ Real-Time PCR Detection System (Cat no. 184-5384,

BioRad) using the QuantiFast SYBR Green PCR (Cat no. 204054, Qiagen) following the manufacturer's recommendations.

**Table 2.5.** qPCR primers used for the detection of ILTV gB gene.

Primer	Sequence (5' - 3')
gB-F	CAGTATCTCGCATCGCCTCAT
gB-R	AGTTCAGGTTCTGTTCCCAGG

**Table 2.6.** qPCR reaction setup and real-time cycler conditions.

Component	Final Concentration	1x, $\mu$ l
2x Quantifast SBYR Green PCR Master Mix	1x	6.25
Primer F	1 $\mu$ M	1.25
Primer R	1 $\mu$ M	1.25
Template DNA	100 ng	1.00
RNase-free water		2.75
Total volume		11.50

STEP	TEMP	TIME
PCR initial activation step	95 °C	5 min
Two-step cycling		
Denaturation	95 °C	10 s
Combined annealing/extension	60 °C	30 s
Number of cycles	35-40	

#### 2.2.4.7.1. Generation of Plasmid Standard

A 148 bp fragment of the ILTV gB gene was amplified from the wild-type ILTV strain genomic DNA by PCR using oligonucleotide primers gB Forward and gB Reverse. Amplification was carried out using OneTaq® 2X Master Mix with standard buffer (Cat no. M0482, NEB) to ensure the addition of an A-overhang at the 3' end of the amplicon to facilitate the subsequent TA cloning. The purified PCR product was cloned in the pCR™II-TOPO™ Vector (Cat no. K465001, Thermo Fisher Scientific) according to the manufacturer's instructions and transformed into *E. coli* as described in Section 2.2.2.1.2.

A 10-fold serial dilution series of the pTOPO-gB, ranging from 10<sup>8</sup> to 10<sup>2</sup> was used to construct the standard curve for gB. The concentration of the plasmid was measured using a fluorometer, and the corresponding copy number was calculated using the following equation (Wilhelm et al., 2003) (**Annex 3**).

DNA (copy)

$$= \frac{6.02 \times 10^{23} \left( \frac{\text{copy}}{\text{mol}} \right) \times \text{Plasmid amount (g)}}{\text{Plasmid length (bp)} \times 660 \left( \frac{\text{g}}{\text{mol}} \right)}$$

C<sub>T</sub> values in each dilution were measured in triplicates using real-time QPCR with the gB primers to generate the standard curve for gB. The C<sub>T</sub> values were plotted against the logarithm of their initial template copy numbers. Each standard curve was generated by a linear regression of the plotted points. Absolute quantification determines the exact copy concentration of the target gene by relating the C<sub>T</sub> value to a standard curve (Y. Yu et al., 2005).

**Table 2.7.** Summary of the components and conditions used for the amplification of ILTV gB using Taq polymerase.

<b>Component</b>	<b>25 <math>\mu</math>l reaction</b>	<b>Final Concentration</b>
10 $\mu$ M Forward Primer	0.5 $\mu$ l	0.2 $\mu$ M
10 $\mu$ M Reverse Primer	0.5 $\mu$ l	0.2 $\mu$ M
Template DNA	1 $\mu$ l	100 ng
OneTaq 2X Master Mix with Standard Buffer	12.5 $\mu$ l	1X
Nuclease-free water	to 25 $\mu$ l	

<b>STEP</b>	<b>TEMP</b>	<b>TIME</b>
Initial Denaturation	94 °C	30 seconds
	94 °C	30 seconds
30 Cycles	45-68 °C	60 seconds
	68 °C	1 minute/kb
Final Extension	68 °C	5 minutes
Hold	4-10 °C	

**Table 2.8.** pTOPO cloning components.

<b>Reagent</b>	<b>Amount, <math>\mu</math>L</b>
PCR Product	4
Salt Solution	1
Sterile Water	1
<b>Final Volume</b>	<b>6</b>

## 2.2.5. Protein Techniques

All procedures were performed at room temperature unless otherwise stated.

### 2.2.5.1. Western Blot

All antibodies (**Table 2.9**) used are listed below:

**Table 2.9.** List of antibodies.

Antibodies	Supplier
Rabbit polyclonal anti-FLAG tag, F7425 (1:2500 dilution)	Sigma, UK
Goat polyclonal anti-rabbit IgG (HRP), ab6721 (1:4000 dilution)	Abcam, UK
Mouse monoclonal anti-alpha tubulin, ab7291 (1:2500 dilution)	Abcam, UK

Confluent cells cultured ( $1.2 \times 10^6$  cells) in 6-well plates were lysed with 100 $\mu$ l NP-40 lysis buffer (Cat. No. J60766.AP, Thermo Fisher Scientific) for 30 minutes and centrifuged at 13,000 x g for 10 min. Samples were kept at -80°C or loaded on the sodium dodecyl sulphate polyacrylamide gel electrophoresis (SDS-PAGE) (Cat no. 4561086, Bio-Rad). **Table 2.10** shows the components used to make the stacking and separating gels. A Mini-PROTEAN tetra system (Cat No. 1658035, Bio-Rad) was used for the SDS-PAGE apparatus. After loading up to 15  $\mu$ l in each lane of the SDSPAGE, the tank was filled with 1x SDS running buffer. The gel was run at 80 volts for 10 minutes and then switched to a constant voltage of 120 volts for approximately 1 hour. The colour pre-stained protein standard with a broad range (Cat no. ab116028, Abcam) was used as a marker. Protein was then transferred from the SDS-PAGE to a nitrocellulose membrane using the trans-Blot Turbo™ Transfer System (Cat no. 1704150, BioRad) according to the guidelines of manufacture. Then the cassette was



disassembled, and the membrane was blocked in 5% (w/v) skimmed milk (Marvel) in PBST/0.1% (v/v) Tween 20 for 1 hour.

All primary antibodies were diluted in 5% (w/v) skimmed milk in PBST, and membrane incubations were conducted on an orbital shaker for 1 hour at room temperature or overnight at 4 °C. Each blot was probed with a mixture of a primary antibody and a loading control at proper concentrations, followed by three washes in PBST. Then the blot was incubated with a secondary fluorescent-tagged antibody at room temperature for 60 minutes in the dark, followed by three washes. The visualisation of the blot was performed using the Biorad Chemidoc MP imaging system (Cat no. 12003154, Bio-rad), according to the manufacturer's protocol. The band intensity was quantified with Image J.

**Table 2.10.** List of components utilised for the SDS-PAGE stacking and resolving gels.

Component	Stacking gel	Resolving gel
	4%	12%
30% Acrylamide/bis	1.98 mL	6.0 mL
0.5M Tris-HCl, pH 6.8	3.78 mL	-
1.5M Tris-HCl, pH 8.8	-	3.75 mL
10% SDS	150 µl	150 µl
dH <sub>2</sub> O	9 mL	5.03 µl
TEMED	15 µl	7.5 µl
10% APS	75 µl	75 µl
<b>Total volume</b>	<b>15 mL</b>	<b>15 mL</b>

## 2.2.6. Assembly of CRISPR/Cas9 Reagents

### 2.2.6.1. sgRNA Design and Synthesis

The web tool CHOPCHOP (<http://chopchop.cbu.uib.no/>) was used to aid in predicting and ranking candidate CRISPR sgRNAs in the genome region of interest. A workflow shows a specific example demonstrating how this website works (**Figure 2.2**).

Briefly, the target sequence of the ILTV genome (*Gallid herpesvirus 1*) (NC006623.1) was pasted into the CHOPCHOP software. All the parameters (e.g., species, protospacer adjacent motif (PAM) type, and CRISPR modes) were inputted correctly. By clicking 'Find Target Sites!', a list of eligible sgRNA candidates with on- and off-target scores was displayed. All evaluated sgRNA sequences were obtained, and more detailed information of interest can be downloaded as an output in Fasta format.

The sequences of all sgRNAs used in this study are detailed in **Table 2.11**. Please note that at the 5' end of the sgRNA oligos were appended with the CACCG sequence. The "CACCG" sequence ensures that the oligo is compatible with the overhangs of the *BbsI*-digested px459v2 vector. The "G" is a requirement of polymerase III promoters and ensures the efficient initiation of the transcription of the gRNA. Additionally, for the reverse complement protospacer, the sequence AAAC was appended to the 5' end. The "AAAC" sequence ensures that the oligo is compatible for cloning into the *BbsI*-digested px459v2 vector. The additional "C" on the 3' end is needed to anneal the sequence to the initiating "G" added to the forward oligo.

Home Instructions Scoring About Updates Submissions Contact FAQ

# STEP 1

# CHOPCHOP



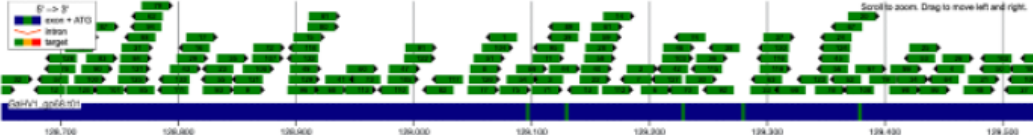
Target:  In:  Using:  For:

RefSeq/ENSEMBL/gene ID or genomic coordinates. Add new species. Change default PAM and guide length in Options. Primers can be adjusted in Options.

Home Instructions Scoring About Updates Submissions Contact FAQ

## STEP 2

### GaHV1\_gp68



Download results:  [View in UCSC genome browser](#)

Rank	Target sequence	Genomic location	Strand	GC content (%)	Self-complementarity	MM0	MM1	MM2	MM3	Efficiency
1	GTAAGTACCAAGTCCACCCCGG	NC_006623.1:129066	-	50	0	0	0	0	0	72.54
2	GGGCTGTTTATCTAGACGTCGG	NC_006623.1:129182	+	45	2	0	0	0	0	73.56
3	CATCCCTGGGTACAGCACCAGGG	NC_006623.1:129105	-	60	3	0	0	0	0	74.55
4	TCGTCGACGTAAGTCCAGCGGG	NC_006623.1:129446	-	60	2	0	0	0	0	76.68
5	GTCGAGAGACATCATGAGCGGG	NC_006623.1:128636	+	45	1	0	0	0	0	68.26
6	CTAGACGTCGGACCAACCCCGG	NC_006623.1:129194	+	60	3	0	0	0	0	69.94
7	GACGCTAGATAAACAGACCCCGG	NC_006623.1:129180	-	45	2	0	0	0	0	68.90
8	GCAGAGAAGACTGCGCTCCGGGG	NC_006623.1:129049	+	65	2	0	0	0	0	68.89
9	CACCGAAGGAGTGTGAGTCGAGG	NC_006623.1:128848	+	60	0	0	0	0	0	66.24
10	TCACAAAAAAGTCTCGGGTGG	NC_006623.1:129530	-	45	0	0	0	0	0	66.18
11	GATCCCTGGTGTGTACCCAGGG	NC_006623.1:129102	+	60	0	0	0	0	0	66.12

Home Instructions Scoring About Updates Submissions Contact FAQ

## STEP 3

Target: **GaHV1\_gp68**  
 Rank: **1**  
 Target sequence: **GTAAGTACCAAGTCCACCCCGG**



Download:

Pair	Left primer coordinates	Left primer	Left primer Tm	Left primer off-targets	Right primer coordinates	Right primer	Right primer Tm	Right primer off-targets	Pair off-targets	Product size
1	NC_006623.1:128975-128997	CATAATCTGAACGGCTCTGTGT	60.2	0	NC_006623.1:129170-129192	AAACAGACCCGGTATATCCCTT	60.0	0	0	217
2	NC_006623.1:128976-128998	ATAATCTGAACGGCTCTGTGTG	60.2	0	NC_006623.1:129170-129192	AAACAGACCCGGTATATCCCTT	60.0	0	0	216
3	NC_006623.1:128975-128997	CATAATCTGAACGGCTCTGTGT	60.2	0	NC_006623.1:129140-129162	CTGAGAGCTGTAGGCTAGAT	60.1	0	0	187
4	NC_006623.1:128976-128998	ATAATCTGAACGGCTCTGTGTG	60.2	0	NC_006623.1:129140-129162	CTGAGAGCTGTAGGCTAGAT	60.1	0	0	186
5	NC_006623.1:128953-128975	GTCATGCTGGGCTCTAATC	60.3	0	NC_006623.1:129170-129192	AAACAGACCCGGTATATCCCTT	60.0	0	0	239

Off-targets		
Location	Number of mismatches	Sequence (including mismatches)
There are no off-targets.		

**Figure 2.2. Example workflow usage of CHOPCHOP web tool. Step 1** shows the home screen of CHOPCHOP website. Top: Links for additional information on

advanced options (“Instructions”), how gRNA ranking is performed (“Scoring”), and general information about the tool (“About,” “Updates”). Help and additional requests can be accessed through “Submission,” “Contact” or “FAQ”. Center: Main fields for gRNA design where one specifies the gene/transcript of interest (“Target”) and selects the genome (“In”) and the planned experiment (“Using”, “For”). Immediately below, additional options can be specified using the grey buttons. Bottom: To perform the search, press the black “Find Target Sites!” button. **Step 2** shows the general results screen for gene knockout using the US4 gene (GaHV1\_gp68) in the ILTV as an example. On the top is the genome view of the gene with identified gRNAs. This view can be toggled left/right and zoomed in/out. The gene model is drawn with the name of each isoform. Thick blue boxes represent exons, thin blue boxes represent untranslated regions, and green lines indicates in-frame start codons. gRNAs are displayed as arrows, with colours matching the scoring. Directionality is indicated by black arrowheads. Immediately below the genome view are options to download all identified gRNA targets (left) or view the results in the UCSC Genome Browser (right). On the bottom is a ranked list of all gRNA targets found, with all features necessary to make an informed decision. Clicking on a gRNA in the list or the graphical representation opens a detailed results view. **Step 3** shows the detailed results view for gRNA rank 1 from Step 2. The top-left corner summarizes details about the specific gRNA hit. Below this is a genome view of the specific target site. This view can be toggled left/right and zoomed in/out. Proposed primer pairs for validation are shown at the top (violet). Immediately below is the gRNA location and directionality (black arrow) with precise dsDNA cut site (light blue). Restriction enzyme sites that can used for mutation validation are also shown (red, green). The genome view is followed by the list of proposed primer pairs with their features, and a list with possible genome off-targets, including location, sequence, and possible mismatches (highlighted in red). In this example, no off-targets were found.

All oligos used in this section were synthesised by Invitrogen (Thermo Fisher Scientific). Synthesised oligo powder was resuspended in nuclease-free water to reach a final concentration of 100  $\mu$ M.

**Table 2.11.** List of the sgRNA oligo sequences as designed and predicted by CHOPCHOP.

<b>Primer</b>	<b>Forward Oligo (5' to 3')</b>	<b>Reverse Oligo (5' to 3')</b>
UL50.1	CACCGTATTCACGCAGGTGACCGAG	AAACCTCGGTCACCTGCGTGAATAC
UL50.2	CACCGATGATATGGTGTCGCACCT	AAACAGGTGCGACACCATATCATC
UL0.1	CACCGTTTACGACGAATCACCCCTAG	AAACCTAGGGTGATTCGTCGTAAAC
UL0.2	CACCGAACGTATCGGATACGGTGGT	AAACACCACCGTATCCGATACGTTC
US4	CACCGTCAGCGGGTACACTTTATA	AAACTATAAAGTGTACCCGCTGAC
sgA	CACCGAGATCGAGTGCCGCATCAC	AAACGTGATGCGGCACTCGATCTC
ICP4.1	CACCGAGCTCCCAGACCTAGGCCG	AAACCGGCCTAGGTCTGGGAGCTC
ICP4.2	CACCGACCATCCTGTTTCGCACCGGA	AAACTCCGGTGCGAACAGGATGGTC
ICP4.3	CACCGTTACCGGTCCGGCGGCCGAA	AAACTTCGGCCGCGGACCGGTAAC

### 2.2.6.2. Assembly of CRISPR/Cas9 Reagents

A cloning vector pX459v2 containing *BbsI* restriction enzyme sites was used for the co-expression of the gRNA and Cas9 protein. The pX459v2 vector carries the Cas9 from *S. pyogenes* with 2A-Puro and the cloning backbone for sgRNA (V2.0) (Addgene plasmid #62988) as described by Ran et al., (2013). The pX459v2 vector contains a hU6 promoter driving the transcription of the gRNA; also, a hybrid cytomegalovirus (CMV) enhancer/chicken  $\beta$ -actin (CAG) promoter is included in the pX459v2 vector to enhance the expression levels of pSpCas9 (BB)-2A-Puro in cells.

The annealed gRNA oligonucleotides were ligated into the pX459v2 vector at the *BbsI* sites. All the procedures are listed below in **Table 2.12**. After this, the reaction was transformed into competent bacterial DH5 $\alpha$  cells (Section 2.2.2.1.2), and the correct insertions were confirmed by PCR and sequencing. The correct pX459v2-gRNA expression construct was then transfected into LMH cells (Section 2.2.1.4).

**Table 2.12. The conditions of CRISPR/Cas9 construct assembly.** Complementary gRNA oligos are synthesised and re-suspended in nuclease free water to reach a final concentration of 100  $\mu$ M (a). Then annealed oligos from reaction is diluted with nuclease free water, followed by linearisation of the pX459v2 vector (b) and the insertion of the annealed sgRNA oligos into the linearised pX459v2 vector at *BbsI* restriction digest sites (c).

		<b>COMPONENT</b>	<b>Amount, <math>\mu</math>l</b>
a. Annealing complementary oligonucleotides		sgRNA F (100 $\mu$ M)	1
		sgRNA R (100 $\mu$ M)	1
		T4 ligation buffer, 10 $\times$	1
		ddH <sub>2</sub> O	7
		<b>PCR Profile</b>	
	37 $^{\circ}$ C	30 min	
	95 $^{\circ}$ C	5 min	
	25 $^{\circ}$ C	5 $^{\circ}$ C/min ramp down	
b. pX459v2 vector linearization		<b>COMPONENT</b>	<b>50 <math>\mu</math>l REACTION</b>
		DNA	1 $\mu$ g
		10X rCutSmart Buffer	5 $\mu$ l (1X)
		<i>BbsI</i> -HF	1.0 $\mu$ l (20 units)
		Nuclease-free Water	to 50 $\mu$ l
	<b>PCR Profile</b>		
	37 $^{\circ}$ C	30 min	
c. Ligation of sgRNA oligos into pX459v2		<b>COMPONENT</b>	<b>10 <math>\mu</math>l reaction, <math>\mu</math>l</b>
		Annealed oligo	1
		Linearised plasmid, 50ng	50 ng
		10X T4 DNA ligase Buffer	1
		T4 DNA ligase	1
	ddH <sub>2</sub> O	3.62	

*Incubate overnight at 4  $^{\circ}$ C*

## 2.2.7. *In silico*-based Techniques

### 2.2.7.1. Sequencing of Philippine Endemic Viral Poultry Strains

Field samples of NDV, IBV, and AIV were collected from different farm locations in the Philippines. Samples were then amplified using primers specific to the antigen of interest. Primers used are listed in **Table 2.13** (Section 2.2.4.3.1). PCR products were then sent for sequencing (Section 2.2.4.7).

Analyses of the ABI and Fasta-formatted sequencing results were carried out through the following steps:

1. Initial validation using NCBI BLAST® (blastn suite, [https://blast.ncbi.nlm.nih.gov/Blast.cgi?PROGRAM=blastn&PAGE\\_TYPE=BlastSearch&LINK\\_LOC=blasthome](https://blast.ncbi.nlm.nih.gov/Blast.cgi?PROGRAM=blastn&PAGE_TYPE=BlastSearch&LINK_LOC=blasthome)). Through the alignment of the query sequences against those present in a selected database, we were able to initially validate the identity of the sequence as well as confirm the sequence directionality (plus or minus strand), percent identity, and gaps.
2. Sequence quality check. Sequences in the minus strand were reverse complemented using the reverse complement online tool (<http://reverse-complement.com>). Once the sequence is in the plus-strand orientation, quality checks and trimming are performed through SnapGene version 7.0.2. Briefly, 'N' base calls were dealt with either by manual editing or deletion, especially with multiple succeeding 'N' base calls at either the 5' or 3' end of the sequence. Once the sequence was cleaned and trimmed, overlapping forward and reverse sequences were merged using the online tool emboss merger (<https://www.bioinformatics.nl/cgi-bin/emboss/merger>). The final sequence will be used for the succeeding analyses.



**Table 2.13.** List of primers for antigen amplification.

Primer	Sequence (5' - 3')
NDV-F-Forward	GACGCAACATGGGTTCCAAATCT
NDV-F-Reverse	CTGCATTCATGCTCTTGTGGTGG
IBV-S1-Forward	AAAGCAACGCCAGTTGT
IBV-S1-Reverse	TAAGCATAACAACAGGTTGC
IBV-S2-Forward	ACTACTACCAAAGTGCCT
IBV-S2-Reverse	ACATCTTGTGCAGTACCATTAACA
AIV-HA-Forward	CTAGCTAGCTCCACCATGGAGATTATCCCCCTGATGGC
AIV-HA-Reverse	GGTACCGGTGCTATCCAGTCCCAGCAGTGG

#### 2.2.7.2. Reference Sequence Data Acquisition

In this project, we aimed to provide an overview of the genotypic and evolutionary identities of the Philippine endemic viral strains. Accordingly, sequences from different geographical locations of the NDV-F and -HN genes, the IBD-S gene, and the AIV-HA gene were retrieved from the NCBI (<https://www.ncbi.nlm.nih.gov>) and Uniprot (<https://www.uniprot.org>) databases for analysis. The analysis also includes known viral genotypes, vaccine strains, and reference genomes.

#### 2.2.7.3. Evolutionary Analysis

Multiple sequence alignments of the amino acid sequence were performed using the ClustalW2 tool included in the MEGA11 software (Tamura et al., 2021). Phylogenetic trees were assembled in MEGA11 software. The evolutionary history was inferred using the neighbor-joining method (Saitou & Nei, 1987). The bootstrap consensus tree inferred from 1000 replicates (Felsenstein, 1985) is taken to represent the evolutionary history of the taxa analysed. Branches corresponding to partitions reproduced in less

than 50% bootstrap replicates are collapsed. The evolutionary distances were computed through various models included in MEGA 11, including a maximum likelihood method based on the JTT matrix-based method (Jones et al., 1992). The rate variation among sites was modelled with a gamma distribution (shape parameter = 1).

#### **2.2.7.4. Protein Analysis**

The ProtParam web server (<http://web.expasy.org/protparam/>) was used to evaluate the physicochemical characteristics of the selected antigens. The analysed characteristics included molecular weight, *in vitro* and *in vivo* half-lives, instability index, theoretical isoelectric point (pI), aliphatic index, and grand average of hydropathicity (GRAVY). Protein structure homology modelling was done through SWISS-MODEL (<https://swissmodel.expasy.org/interactive>), providing initial structural information and insertion and deletion sites as well as different levels of complexity. The antigen amino acid sequence was analysed for its immunological properties. Both AntigenPro (<http://scratch.proteomics.ics.uci.edu/>) and VaxiJen v2.0 (<http://www.ddg-pharmfac.net/vaxijen/VaxiJen/VaxiJen.html>) were utilised to assess the antigenicity of the antigens. The VaxiJen v2.0 server was used with viral, bacteria, and parasite models, and a 0.7 threshold was used in both.

### **2.2.8. Statistical Analysis**

The means were compared using the student's t-test, where only two groups were involved. When multiple comparisons were required for a single factor, experimental means were compared using a one-way analysis of variance (one-way ANOVA). p values were calculated with GraphPad Prism 8. The data usually represents the average of three technical replicates with standard deviation (S.D.). ns: non-significant;  $p > 0.05$ , \* $p < 0.05$ , \*\* $p < 0.01$ , \*\*\* $p < 0.001$ .

# CHAPTER 3

## Genetic Characterisation of Field Strains of Important Viral Diseases in Commercial Poultry

### 3.1. Introduction

Traditional approaches to vaccine development, such as the use of inactivated or live attenuated viruses, are associated with some drawbacks, including the time-consuming nature of the process and challenges in the production of proteins and pathogens (Dangi et al., 2018). This impedes the advancement of the development of innovative vaccinations for prospective pandemics. To tackle these concerns, several efforts have been proposed to devise recombinant vaccines through the process of cloning, expression, and purification of genes derived from pathogenic organisms. These genes are subsequently employed as prospective vaccine candidates (Nascimento & Leite, 2012).

*In silico* approaches in reverse vaccinology (RV) offer great importance in the development of novel recombinant vaccines. This methodology enables the generation of comprehensive preliminary predictions regarding potential vaccine candidates through the analysis of genome sequences. The tool predicts the antigenicity, B and T cell epitope regions, signal peptide, subcellular localisation, and solubility of the target proteins (Can, Alak, et al., 2020; Can, Köseoğlu, et al., 2020). The examination of docking plays a vital role in the *in silico* technique of reverse

vaccinology, as it provides evidence of the interaction between anticipated epitopes and specific alleles of major histocompatibility complex class I (MHC-I) and class II (MHC-II). The outcomes of these predictions play a critical role in mitigating failures in wet laboratory experiments or clinical trials (Can, Köseoğlu, et al., 2020; Dangi et al., 2018).

The development of novel recombinant viral vectors against economically important poultry diseases starts with the identification of appropriate antigens. These antigens will determine the potential of the viral vaccine vector to confer protection against existing field strains and possible emerging variants through antigenic variation (Zenglei Hu et al., 2022; Vilela et al., 2020). The careful consideration of vaccine antigens is of utmost importance, as it dictates the potential for achieving sufficient protective immunity via the utilisation of either a single antigen or a combination of several antigens. The precise characteristics and mechanisms of protective antigens are still not fully understood, which may impede the ability to effectively detect and assess them. Vaccine development is subject to several issues that impact its efficacy, including the intrinsic diversity of antigens and the requirement to preserve their original conformation to ensure an adequate immune response upon immunisation. Various elements and restrictions exert an impact on the formulation and assessment of methods pertaining to antigen identification and evaluation (Chambers et al., 2016).

This chapter examines three poultry viruses of significant economic importance, namely NDV, IBV, and AIV. Field samples were collected from the Philippines (through the BBSRC-funded project (BB/R012695/1), where the aforementioned poultry diseases are present and widespread, resulting in significant economic losses as well

as potential human health concerns (Cáceres et al., 2021). In this study, we employed *in silico* methods to analyse the viral field strains endemic to the Philippines, with a major emphasis on comparing and selecting suitable antigens for vaccine construction. Providing us with the necessary information to design the antigenic proteins and epitopes that have the potential to provide broad protection against economically important poultry viruses globally.

### **3.1.1. Aims**

The objective of this chapter is to identify potential antigenic proteins and epitopes that may be utilised for the creation of a putative vaccine candidate or serological diagnostic test through the application of an *in-silico* approach.

Specifically:

1. Sequence-based characterisation of NDV, IBV, and AIV putative antigenic sequence.
2. Demonstrate the evolutionary relationship between the Philippine strain and existing global strains through phylogenetic analysis and sequence similarity.
3. Explore potential correlations between viral antigenic sequences and the identification of putative antigens.

## 3.2. Results

The objective of this chapter was to conduct an analysis of the complete genomes of NDV, IBV, and AIV. The reference genome accession numbers for these viruses are NC\_039223.1, AJ311317, and NC\_004908.1, respectively. The purpose of this analysis was to identify potential antigenic proteins and epitopes that could be utilised in the development of a vaccine candidate or serological diagnostic assay. This analysis was conducted using a reverse vaccinology approach, as previously described (Can, Köseoğlu, et al., 2020; Dangi et al., 2018).

A series of *in silico* investigations were performed on proteins derived from the NDV, IBV, and AIV genomes. These analyses involved the prediction of various physico-chemical properties, secondary structure, subcellular localisation, transmembrane helices, antigenicity, and the presence of signal peptides. In addition to the aforementioned factors, the study also made predictions for B/T cell epitopes, MHC I, and MHC II epitopes.

### 3.2.1. *In silico* Characterisation of Antigenic Proteins and Epitopes of NDV, IBV, and AIV

The physico-chemical characteristics of the reference genome proteins were analysed by utilising the Expasy ProtParam online tool (<https://web.expasy.org/protparam/>) (Gasteiger et al., 2005) for prediction purposes. The solubility prediction was conducted using SolPro, which may be accessed at the following URL: <http://scratch.proteomics.ics.uci.edu/> (J. Cheng et al., 2005). The prediction of secondary structures was carried out using the GOR IV web server, which may be accessed at [https://npsa-prabi.ibcp.fr/cgi-bin/npsa\\_automat.pl?page=/NPSA/npsa\\_gor4.html](https://npsa-prabi.ibcp.fr/cgi-bin/npsa_automat.pl?page=/NPSA/npsa_gor4.html) (Garnier et al., 1996). In general, the range of amino acids observed varied from 57 to 6629. In the case of NDV, the L protein, weighing approximately 248 kDa, is the largest protein, whereas the M protein, weighing approximately 39 kDa, is the smallest. In contrast, for IBV, the replicase polyprotein 1ab, weighing approximately 441 kDa, is the largest protein, while protein 3a, weighing approximately 6.6 kDa, is the smallest. Lastly, in the case of AIV, the largest protein is PB2, weighing approximately 85 kDa, and the smallest protein weighs approximately 24 kDa (**Table 3.1**). Upon analysis of all proteins encoded by the full genome, it was determined that the theoretical isoelectric point (PI) value ranged from 3.7 to 10.18. The half-life of all proteins was calculated to be 30 hours. Based on the instability index, it was observed that the P, M, and L proteins of NDV exhibited instability, but the NP, F, and HN proteins showed stability. In contrast, it has been observed that the proteins 3a, 3b, M, 5b, and N of IBV exhibit instability, whereas replicase polyproteins 1ab, S, 3c, and 5a demonstrate stability. In the study, it was shown that AIV's PB2, PA, NP, and ND exhibited instability, but PB1, HA, NA, and M demonstrated stability. The aliphatic index exhibited considerable variability, with values ranging from 50.42 to 167.54 across all proteins. Most proteins, with the



exception of NDV M and F, IBV S, 3a, 3c, M, and 5a, as well as AIV PA, exhibited a negative grand average hydropathicity value (**Table 3.1**).

Based on the findings derived from the analysis of structural proteins, it was seen that the proportion of the alpha helix conformation ranged approximately from 8% to 52%. Similarly, the extended strand conformation exhibited a range of about 8% to 40%, while the random coil conformation ranged approximately from 32% to 61% (**Table 3.2**).

**Table 3.1.** Physico-chemical parameter results predicted by the ExPASyProtParam.

Virus	Protein name	Number of amino acids	Molecular weight	Theoretical PI	Total number of negatively charged residues (Asp + Glu)	Total number of positively charged residues (Arg + Lys)	The estimated half-life (hour)	The instability index (II)	Aliphatic index	Grand average of hydropathicity (GRAVY)
NDV	NP	489	53320	5.57	54	47	30	39.71/Stable	73.68	-0.366
	P	395	42107	6.68	40	38	30	47.82/Unstable	64.05	-0.708
	M	364	39867	9.57	31	46	30	40.81/Unstable	99.56	0.005
	F	553	58940	8.59	37	43	30	29.99/Stable	107.41	0.174
	HN	571	62595	7.19	53	53	30	33.20/Stable	82.63	-0.162
	L	2204	248492	6.91	240	234	30	45.42/Unstable	96.84	-0.130

	replicase									
IBVS	polyprotein	6629	744432	6.17	704	645	30	32.20/Stable	88.86	-0.015
	1ab									
	S	1162	128047	7.71	81	84	30	35.53/Stable	86.05	0.012
	3a	57	6668	7.85	2	3	30	74.13/Unstable	167.54	1.021
	3b	64	7442	3.79	14	2	30	57.20/Unstable	86.72	-0.192
	3c	108	12248	8.56	8	10	30	17.36/Stable	94.91	0.011
	M	225	25476	8.54	15	19	30	51.17/Unstable	94.84	0.202
	5a	65	7505	10.18	3	9	30	34.04/Stable	145.38	0.549
	5b	82	9334	9.07	7	11	30	55.92/Unstable	71.46	-0.691
	n	409	45032	9.61	53	72	30	40.05/Unstable	50.42	-1.034
AIV	PB2	759	85977	9.43	87	105	30	45.42/Unstable	87.68	-0.307
	PB1	758	86300	9.25	82	101	30	39.12/Stable	72.82	-0.492
	PA	716	82679	5.46	114	95	30	49.12/Unstable	78.06	0.474

HA	492	55069	5.98	54	45	30	36.29/Stable	80.85	-0.424
NP	490	55342	9.72	54	70	30	44.76/Unstable	70.51	-0.537
NA	469	51887	6.51	45	43	30	31.41/Stable	76.84	-0.260
M	252	27880	9.32	24	30	30	37.56/Stable	84.05	-0.229
NS	217	24538	5.65	33	29	30	42.15/Unstable	89.4	-0.378

---

**Table 3.2.** Secondary structures results predicted by GOR IV.

<b>Virus</b>	<b>Protein name</b>	<b>Alpha helix (%)</b>	<b>Extended strand (%)</b>	<b>Random coil (%)</b>
NDV	NP	41.72	15.13	43.15
	P	32.41	8.1	59.49
	M	26.92	20.88	52.2
	F	27.86	24.95	47.2
	HN	20.14	21.54	58.32
	L	40.43	14.93	44.65
IBVS	replicase polyprotein 1ab	24.39	26.4	49.21
	replicase polyprotein 1a	26.27	26.02	47.71
	S	20.91	29.35	49.74
	3a	29.82	29.82	40.35
	3b	9.38	32.81	57.81
	3c	34.26	24.07	41.67
	M	10.67	40.44	48.89
	5a	52.31	15.38	32.31

	5b	31.71	10.98	57.32
	N	23.96	14.18	61.86
AIV	PB2	38.47	20.42	41.11
	PB1	40.24	16.75	43.01
	PA	37.01	15.5	47.49
	HA	19.92	30.69	49.39
	NP	39.59	13.27	47.14
	NA	8.96	34.97	56.08
	M	52.38	13.1	34.52
	NS	47.93	11.98	40.09

All the proteins, except for IBV 3a, 3c, and 5a, were identified as potential antigens. The proteins from the reference genome, as well as expected epitopes, were subjected to analysis utilising the Vaxijen v2.0 web server. This server, accessible at <http://www.ddg-pharmfac.net/vaxijen/VaxiJen/VaxiJen.html>, was utilised to predict the antigenicity of these proteins, employing a threshold value of 0.4 (Doytchinova & Flower, 2007). The antigenicity value exhibited a range of 0.2325 to 0.7241. In terms of the NDV, the HN protein exhibited the highest level of antigenicity, while the NP protein had the lowest level of antigenicity. It is noteworthy that NDV-HN had the greatest antigenicity value, whereas NDV-F demonstrated a closely comparable antigenicity value. The predominant NDV vaccines currently available are formulated using the NDV-F antigen. The N protein had the greatest antigenicity value among the potential antigen findings of IBV, whereas the replicase polyprotein 1ab displayed the lowest value. In contrast, it is noteworthy that the AIV proteins had the highest antigenicity value in the NA protein, while the HA protein displayed the lowest antigenicity value. This observation is particularly intriguing considering that many vaccines have been developed based on the HA protein (**Table 3.3**).

To further validate the subcellular localisation of viral proteins within host cells during infection, the Virus-mPLoc tool was utilised, which can be accessed at <http://www.csbio.sjtu.edu.cn/bioinf/virus-multi/> (Shen & Chou, 2010). The TMHMM Server v. 2.0 (<http://www.cbs.dtu.dk/services/TMHMM/>) was employed for predicting the quantity of transmembrane helices (Krogh et al., 2001). The transmembrane helices showed a range of 0 to 18 among the proteins of NDV, IBV, and AIV. The majority of the proteins examined did not possess transmembrane helices, with the exception of NDV-F/HN/L, IBV-replicase1ab/S/3a/3c/M, and AIV-NA. Upon analysis

of subcellular localisation predictions, it was shown that the NDV NP, P, and L proteins are predicted to be located within the cytoplasm of the host. The localisation of F and HN proteins was expected to be within the host cell membrane, whereas M protein was anticipated to be present in the host cell membrane, cytoplasm, and nucleus. The localisation of IBV 3a, 3b, and 5a proteins was expected to be located inside the cytoplasm of the host, whereas 3c and M proteins were predicted to be localised within the host cell membrane. The localisation of IBV-S and -N proteins has been predicted to occur within the endoplasmic reticulum of the host. Regarding AIV, it was anticipated that the PB2 and PB1 proteins would localise inside the cytoplasm and nucleus of the host, while the PA and NA proteins were anticipated to reside within the host cell membrane. The localisation of AIV NP, M, and NS proteins within the host nucleus was determined and documented in **Table 3.3**.

Furthermore, in the attempt to predict linear B cell epitopes of the NDV, IBV, and AIV proteins, we employed the web-based programmes Bcepred and Bepipred Linear Epitope Prediction 2.0, which were accessed through the online servers of the Immune Epitope Database (IEDB). The Bcepred server can be found at <http://crdd.osdd.net/raghava/bcepred/>, while the IEDB server is available at <https://www.iedb.org/> (Vita et al., 2019). Numerous linear B cell epitopes were predicted for the NDV-F and -HN, IBV-S, and AIV-HA and -NA proteins by the utilisation of Bcepred and IEDB. The epitopes that were identified in both Bcepred and IEDB prediction tools and subsequently confirmed as potential antigens were compiled and shown in **Table 3.4**. The predictions obtained indicated that the majority of epitopes exhibited higher levels of antigenicity compared to their respective proteins. The proteins that were analysed exhibit varying levels of antigenicity, with the highest



values recorded as follows: NDV-F, NDV-HN, IBV-S, AIV-HA, and AIV-NA epitopes are 1.42, 1.62, 1.22, 1.51, and 1.72, respectively. The epitopes are represented by the sequences DKVNVRLTS, TGANPNP, IGYQSTNST, and LHFQNE. **Table 3.4** displays all the predicted potential antigenic epitopes.

Furthering our understanding of predicting antigenic epitopes, we have performed the analysis of major histocompatibility complex class I (MHC-I) and class II (MHC-II) epitopes in the structural proteins of the reference genome and proteins containing a signal peptide using the Immune Epitope Database (IEDB), available at <https://www.iedb.org/> (Vita et al., 2019). In the analysis, a total of twelve MHC-I alleles were employed for the prediction of MHC-I epitopes. These alleles, namely A01.01, A02.01, A03.01, A24.02, A26.01, B07.02, B08.01, B27.05, B39.01, B40.01, B58.01, and B15.01, were selected as representatives of the HLA super-type. In the analysis, a total of seven distinct MHC-II alleles were utilised for the prediction of MHC-II epitopes. These alleles include DRB1.03.01, DRB1.07.01, DRB1.15.01, DRB3.01.01, DRB3.02.02, DRB4.01.01, and DRB5.01.01. A lot of MHC-I epitopes were predicted as probable antigens (**Table 3.5**). The antigenicity values associated with epitopes were often seen to be higher in comparison to the antigenicity values of their respective proteins. The epitopes (GEFDATYQKNISIL) and (RVQQAILSIL) were identified as having the greatest antigenicity values (1.0369 and 1.1574, respectively) among the NDV proteins. These epitopes had been predicted to be present in the F and HN proteins, respectively. The epitope (KAGGPITYK) of the IBV-S protein had the greatest antigenicity value (1.4952). Furthermore, it is worth noting that the AIV-HA proteins exhibit epitopes with the highest antigenicity values, namely (SEIEARLNM) and (LATTVTLHF), which have been measured at 1.1402 and 1.1589, respectively.

All predicted epitopes have a percentile rank ranging from 0.02 to 0.1, demonstrating a robust binding affinity between the epitope and MHC-I alleles (Can, Köseoğlu, et al., 2020).

**Table 3.3.** Transmembrane helices, localisation and antigenicity results predicted by TMHMM, Virus-mPLOC and Vaxijen, respectively.

<b>Virus</b>	<b>Protein name</b>	<b>TMHMM</b>	<b>Virus-mPLOC</b>	<b>Vaxijen v2.0 value</b>
NDV	NP	0	Host cytoplasm	0.4078 (probable antigen)
	P	0	Host cytoplasm	0.4804 (probable antigen)
	M	0	Host cell membrane. Host cytoplasm. Host nucleus.	0.5044 (probable antigen)
	F	2	Host cell membrane.	0.5530 (probable antigen)
	HN	1	Host cell membrane.	0.5624 (probable antigen)
	L	0	Host cytoplasm.	0.4450 (probable antigen)
IBV	replicase polyprotein 1ab	18	ND	0.4313 (probable antigen)
	replicase polyprotein 1a	18	ND	0.4269 (probable antigen)
	S	1	Host endoplasmic reticulum	0.4583 (probable antigen)
	3a	1	Host cytoplasm	0.2325 (NON-antigen)
	3b	0	Host cytoplasm	0.497 (probable antigen)
	3c	2	Host cell membrane	0.374 (NON-antigen)
	M	3	Host cell membrane	0.4006 (probable antigen)
	5a	0	Host cytoplasm	0.2144 (NON-antigen)

	5b	0	Host nucleus	0.51 (probable antigen)
	N	0	Host endoplasmic reticulum	0.7241 (probable antigen)
AIV	PB2	0	Host cytoplasm. Host nucleus.	0.5259 (probable antigen)
	PB1	0	Host cytoplasm. Host nucleus.	0.5041 (probable antigen)
	PA	0	Host cytoplasm.	0.5232 (probable antigen)
	HA	0	Host cell membrane	0.4397 (probable antigen)
	NP	0	Host nucleus	0.5405 (probable antigen)
	NA	1	Host cell membrane	0.6011 (probable antigen)
	M	0	Host nucleus	0.4696 (probable antigen)
	NS	0	Host nucleus	0.4613 (probable antigen)

---

ND (Not Detected)- Virus-mPLoc algorithmn was not able to perform the test due to computational limitations.

**Table 3.4.** B cell epitopes predicted by both Bcepred and IEDB and antigenicity value predicted by Vaxijen v2.0.

<b>Virus</b>	<b>Protein name</b>	<b>Antigenicity value</b>	<b>B cell epitopes</b>	<b>Antigenicity value for epitopes</b>
NDV	F	0.5530 (probable antigen)	NMPKDKEACAKAPLDAYNR	-0.0179 (non-antigen)
			QGSVATSGGRRQ	0.5669 (probable antigen)
			GPQITSPALTQL	0.4637 (probable antigen)
			LTKLGVGNNQLS	0.8365 (probable antigen)
			SVIEKLDTSYCIE	0.412 (probable antigen)
			TRIVTFPMSP	0.4618 (probable antigen)
			YSKTEGALT	0.7162 (probable antigen)
			ILDSQVIVTGNLDIS	0.7208 (probable antigen)
			DKVNVRLTS	1.4286 (probable antigen)
NDV	HN	0.5624 (probable antigen)	VMLENEEREAK	0.9112 (probable antigen)
			YSMGTSTP	0.3428 (non-antigen)
			IAISKTE	1.6242 (probable antigen)
			TSLSSSQ	0.2866 (non-antigen)
			YQINGASNNSG	0.012 (non-antigen)
			IPAPTTGSGC	-0.157 (non-antigen)

			GVLRTSAT	0.1038 (non-antigen)
			INLDDTQNRKSCS	1.1857 (probable antigen)
			SKVTETEE	0.8353 (probable antigen)
			GGLKPNSP	0.4523 (probable antigen)
			RMAKSSYKPGRFGG	0.9639 (probable antigen)
			AVFDDISRSRVTRVSSSST	0.0719 (non-antigen)
IBV	S	0.4583 (probable antigen)	VNISSEFNNAGSSSG	0.6477 (probable antigen)
			ILCDGSP	-0.4232 (non-antigen)
			IVYRENS	1.072 (probable antigen)
			TGANPNP	1.2221 (probable antigen)
			YQTKTA	1.0952 (probable antigen)
			PLQGGCK	0.7676 (probable antigen)
			LVYVTKSGGS	0.5791 (probable antigen)
			NIYGRT	-0.2949 (non-antigen)
			GILTSRNETG	1.0589 (probable antigen)
			IKITNGTRRFR	1.0172 (probable antigen)
			PLMSKCGKKS	0.5522 (probable antigen)

AIV	HA	0.5232 (probable antigen)	IVTTSNA	0.7831 (probable antigen)
			IGYQSTNST	1.5192 (probable antigen)
			VTYSGTS	0.8192 (probable antigen)
			RWLTHKS	-1.8023 (non-antigen)
			AQYTNTEG	0.3787 (non-antigen)
			NLYKKTDDT	0.1291 (non-antigen)
			PLVNGQQ	1.2125 (probable antigen)
			QTLRVRSNG	0.3307 (non-antigen)
			GMAADKEST	0.9249 (probable antigen)
			DKITSKV	0.3732 (non-antigen)
AIV	NA	0.6011 (probable antigen)	LHFKQNE	1.7294 (probable antigen)
			RNWSKPQ	-0.1237 (non-antigen)
			FAPFSKDNS	0.846 (probable antigen)
			PYVSCSP	0.9301 (probable antigen)
			TTLDNKHSN	1.5257 (probable antigen)
			IAWSSSS	0.974 (probable antigen)
			VCVTGDD	0.2885 (non-antigen)

VMTDGGASGRAD	0.5806 (probable antigen)
GLVGDTPRNEDSSSNSNCKDPNNERGN	0.5438 (probable antigen)
VWMGRTISKDSRSG	1.1047 (probable antigen)
WTMANSKSQV	0.5077 (probable antigen)
GIFSVEG	1.0312 (probable antigen)
ELIRGRP	0.2952 (non-antigen)

---



**Table 3.5.** Epitopes specific to selected MHC-I alleles.

<b>Virus</b>	<b>Proteins</b>	<b>Allele</b>	<b>Start</b>	<b>End</b>	<b>Peptide</b>	<b>Percentage Rank</b>	<b>Antigenicity</b>
NDV	F	HLA-B*40:01	18	31	GEFDATYQKNISIL	0.04	1.0369 (probable antigen)
		HLA-B*58:01	37	45	VAVGKMQQF	0.09	0.8708 (probable antigen)
		HLA-A*26:01	48	57	SVIEELDTSY	0.02	0.4218 (probable antigen)
		HLA-A*02:01	1	9	QLLGIQVNL	0.02	0.7072 (probable antigen)
		HLA-B*07:02	17	25	SPALTQLTI	0.07	0.9003 (probable antigen)
		HLA-B*07:02	11	20	APLMLITRTM	0.08	0.7482 (probable antigen)
NDV	HN	HLA-A*01:01	50	58	YTDPYPLIF	0.01	0.9134 (probable antigen)
		HLA-A*26:01	4	12	DISDVTSFY	0.01	0.7315 (probable antigen)
		HLA-A*03:01	18	27	RVQQAILSIL	0.03	1.1574 (probable antigen)
		HLA-B*08:01	56	64	LIFHRNHTL	0.02	0.8004 (probable antigen)
		HLA-A*01:01	36	45	PSFDMSTTHY	0.04	0.8922 (probable antigen)
IBV	S	HLA-A*01:01	28	37	VTDSAVSYNY	0.01	0.936 (probable antigen)
		HLA-B*40:01	30	38	REYNGLLVL	0.01	0.5837 (probable antigen)
		HLA-B*40:01	43	51	GEFNISLLL	0.01	0.9489 (probable antigen)
		HLA-B*40:01	29	38	AREYNGLLVL	0.04	0.4692 (probable antigen)
		HLA-A*01:01	42	50	ITAEMQALY	0.02	0.7679 (probable antigen)

		HLA-A*03:01	51	59	KAGGPITYK	0.02	1.4952 (probable antigen)
		HLA-A*02:01	24	32	VLIPNSFNL	0.03	0.5258 (probable antigen)
		HLA-A*26:01	27	35	NVTDSAVSY	0.03	0.9915 (probable antigen)
		HLA-B*58:01	33	42	LSILKTYIKW	0.08	0.6289 (probable antigen)
AIV	HA H9N2	HLA-B*07:02	12	20	KPMIGPRPL	0.01	1.0267 (probable antigen)
		HLA-A*01:01	54	63	PTDTEQNNLY	0.01	0.499 (probable antigen)
		HLA-B*07:02	42	50	VPVTHTKEL	0.02	1.328 (probable antigen)
		HLA-B*40:01	56	65	HEFSEIEARL	0.04	0.9517 (probable antigen)
		HLA-B*40:01	59	67	SEIEARLNM	0.04	1.1402 (probable antigen)
		HLA-A*03:01	27	36	RIDYYWSVLK	0.06	0.7938 (probable antigen)
		HLA-A*01:01	17	25	NADKICIGY	0.07	0.8506 (probable antigen)
AIV	NA	HLA-A*01:01	27	36	MADYSIDSSY	0.04	0.8233 (probable antigen)
		HLA-B*58:01	29	37	LATTVTLHF	0.08	1.1589 (probable antigen)
		HLA-B*44:03	5	14	KELCPKIVEY	0.05	1.1453 (probable antigen)

In a comparable manner, various MHC-II epitopes were identified as potential antigens, as seen in **Table 3.6**. The F and HN proteins of NDV were shown to include predicted epitopes, specifically GRRQKRFI~~GA~~VIGSV in the F protein and YPLIFHRNHTLRGVF in the HN protein. The antigenicity values of these epitopes were determined to be similar to those of their corresponding proteins. The epitope SAVSYNYLADAGLAI had the greatest antigenicity values within the IBV-S protein. The AIV-HA did not exhibit any expected antigenic epitopes, but a predicted epitope (VCFLMQIALATTVT) with an antigenicity value of 1.1186 was identified for the AIV-NA. It is noteworthy that MHC-I epitopes exhibited a higher abundance when compared to MHC-II epitopes.

**Table 3.6.** Epitopes specific to selected MHC-II alleles.

Virus	Proteins	Allele	Start	End	Peptide	Percentage Rank	Antigenicity
NDV	F	HLA-DPA1*02:01/DPB1*14:01	111	125	GRRQKRFIGAVIGSV	0.1	0.8306 (probable antigen)
NDV	HN	HLA-DRB3*02:02	474	488	YPLIFHRNHTLRGVF	0.1	0.4636 (probable antigen)
IBV	S	HLA-DRB3*01:01	34	48	SYNYLADAGLAILDT	0.02	0.798 (probable antigen)
		HLA-DRB3*01:01	31	45	SAVSYNYLADAGLAI	0.05	0.9014 (probable antigen)
		HLA-DRB3*01:01	33	47	VSYNYLADAGLAILD	0.02	0.9472 (probable antigen)
		HLA-DRB3*01:01	32	46	AVSYNYLADAGLAIL	0.03	0.8245 (probable antigen)
		HLA-DRB3*01:01	35	49	YNYLADAGLAILDTS	0.03	0.8156 (probable antigen)
AIV	NA	HLA-DRB1*01:01	20	34	VCFLMQIAILATTVT	0.1	1.1186 (probable antigen)

### 3.2.2. Phylogenetic Analysis

Having predicted the antigenicity of specific proteins and epitopes of NDV, IBV, and AIV. It is now our aim to validate the antigenicity of these protein antigens using field strains collected in the Philippines. Phylogenetic analyses of the field viral strain sequence of NDV-F and -HN genes, the IBV-S gene, and AIV were performed through the use of MEGA software (Tamura et al., 2021).

#### 3.2.2.1. NDV-F Gene

A total of 57 complete NDV-F gene sequences were used to infer the phylogenetic tree shown in **Figure 3.1**. Phylogenetic analysis based on sequences of F genes revealed that the Philippine isolates belonged to sub-genotype VII, which are known to be virulent NDV strains. The NDV genotypic classification used was based on the updated NDV nomenclature as described by Dimitrov et al., (2019). The NDV reference sequence used in this chapter is summarised in **Annex 1**.

To provide further understanding of the characteristics of the PH NDV isolates, molecular pathotyping was performed by analysing the amino acid sequences of the proteolytic cleavage site (residues 112-117) of the F protein. The Philippine NDV-F strain has the <sup>112</sup>RRQKRF<sup>117</sup> pattern (as highlighted in the black box), which bears a striking resemblance to the velogenic reference NDV-F isolate (AEZ00711) that is already documented (**Figure 3.2**). Additionally, all N-linked glycosylation sites at residues 85, 191, 366, 447, 471, and 541 are conserved in the selected Philippine strain; previous studies suggest that N-glycosylation residues might play an important role in fusion promotion (McGinnes et al., 2001). **Figure 3.3** provides a detailed examination of the three-dimensional representation of the NDV-F protein. The amino

acid motifs corresponding to the cleavage sites (<sup>112</sup>RRQKRF<sup>117</sup>) of the Philippine isolate NDV-F are presented and thoroughly examined. NDV may be categorised into three pathotypes, namely velogenic, mesogenic, and lentogenic, based on the reported pathogenicity in susceptible chickens (Stear, 2005). Virulent strains of avian pathogens elicit systemic infection and induce severe lesions in chickens (Miller et al., 2010). The amino acid present at the cleavage site of the F protein plays a crucial role in determining the level of virulence exhibited by these strains (Peeters et al., 1999).

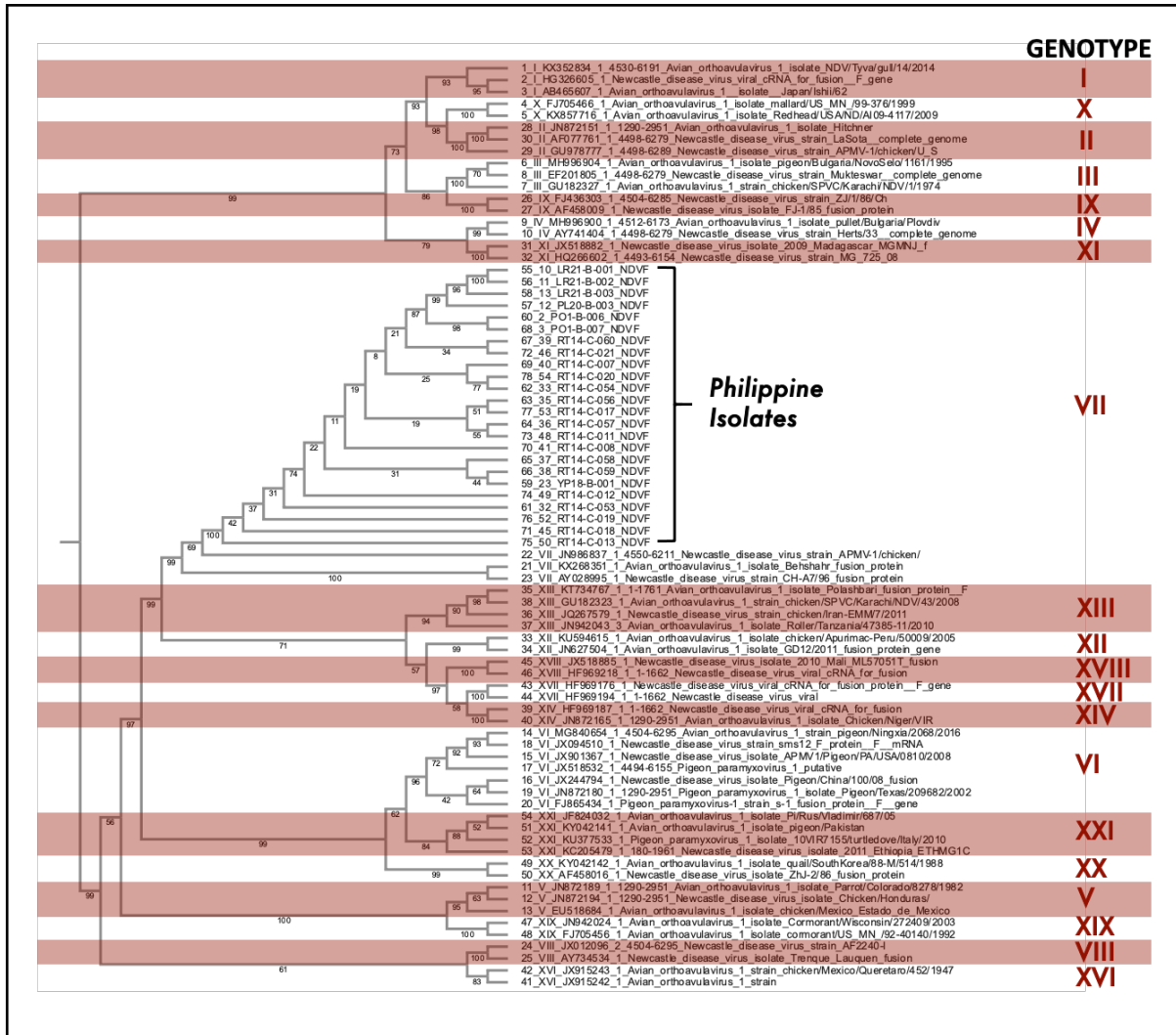


**Figure 3.1. Phylogenetic analysis of the NDV-F complete gene shows the lineage of the Philippine isolates.** The evolutionary history was inferred using the neighbor-joining method. The optimal tree is shown. The percentage of replicate trees in which the associated taxa clustered together in the bootstrap test (1000 replicates) are shown above the branches (Tamura et al., 2021). Reference sequences used: HQ39795, GQ245777, FJ597580, AY626268, and vaccine strains (AF077761 and JN872151). It is worth noting that the PH isolates clustered with Genotype VII.

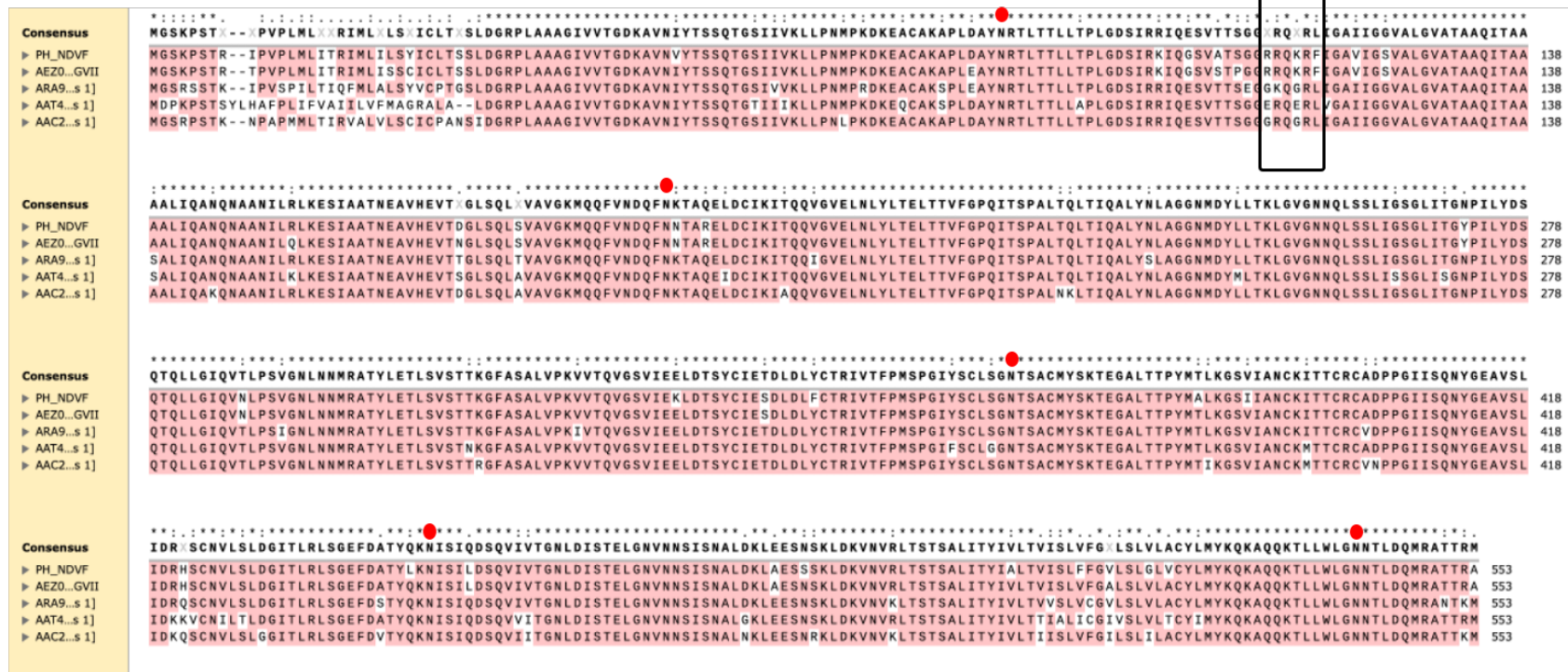


**Figure 3.2. Multiple sequence analysis of the Philippine NDV-F gene.** The image shows a comprehensive investigation of the F gene of NDV in the Philippines by multiple sequencing analyses. Molecular pathotyping was performed by analysing the amino acid sequences of the proteolytic cleavage site (residues 112-117) of the F protein. The Philippine NDV-F strain has the <sup>112</sup>RRQKRF<sup>117</sup> pattern (as highlighted in the black box), which bears a striking resemblance to the virulent reference NDV-F isolate (AEZ00711) that is already documented. Highlighted in pink are amino acids that match the consensus sequence. The red dot denotes N-linked glycosylation sites.



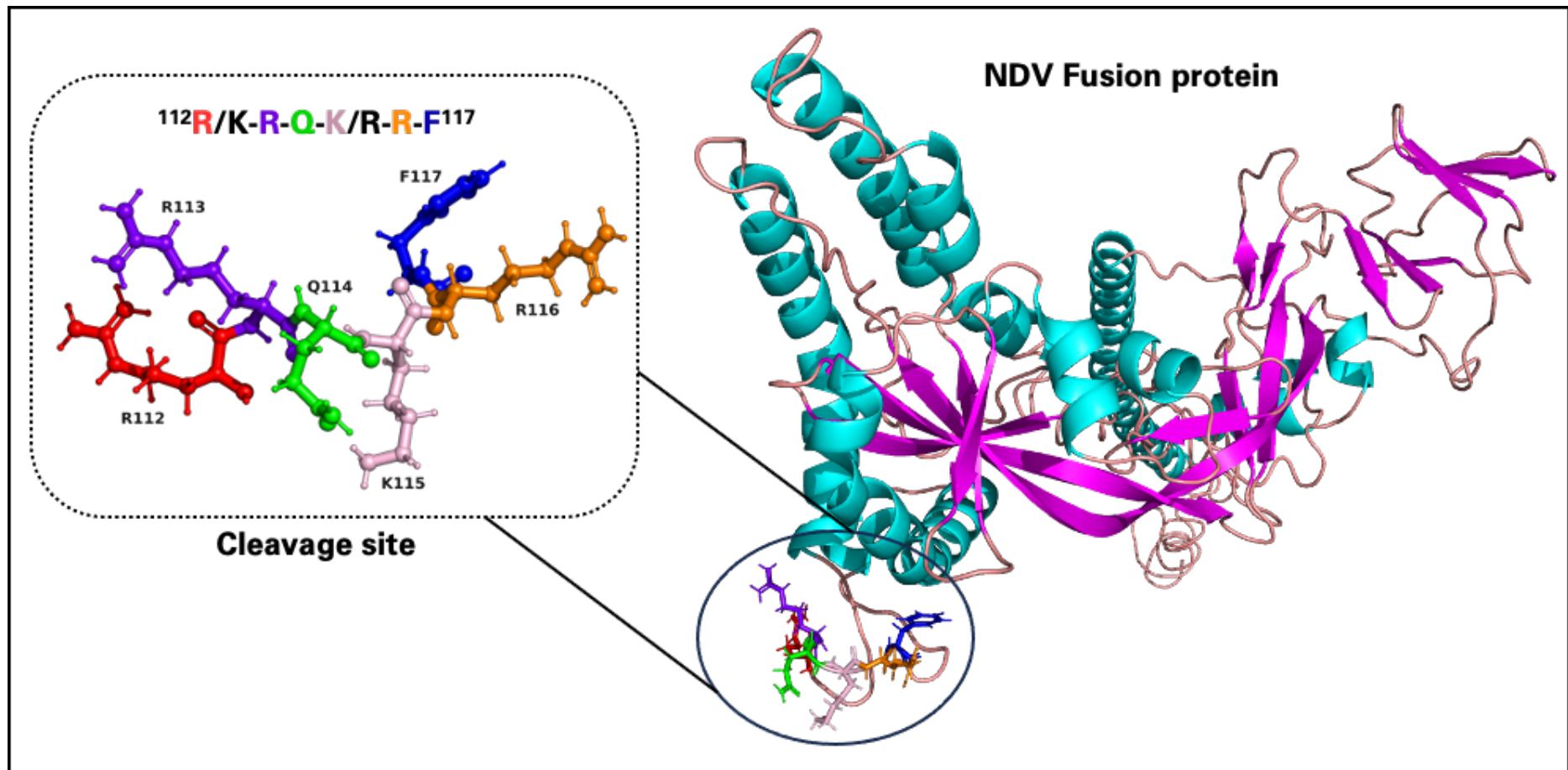


**Figure 3.3. Representative NDV-F protein cleavage site.** The amino acid motifs representing the cleavage sites ( $^{112}\text{RRQKRF}^{117}$ ) of the Philippine isolate NDV-F are shown. The illustration depicts the representation of each amino acid residue as a ball and stick model, with distinct colours assigned to each. The virulence of strains is responsible for inducing systemic infection and causing severe lesions in chickens. The primary factor determining virulence is the specific amino acid present at the cleavage site of the F protein.

### 3.2.2.2. IBV-S Gene

The phylogenetic tree (**Figure 3.4**) was generated by employing a dataset comprising the PH IBV strain and 68 reference strains, which encompassed established genotypes and lineages (Yuqiu Chen et al., 2017; L. Jiang et al., 2017; Valastro et al., 2016) (**Annex 1**). The Mega version 11 software (Tamura et al., 2021) was utilised for this purpose. To evaluate the reliability of the branches, we employed the neighbor-joining method and performed 1000 bootstrapping repetitions. The findings indicated that our IBV PH strain had a similar clustering pattern to IBV GI viruses. Although the results indicated a 100% resemblance between the PH strain and the Moroccan GI-13 strain, it is important to note that the depth of the sequence comparison study conducted may not provide sufficient definitive proof. The GI-13 lineage is widely distributed across many regions of the globe. Previous studies have examined a total of 70 viruses belonging to this lineage, encompassing both vaccine strains and naturally occurring virulent field strains. These viruses were previously classified as the 793B type, which is also referred to as 4/91 and CR88 (Valastro et al., 2016).

Alignment of the partial S1 glycoprotein sequence of Philippine IBV isolates with that of the published IBV strain identified most sequence variations between residues 50–77 and 117–141 (**Figure 3.5**). Both of these sequence regions correspond to known hyper-variable regions (HVR) (Yan et al., 2021). The hyper-variable regions (HVRs) of the S1 gene influence the antigenic relatedness and receptor binding with host cells; therefore, most studies have utilised the S1 subunit for IBV genotyping and classification (Yan et al., 2021). HVR1 and HVR2 contain sequences that have been associated with specific IBV serotypes (Cavanagh et al., 1988; Kusters et al., 1989) and serotype-specific neutralising epitopes (Kant et al., 1992). **Figure 3.6** presents an

in-depth look at the structural characteristics of the IBV-S protein. The consensus motif R-X-[K/R]-R↓S (Kusters et al., 1989; Valastro et al., 2016), consisting of four amino acid residues, was identified as the furin recognition motif at the S1/S2 cleavage site. This motif was also emphasised in the image.

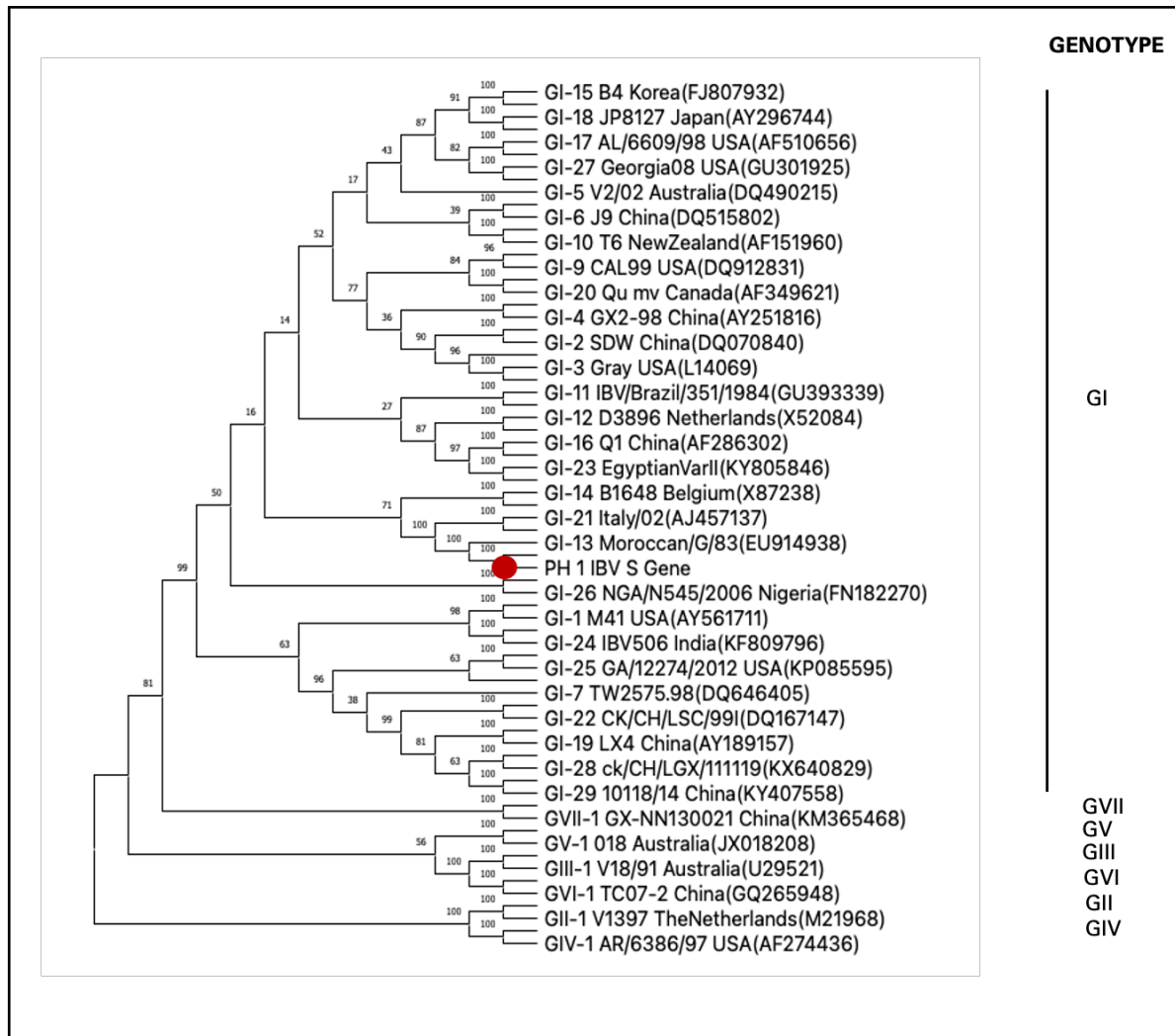


**Figure 3.4. Phylogenetic analysis of the IBV-S gene showing lineage of the Philippine isolates (PH 1 IBV S Gene).** The evolutionary history was inferred using the neighbor-joining method. The optimal tree is shown. The percentage of replicate trees in which the associated taxa clustered together in the bootstrap test (1000 replicates) are shown above the branches (Tamura et al., 2021). The red dot on the phylogenetic tree represents the placement of the Philippine isolate, which is seen to be closely grouped within the IBV GI genotype.

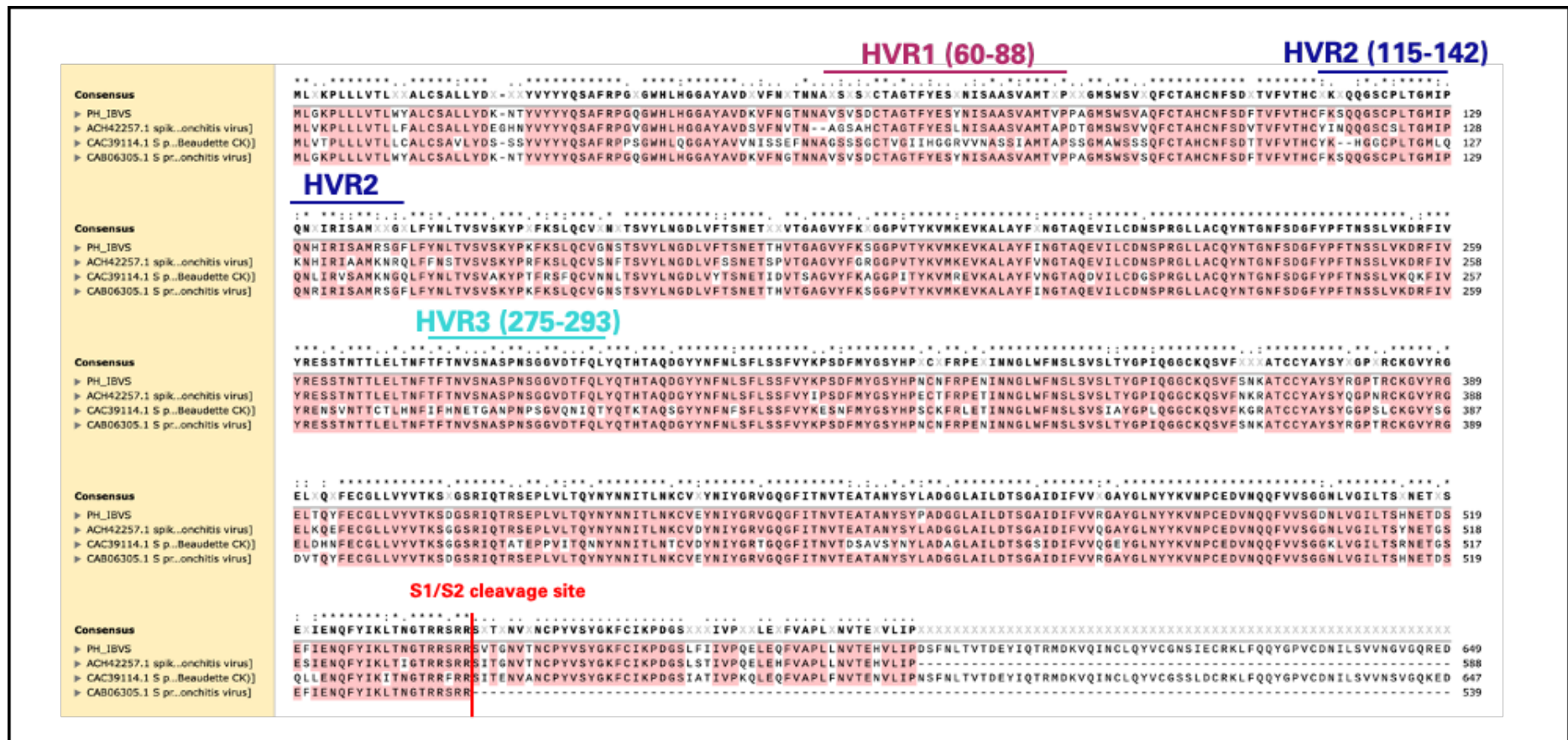


**Figure 3.5. Multiple sequence analysis of the Philippine IBV-S gene.** The image shows a comprehensive investigation of the S gene of IBV in the Philippines by multiple sequencing analyses. The three hyper-variable regions (HVR1, HVR2, and HVR3) of the IBV-S are shown here, denoted by the black line above the alignment. The hyper-variable regions (HVRs) of the S1 gene influence the antigenic relatedness and receptor binding with host cells; therefore, most studies have utilised the S1 subunit for IBV genotyping and classification. The PH isolates were compared to reference and vaccine isolates of IBV-S. Highlighted in pink are amino acids that match the consensus sequence. Multiple substitutions can be observed within the HVRs.

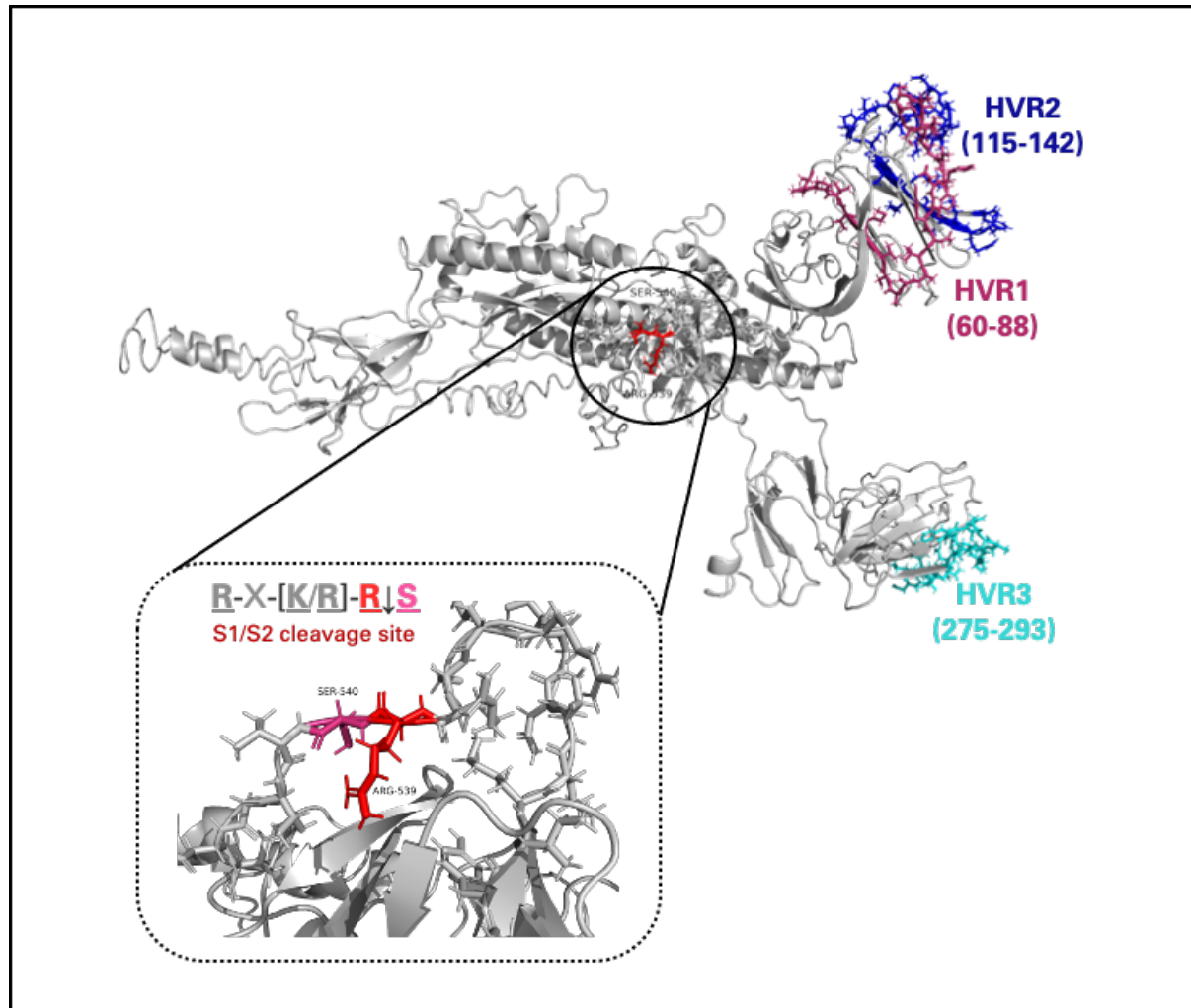


**Figure 3.6. Representative furin recognition consensus motif of the IBV-S protein.** All S-gene sequences contain the canonical 4 amino acid (aa) residue furin recognition consensus motif R-X-[K/R]-R↓S at the S1/S2 cleavage site (X is any residue, ↓ is cleavage position, and underlined residues are conserved). Hypervariable regions were highlighted and shown in different colours.

### 3.2.2.3. AIV-HA (H9N2) Gene

The phylogenetic study involved the use of 177 gene sequences of AIV-HA (H9N2). The findings indicated that the Philippine AIV-HA (H9N2) isolate was classified under the A genotype, more precisely the A5 genotype. The A series genotype, encompassing genotypes A0-A9, had a distribution over Asia, the Middle East, and Europe (G. Dong et al., 2011) (**Figure 3.7**).

By using molecular pathotyping, we successfully identified the sequence motif at residues 335-341 of the connecting peptides (HA1-HA2) in the PH-HA protein as <sup>335</sup>KSSR/GLF<sup>341</sup> (**Figure 3.8**). Prior research has demonstrated a slightly different sequence motif of <sup>335</sup>RSSR/GLF<sup>341</sup>, which is suggestive of reduced pathogenicity (J.-H. Liu et al., 2004). According to previous studies (Chrzastek et al., 2018; J.-H. Liu et al., 2004), it has been shown that this particular motif is commonly seen in LPAIV H9N2 viruses originating from the Middle East and Asia (Chrzastek et al., 2018). Furthermore, these viruses have shown a high level of adaptation to poultry (Aamir et al., 2007). Consistent with our findings, previous research has indicated that AIV H9N2 viruses have the potential to undergo specific substitutions at the linking peptide sequence between the HA1 and HA2 domains, resulting in the acquisition of the dibasic pattern K-S-S-R at the cleavage site (Ghorbani et al., 2016). This alteration has been associated with an enhanced pathogenicity of the viruses (Soda et al., 2011) (**Figure 3.9**).



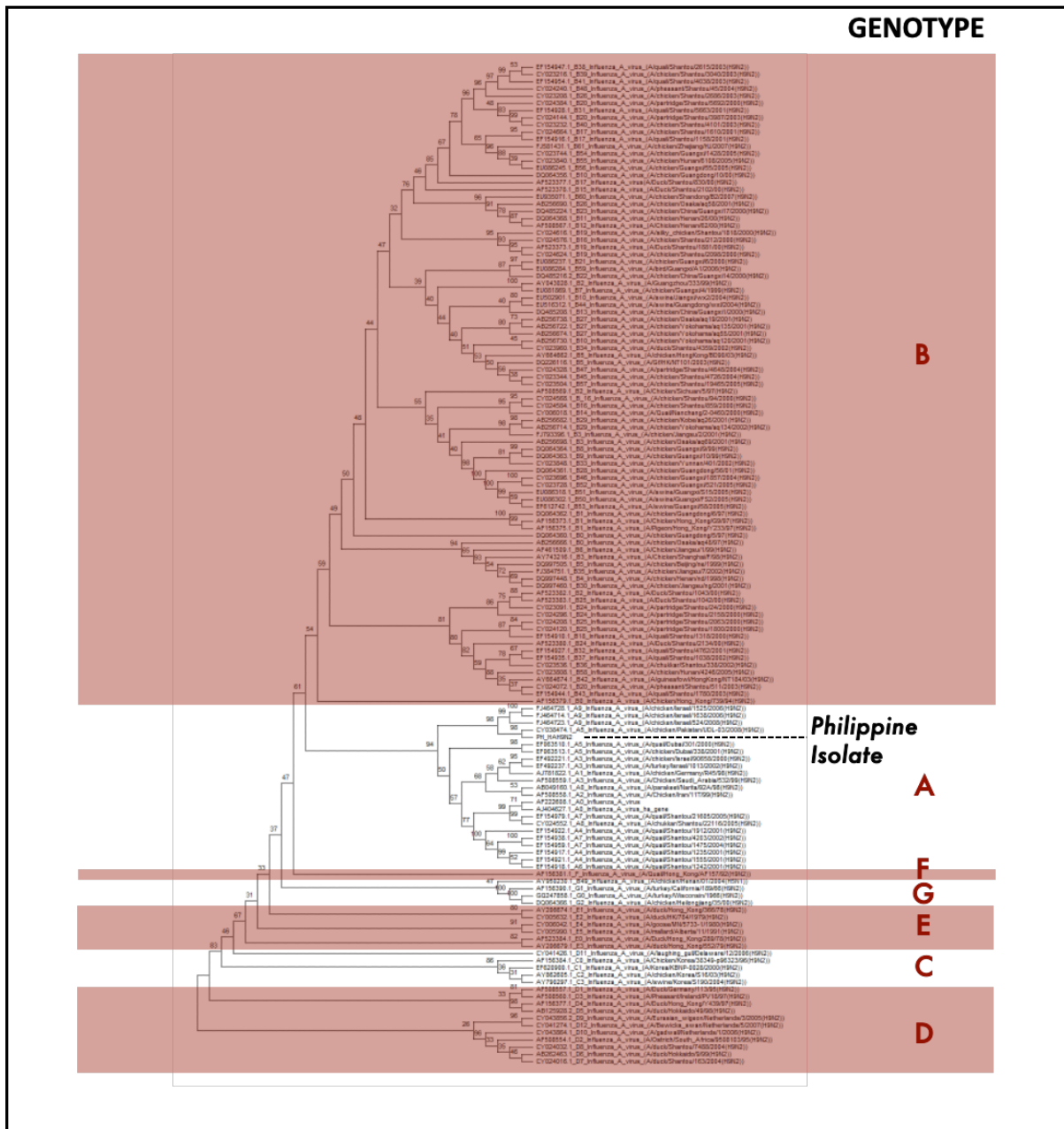


**Figure 3.7. Phylogenetic analysis of the AIV-HA complete gene showing lineage of the Philippines isolates (PH\_HAH9N2).** The evolutionary history was inferred using the neighbor-joining method. The optimal tree is shown. The percentage of replicate trees in which the associated taxa clustered together in the bootstrap test (1000 replicates) are shown above the branches (Tamura et al., 2021). Within the seven genotypic clusters of AIV H9N2 viruses (A-G) shown in the phylogenetic tree, the Philippines isolate clustered with the A genotype.

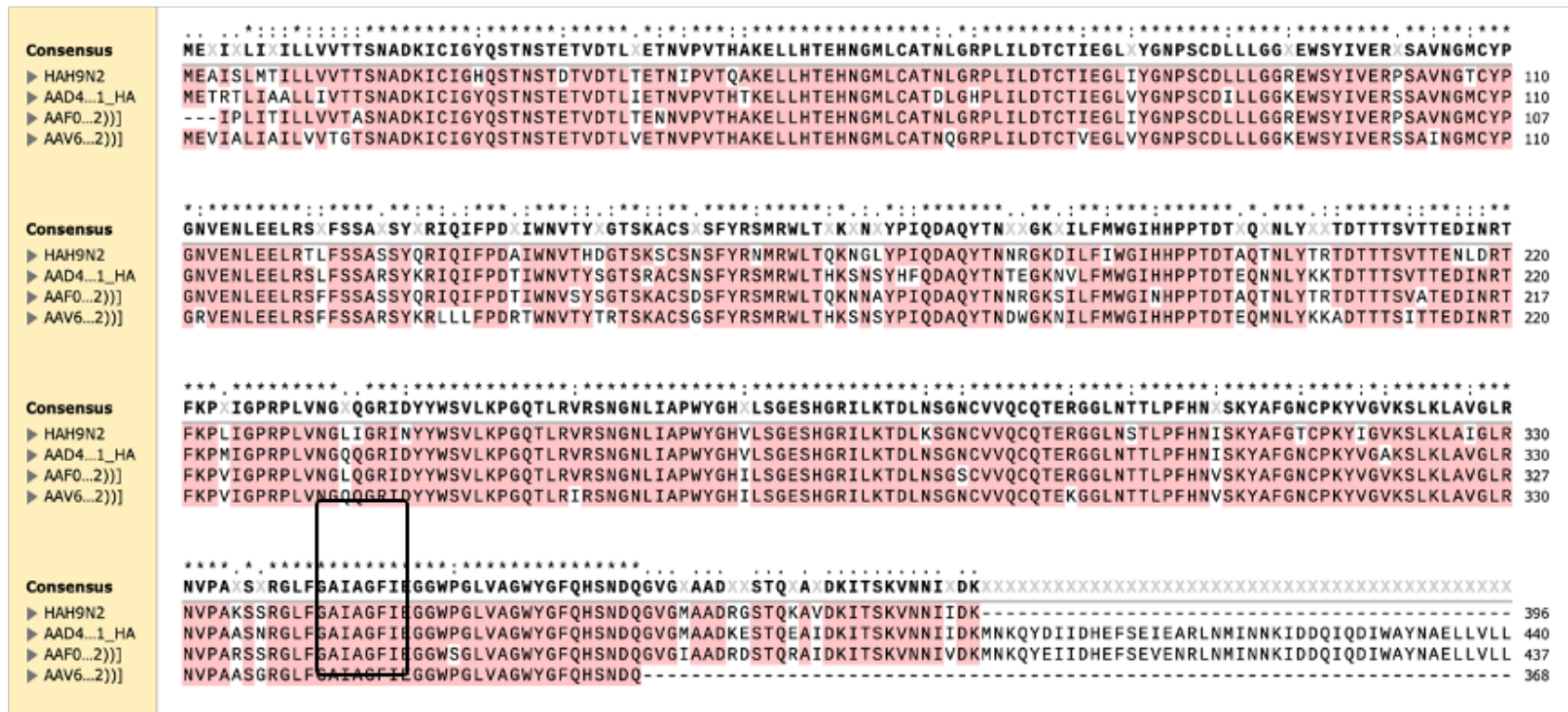


**Figure 3.8. Comprehensive analyses of the amino acid residue of the Philippine AIV-HA (H9N2) gene.** The image shows a comprehensive investigation of the HA gene of AIV in the Philippines by multiple sequencing analyses. Molecular pathotyping was performed by analysing the amino acid sequences of the sequence motif at HA1-HA2 connecting peptides (residues 335-341) of the HA protein. The Philippine AIV strain has the <sup>335</sup>KSSR/GLF<sup>341</sup> pattern (as highlighted in the black box). Highlighted in pink are amino acids that match the consensus sequence.



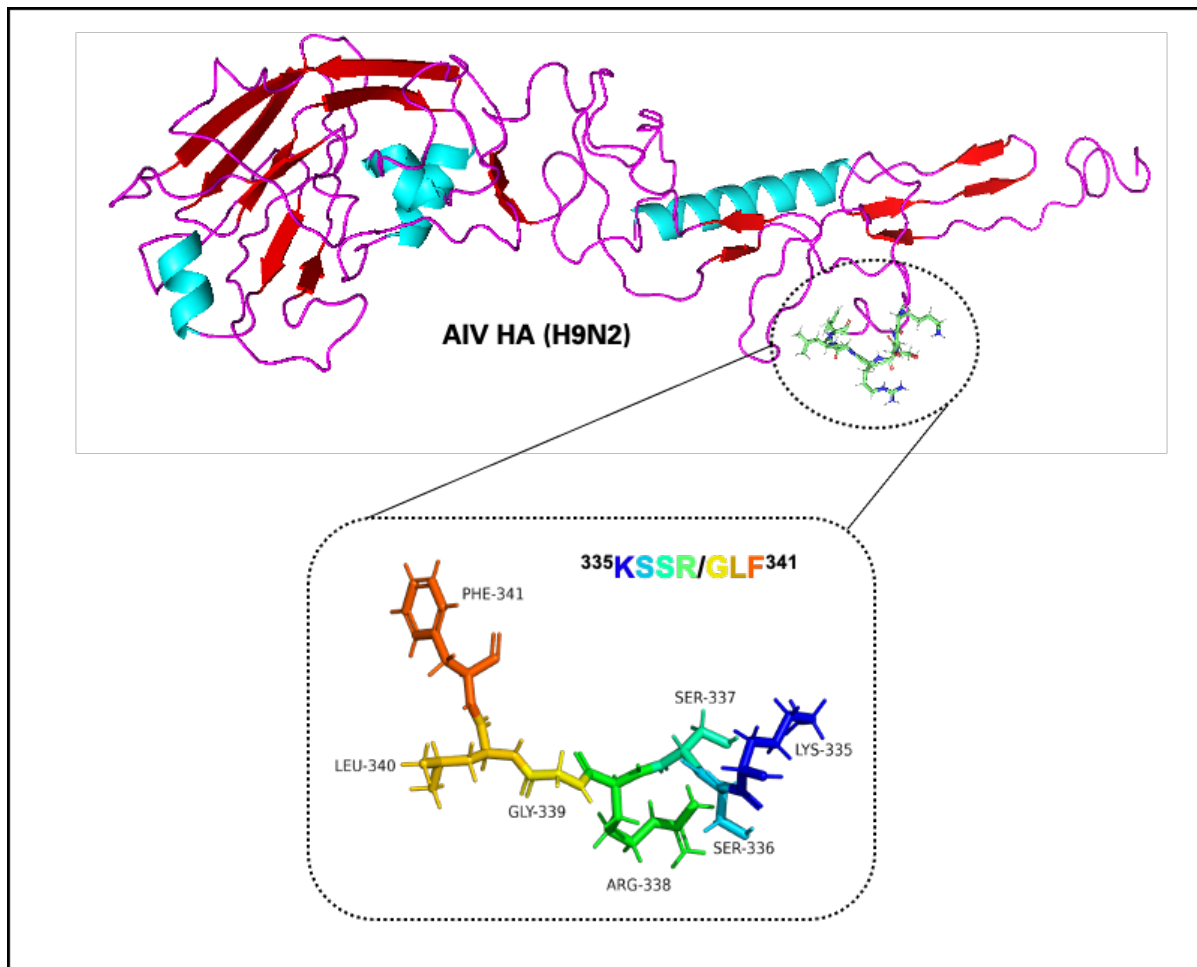


**Figure 3.9. Representative AIV-HA protein cleavage site.** The provided image is a representative three-dimensional cartoon representation of the AIV-HA gene. The protein motif HA1-HA2 is encircled (in back dots). The provided image displays a magnified view of the amino acid residues of the  $^{335}\text{KSSR/GLF}^{341}$  protein motif. The representation of each residue is depicted using distinct colours.

### 3.3. Chapter Discussion

The use of reverse vaccinology plays a pivotal role in the development of recombinant vaccines through its ability to facilitate *in silico* analysis of pathogen genomes. This methodology facilitates the identification of proteins that possess high antigenicity and are secreted, both of which are crucial attributes for the production of vaccines. The main goals of this chapter are to (1) identify antigenic proteins and epitope regions that are specifically recognised by the B and T cell components of the adaptive immune response for the creation of vaccines or serological diagnostic assays (Can, Köseoğlu, et al., 2020; Dangi et al., 2018) and (2) characterise antigenic proteins isolated from the Philippine viral field strains (NDV, IBV, and AIV).

For the first part of this chapter, the potential antigenicity of all proteins from NDV, IBV, and AIV, with the exception of IBV 3a, 3c, and 5a, had been predicted. The predicted antigenicity values for the potential vaccine candidate proteins, namely NDV-F, NDV-HN, IBV-S, and AIV-HA, did not exhibit significant differences. However, based on the findings of *in silico* analysis, NDV-F, NDV-HN, IBV-S, and AIV-HA proteins were identified as superior vaccine candidates compared to the other proteins. The physicochemical investigation revealed that the NDV-HN and AIV-HA proteins exhibit a negative GRAVY value, suggesting their hydrophilic nature and favourable interaction with surrounding water molecules (Droppa-Almeida et al., 2018). The proteins NDV-F, NDV-HN, IBV-S, and AIV-HA possess stable and soluble properties that are crucial factors in conducting biophysical studies relevant to the development of epitope-based vaccines. Furthermore, the NDV-HN, IBV-S, and AIV-HA proteins have a moderate aliphatic index, suggesting their stability throughout a broad range of temperatures (Shey et al., 2019). These proteins also include less than two

transmembrane helices, which facilitates their cloning, expression, and purification processes (Meunier et al., 2016). Additionally, they have a substantial molecular weight and an estimated half-life exceeding 10 hours. These qualities demonstrate the potential of NDV-F, NDV-HN, IBV-S, and AIV-HA proteins as viable candidates for vaccine antigens. When analysing the secondary structure of NDV-F, NDV-HN, IBV-S, and AIV-HA proteins, it was shown that random coils accounted for more than 49% of the overall structure. The detection of this highly predicted random coil structure indicates that these proteins possess an affinity for antibody recognition (Shaddel et al., 2018). The findings presented here are consistent with prior research that employed the NDV-F, NDV-HN, IBV-S, and AIV-HA proteins as the preferred antigens for vaccine production (L. Liu et al., 2019; Lüschow et al., 2001; Paldurai et al., 2014; Tan et al., 2016; Zahid et al., 2020).

Epitope regions that are unique to B and T cells were predicted in all proteins, namely NDV-F, NDV-HN, IBV-S, AIV-HA, and AIV-NA. Additionally, antigenicity analysis was conducted for all the anticipated epitopes (Doytchinova & Flower, 2007). The observations associated with B-cell epitopes showed a substantial presence of epitopes that exhibited a high degree of antigenicity. The antigenicity value was very high for DKVNVRLTS, IAISKTE, TGANPNP, IGYQSTNST, and LHFQNE, corresponding to NDV-F, NDV-HN, IBV-S, AIV-HA, and AIV-NA proteins. In the same way, the study also made predictions for epitopes that exhibited high levels of antigenicity for both MHC-I and MHC-II alleles. Among these predicted epitopes, for MHC-I alleles, GEFDATYQKNISIL, RVQQAILSIL, KAGGPITYK, SEIEARLNM, and LATTVTLHF epitopes belonging to NDV-F, NDV-HN, IBV-S, AIV-HA, and AIV-NA proteins had very high antigenicity values, whereas for MHC-II alleles,

GRRQKRFIGAVIGSV, YPLIFHRNHTLRGVF, VSYNYLADAGLAILD, and VCFLMQIAILATTVT epitopes belonging to NDV-F, NDV-HN, IBV-S, and AIV-NA proteins also had significant antigenicity values.

The results of this study suggest that a combination of these epitopes has the potential to elicit a neutralising antibody response or be utilised in the creation of an epitope-based peptide vaccine due to their affinity for both B and T cells (Can, Köseoğlu, et al., 2020). Furthermore, it was hypothesised that these epitopes possess the potential to serve as antigens capable of capturing antibodies against NDV, IBV, and AIV in enzyme-linked immunosorbent assays (ELISA) or Western blotting assays performed during viral infection (Can, Köseoğlu, et al., 2020; Droppa-Almeida et al., 2018; Ghorbani et al., 2016; Zenglei Hu et al., 2020; Valastro et al., 2016).

In the subsequent section of this chapter, viral isolates obtained from the Philippines were characterised using *in silico*-based methodologies. The lineage of the Philippine isolates of NDV-F, NDV-HN, IBV-S, and AIV-HA proteins was determined using phylogenetic analysis (Cavanagh et al., 1988; Ghorbani et al., 2016; T. A. Khan et al., 2010; Selim et al., 2018). The Philippine NDV-F isolate exhibited clustering with the velogenic genotype VII of NDV (Dimitrov et al., 2019). The IBV isolate from the Philippines was shown to be closely related to IBV genotype I. This genotype includes both vaccine strains and naturally occurring virulent field strains (Valastro et al., 2016). Moreover, the Philippine AIV-HA H9N2 isolate had a close genetic relationship with the AIV H9N2 genotype A, which includes genotypes A0-A9. This particular genotype has been found in several regions, including Asia, the Middle East, and Europe (Ghorbani et al., 2016).

Moreover, in order to achieve a comprehensive understanding of the virulence characteristics shown by the isolates from the Philippines, we conducted a molecular pathotyping analysis. This involved aligning the reference genome sequences of each isolate with those obtained from the Philippine isolates. Through the implementation of this methodology, we were able to enhance the reliability of the findings derived from the phylogenetic studies.

The Philippine NDV isolate is related to genotype VIId viruses seen in Israeli, Chinese, Korean, and other Middle Eastern strains (Selim et al., 2018). This relationship is determined based on the F protein cleavage site, which contains a sequence of basic amino acids ( $^{112}RRQKRF^{117}$ ). Previous research has classified NDVs based on the cleavage site of the F gene, resulting in the identification of various sublineages. Specifically, sublineages 7a-, 7b-, and 7d-group I are characterised by the presence of four basic amino acids (RRQKR/F), whereas sublineages 7c- and 7d-group II exhibit five basic amino acids (RRRKR/F) (Cattoli et al., 2010; Dimitrov et al., 2019).

The antigenic relatedness and receptor interaction with host cells are influenced by the hyper-variable regions (HVRs) of the S1 gene. As a result, several studies have focused on using the S1 subunit for the genotyping and classification of IBV (Valastro et al., 2016). Through the HVRs of the Philippine IBV isolate, we were able to categorise the isolate together with genotype I (GI). However, some researchers have documented that the genetic classification utilising the hypervariable region 1 (HVR1) of the S1 gene exhibits discrepancies when compared to the groupings established through the entirety of the S1 gene. Thus, it is worth considering using the complete

S1 gene sequence for future designations of novel IBV lineages or genotypes (Kusters et al., 1989; Valastro et al., 2016).

The PH AIV strain shared sequence similarity to the A series genotype, encompassing genotypes A0-A9, had a distribution over Asia, the Middle East, and Europe (G. Dong et al., 2011; Ghorbani et al., 2016). It is noteworthy that our findings revealed precise alterations occurring at the linking peptide sequence between HA1 and HA2, resulting in the acquisition of the dibasic pattern K-S-S-R at the cleavage site (Ghorbani et al., 2016). This alteration significantly enhances the pathogenicity of the observed strains (Soda et al., 2011; Tombari et al., 2011).

Taken together, the utilisation of computer-based methodology has significantly enhanced the reliability and validity of *in silico* approaches in the realm of biological research, specifically in the realm of predicting potential vaccine candidate proteins. By employing computational methods, we successfully validated prospective antigenic proteins and predicted epitopes that hold promise for their application in the development of a vaccine candidate or serological diagnostic screening. The results of this study indicate that the combination of these epitopes exhibits promise in inducing a neutralising antibody response or serving as a feasible approach for epitope-based peptide vaccination. Furthermore, we successfully confirmed the antigenicity of these protein antigens by using field strains obtained from the Philippines.

# CHAPTER 4

## Establishment of CRISPR/Cas9 Approach for the Generation of Recombinant ILTV

### 4.1. Introduction

The CRISPR-associated protein nuclease (Cas) system has emerged as a groundbreaking method for gene editing (Doudna & Charpentier, 2014). This innovative technique offers a precise, cost-effective, and user-friendly platform that may be used in several fields, including avian virology. The use of CRISPR/Cas9 technology offers valuable resources for elucidating the fundamental aspects of virus research (Teng et al., 2021). This encompasses the investigation of host and virus interactions, gene therapy applications, shedding light on viral gene functionality, the facilitation of antiviral treatment, and the development of recombinant vaccines (Doudna & Charpentier, 2014; Vilela et al., 2020; Wright et al., 2016).

Application of the CRISPR/Cas9 system in virology research has significantly increased in the last decade (Teng et al., 2021). In principle, the use of the CRISPR/Cas9 system is not only limited to selectively editing specific nucleotides within the genomes of humans, animals, and plants, but it also has the ability to modify the viral genomes (H. Lin et al., 2021). Moreover, the potential application of the CRISPR/Cas9 machinery for eliminating viral infections from cells extends to a wide

range of DNA or RNA viruses that possess a DNA intermediate in its life cycle (Doudna & Charpentier, 2014; H. Lin et al., 2021). Hence, the utilisation of the CRISPR/Cas9 technique presents significant potential for selectively targeting various stages of the viral life cycle and possesses the capacity to facilitate effective and persistent genetic therapy against infectious viruses (Bakhrebah et al., 2018; Jinek et al., 2013; Vilela et al., 2020).

The CRISPR/Cas9 system has been effectively utilised for gene editing across a diverse range of viral species, primarily in the context of viral gene therapy, functional investigation of viral virulence factors, and the development of recombinant vaccines (Bi et al., 2014; Ebina et al., 2013; H. J. Lee et al., 2017; Suenaga et al., 2014; N. Tang et al., 2021; X. Xu et al., 2016; Y. Zhao et al., 2020). Ebina et al. (2013) have demonstrated the successful application of CRISPR/Cas9 gene editing techniques in viral gene therapy and functional investigation of viruses (Ebina et al., 2013). Specifically, it has been proven that it is feasible to edit viral genomes that are integrated within the host genome. In their study, they effectively suppressed the expression of HIV-1 *in vitro* using CRISPR/Cas9. These results have led to other investigations with the objective of rendering HIV-1 inactive and eradicating it by means of genome editing (Ebina et al., 2013; W. Hu et al., 2014; Lebbink et al., 2017; H.-K. Liao et al., 2015; Mefferd et al., 2018). Additional research has been conducted to explore the application of the CRISPR/Cas9 gene editing technique in the context of viral-related human diseases. This includes investigations into the potential use of this technique in oncogenic viruses such as the hepatitis B virus (HBV), which has been associated with the development of liver cancer (Kennedy et al., 2015; S. R. Lin et al., 2014; Jie Wang et al., 2015; S. Zhen et al., 2015). Furthermore, studies have also focused on high-risk human papillomavirus (HR-HPV), which is known to cause



cervical cancer (Bortnik et al., 2021; Zheng Hu et al., 2014; Shuai Zhen et al., 2014). Additionally, investigations have been conducted on human endogenous retroviruses-K (HERVs), which have been suggested to be associated with the progression of prostate cancer and motor neuron diseases (Ibba et al., 2018).

The capacity of the CRISPR/Cas9 system to directly induce double-strand breaks (DSBs) in the DNA viral genome has facilitated the editing of herpesviruses' genomes (Teng et al., 2021). These viruses comprise a wide range of major diseases affecting humans, poultry, and livestock. Recent studies have employed the CRISPR/Cas9 system as a potential antiviral strategy to disrupt human herpesvirus infection *in vitro* (Suenaga et al., 2014; van Diemen & Lebbink, 2017). These studies have demonstrated the inhibitory effects of CRISPR/Cas9 on the replication of Epstein-Barr virus (EBV), human cytomegalovirus (HCMV), and herpes simplex virus type 1 (HSV-1) in cell culture models (Roehm et al., 2016; Van Diemen et al., 2016; X. Xu et al., 2016). Additionally, the CRISPR/Cas9 system has been utilised for gene editing of EBV (Jianbin Wang & Quake, 2014; K.-S. Yuen et al., 2017; K. S. Yuen et al., 2018).

In addition to investigations into gene function, gene therapy, and virus-host interactions, the utilisation of CRISPR/Cas9-based gene-editing technology has been extensively employed in vaccine research (Liang et al., 2016; L. Liu et al., 2019; N. Tang et al., 2021). This technology is highly efficient, specific, versatile, flexible, simple, and cost-effective in comparison to alternative methods of viral genome editing. Consequently, it has proven to be an effective and powerful approach for the advancement of genetically engineered vaccines (Atasoy et al., 2019; Liang et al., 2016; Okoli et al., 2018; M. Yuan et al., 2015). At present, there has been a noticeable increase in the number of studies related to the development of animal anti-viral

vaccines through the use of the CRISPR/Cas9 system (Bortnik et al., 2021; Ebina et al., 2013; Mayo-Muñoz et al., 2018). Virus species that were reconstituted for vaccine development using CRISPR/Cas9-based genome editing technology include a range of viruses, namely PRV (Liang et al., 2016; Y. D. Tang et al., 2016; A. Xu et al., 2015; Y. Zhao et al., 2020), ASFV (Borca et al., 2018), HVT (Chang et al., 2019; L. Liu et al., 2019; N. Tang et al., 2018, 2020), DEV (Chang et al., 2018; Zou et al., 2017), ILTV (Atasoy et al., 2019), and CDV (Gong et al., 2020).

The efficacy of the CRISPR/Cas9 gene editing technique in manipulating viral genomes, including the ILTV, has been established through previously mentioned studies. In our research group, Atasoy et al. 2019 have demonstrated the use of CRISPR/Cas9 in deleting the ILTV TK and US4 genes while simultaneously introducing an NDV-F gene, therefore facilitating the development of a stable vaccine vector. However, compared to other double-stranded DNA viruses, the genome of ILTV has not been extensively evaluated for the presence of regions that can be targeted for CRISPR/Cas9-mediated knock-in or knockout. Although the overall biology of the ILTV has been comprehensively investigated and analysed, there remains a lack of research pertaining to the specific study of gene inactivation and elimination as a potential technique for disease prevention in the future (Atasoy et al., 2019; Fuchs et al., 2007; S.-W. Lee et al., 2011).

### **4.1.1. AIMS**

This chapter aims to demonstrate a proof-of-concept that provides a comprehensive analysis of the potential of CRISPR/Cas9 gene editing technology as a method of choice for vaccine development and disease prevention.

Specifically:

1. Functionally validate the expression of GFP in attenuated recombinant ILTV.
2. Develop a versatile, adaptable, and innovative donor plasmid with multiple cloning sites into which multiple genes can be inserted.
3. Demonstrate the effectiveness of CRISPR/Cas9 in creating incisions in the ILTV genome leading to gene knockout or knock-in.
4. Demonstrate the ability of ILTV as a putative vaccine vector through the insertion of NDV-F antigen.
5. Provide an overview of the possible regions of insertion in the ILTV genome.

## 4.2. General Workflow

To provide a more comprehensive presentation of the progression throughout this chapter, **Figure 4.1** presents a concise overview of the order of outcomes and the sequential execution of the whole process. The results include three main parts. Firstly, it involves the propagation of the attenuated ILTV that expresses the GFP reporter marker. Secondly, it entails the assembly of the donor plasmid, which utilises pCDNA3.0 as the backbone vector and incorporates a gene fragment consisting of two multiple cloning sites: MCS1 and MCS2. Lastly, it involves the implementation of CRISPR-Cas9-based knock-in and knockout experiments.

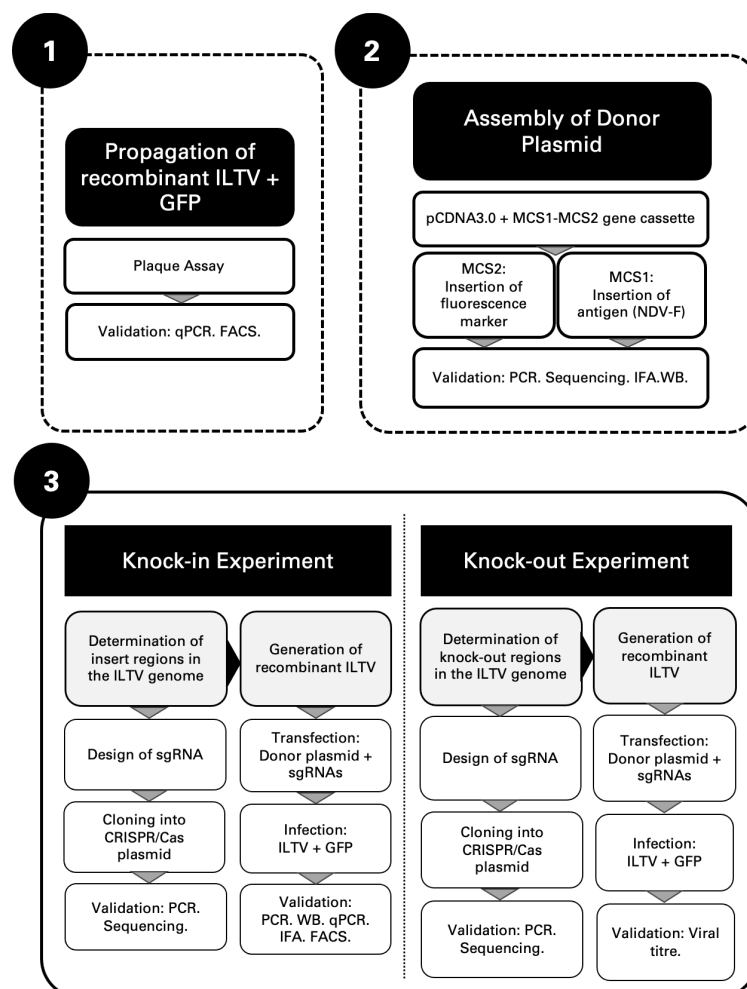


**Figure 4.1. Schematic representation of the workflow used in this chapter.** The results of this chapter were presented in three sections: **(1)** propagation of the recombinant attenuated ILTV containing the GFP insert; **(2)** construction of the donor plasmid; and **(3)** implementation of the CRISPR/Cas9-based knock-in and knockout experiments.

## 4.3. Results

### 4.3.1. Propagation of Recombinant ILTV + GFP

Previous studies in our lab resulted in the creation of an attenuated recombinant ILTV expressing the GFP fluorescence marker (Atasoy et al., 2019). Genetic impairment of the ILTV was achieved through the replacement of the thymine kinase (TK) gene of the ILTV with the GFP fluorescence gene through the CRISPR/Cas9 gene editing system, rendering the resulting recombinant ILTV inactive and providing a system to detect ILTV infection through the presence of the GFP signal in the ILTV-infected host cells (**Figure 4.2.A**) (Atasoy et al., 2019). Once infection in the LMH cells has been established, a green fluorescence signal can be observed under the microscope (**Figure 4.2.B**). A plaque assay experiment was performed to further measure the effectivity and infectivity of the recombinant ILTV-GFP for downstream applications (**Figure 4.2.C**). Serial dilutions and plaque counting revealed the ILTV-GFP viral titre to be  $1.8 \times 10^7$  PFU/mL. These results were compared to the ILTV-WT ( $1.3 \times 10^8$  PFU/mL). There was a significant difference in viral titre between the ILTV-WT ( $M = 1.3 \times 10^8$ ,  $SD = 5.1 \times 10^7$ ) and the ILTV-GFP ( $M = 1.8 \times 10^7$ ,  $SD = 9.1 \times 10^6$ );  $t(4) = 3.67$ ,  $p = .021$ . Moreover, to establish evidence of infectivity and replication rate between recombinant ILTV-GFP and ILTV wild-type, further studies were conducted, which encompassed a kinetics study and flow cytometry analysis. The experimental results demonstrated a significant difference in the replication kinetics of ILTV-WT and ILTV-GFP, indicating that ILTV-GFP exhibited superior replication capabilities. The flow cytometry findings further confirmed the infectivity and spread of ILTV-GFP (**Figure 4.2.E.F**).

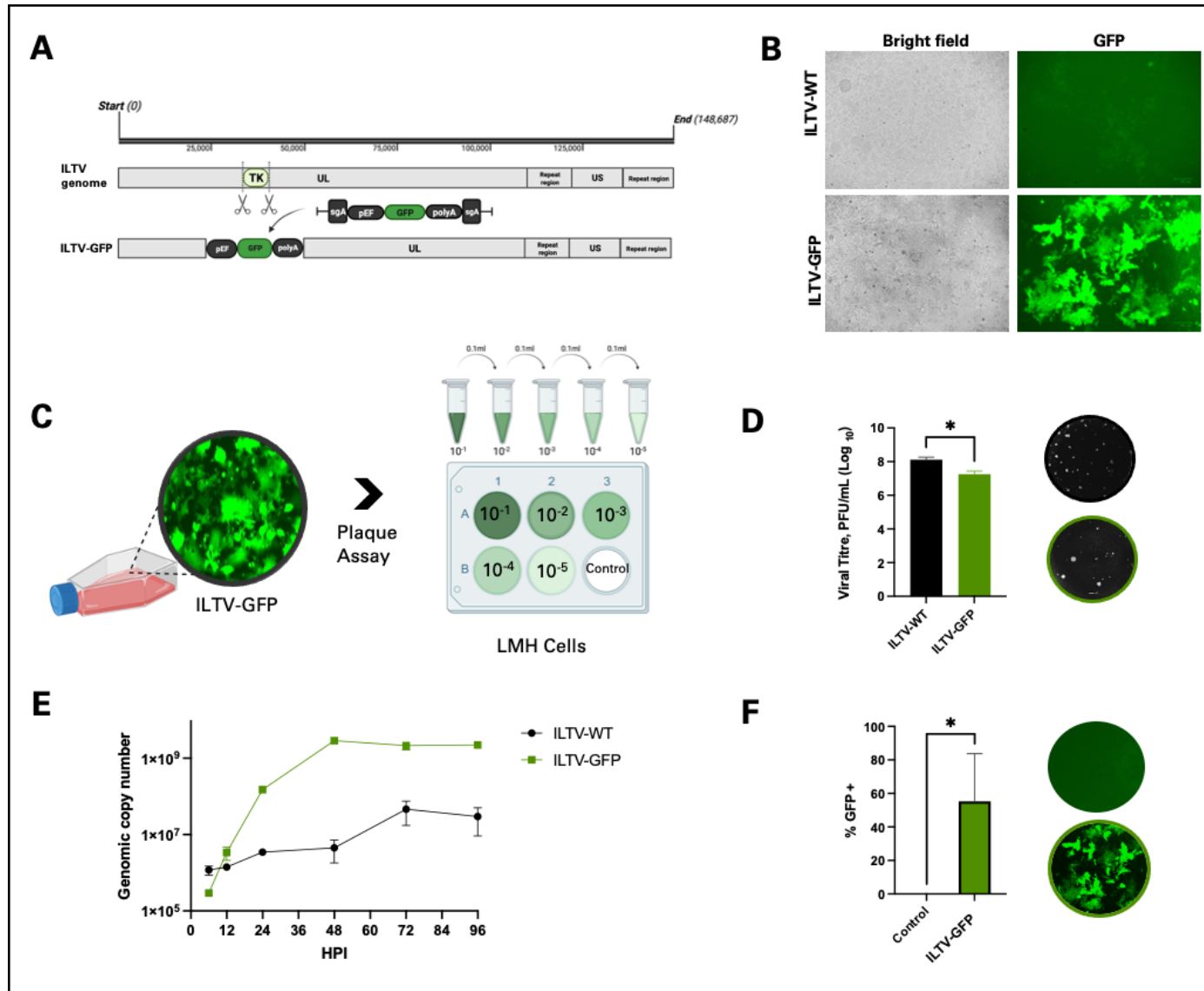


**Figure 4.2. Propagation and validation of the attenuated recombinant ILTV expressing the GFP fluorescence marker. (A)** CRISPR/Cas9 was used to attenuate the ILTV genome (grey coloured box) through the insertion of the GFP fluorescence marker at the TK region in the ILTV genome. **(B)** Confirmation of the infectivity of the recombinant ILTV-GFP was facilitated through the

infection of host cells (LMH). Once the ILTV infection in the host has been established, green fluorescence can be observed under the microscope. **(C)** The viral titre of the recombinant ILTV-GFP was measured through a plaque assay. **(D)** Determination of the viral titre was done by counting the number of plaques formed per well dilution. Comparison showed significance in viral titre between the ILTV-WT ( $M = 1.3 \times 10^8$ ,  $SD = 5.1 \times 10^7$ ) and ILTV-GFP ( $M = 1.8 \times 10^7$ ,  $SD = 9.1 \times 10^6$ );  $t(4) = 3.67$ ,  $p = .021$ . **(E)** qPCR data analysis represents the comparison of genomic copy numbers between the ILTV-WT and recombinant ILTV-GFP through different time points (MOI = 1.0). **(F)** Graphical representation of the comparison in percent GFP positive between the uninfected control cells and cells infected with recombinant ILTV-GFP. A significant difference was observed between the uninfected control and ILTV-GFP. Data analysis is based on one experiment with three technical replicates.

#### **4.3.2. Assembly of Donor Plasmid**

The donor plasmid used in this present study was previously assembled in prior experiments performed in our laboratory (Atasoy et al., 2019). To create a CRISPR/Cas9 experimental workflow, the assembly of a versatile, adaptable, and innovative donor plasmid is an essential step. The donor plasmid described in this study was created through the restriction digestion of the mammalian expression vector pcDNA-EGFP (shown by the colour black) using *MfeI* and *BbsI* restriction enzymes (**Figure 4.3.A**). The digested pcDNA-EGFP will serve as the plasmid backbone. Additionally, the synthetic MCS1-MCS2 fragment (represented by the colour red) was cleaved at its 5' and 3' ends using *BsmBI*. The design of the synthetic MCS1-MCS2 fragment incorporates two crucial elements. Firstly, it includes two multiple cloning sites (MCS1 and MCS2) that allow for the insertion of multiple genes. Specifically, the gene of interest can be inserted into MCS1, while a reporter fluorescence gene can be inserted into MCS2. Secondly, the fragment contains *LoxP* sites positioned in the same direction, flanking the MCS2 region. These *LoxP* sites

facilitate the excision of the entire MCS2 region using Cre-Lox recombinase technology. This excision process enhances flexibility in downstream applications, such as the conditional knockout of the fluorescence marker in MCS2. Please refer to **Figure 4.3.B** for a visual representation of this design. The process of ligation and end-joining of the cleaved pcDNA-EGFP and synthetic MCS1-MCS2 fragments was successfully carried out using DNA ligase. A summary of the elements of the MCS1-MCS2 synthetic gene cassette is shown in **Table 4.1**. This resulted in the assembly of the donor plasmid pcDNA-MCS1-MCS2, as seen in **Figure 4.3.C**. In order to confirm the presence of the MCS1-MCS2 fragment inside the donor plasmid, the recombinant donor plasmid underwent restriction digestion utilising the *BsmBI* fragment. The gel electrophoresis picture displays distinct bands resulting from the application of the restriction enzyme *BsmBI*. These bands correspond to the synthetic MCS1-MCS2 fragment, measuring about 2500 bp; the pcDNA backbone fragment, measuring approximately 4455 bp; and the undigested donor plasmid, measuring approximately 7000 bp (**Figure 4.3.D**).





ligase, resulting in the formation of the donor plasmid pcDNA-MCS1-MCS2. **(D)** The gel electrophoresis image showing the bands after the treatment with restriction enzyme *BsmBI*: synthetic MCS1-MCS2 fragment (around 2500 bp), pcDNA backbone fragment (around 4455 bp), and undigested donor plasmid (around 7000 bp).

**Table 4.1.** Summary of the components and purpose of the MCS1-MCS2 gene fragment.

<b>MCS1-MCS2 Gene</b>	
<b>Cassette component</b>	<b>Purpose</b>
<i>BsmBI</i>	<i>BsmBI</i> Restriction site
sg-A	For releasing gene cassette from the donor plasmid
pCMV	Human cytomegalovirus (CMV) immediate early promoter to promote constitutive expression of the inserts in the MCS1.
MCS1	For the easy insertion of foreign DNA fragments
flag	Protein tag
bGH polyA	expression terminator
LoxP	34 bp Cre recombinase recognition site for the excision of the fluorescence marker at MCS2
pEF	EF1 alpha promoter
MCS2	For the easy insertion of foreign DNA fragments
V5	Protein tag

#### 4.3.2.1. Assembly and Cloning of the Fluorescent Marker Into the Multiple Cloning Site 2 (MCS2)

The donor plasmid pcDNA-MCS1-MCS2 was used to create a version of the plasmid that will carry a reporter gene and will fluoresce red under the microscope when expressed. The mammalian expression vector, pcDNA3-mRFP (Addgene plasmid #13032), which contains the mRFP gene, was used as the template for the amplification of the mRFP1 gene (**Figure 4.4.A**). The primer design for the amplification of mRFP incorporated recognition sites for the *EcoRI* and *XbaI* restriction enzymes. The forward primer sequence was 5' CCGGAATTCTCCACCATGGCCTCCTCCGAGGACG 3', which included the *EcoRI* recognition site. The reverse primer sequence was 5' GTACTCTAGAGGCGCCGGTGGAGTGGC 3', and it contained the *XbaI* recognition site. The mRFP fragment was amplified using the polymerase chain reaction (PCR), resulting in a band size of about 700 base pairs (**Figure 4.5.B**). To enable the cloning of the mRFP fragment into the multiple cloning site 2 (MCS2) of the recipient vector (pcDNA-MCS1-MCS2), both the mRFP insert and the recipient vector (pcDNA-MCS1-MCS2) were subjected to digestion using the restriction enzymes *EcoRI* and *XbaI* (**Figure 4.4.C**). Following this, DNA ligase was applied to promote the fusion of the mRFP insert and the recipient vector. The resulting donor plasmid, pcDNA-MCS1-mRFP, which had been ligated, was propagated by means of transformation into DH5 $\alpha$ -competent *E. coli* cells (**Figure 4.4.D**). The selection process involved the identification and isolation of positive colonies, followed by the purification of plasmid DNA for subsequent Sanger sequencing analysis. The Sanger sequencing analysis confirmed that there was a 100% sequence similarity in the nucleotide sequence between the wild-type plasmid pcDNA3-mRFP and the mRFP fragment present in the

donor plasmid pcDNA-MCS1-mRFP (**Figure 4.4.F**). To further confirm the successful integration of the mRFP gene into the donor plasmid (pcDNA-MCS1-mRFP), expression analysis was conducted by transfecting the purified plasmid DNA into DF1 cells. The presence of red fluorescence was detected 36 hours after transfection, as seen in **Figure 4.4.E**.

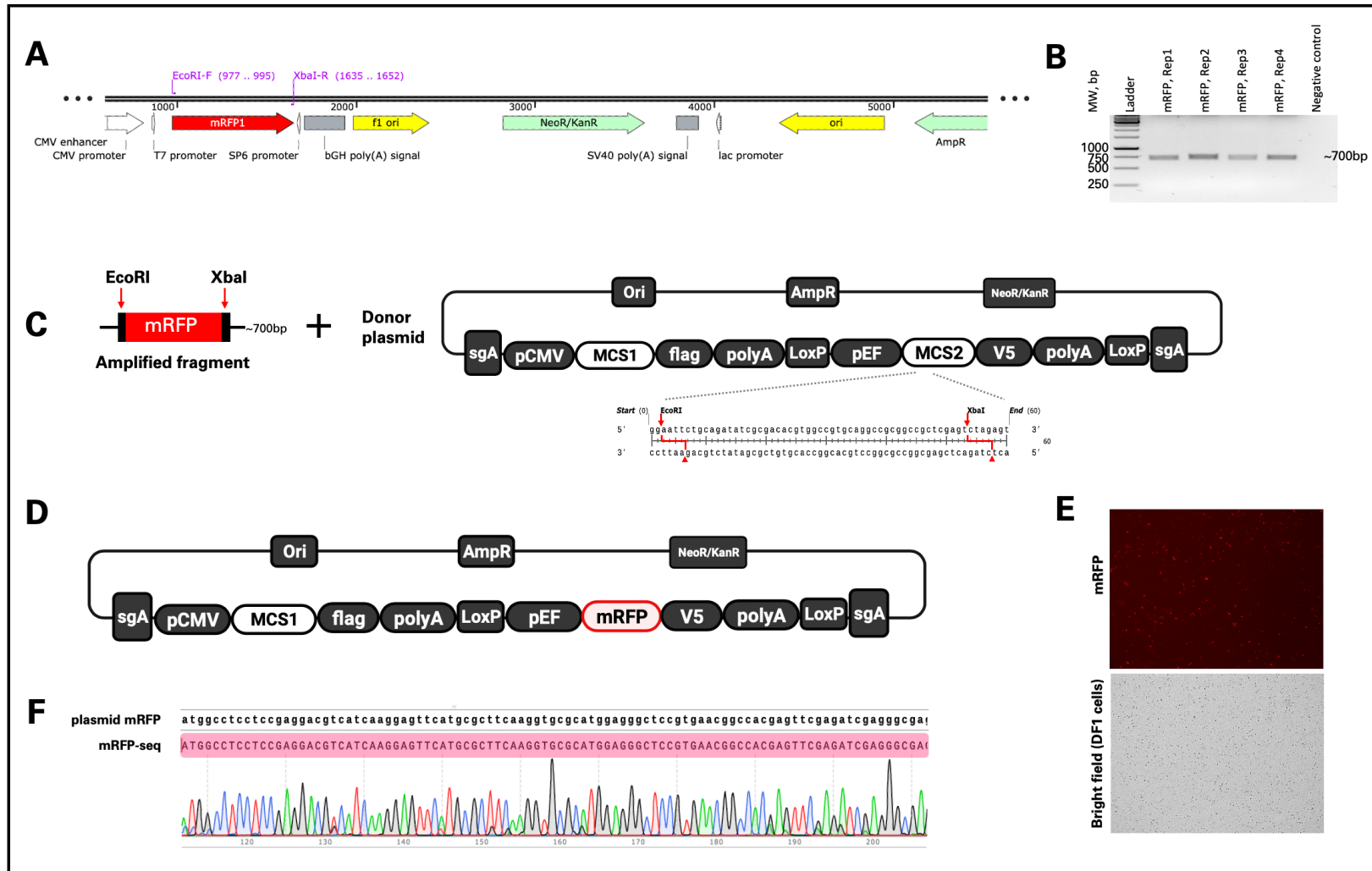


**Figure 4.4. Assembly and validation of the recombinant donor plasmid pCDNA-MCS1-mRFP.** The mRFP gene fragment was inserted into the multiple cloning site 2 (MCS2) of the donor plasmid pcDNA3-MCS1-MCS2. **(A)** Fragment representation of the pcDNA3-mRFP mammalian expression vector (Addgene plasmid #13032) highlighting the mRFP1 gene (shown by a red-coloured

box). Forward and reverse primers, *EcoRI*-F and *XbaI*-R were designed to amplify the mRFP1 fragment. **(B)** Gel electrophoresis image showing the amplified mRFP1 gene, approximately 700 bp in size. The image shows one experiment with at least three biological replicates. **(C)** Cloning of the amplified mRFP gene fragment with *EcoRI* restriction sites at the 5' end and *XbaI* at the 3' end together with the donor plasmid pcDNA3-MCS1-MCS2 through restriction enzyme digestion using *EcoRI* and *XbaI*. **(D)** DNA ligation was carried out to fuse the mRFP fragment to the recipient donor plasmid pcDNA-MCS1-MCS2, creating the recombinant donor vector, pcDNA-MCS1-mRFP. **(E)** Microscopic image showing the expression of the mRFP as shown by red fluorescence in DF1 cells. **(F)** Sanger sequencing results showing 100% similarity between the wild-type plasmid pcDNA3-mRFP and pcDNA-MCS1-mRFP (highlighted in pink). Images were taken using the Zoe Fluorescent Cell Imager (BioRad).

#### **4.3.2.2. Assembly and Cloning of the Target Antigen NDV-F Into the Multiple Cloning Site 1 (MCS1)**

The final stage in the construction of the donor plasmid is the insertion of the target gene of interest, namely the NDV-F gene, into the multiple cloning site 1 (MCS1) of the pcDNA-MCS1-mRFP plasmid. The plasmid DNA harbouring the NDV genotype VII Egypt isolate was used as the template for the amplification of the F gene, as seen in **Figure 4.5.A**. The primers were strategically designed to facilitate the amplification of the NDV-F gene, incorporating specific recognition sites for the restriction enzymes *NheI* (5'-CTAGCTAGCTCCACCATGGGCTCCAAACTTTCTA-3') and *KpnI* (5'-GCCGGTACCTGCTCTTG TAGTGGCTCT-3'). PCR was employed to perform positive amplification of the NDV-F gene, resulting in the detection of a band with an estimated size of 1600 bp (**Figure 4.5.B**). To facilitate the insertion of the NDV-F fragment into the multiple cloning site 1 (MCS1) of the recipient vector (pcDNA-MCS1-mRFP), both the NDV-F insert and the recipient vector (pcDNA-MCS1-mRFP) underwent restriction enzyme digestion utilising the restriction enzymes *NheI* and *KpnI*

**(Figure 4.5.C).** Subsequently, the use of DNA ligase facilitated the fusing of the NDV-F insert and the recipient vector. The donor plasmid, pcDNA-NDVF-mRFP **(Figure 4.5.D)**, obtained after ligation, was propagated by transformation into DH5 $\alpha$ -competent *E. coli* cells. Positive colonies were then subjected to a purification process to obtain purified plasmid DNA for further examination using Sanger sequencing. The Sanger sequencing study provided confirmation of a complete sequence identity of 100% between the wild-type Genotype VII Egypt NDV-F gene and pcDNA-NDVF-mRFP **(Figure 4.5.E)**.

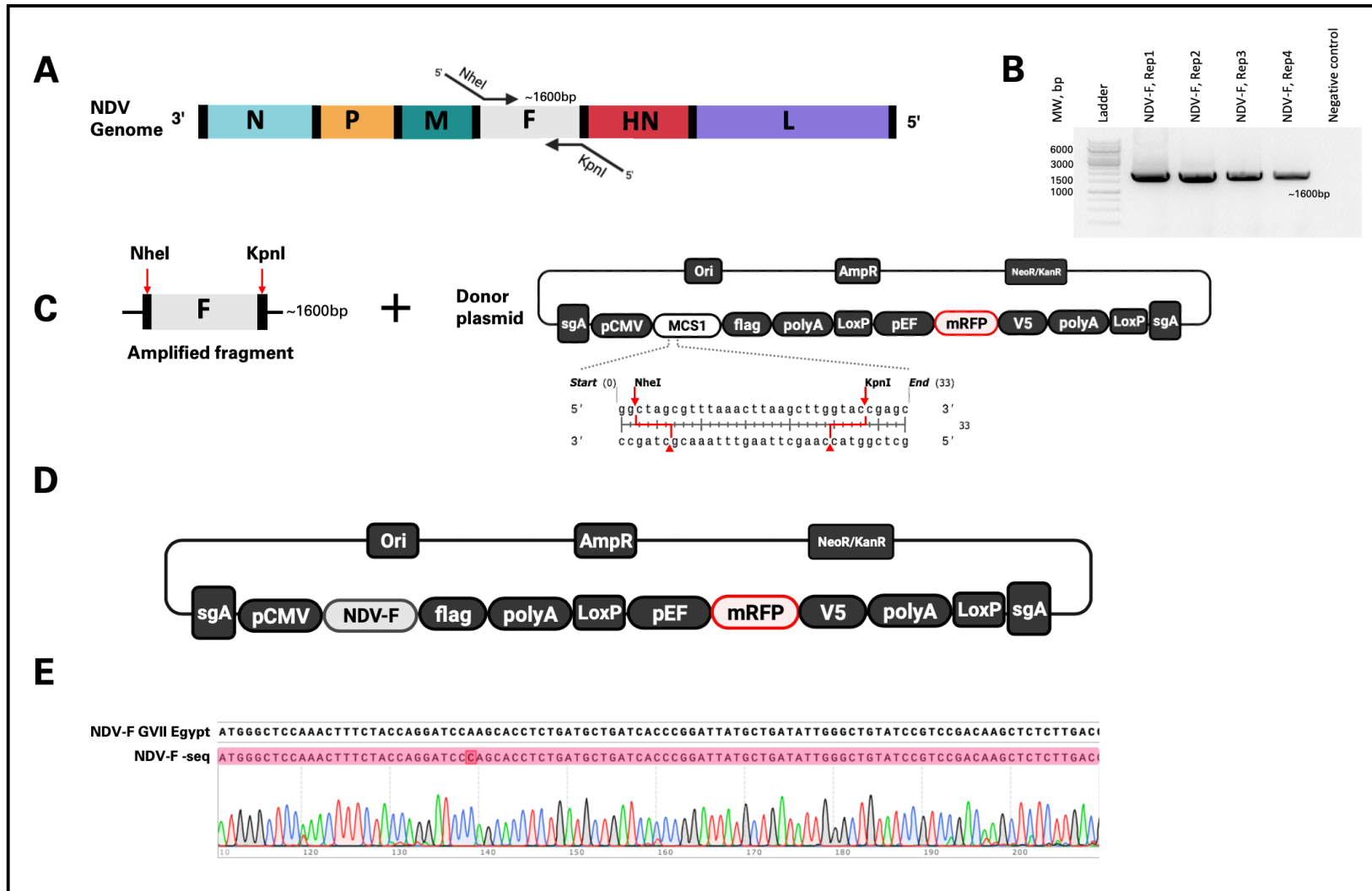


**Figure 4.5. Assembly and sequence validation of the recombinant donor plasmid pCDNA-NDVF-mRFP.** The NDV-F gene fragment was inserted into the multiple cloning site 1 (MCS1) of the donor plasmid pCDNA-MCS1-mRFP. **(A)** Fragment representation of the NDV genome. Primers were designed to amplify the NDV-F gene to contain restriction enzyme sites *NheI* (5' end) and



*KpnI* (3' end). **(B)** Gel electrophoresis image showing the amplified NDV-F gene, approximately 1600 bp in size. The image shows one experiment with at least three biological replicates. **(C)** Cloning of the amplified NDV-F gene fragment and donor plasmid pcDNA-MCS1-mRFP through restriction enzyme digestion using *NheI* and *KpnI*. **(D)** DNA ligation was carried out to fuse the NDV-F fragment to the recipient donor plasmid pcDNA-MCS1-mRFP, creating the recombinant donor vector pcDNA-NDVF-mRFP. **(E)** Sanger sequencing results shows 100% similarity between the wild-type NDV-F gene Genotype VII Egypt and pcDNA-NDVF-mRFP (highlighted in pink).

#### 4.3.2.3. Functional Validation of the Donor Plasmid pcDNA-NDVF-mRFP

The pcDNA-NDVF-mRFP plasmid was subjected to further expression studies to validate its final donor plasmid form. This investigation aimed to confirm the expression of the mRFP gene in the multiple cloning site 2 (MCS2) as red fluorescence and the functional expression of the NDV-F gene. A transfection experiment was performed in order to investigate the expression of the mRFP gene in DF1 cells. The expression of the mRFP gene in DF1 cells was seen through microscopy imaging taken 36 hours after transfection (**Figure 4.6.A**). The expression and localisation investigation of the NDV-F protein was conducted using western blotting tests and an immunofluorescence assay. The expression study utilises the anti-FLAG primary antibody for the purpose of labelling the NDV-F protein. Subsequently, the Goat anti-Rabbit IgG, which is tagged with Alexa fluor 488, is employed. As a consequence of this process, a positive band of the NDV-F gene, measuring about 55 kDa in size, is observed (**Figure 4.6.B**). The immunofluorescence experiment was conducted to verify the expression and localisation of the NDV-F protein. The confocal imaging findings demonstrated the presence of the NDV-F protein, which was tagged with anti-FLAG-specific antibody, and its specific localisation inside the cytoplasm of the DF1 cells (**Figure 4.6.C**). Throughout this chapter, the pcDNA-NDVF-mRFP plasmid was used as the donor plasmid.

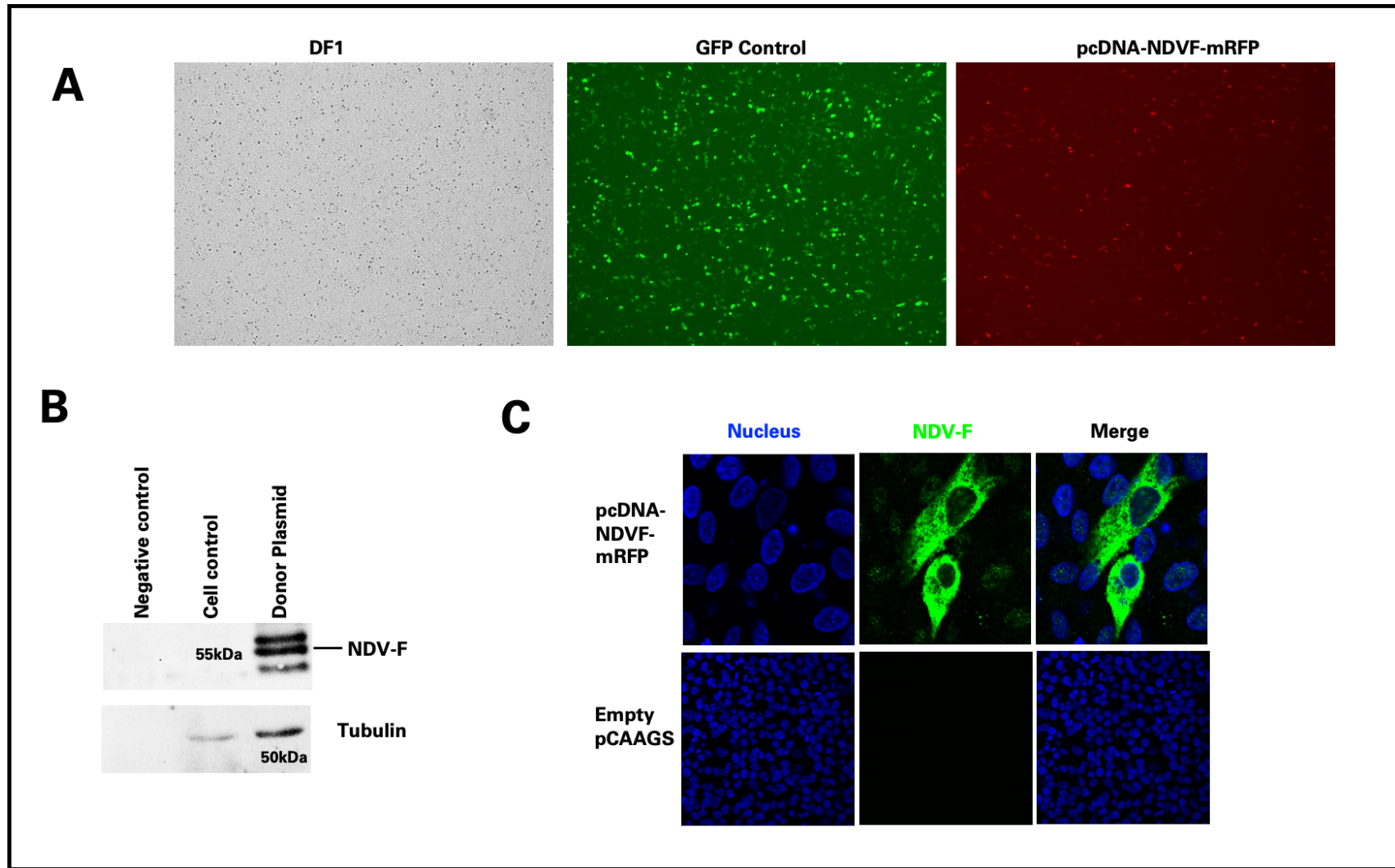


**Figure 4.6. GFP protein expressed at the protein level in plasmid pcDNA-NDVF-mRFP.** DF1 cells were transfected with the donor plasmid pcDNA-NDVF-mRFP. **(A)** Microscope image of the transfected DF1 cells, 36 hours post-transfection, showing the

expression of the mRFP gene in pcDNA-NDVF-mRFP (shown as red fluorescence). pCAAG-GFP was used as the transfection control. **(B)** Western blot image showing the detection of NDV-F (approximately 55 kDa) using ANTI-FLAG followed by Goat anti-Rabbit IgG labelled with Alexa fluor 488. Beta-tubulin was used as the loading control for the western blot experiment, as well as for all other experiments conducted within the scope of this work. **(C)** Confocal immunofluorescence image showing the NDV-F protein location. The nucleus (blue) and NDV-F (green) were labelled with DAPI and anti-FLAG-specific antibodies, respectively. Empty plasmid-transfected cells served as negative control.

### 4.3.3. Knock-in Experiments

#### 4.3.3.1. Design, Assembly, and Cloning of sgRNAs

Atasoy et al. earlier devised a set of five single-guide RNAs (sgRNAs) with the purpose of selectively targeting distinct areas of the ILTV genome. The aforementioned regions are denoted as UL0, UL50, and US4. Accessory single-guide RNA (sgRNA) A was also engineered to enhance the enzymatic cleavage of the gene cassette from the donor plasmid. **Table 4.2** presents a summary of the sgRNAs that were developed specifically for the purpose of this investigation. **Figure 4.7** provides further visual representation of the precise positions of the single-guide RNA (sgRNA) target sites within the genome of the ILTV. The parameters of these single-guide RNAs (sgRNAs) were assessed by the use of NCBI-BLAST and Chop-Chop web-based *in silico* resources.

The CRISPR/Cas9-sgRNA (pX459v2-sgRNAs) construct utilised in this chapter was generated by prior experimental procedures conducted within our laboratory (Atasoy et al., 2019). The in-silico cloning process was visually depicted using a diagram generated by the software SnapGene version 7.0.2 (**Figure 4.8**). To facilitate the

integration of the sgRNA oligo fragment into the CRISPR/Cas9 construct pX459v2, both the sgRNA insert and the recipient vector (pX459v2) underwent digestion using the restriction enzyme *BbsI* (**Figure 4.8.A.B**). Subsequently, the use of DNA ligase facilitated the fusing of the sgRNA insert and the recipient vector. The CRISPR/Cas9-sgRNA plasmid, pX459v2-sgRNAs (**Figure 4.8.C**), was propagated by transformation into DH5 $\alpha$ -competent *E. coli* cells after ligation. The selection approach encompassed the detection and isolation of positive colonies through colony PCR, employing the forward HU6 universal primer (5'-GACTATCATATGCTTACCGT-3') and the sgRNA reverse oligo as the reverse primer (**Figure 4.9.A**). The purified plasmids were submitted for Sanger sequencing. The Sanger sequencing verified a complete sequence similarity of 100% in the alignment of nucleotide sequences between the sgRNA oligos and the sequenced pX459v2-sgRNAs. The sequencing primer employed in this study was the HU6 universal primer. **Figure 4.9.B** illustrates the identification of positive guide RNAs, which are visually distinguished by the colour pink highlight. These CRISPR/Cas9-sgRNA plasmids will be used for the generation of recombinant ILTV.

**Table 4.2.** Guide RNAs designed to target the UL0/UL50/US4 region of the ILTV genome.

sgRNA	Target Sequence	PAM	Forward Oligo (5' to 3')	Reverse Oligo (5' to 3')	Gene Locus	Reference
UL50.1	TATTCACGCAGGTGACCGAG	TGG	CACCGTATTCACGCAGGTGACCGAG	AAACCTCGGTACCTGCGTGAATAC	UL50	(Atasoy et al., 2019)
UL50.2	ATGATATGGTGTGCGCACCT	GGG	CACCGATGATATGGTGTGCGCACCT	AAACAGGTGCGACACCATATCATC		
UL0.1	TTTACGACGAATCACCCCTAG	CGG	CACCGTTTACGACGAATCACCCCTAG	AAACCTAGGGTGATTCGTCGTAAAC	UL0	(Atasoy et al., 2019)
UL0.2	AACGTATCGGATACGGTGGT	CGG	CACCGAACGTATCGGATACGGTGGT	AAACACCACCGTATCCGATACGTTTC		
US4	TCAGCGGGTACACTTTATA	GGG	CACCGTCAGCGGGTACACTTTATA	AAACTATAAAGTGTACCCGCTGAC	US4	(Atasoy et al., 2019)
sgA	AGATCGAGTGCCGCATCAC	CGG	CACCGAGATCGAGTGCCGCATCAC	AAACGTGATGCGGCACTCGATCTC		(Xiangjun He et al., 2016)

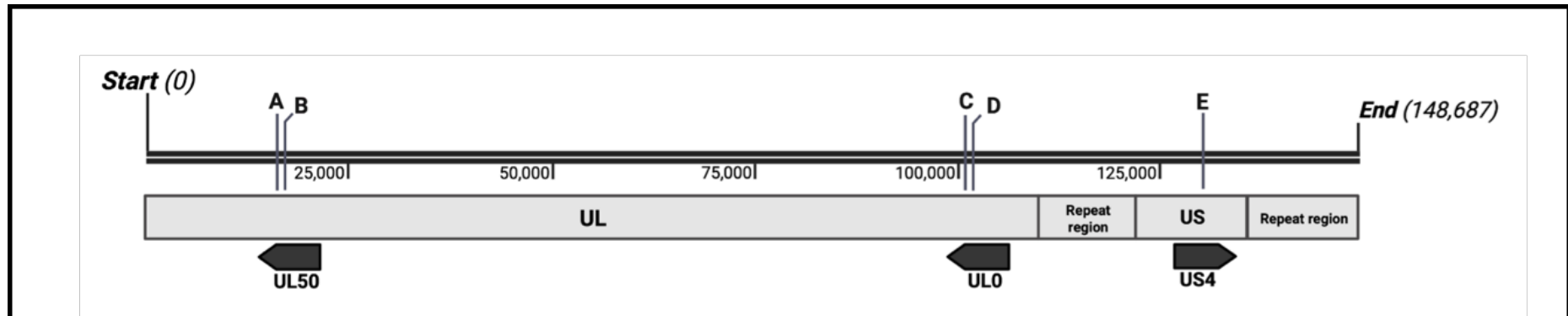


**Figure 4.7. Diagram illustrating the positioning of the guide RNA inside the genome of the ILTV.** The approximate location of the 28-31 bp guides is represented by the letters A-E. The design of the guide RNAs was based on three specific genomic regions, such as: UL50 **(A)** sgRNA-UL50.1 (18,078...18,098), **(B)** sgRNA-UL50.2 (18,436 ... 18,456), UL0 **(C)** sgRNA-UL0.1 (109,020 ... 109,039), **(D)** sgRNA-UL0.2 (109,296 ... 109,319), and US4 **(E)** sgRNA-US4 (128,564 ... 128,584).

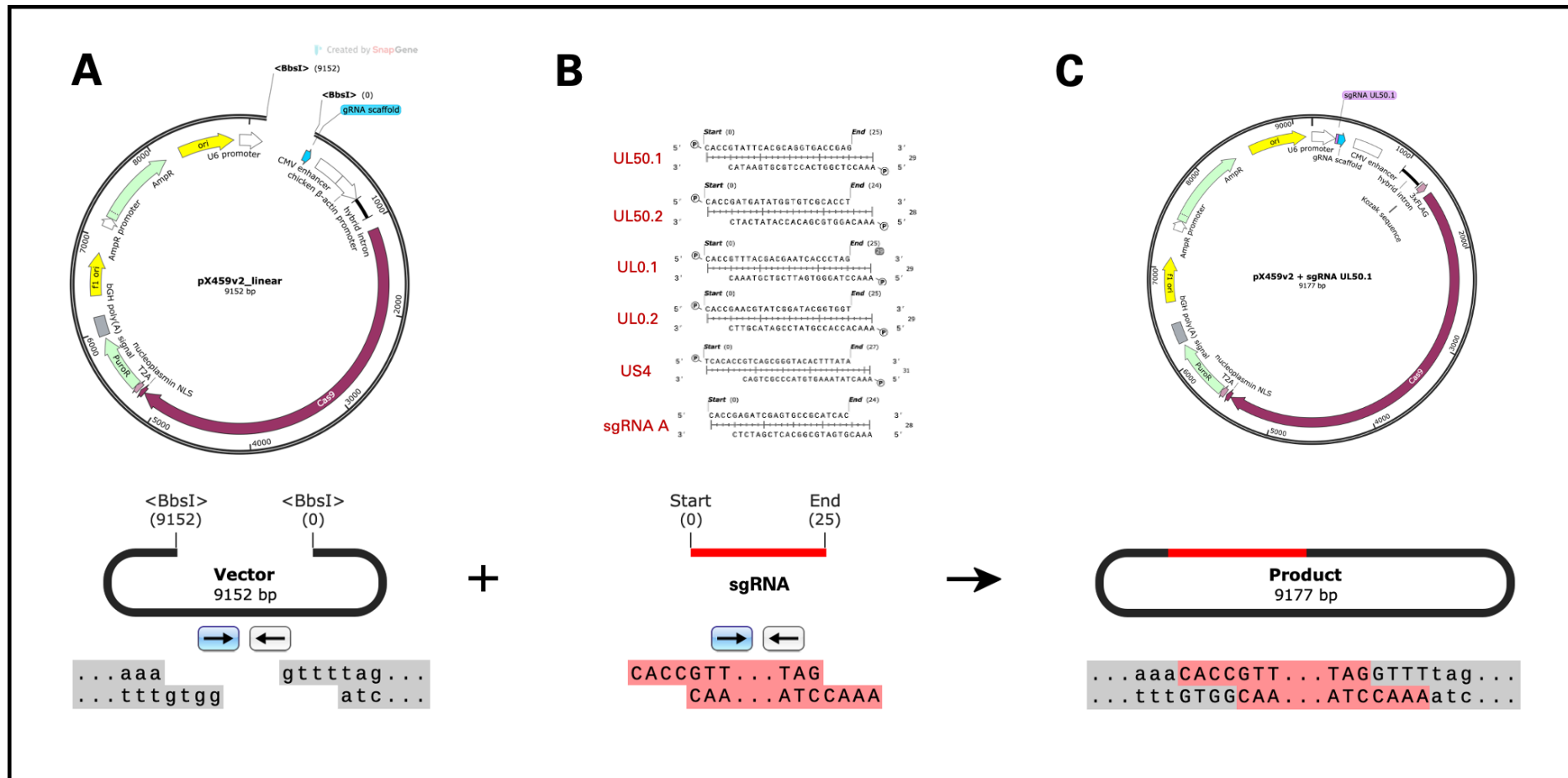


**Figure 4.8. Diagrammatic representation of the assembly of the sgRNAs into the CRISPR/Cas9 plasmid (pX459v2).** Guide RNA and accessory gRNA constructs were used to edit the ILTV genome. **(A)** Digestion of the plasmid containing CRISPR/Cas9 (pX459v2) and **(B)** sgRNA with *BbsI* allows the insertion of the annealed sgRNA oligos through replacing the type II restriction enzyme site. **(C)** Assembled CRISPR/Cas9 plasmid map, pX459v2-sgRNAs. In-silico analysis was done using SnapGene version 7.0.2.

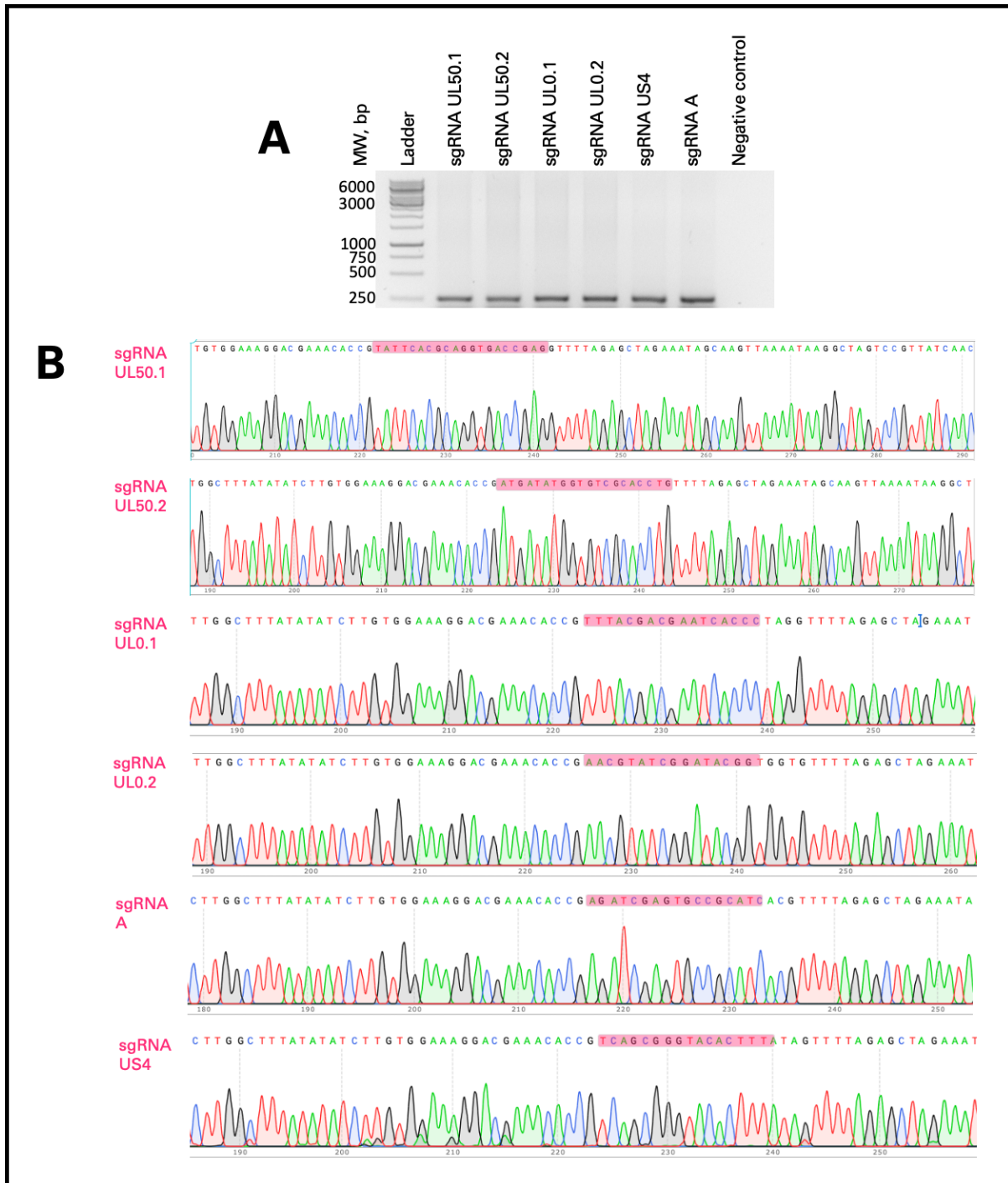


**Figure 4.9. Molecular and sequence validation of pX459v2-sgRNAs.** Validation of the cloning of the guide RNAs into the pX459v2. **(A)** A gel electrophoresis image showing the positive bands at approximately 250 bp indicates the amplification of the sgRNA amplicon. Purified pX459v2-sgRNA plasmids were amplified through the forward HU6 universal primer (5'-GACTATCATATGCTTACCGT-3') and sgRNA reverse oligo. **(B)** Sanger sequencing results show 100% identity between the annealed sgRNA oligos and the sequenced pX459v2-sgRNAs. The sequencing primer used was the HU6 universal primer (5'-GACTATCATATGCTTACCGT-3'). Positive guide RNAs are highlighted in pink.



#### 4.3.3.2. Generation of Recombinant ILTV with NDV-F Knock-in

The generation of the recombinant ILTV with NDV-F gene cassette knock-in required multiple parts to come together: (1) the recombinant ILTV-GFP, which expresses the GFP gene; (2) the donor plasmid pcDNA-NDVF-mRFP, which carries the NDV-F gene and mRFP reporter gene; and (3) the CRISPR/Cas9-sgRNA plasmid pX459-sgRNAs, which will cut the ILTV genome at the specific regions (UL0, UL50, and US4).

The process required is separated into two major parts: the transfection of the donor plasmid (pcDNA-NDVF-mRFP) and the CRISPR/Cas9-sgRNA plasmids (pX459v2-UL0, pX459v2-UL50, and pX459v2-US4) in LMH cells (**Figure 4.10.A**). During incubation, the accessory guide RNA A (pX459v2-sgRNA-A) will recognise and cleave the sgRNA-A site of the donor plasmid, releasing the NDVF-mRFP gene cassette (inside the MCS1 and MCS2, respectively). At 36 hours post-transfection, immediately after observing the presence of the red fluorescence under the microscope indicating the expression of the mRFP protein, the LMH cells were infected with recombinant ILTV-GFP. This will enable the CRISPR/Cas9-guideRNAs (pX459v2-UL0, pX459v2-UL50, and pX459v2-US4) to scan the ILTV genome and make the necessary cleavage, allowing the introduction of the NDVF-mRFP gene cassette into the ILTV genome (regions UL0, UL50, and US4, respectively), ultimately leading to non-homology targeting or non-homologous end joining. At 24-hour post-infection, LMH cells were observed under the microscope for the co-expression of the GFP protein (green fluorescence), indicating the successful infection of the ILTV-GFP, and the mRFP protein (red fluorescence), indicative of the expression of the mRFP reporter gene inside the gene cassette carried by the donor plasmid pcDNA-NDVF-mRFP (**Figure 4.10.B**).

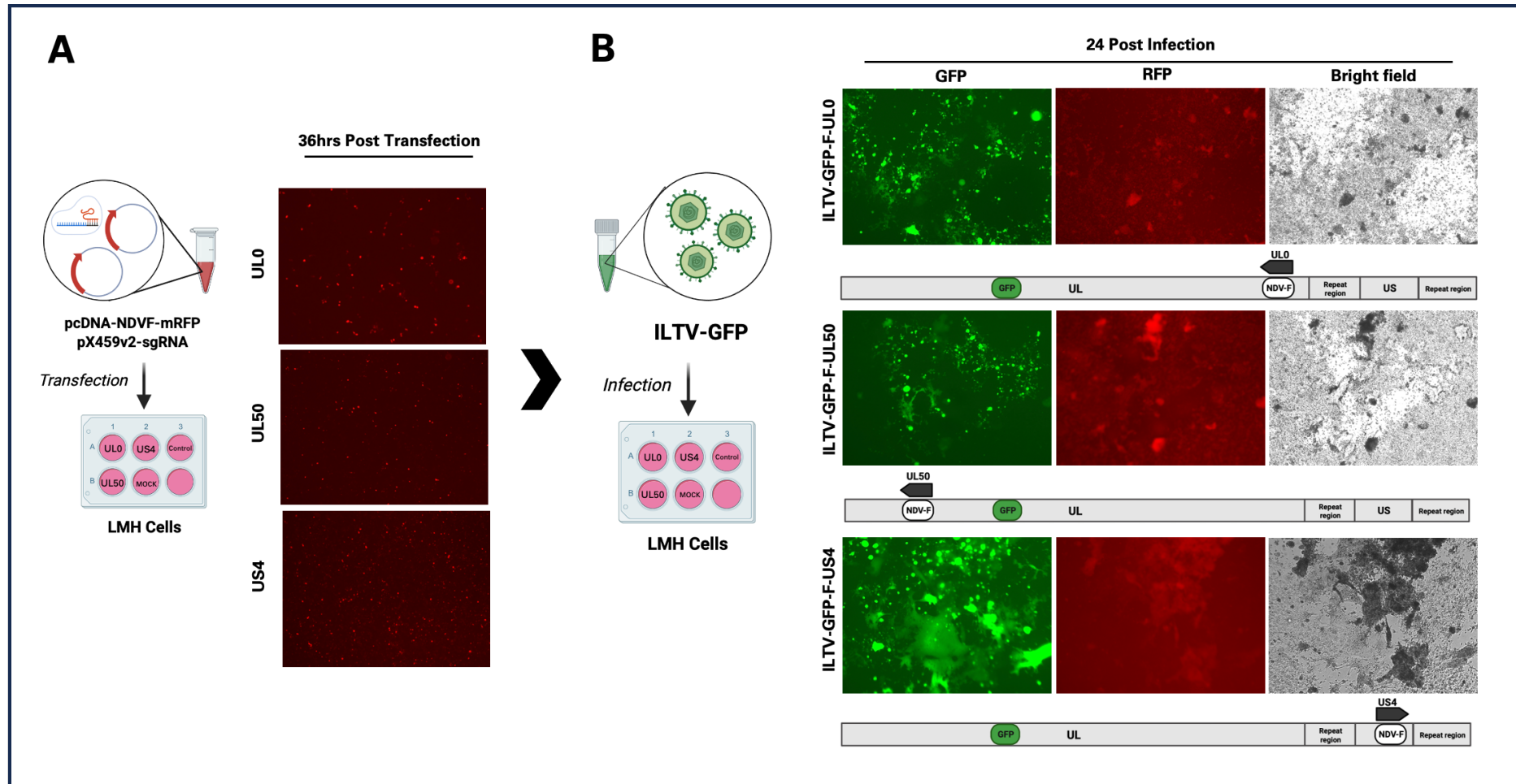


**Figure 4.10. Illustrative representation of the workflow used for the generation of recombinant ILTV with NDV-F-mRFP knock-in.** The workflow includes two important parts: **(A)** Transfection of the LMH cells with pX459v2-sgRNA plasmids (CRISPR/Cas9-sgRNA plasmid) and pcDNA-NDVF-mRFP (donor plasmid). At 36 hours post-transfection, microscope imaging shows red fluorescence detecting the presence of pcDNA-NDVF-mRFP in LMH cells. **(B)** Subsequent to the detection of the red fluorescence

in LMH cells, infection with ILTV-GFP was performed. At 24 hours post-infection, microscope imaging shows the LMH cells fluorescing green, indicating the presence of ILTV-GFP. LMH cells co-expressing the GFP (green signal) and mRFP (red signal) were collected for purification and further passaging. The predicted location of the NDV-F-mRFP insertion in the ILTV genomic regions UL0, UL50, and US4 was diagrammatically illustrated as well. Images were taken using the Zoe Fluorescent Cell Imager (BioRad).

#### **4.3.3.3. Characterisation of the Recombinant ILTV with NDV-F Knock-in**

The analysis of the three recombinant ILTVs (ILTV-GFP-NDVF-UL0, -UL50, and -US4) was conducted using molecular and imaging approaches.

##### **4.3.3.3.1. Validation of NDV-F Knock-in**

The PCR amplification method was utilised to confirm the existence and integration of the NDV-F-mRFP gene cassette into the recombinant ILTV genome. The confluent LMH cells were infected with three recombinant ILTV strains on a 6-well plate. The cells were collected 36 hours after infection, and further techniques were carried out to extract DNA and protein. The DNA that was obtained was subjected to amplification using primers specific to the NDV-F gene, namely Fclone-F (5'-CTAGCTAGCTCCACCATGGGCTCCAACTTTCTA-3') and Fclone-R (5'-GCCGGTACCTGCTCTTG TAGTGGCTCT-3'). **Figure 4.11.B** illustrates the detection of the NDV-F amplicon, which is about 1600 bp in length, in all three of the recombinant ILTV samples. The protein derived from the infected LMH cells was analysed for the presence of the NDV-F protein using an anti-FLAG primary antibody and Goat anti-Rabbit IgG, which was labelled with Alexa fluor 488. The use of blot imaging revealed

the consistent expression of a 55 kDa band throughout all three recombinant ILTVs (**Figure 4.11.C**).

The localisation of the ILTV NDV-F protein was validated by the outcome of an immunofluorescence experiment. The recombinant ILTV strains were used to infect LMH cells in a 24-well plate. The cells were fixed and labelled with anti-FLAG and Goat anti-Rabbit IgG (H+L) Cross-Adsorbed Secondary Antibody, Alexa Fluor 594 (red), at 36 hours post-infection. The localisation of the NDV-F protein in LMH cells is detected in the cytoplasm after infection with recombinant ILTV strains, as shown in **Figure 4.12** by confocal microscopy imaging.

#### **4.3.3.3.2. Functional Validation of the Recombinant ILTVs**

In order to confirm the comparability of infectivity and replication rate between the recombinant ILTVs and the ILTV wild-type, further studies were conducted, including a plaque assay, a kinetics study, and flow cytometry analysis. The LMH cells were infected with the recombinant strains. After 72 hours of infection, the cells were treated with a fixative and stained using a 0.5% crystal violet solution. Following a washing step, the number of individual plaques was determined and used to calculate the viral concentration. The viral concentration (PFU/mL) of the recombinant strains was compared to that of ILTV-WT (**Figure 4.13**).

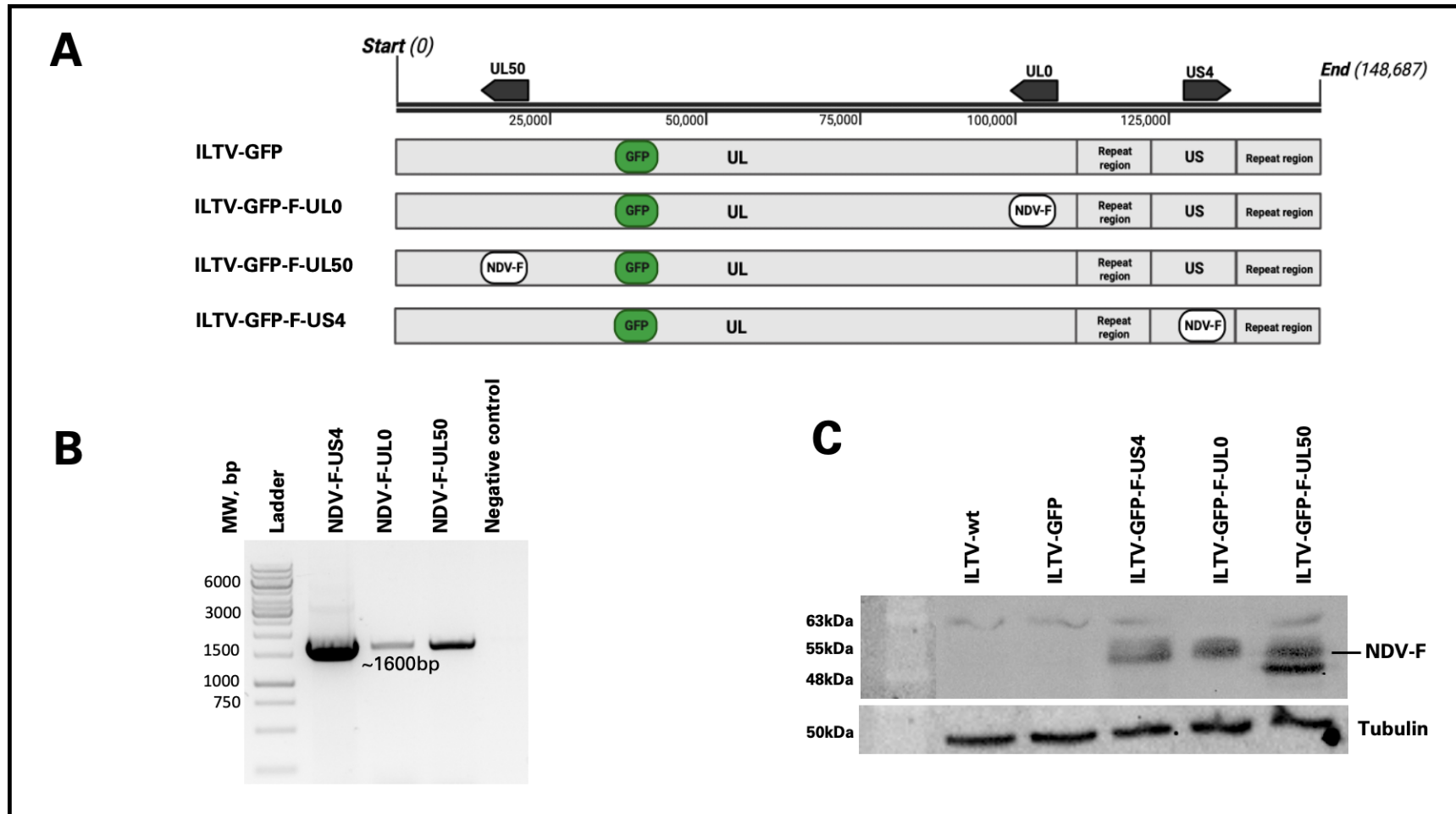


**Figure 4.11. The NDV-F gene is expressed at the molecular and protein levels in LMH cells post-infection with recombinant ILTV strains.** (A) Illustrative representation of the predicted insertion of the NDV-F gene in the ILTV genomic regions UL0, UL50, and US4. The recombinant ILTVs were denoted as ILTV-GFP-F-UL0, ILTV-GFP-F-UL50, and ILTV-GFP-F-US4. (B) Gel electrophoresis image showing the amplification of the NDV-F gene fragment using NDV-F gene specific primers (Fclone-F 5'-CTAGCTAGCTCCACCATGGGCTCCAAACTTTCTA-3' and Fclone-R 5'-GCCGGTACCTGCTCTTGTAAGTGGCTCT-3'). (C) Western blot image showing the presence of the NDV-F protein (approximately 55 kDa) in all the recombinant ILTVs, indicating the expression of NDV-F in all the recombinant ILTVs.

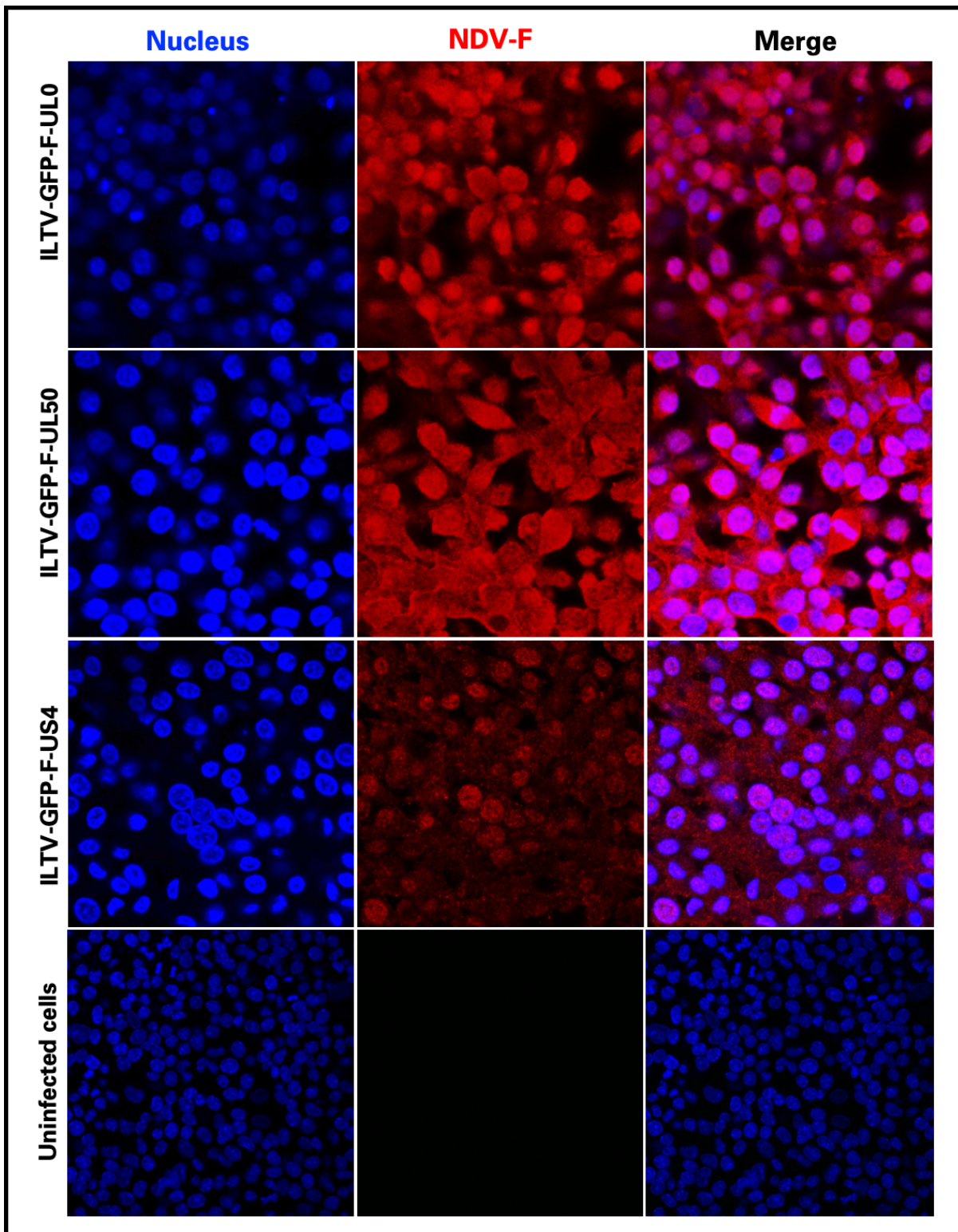


**Figure 4.12. NDV-F protein localised expression in the cellular cytoplasm of LMH cells post-infection of recombinant ILTV strains.** Confocal microscopy images show the NDV-F protein localisation. LMH cells were infected with the recombinant ILTV-GFP-UL0, ILTV-GFP-UL50, and ILTV-GFP-US4 at day 2 post-infection. The nucleus (blue) and NDV-F (red) were labelled with DAPI stain and anti-FLAG-specific antibodies, respectively. Uninfected cells served as negative control.

The quantitative polymerase chain reaction (qPCR) study was conducted in order to assess *in vitro* growth kinetics. LMH cells were subjected to infection with recombinant ILTV strains at a multiplicity of infection (MOI) of 1.0. Subsequently, DNA extraction was performed at certain time intervals following infection, namely 6-, 12-, 24-, 48-, 72-, and 96-hours post-infection (HPI) (**Figure 4.14**). The determination of genomic copy number per time point was conducted using a standard curve that was generated by employing the cloned ILTV gB gene in the pTOPO plasmid. This plasmid was serially diluted from  $10^2$  to  $10^8$ ; however, the specific data is not presented in this context (**Annex 3**).

The infectivity of the recombinant ILTVs was assessed by conducting flow cytometry analysis to evaluate GFP expression. LMH cells were infected with the recombinant ILTV strains. Subsequently, at 36 hours post-infection, the cells were fixed and subjected to staining. The analysis of the percentage of cells expressing GFP demonstrated no statistically significant variations when comparing uninfected control cells with cells that were infected with recombinant ILTV strains (**Figure 4.15.A**). **Figure 4.15.B** displays microscopic images illustrating the production of GFP in LMH cells infected with recombinant ILTV.



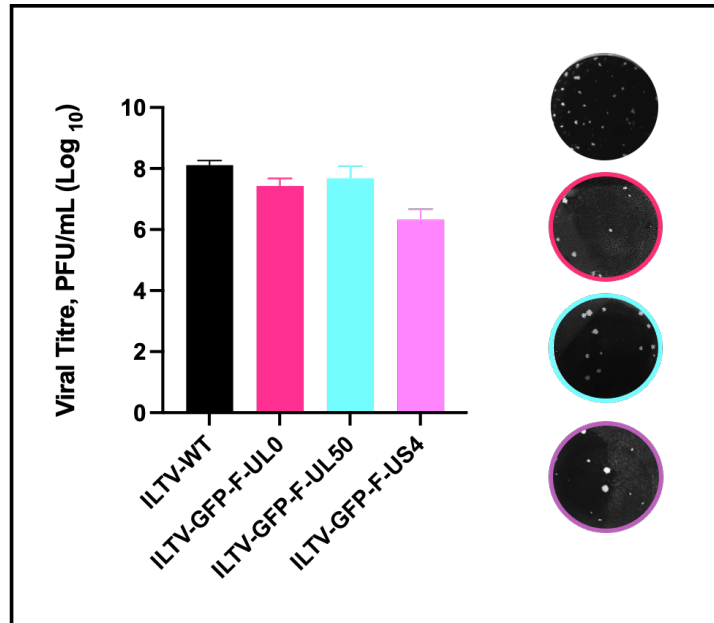


**Figure 4.13. Viral infectivity of the recombinant ILTV strains is not significantly different from the ILTV-WT.** Plaque assay-based quantification of the infectious virus between the ILTV-WT and recombinant ILTVs (ILTV-GFP-F-UL0, ILTV-GFP-F-UL50, and ILTV-GFP-F-US4). Comparative analysis through a one-way ANOVA revealed that there was no statistically significant difference in mean viral titre between the ILTV wild type and ILTV-GFP-F-UL0 ( $p = >0.9999$ ), the ILTV wild type and ILTV-GFP-F-UL50 ( $p = >0.9999$ ), or ILTV wild type and ILTV-GFP-F-US4 ( $p = >0.9999$ ). Error bars show the mean with standard deviation (SD). \* $p < 0.05$ , \*\* $p < 0.01$ , \*\*\* $p < 0.001$  using one-way ANOVA. Data analysis is based on one experiment with three technical replicates.

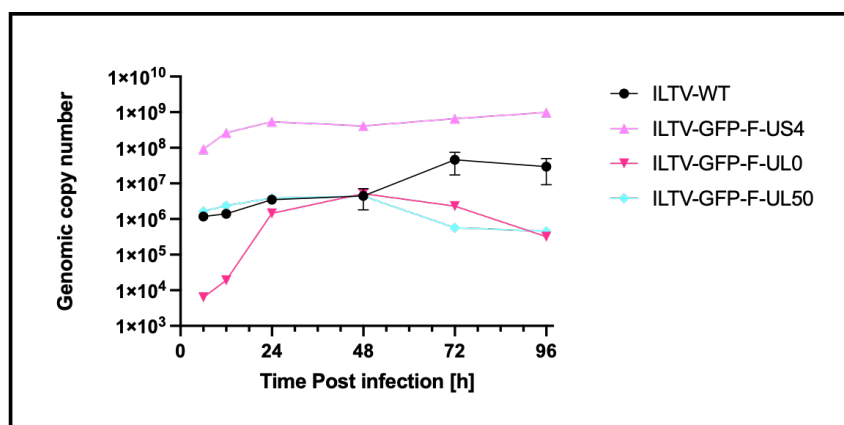


**Figure 4.14. Comparison of the replication kinetics of the ILTV-WT and recombinant ILTV strains.** qPCR data analysis represents the comparison of genomic copy numbers between the ILTV-WT and recombinant ILTVs (ILTV-GFP-F-UL0, ILTV-GFP-F-UL50, and ILTV-GFP-F-US4) through different time points (MOI = 1.0). Data analysis is based on one experiment with three technical replicates.



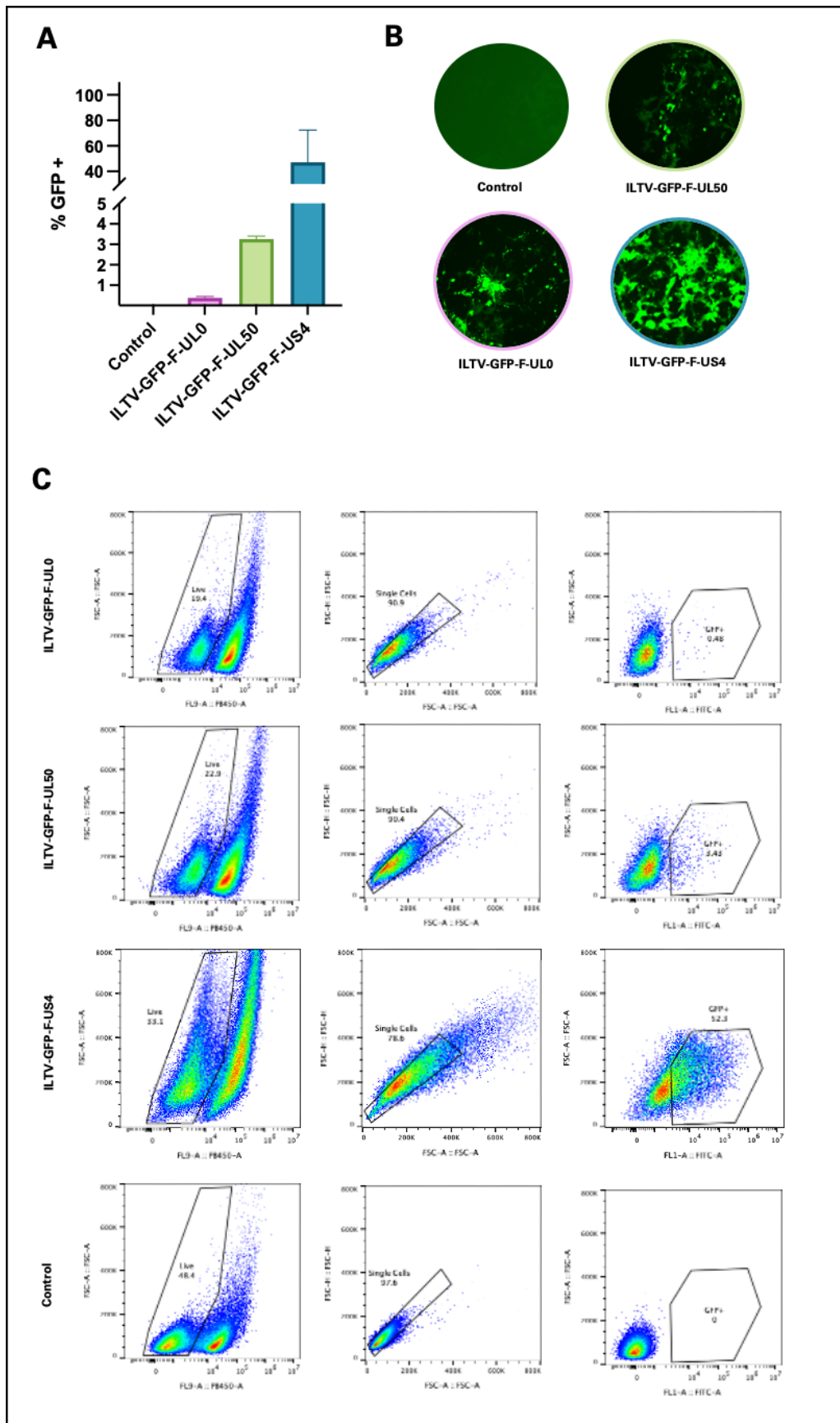


**Figure 4.15. Trend towards an increase in GFP positivity in LMH cells post-viral infection.** LMH cells were infected with recombinant ILTV-GFP-UL0, ILTV-GFP-UL50, and ILTV-GFP-US4 at 36 hours post-infection. Flow cytometry analysis was

performed to determine the infectivity of the recombinant ILTVs through GFP expression. **(A)** Graphical representation of the comparison in percent GFP positive between the uninfected control and recombinant ILTV-GFP-UL0, ILTV-GFP-UL50, and ILTV-GFP-US4. **(B)** Microscopic images showing the expression of GFP in recombinant ILTV-infected LMH cells. **(C)** The provided information represents the gating approach employed for the identification of GFP-positive cells in the LMH cell population. The viral particles were fluorescently marked with GFP, while the viability of the cells was determined using the live/dead staining kit. The process of gating was conducted via the FlowJo software. Data analysis is based on one experiment with three technical replicates.

#### **4.3.4. Knockout Experiments**

##### **4.3.4.1. Assembly and Construction of the ICP4 sgRNAs**

A total of three sgRNAs were designed to perform the ICP4 gene knockout. The sgRNA targeting the ICP4 gene was designed to cut the gene at the proximal, middle, and distal locations of the gene, as shown in **Figure 4.16**.

To facilitate the integration of the ICP4 sgRNA oligo fragment into the CRISPR/Cas9 construct pX459v2, both the sgRNA insert and the recipient vector (pX459v2) underwent digestion using the restriction enzyme *BbsI* (**Figure 4.17.A.B**). Subsequently, the use of DNA ligase facilitated the fusing of the sgRNA insert and the recipient vector. The CRISPR/Cas9-sgRNA plasmid, pX459v2-sgRNAs (**Figure 4.17.C**), was propagated by transformation into DH5 $\alpha$ -competent *E. coli* cells after ligation. The selection approach encompassed the detection and isolation of positive colonies through colony PCR, employing the forward HU6 universal primer (5'-GACTATCATATGCTTACCGT-3') and the sgRNA reverse oligo as the reverse primer (**Figure 4.18.A**). The purified plasmids were submitted for Sanger sequencing. The

Sanger sequencing verified a complete sequence similarity of 100% in the alignment of nucleotide sequences between the sgRNA oligos and the sequenced pX459v2-sgRNAs. The sequencing primer employed in this study was the HU6 universal primer. **Figure 4.18.B** illustrates the identification of positive guide RNAs, which are visually distinguished by the colour pink. These CRISPR/Cas9-sgRNA plasmids will be used for ILTV ICP4 gene knockout experiments.

#### **4.3.4.2. Generation of ICP4 Knockout Recombinant ILTV**

The production of recombinant ILTV knockout progenies and further passaging until passage II resulted in the successful creation of the putative recombinant ILTV with ICP4 knockout. The proof-of-concept study consisted of three primary procedures: transfection of ICP4 sgRNA plasmids at a concentration of 1 ug per sgRNA; infection of recombinant ILTV expressing a GFP signal at a multiplicity of infection (MOI) of 1.0; and subsequent collection of the recombinant ILTV containing potential ICP4 knockout progeny. The procedure was replicated for two separate passages, whereby the recombinant ILTV with ICP4 knockout offspring that had been collected was used for the infection in the subsequent passage. In the first passage, the infection was conducted using recombinant ILTV progeny with a knockout of the ICP4 gene, derived from passage 0. In the second passage, recombinant ILTV with ICP4 knockout progeny from passage I was used for infection. The downstream tests utilised the progeny of passage II, which consisted of the final recombinant ILTV with a putative knockout of the ICP4 gene (**Figure 4.19**).

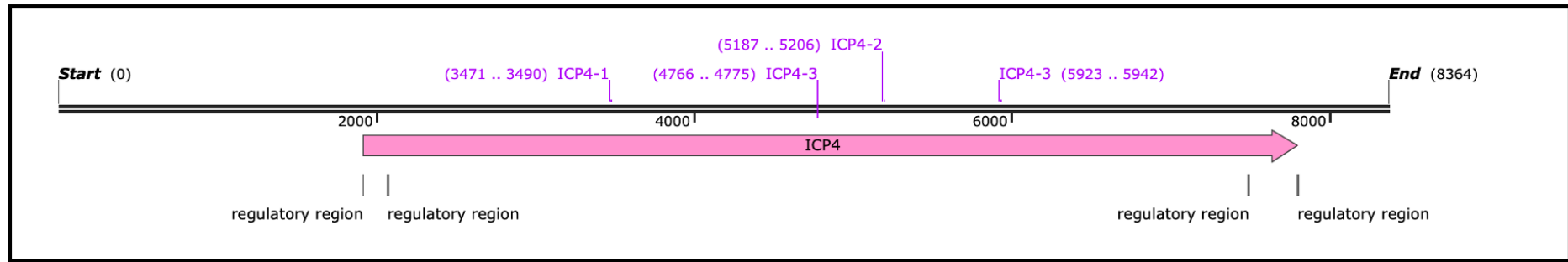


**Figure 4.16. Diagram illustrating the positioning of the guide RNA inside the ILTV ICP4 genomic region.** The location of the 28-31 bp guides is indicated by the sgRNA names in purple text. The design of the guide sgRNAs were based on the ILTV ICP4 genomic region: ICP4-1 (3471 ... 3490), ICP4-2 (5187 ... 5206), ICP4-3 (4766 ... 4775), and ICP4-3 (5923 ... 5942).



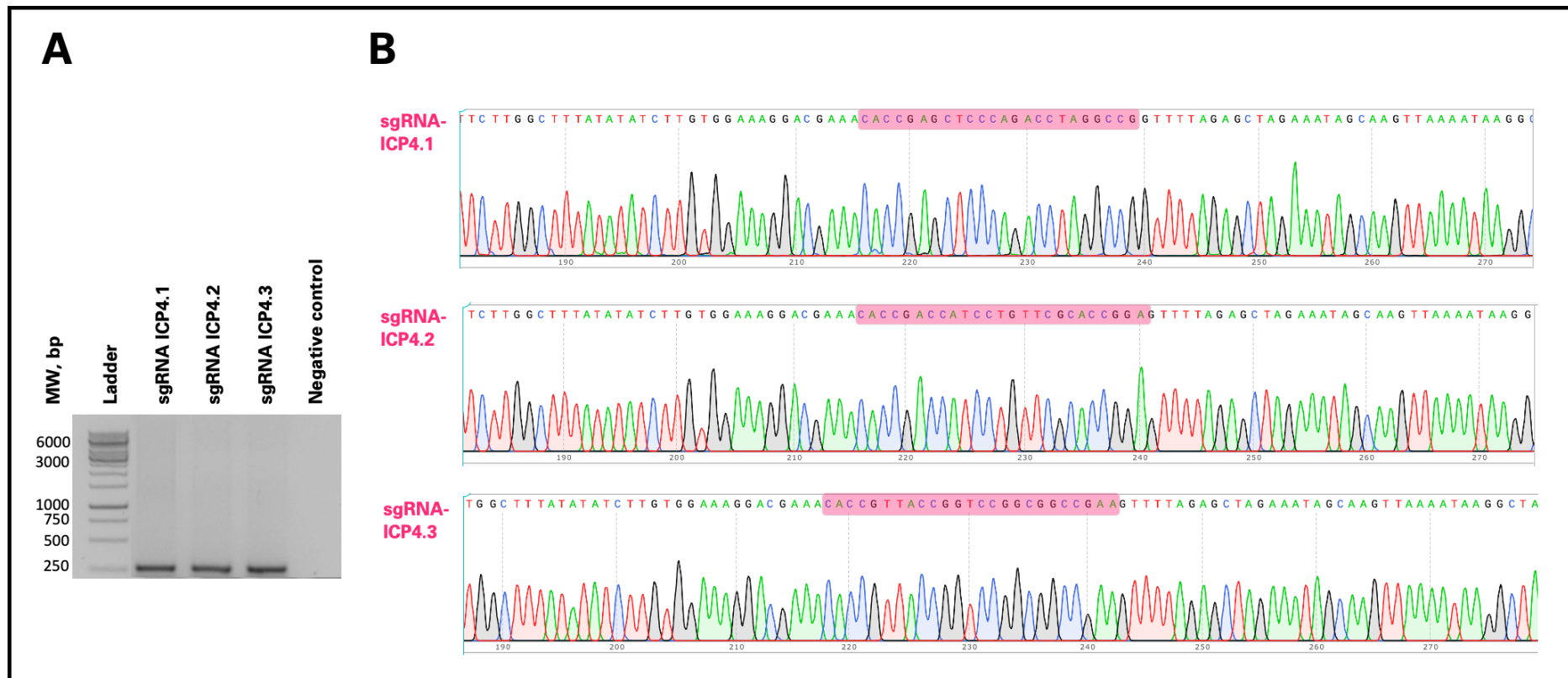


**Figure 4.18. Molecular and sequence validation of pX459v2-sgRNAs.** Validation of the cloning of the guide RNAs into the pX459v2. **(A)** Gel electrophoresis image show the positive bands at approximately 250 bp indicates the amplification of the sgRNA amplicon. Purified pX459v2-sgRNA plasmids were amplified through the forward HU6 universal primer (5'-GACTATCATATGCTTACCGT-3') and sgRNA reverse oligo. **(B)** Sanger sequencing results show 100% identity between the annealed sgRNA oligos and the sequenced pX459v2-sgRNAs. The sequencing primer used was the HU6 universal primer (5'-GACTATCATATGCTTACCGT-3'). Positive guide RNAs are highlighted in pink.

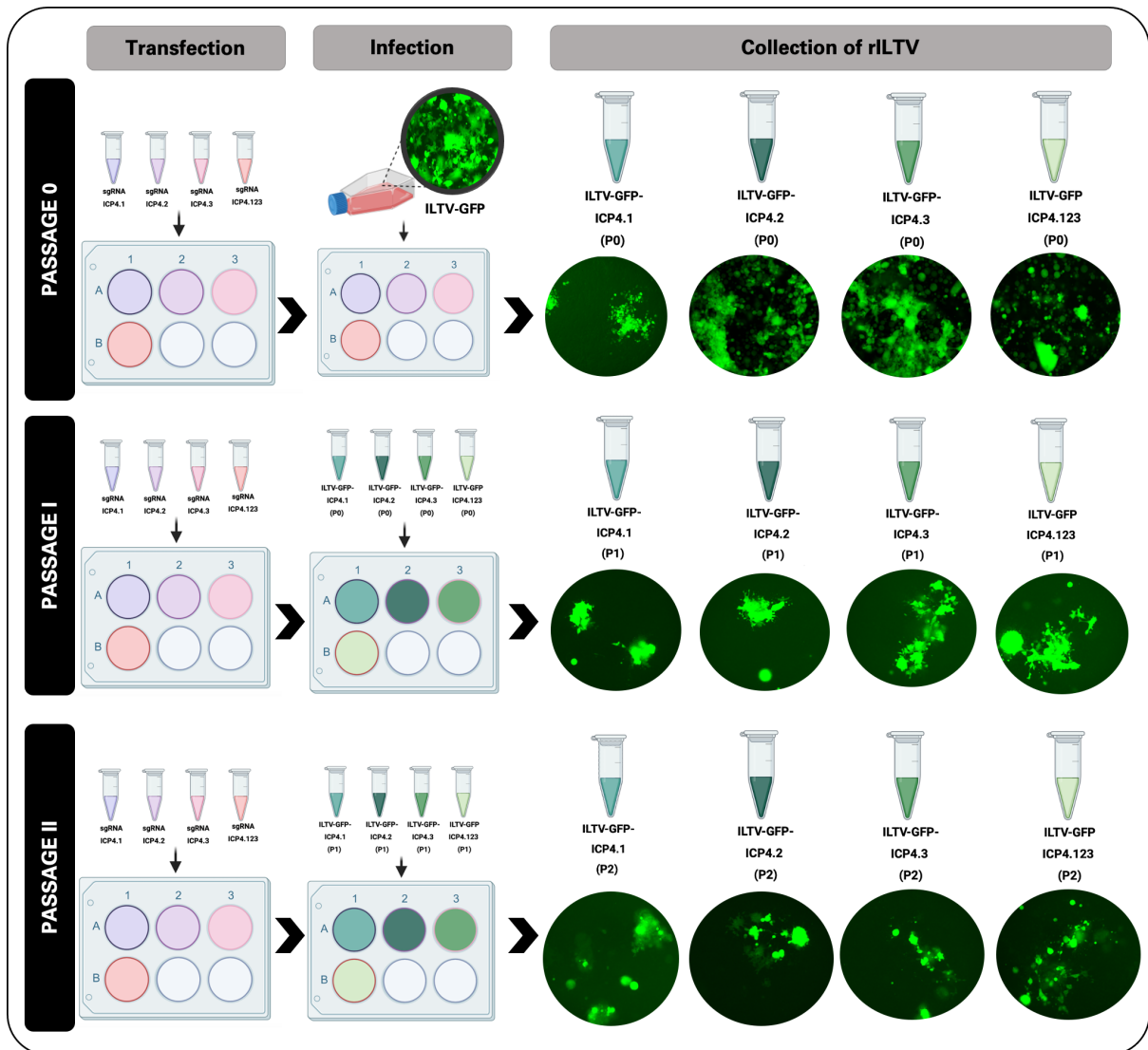


**Figure 4.19. Illustrative representation of the workflow used to generate recombinant ILTV with ICP4 knockout.** The workflow is divided into three main processes: transfection of ICP4 sgRNA plasmids (1  $\mu$ g per sgRNA), infection of recombinant ILTV expressing GFP signal (green) (MOI = 1.0), and collection of the recombinant ILTV with putative ICP4 knockout. These steps were repeated for two passages, each time using the collected recombinant ILTV with an ICP4 knockout for the infection in the succeeding passage. In passage I, recombinant ILTV with an ICP4 knockout from passage 0 was used for infection. In passage II, recombinant ILTV with an ICP4 knockout from passage I was used for infection. The final recombinant ILTV with ICP4 knockout from passage II was used for downstream experiments.

#### 4.3.4.3. Validation of the ICP4 Knockout Recombinant ILTV

The assessment of the relative change in viral concentration between recombinant ILTV with ICP4 knockout and ILTV-WT was performed using a plaque assay-based method. The LMH cells were subjected to infection by recombinant ILTVs with ICP4 knockouts (passage II). After 72 hours of infection, the samples were fixed and treated with crystal violet staining. The statistical analysis reveals a highly significant difference in the means of the viral concentration when comparing ILTV-WT and ILTV-GFP-ICP4.1, ILTV-WT and ILTV-GFP-ICP4.2, ILTV-WT and ILTV-GFP-ICP4.3, as well as ILTV-WT and ILTV-GFP-ICP4.123 (refer to **Figure 4.20.A.B**). The data is from one experiment with three technical repeats. Error bars show the mean with standard deviation (SD). \* $p < 0.05$ , \*\* $p < 0.01$ , \*\*\* $p < 0.001$  using one-way ANOVA.



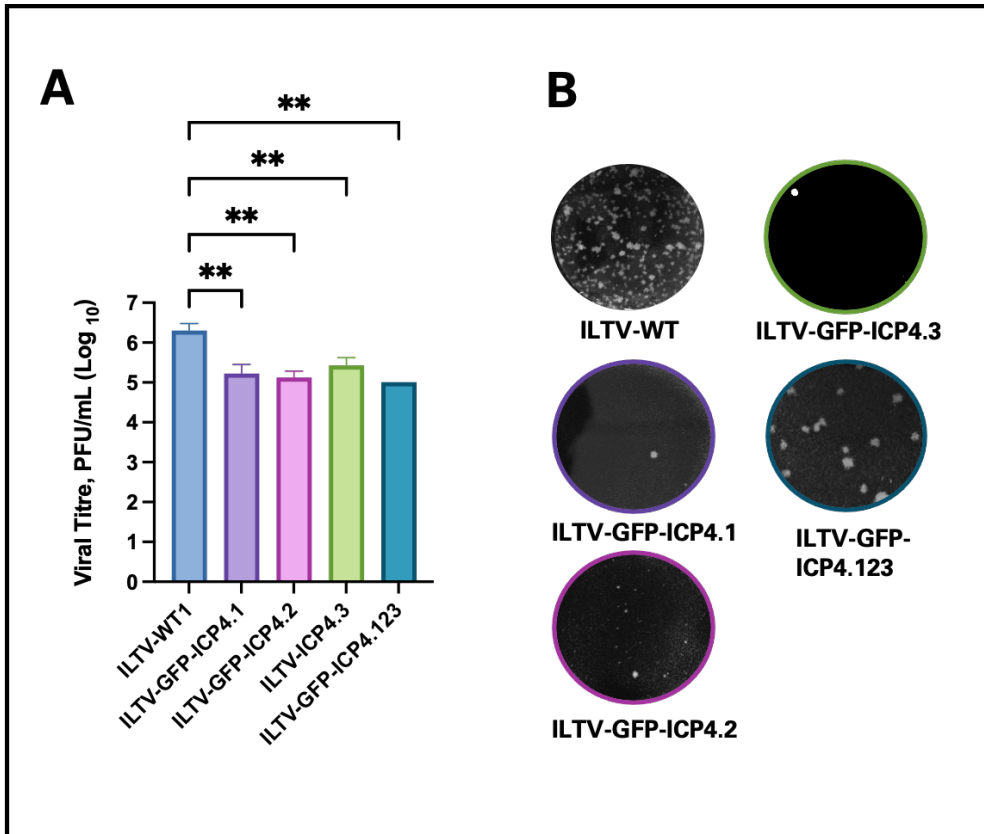


**Figure 4.20. Viral infectivity significantly decreased in recombinant ILTV strains with ICP4 gene knockout.** Plaque assay-based quantification of the relative change in viral concentration in recombinant ILTV with ICP4 knockout versus ILTV-WT. LMH cells were infected with the recombinant ILTVs with ICP4 knockouts (passage II), at 72 hours post-infection, samples were stained with crystal violet. **(A)** Statistical analysis shows a very significant difference in the means of the viral concentration between ILTV-WT and ILTV-GFP-ICP4.1; ILTV-WT and ILTV-GFP-ICP4.2; ILTV-WT and ILTV-GFP-ICP4.3; and ILTV-WT and ILTV-GFP-ICP4.123. **(B)** The plaque analyses illustrate the quantification of individual plaques. The data is from one experiment with three technical repeats. Error bars show the mean with standard deviation (SD). \* $p < 0.05$ , \*\* $p < 0.01$ , \*\*\* $p < 0.001$  using one-way ANOVA.

## 4.4. Chapter Discussion

The investigation of the potential of CRISPR/Cas9 in the development of recombinant ILTV strains has significant importance for the future of poultry disease prevention (Collett et al., 2020). The production and characterisation of the recombinant ILTV were facilitated by the use of several methodologies and techniques. The gene editing procedure employed the CRISPR/Cas9 system, which was guided by *in silico* sgRNA design. The assembly and propagation of the donor plasmids and sgRNAs were facilitated using cloning and molecular biology techniques, including restriction digestion and ligation. The donor plasmids were characterised through western blotting and IFA, while the selection and validation of recombinant ILTV strains were performed using molecular, protein, and imaging tools.

As previously mentioned, Atasoy et al. have implemented a study whereby they utilised the CRISPR/Cas9 system to delete the ILTV TK and US4 genes. Additionally, they introduced a GFP marker and the NDV-F gene in a synchronous manner. The recombinant strain of ILTV-GFP and the donor plasmid utilised in this investigation were created by the researchers (Atasoy et al., 2019). Prior studies have demonstrated that the TK gene of the herpesvirus, which is associated with virulence, is not necessary for the development and replication of the virus (Field & Wildy, 1978; S. Kit et al., 1985; Slater et al., 1993; Tenser et al., 1983); therefore, it has been a focus for the development of gene-deleted attenuated vaccines and recombinant viral vectors carrying inserted and expressed exogenous genes. (Nishikawa et al., 2000; Xuan et al., 1998).

In this chapter, the ILTV-GFP strain and the donor plasmid were first described and confirmed using various methodologies, including molecular methods, viral quantification, protein expression analysis, Sanger sequencing, and immunofluorescence assays. It was proposed in previous studies that the insertion of the GFP reporter gene into a certain region of the ILTV genome might cause toxicity and affect plaque formation (Fuchs et al., 2000; Veits et al., 2003). Our results through viral quantification using plaque assays and image analysis demonstrated that the final titres of the wild-type and recombinant strains are very similar. As well, the GFP protein is being expressed without any indication of negative effects such as loss of functionality and instability (Fuchs et al., 2000).

In contrast, the donor plasmid was evaluated using molecular and protein analysis, DNA sequencing, and an immunofluorescence test, which provided confirmation of the expression of the NDV-F and mRFP genes in DF1 cells. The results of the above methodologies have established the presence of the GFP signals emitted by the ILTV-GFP strain as well as validated its viral infectivity. Furthermore, the verification of the assembly of crucial components, including the mRFP (a fluorescence marker) and gene insert, within the donor plasmid yielded essential functional insights into the *in vitro* expression of the donor plasmid.

Due to the inherent advantages of herpesvirus-based vectors, they have been widely used in the development of several vaccines and treatments (Kamel & El-Sayed, 2019). Techniques used for generating recombinant herpesvirus include bacterial artificial chromosome (BAC), *en passant* mutagenesis, homologous recombination, codon optimisations in vectrology, and CRISPR/Cas9 gene editing technology (Kamel

& El-Sayed, 2019). Through these techniques, various animal herpesvirus-based recombinant viral vectors were developed both for research and commercial studies (Kamel & El-Sayed, 2019), including canine herpesvirus, feline herpesvirus, pseudorabies, bovine herpesvirus type 1, bovine herpesvirus 4, equine herpesvirus, and the herpesvirus of turkey. However, in terms of poultry herpesviruses, ILTV has not been extensively evaluated for its full potential as a candidate recombinant viral vector compared to HVT and MDV (Gergen et al., 2019; L. Liu et al., 2019; Y. Liu et al., 2020; N. Tang et al., 2018, 2019).

In order to evaluate the ability of the ILTV genome to accommodate foreign gene inserts and the versatility of CRISPR/Cas system gene editing technology, we designed a total of three guide RNA sequences that target three distinct genomic locations within the ILTV genome, specifically UL0, UL50, and US4. The aim of this is to evaluate the stability of the NDV-F integration inside three distinct genomic areas of ILTV and to provide a functional comparison of the recombinant viral vector strains created through the insertion of foreign genes in three different genomic locations. These ILTV genomic target regions are situated at the beginning of the ILTV genome (UL50) near the 5' terminal repeat region, at the end of the UL region near the internal repeat region bordering the UL and US regions (UL0), and in the middle of the US region (US4).

Three recombinant ILTV strains, namely ILTV-GFP-F-UL0, ILTV-GFP-F-UL50, and ILTV-GFP-F-US4, were generated using these three areas. The molecular and protein-level examinations of the recombinant ILTV strains demonstrated the presence of the NDV-F gene, confirming the effective application of CRISPR/Cas9

technology for modifying the ILTV genome and enabling the integration of the NDV-F gene. The localisation study provided confirmation of NDV-F gene expression within the cytoplasm of LMH cells following infection with ILTV strains. This observation is consistent with other research that has reported the accumulation and maturation of ILTV virions in the cytoplasm throughout the process of ILTV replication within host cells, ultimately leading to exocytosis or cell lysis (Gowthaman et al., 2020).

The stability and viral fitness of genetically engineered viral genomes with foreign gene insertions have consistently undergone extensive testing. The experiment involved assessing the infectivity of recombinant ILTV strains with a knock-in of the NDV-F gene in comparison to the ILTV wild-type strain. The quantification of viral infectivity using the plaque assay method revealed no statistically significant difference in infectivity between the wild-type ILTV strain and the recombinant ILTV strains (ILTV-GFP-F-UL0, ILTV-GFP-F-UL50, and ILTV-GFP-F-US4). All three genes, UL0, UL50, and US4, were shown to be non-essential for replication of ILTV in cell culture, as has been observed in previous studies (Devlin et al., 2006; Fuchs et al., 2000; Veits et al., 2003).

Additionally, a kinetics study was conducted using quantitative polymerase chain reaction (qPCR) to further quantify the presence of ILTV viral DNA over a period of time. This was achieved by amplifying the ILTV gB gene. The data obtained from the kinetics time point indicates two key findings. (1) The genomic copy number of the recombinant ILTV strains is found to be comparable to that of the ILTV-WT strain. In fact, in one instance, the recombinant ILTV strain with the NDV-F knock-in in the US4 region exhibited even better results. This result is consistent with the findings of Devlin

et al., 2006, showing that the deletion of the US4 gene rendered the recombinant ILTV strain with no deficiency in cell-to-cell spread (Devlin et al., 2006). (2) The replication of the recombinant ILTV strains with gene inserts at US4 and UL50 aligns with findings from other *in vitro* studies on the ILTV replication cycle. These studies have shown that viral progeny production occurs approximately 8 to 12 hours after infection, reaching the highest concentration around 24 to 30 hours post-infection. Additionally, latency establishment takes place within 7 to 10 days post-infection, as reported by Bagust and Johnson (1995) and Davison et al. (1989). However, the ILTV strains with inserts at UL0 appeared to be slightly delayed, implicating that UL0 might have a beneficial function in the early steps of viral replication (Veits et al., 2003).

Lastly, the cellular infectivity of the recombinant ILTV strains, including NDV-F knock-ins, was examined by flow cytometry. In this experiment, the GFP was employed as a marker to examine the presence of viral particles within the infected LMH cells. The results revealed a noticeable trend indicating an elevation in GFP positivity among the LMH cells after viral infection. The findings of this study suggest that the recombinant ILTV strains with the NDV-F knock-in mutation retained their infectivity. The flow cytometry findings of this study have the potential to be utilised in future investigations, including the examination of the *in vivo* behaviour of recombinant ILTV viral vector vaccine strains, as demonstrated in animal testing (De Baets et al., 2015). Flow cytometry studies have been employed as a technique for quantifying infectious virus titre, using its capacity to generate extensive datasets through the swift study of several individual cells (Grigorov et al., 2011; Z. Li et al., 2010; Logan et al., 2019; Lonsdale et al., 2003). Nevertheless, the utilisation of fluorescent reporter proteins requires a meticulously designed cell line or virus, a process that can be time-intensive

to establish (Logan et al., 2019). The recombinant ILTV viral strain, which carries a GFP reporter protein, has been successfully developed in this study using CRISPR/Cas9 gene editing technology, therefore circumventing the conventional labour-intensive approach. Our flow cytometry data successfully captured the effectiveness and efficiency of these recombinant ILTV strains, serving as a potential reference point for the creation of a rapid, high-throughput approach for infectious virus titration and GFP-based flow cytometry antiviral assay.

The targeted disruption of one or more essential genes can result in a reduction of viral replication within the cells of the host organism (M. Chen et al., 2008; Roehm et al., 2016). The application of CRISPR/Cas9 technology has facilitated the generation of a recombinant ILTV strain, wherein the ILTV ICP4 gene has been effectively disrupted. The study conducted by Challagulla et al. (2021) has demonstrated the crucial involvement of ICP4 in the process of ILTV viral replication. Three guide RNAs were developed with the purpose of disrupting the ICP4 gene inside the genome of ILTV. The production of the recombinant ILTV involved a sequential method of transfection-infection passaging of the recombinant ILTV progenies. Subsequently, during the second passage, the final recombinant ILTV strain with a predicted ICP4 knockout was validated by assessing the viral titre through counting the plaque-forming unit present. The analysis of the plaque assay demonstrated a notable decrease in replication of the recombinant ILTV strain in comparison to the wild-type ILTV. This proves the important role ICP4 plays in the ILTV replication cycle (M. Chen et al., 2008). *In vitro* characterisation of three sgRNAs targeting ILTV ICP4 showed successful inhibition of ILTV replication in LMH. While there was a decrease in the quantity of plaques formed, there was no significant variation in the diameters of

plaques among the different treatment groups. The findings of this study are consistent with prior research on the use of gene editing techniques (RNAi) to specifically target the ICP4 gene, therefore impeding viral replication (M. Chen et al., 2008; Lambeth et al., 2009). Our experimental design involved the use of three guide RNAs (gRNAs) that spanned the entirety of the ICP4 gene. Consequently, our targeting strategy can provide two potential outcomes: (i) a precise deletion of the complete ICP4 gene or (ii) the occurrence of mutations at the three specific gRNA loci within the ICP4 gene. The present preliminary investigation relative to the deletion of the ILTV ICP4 gene presents an exciting possibility for the development of innovative approaches aimed at treating ILTV infections.

Taken together, this chapter effectively demonstrated the efficacy of CRISPR/Cas9 in the creation of recombinant ILTV strains that incorporate foreign gene inserts, as well as ILTV strains with reduced replication potential. This chapter also demonstrates the stability and flexibility of recombinant ILTV strains containing inserted foreign genes and offers insights into potential sites within the ILTV genome where foreign gene insertion could be possible. While the CRISPR/Cas9-based gene knock-in system was first tested in the NDV-F gene, our objective is to employ this method for the development of other recombinant ILTV strains. These strains would function as viral vectors, capable of transporting antigens derived from various avian diseases.



# CHAPTER 5

## Construction of Recombinant ILTV-expressing NDV-F Gene Variants

### 5.1. Introduction

Emerging and re-emerging pathogens have a substantial influence on the economies and public health of nations around the globe (Gummow, 2010). Vaccination has been widely acknowledged as the most efficacious method for safeguarding individuals from infection throughout the course of battling infectious illnesses. The field of vaccine development is seeing tremendous advancements due to the progress made in immunology, molecular biology, and microbiology (Zenglei Hu et al., 2020). Recombinant viral vectors offer a robust and promising framework for the production of vaccines that are safe, immunogenic, and efficacious (Aida et al., 2021; Lauer et al., 2017; Naim, 2013). This approach eliminates the need for cultivating and manipulating live pathogens, especially those that pose a fatal threat to both humans and animals. The use of recombinant viral vectors as the basis for vaccinations has resulted in significant breakthroughs (Marín-López & Ortego, 2016). These vaccines have become safer and more potent, making them an effective tool for vaccine development. Additionally, they have demonstrated the ability to produce long-term immunity, as supported by studies conducted by Lauring et al. (2010) and Lino et al. (2018) (Lauring et al., 2010; Lino et al., 2018).

The need for highly effective vaccines has witnessed a significant surge in response to the need for addressing emerging and re-emerging infectious illnesses, as well as mitigating the limitations associated with conventional vaccine types such as live attenuated and inactivated vaccines (Fauci, 2005; Kanekiyo et al., 2019; Liverani et al., 2013; Vilela et al., 2022). Viral vector-based vaccines, which utilise the delivery of one or more genetically engineered viral antigens, exhibit significant versatility and provide several benefits compared to conventional vaccination technologies (Yokoyama et al., 1997). This method employs either living vectors, which may have replicative properties but are frequently attenuated, or non-replicating vectors (Rauch et al., 2018). Replicating viral vector vaccines possess the attributes of live vaccines, eliminating the necessity for complete pathogen involvement or pathogen cultivation. Additionally, these vaccines have the capability to intracellularly administer foreign antigens, thereby eliciting humoral, cellular, and mucosal immune responses (Bukreyev & Collins, 2008).

NDV is an economically important pathogen, devastating the poultry industry (Imran et al., 2020). Vaccination is still the most effective approach to preventing the disease. NDV vaccines are effective in suppressing large-scale outbreaks globally. However, due to mutations, small-scale outbreaks, and new strains with higher virulence emerging, there is a need for a novel vaccine against NDV (Sakaguchi et al., 1998; X. Yuan et al., 2012; M. Zhang et al., 2017).

After almost a century since its initial appearance, NDV has gone through significant evolutionary changes, leading to a notable diversity in its genetic makeup, virulence levels, antigenic properties, and ability to infect various hosts (Zenglei Hu et al., 2022).

Furthermore, the phenomenon of antigenic variation, which is a significant indication of viral evolution, can lead to immune resistance and inadequate immunity against prevailing viral field strains (Zenglei Hu et al., 2022). The comparison of commercial and experimental ND vaccines has significant importance in the context of effective vaccination programmes and the identification of development pathways for next-generation vaccines (Zenglei Hu et al., 2022; Sultan et al., 2021). This is mostly because of the lack of similarity observed between prevailing field strains and existing vaccines (Yonghua Li et al., 2021; C. Meng et al., 2018). The development of novel vaccine responses to emerging and existing field NDV strains is widely recognised (DiNapoli et al., 2007; Panda et al., 2004). Strategies that enhance the immunogenicity of recombinant viral vectors through adjuvants in the form of tags have been previously studied (Du et al., 2011; Loureiro et al., 2011; F. Yu et al., 2015).

In the context of vaccines, enhancers or adjuvants refer to components that have the ability to augment and/or modulate immune responses specific to antigens (Chambers et al., 2016). Modern vaccines are developed using deliberately designed recombinant antigens that consist of precisely purified components possessing desirable safety properties (Reed et al., 2013). Two commonly investigated enhancers for poultry vaccine development are Foldon (Fd) and the IgY Fc domain (Du et al., 2011; F. Yu et al., 2015). Foldon is a naturally occurring trimerization domain that aids in stabilising protein trimer or oligomer structures (J. Li et al., 2013; F. Yu et al., 2015). This stabilisation enhances the immunogenicity and antiviral activity of recombinant proteins. On the other hand, the IgY Fc domain improves antigen processing efficiency, thereby augmenting the immunological response triggered by the antigen (Du et al., 2011; Jegaskanda, 2018; B. Zhao et al., 2018). Additionally, it facilitates

binding to antigen-presenting cells (APCs) or cells expressing Fc receptors and assists in the proper folding of F proteins post-expression. Evidence of enhanced immunity has been shown in studies fusing the human immunoglobulin Fc domain (HuFc) to glycoproteins (Schmidt, 2009; M.-Y. Zhang et al., 2009).

Currently, there is a lack of research evaluating the efficacy of foldon and fc domain enhancers in the context of NDV-F antigen. Furthermore, it is vital to investigate the advancement of a viral vaccine vector that integrates the NDV-F gene fused with Fc or Fd enhancers and evaluate its efficacy.

### **5.1.1 Aims**

The objective of this chapter is to utilise the CRISPR/Cas9 gene editing technology to demonstrate the potential of ILTV as a vaccine vector capable of delivering foreign antigen inserts.

Specifically:

1. Develop a gene cassette with the NDV-F gene fused with enhancers.
2. Perform *in silico*-based analyses on the predicted protein sequences of the NDV-F protein fused with enhancers.
3. Functionally validate the donor plasmid carrying the NDV-F gene fused with enhancers.
4. Demonstrate the effectiveness of CRISPR/Cas9 in creating incisions in the ILTV genome leading to the insertion of the NDV-F gene fused with enhancers.
5. Demonstrate the ability of ILTV as a putative vaccine vector through the insertion of NDV-F antigen fused with enhancers.

## 5.2. Results

In order to conduct an extensive investigation of the ILTV's potential as a vaccine viral vector, we have devised a systematic procedure that facilitates the manipulation of the NDV-F gene insert by fusing enhancers at the 3' end of the NDV-F gene fragment. This approach will further assess the stability of the inserts and examine their potential impact on the replication and virulence of ILTV. The genome of ILTV is currently estimated to be around 149,000 bases in length. The introduction of foreign genes of different sizes into this genome may potentially impact insert stability, viral replication, and virulence (Willemsen & Zwart, 2019).

### 5.2.1. *In silico* Characterisation of NDV-F Gene Variants

By employing an in-silico approach for vaccine design, this chapter successfully devised three variations of NDV-F, each incorporating distinct enhancers: foldon, chicken IgY Fc domain, and chicken IgY Fc domain tail region. The selection of these enhancers was conducted with detailed attention, taking into consideration prior publications (Jegaskanda, 2018; Loureiro et al., 2011; F. Yu et al., 2015) and their demonstrated capacity to augment the immune response. The selection of the NDV-F protein as the preferable antigen was mainly driven by its significant role in both virulence and infectivity. **Figure 5.1** presents a visual representation of the *in silico*-driven design of the NDV-F gene cassette combined with enhancers. The *in silico* study was conducted using the amino acid sequence of the whole proteome of NDV, as provided by the NCBI Reference Sequence NC\_039223.1. The choice of the NDV-F protein among the six transcriptional units was determined based on its potential for antigenicity. The F protein sequence of NDV is combined with enhancers, namely

Foldon (Fd), the Fc domain of chicken immunoglobulin Y (IgY) (Fc), and the FcTail, a fragment of the chicken IgY Fc domain. The gene cassettes NDVF-Fd, NDVF-Fc, and NDVF-FcTail were generated by the fusion of the NDV-F protein with enhancer elements. The physicochemical features of the NDV-F variations were assessed by analysing their secondary protein structure, which involved predicting protein folding, determining the number of amino acids, the instability index, and calculating the molecular weight. Finally, web-based algorithms (Swiss model) were employed to predict the tertiary structure of the NDV-F variants. **Table 5.1** is a summary of the physico-chemical and antigenic features that have been inferred from the protein sequences of the F variant of NDV. The protein sequence analysis was conducted utilising the ProtParam, Swiss-model, and Translate tools available on the Swiss Bioinformatics Resource Portal. Additional research was conducted to explore the predictive capabilities of antigens using the VaxiJen online algorithm (<http://www.ddg-pharmfac.net/vaxijen/>). The NDV-F variants were synthetically synthesised and will serve as the gene inserts in this chapter.



**Table 5.1.** Summary of the physico-chemical and antigenic properties deduced from the NDV-F variant protein sequences as well as the NDF wild type.

NDV-F Variant	No. of Amino acid	Molecular weight, kDa	Instability Index	Protective antigen
NDVF-Fd	557	60	28.48 (Stable)	0.51 (Probable Antigen)
NDVF-Fc	755	81	38.49 (Stable)	0.54 (Probable Antigen)
NDVF-FcTail	559	60	30.59 (Stable)	0.54 (Probable Antigen)
NDVF-WT	551	58	31.0 (Stable)	0.55 (Probable Antigen)

### 5.2.2. Cloning and Validation of Gene Cassettes

The donor plasmid pCDNA3-MCS1-mRFP, which was previously created and discussed in Chapter 4, was utilised to create donor plasmids that harbour the NDV-F variations in MCS1. **Figure 5.2.A** illustrates a schematic depiction of the donor plasmid pCDNA3-MCS1-mRFP. To enable the integration of the NDV-F variant fragment into the multiple cloning site 1 (MCS1) of the recipient vector (pcDNA-MCS1-mRFP), both the NDV-F variant insert and the recipient vector (pcDNA-MCS1-mRFP) were subjected to restriction enzyme digestion using the enzymes *NheI* and *Clal* (**Figure 5.2.B**). Following this, the use of DNA ligase enabled the fusion of the NDV-F variant insert with the recipient vector. The final construct map of the NDV-F variants, namely pcDNA3-NDVF-Fd, pcDNA3-NDVF-Fc, pcDNA3-NDVF-FcTail, and pcDNA3-NDVF-WT, is depicted in **Figure 5.2.C**. This map was acquired subsequent to ligation and was then propagated by transformation into DH5 $\alpha$ -competent *E. coli* cells.

The molecular and protein levels were used to evaluate the expression of the NDV-F variants in the purified plasmids. The examination of molecular, protein, and imaging data was conducted using DF1 cells that had been transfected. PCR amplification of the NDV-F variant was performed using the MCS1-specific primers, namely CMV-



MCS1-F (5'-AGAACCCACTGCTTACTGGCTT-3') and CMV-MCS1-R (5'-AACTAGAAGGCACAGTCGAGGC-3'). The electrophoresis image obtained from this amplification process revealed the molecular sizes of the NDV-F variant genes as follows: NDVF-Fd (~1.8 kb), NDVF-Fc (~2.3 kb), and NDVF-FcTail (~1.9 kb). The size of NDVF-WT is estimated to be around 1.6 kb, as seen in **Figure 5.3.A**. In order to provide a more comprehensive characterisation of the NDV-F variant donor plasmids, a western blot analysis was conducted to ascertain the expression of the NDV-F variants in DF1 cells. The Western blot analysis depicted an image illustrating the identification of NDV-F variants, namely, NDVF-Fd (~60 kDa), NDVF-Fc (~81 kDa), NDVF-FcTail (~60 kDa), and NDVF-WT (about 55 kDa). This detection was achieved by employing ANTI-FLAG as the primary antibody, followed by the application of Goat anti-Rabbit IgG conjugated with Alexa fluor 488, which emitted a brilliant green fluorescence signal. The beta-tubulin protein was utilised as the loading control in the western blot experiment as well as in other studies conducted in the scope of this research (**Figure 5.3.B**). The purpose of the immunofluorescence experiment was to validate the expression and spatial distribution of the different versions of the NDV-F protein. The confocal imaging results revealed the existence of the NDV-F protein variants, which were labelled with anti-FLAG, and their distinct location inside the cytoplasm of the DF1 cells (**Figure 5.3.C**).

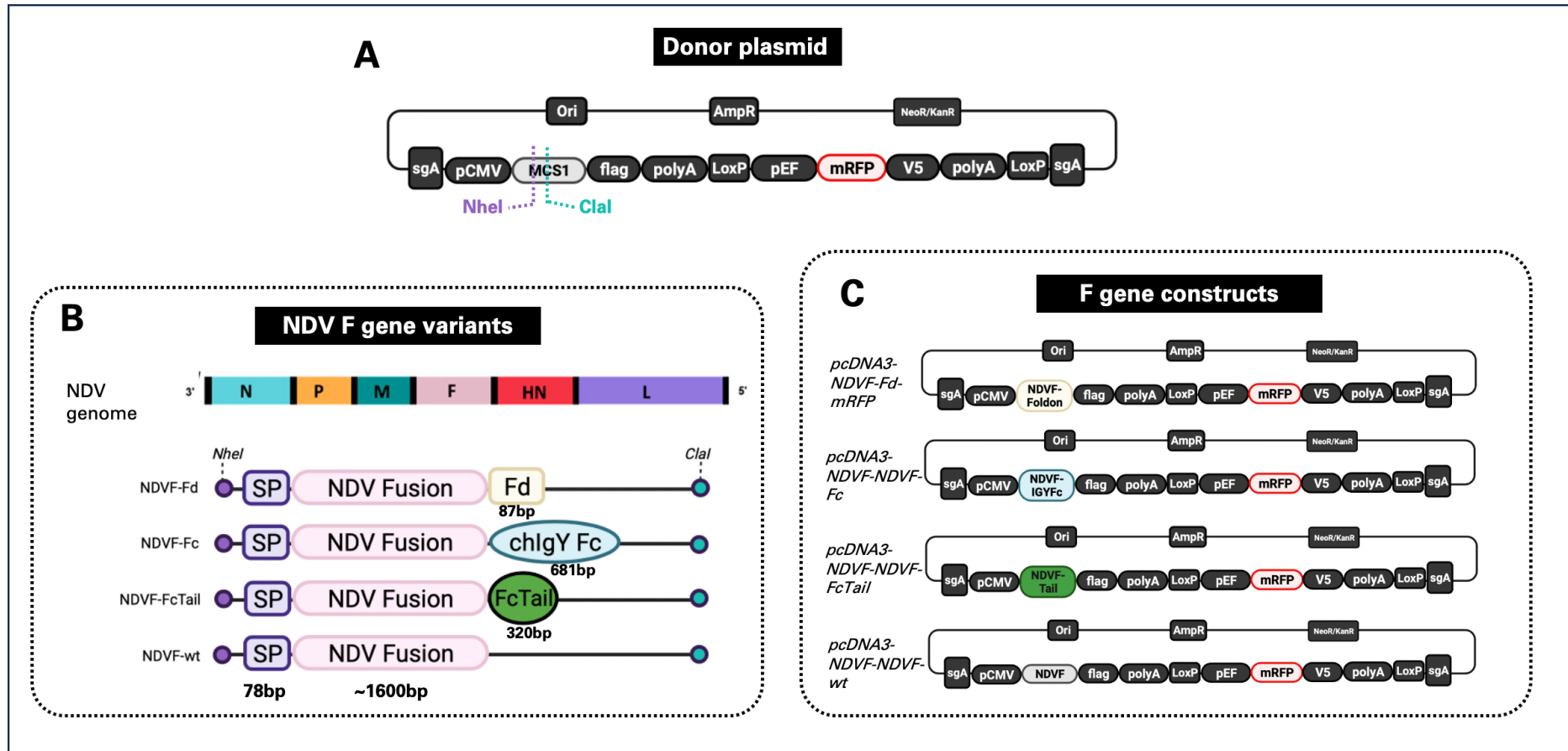


**Figure 5.2. A schematic representation illustrating the structural organisation of the donor plasmid construct map for the NDV-F variants. (A)** The previously generated donor plasmid pCDNA3-MCS1-mRFP, as described in Chapter 4, was employed to generate donor plasmids containing the NDV-F variants in MCS1. **(B)** The insertion of the NDV-F variants into the donor plasmid was accomplished by means of restriction digestion utilising *NheI* and *ClaI* restriction enzymes. The final construct map of the NDV-F variants, namely pcDNA3-NDVF-Fd, pcDNA3-NDVF-Fc, pcDNA3-NDVF-FcTail, and pcDNA3-NDVF-WT, is presented in **(C)**.

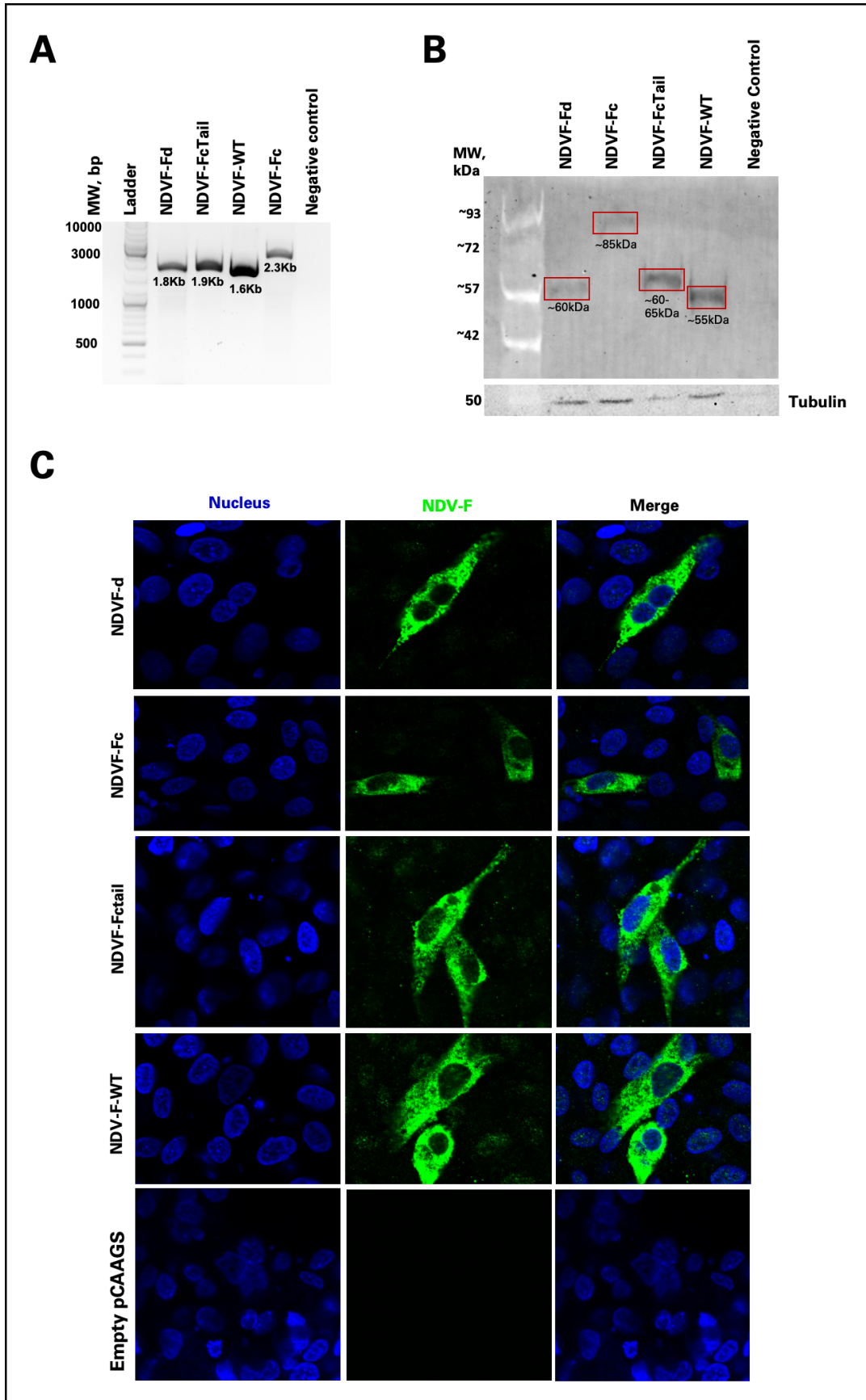


**Figure 5.3. NDV-F variant expression assessed at the molecular and protein levels.** Purified plasmids were assessed at the molecular and protein levels for the

expression of the NDV-F variants. Transfected DF1 cells were used for the protein and imaging analyses. **(A)** Primers (CMV-MCS1-F 5'-AGAACCCACTGCTTACTGGCTT-3' and CMV-MCS1-R 5'-AACTAGAAGGCACAGTCGAGGC-3') flanking the MCS1 region of the donor plasmid were used for the amplification of the NDV-F variants. NDV-F variant gene amplification molecular size is as follows: NDVF-Fd (~1.8 kb), NDVF-Fc (~2.3 kb), and NDVF-FcTail (~1.9 kb). NDVF-WT is approximately 1.6 kb in size. **(B)** Western blot image showing the detection of NDV-F variants, NDVF-Fd (~60 kDa), NDVF-Fc (~81 kDa), NDVF-FcTail (~60 kDa), and NDVF-WT (approximately 55 kDa) using ANTI-FLAG followed by Goat anti-Rabbit IgG labelled with Alexa fluor 488. Beta-tubulin was used as the loading control for the western blot experiment, as well as for all other experiments conducted within the scope of this work. **(C)** Confocal immunofluorescence image showing the NDV-F protein variant location. The nucleus and NDV-F variants (green) were labelled with DAPI and anti-FLAG, respectively. Empty plasmid-transfected cells served as negative control.

### 5.2.3. Generation of Recombinant ILTV Variants

The generation of the recombinant ILTV with a cassette knock-in of NDV-F gene variants involved the assembly of multiple components. These components included: (1) the recombinant ILTV-GFP, which expresses the GFP gene; (2) the donor plasmid pcDNA-NDVF-Variant-mRFP, which carries the NDV-F gene variants and a reporter gene encoding mRFP; and (3) the CRISPR/Cas9-sgRNA plasmids, specifically pX459v2-US4, which were designed to induce double-strand breaks in the ILTV genome at the US4 region.

The procedure involves two main components: the transfection of the donor plasmid (pcDNA-NDVF-Variant-mRFP) and the CRISPR/Cas9-sgRNA plasmid (pX459v2-US4) into LMH cells (**Figure 5.4.A**). During the process of incubation, the accessory guide RNA-A (pX459v2-sgRNA-A) will precisely identify and cleave the specific sgRNA A site present in the donor plasmid, resulting in the liberation of the NDVF-Variant-mRFP gene cassette. At 36 hours following transfection, subsequent to the visual detection of red fluorescence by microscopic examination, the LMH cells were subjected to infection with recombinant ILTV-GFP (**Figure 5.4.B**). The use of the CRISPR/Cas9-guideRNA (pX459v2-US4) system facilitates the analysis of the ILTV genome and facilitates the precise cleavage required for the integration of the NDVF-Variant-mRFP gene cassette into the ILTV genome (specifically in the US4 genomic region). Consequently, this process results in non-homology targeting. At the 24-hour time point following infection, LMH cells were examined using microscopy to assess the simultaneous presence of the GFP protein, which emits green fluorescence, indicating the effective infection of the ILTV-GFP, and the expression of the mRFP reporter gene within the gene cassette carried by the donor plasmid pcDNA-NDVF-

mRFP, which emits red fluorescence. The genetically modified ILTV-GFP-NDVF variants, which were derived from viral progenies, were exposed to the Cre enzyme for treatment. The enzyme recognises the LoxP region present in the ILTV-GFP-NDVF variant genome, leading to the excision of the adjacent genomic region, including the mRFP gene, hence inducing a heritable deletion of the gene. The deletion event leads to the manifestation of GFP with a positive expression in the viral progeny, whereas the expression of mRFP is absent. The diagram depicted in **Figures 5.5, 5.6, and 5.7** illustrates the subject matter under discussion.

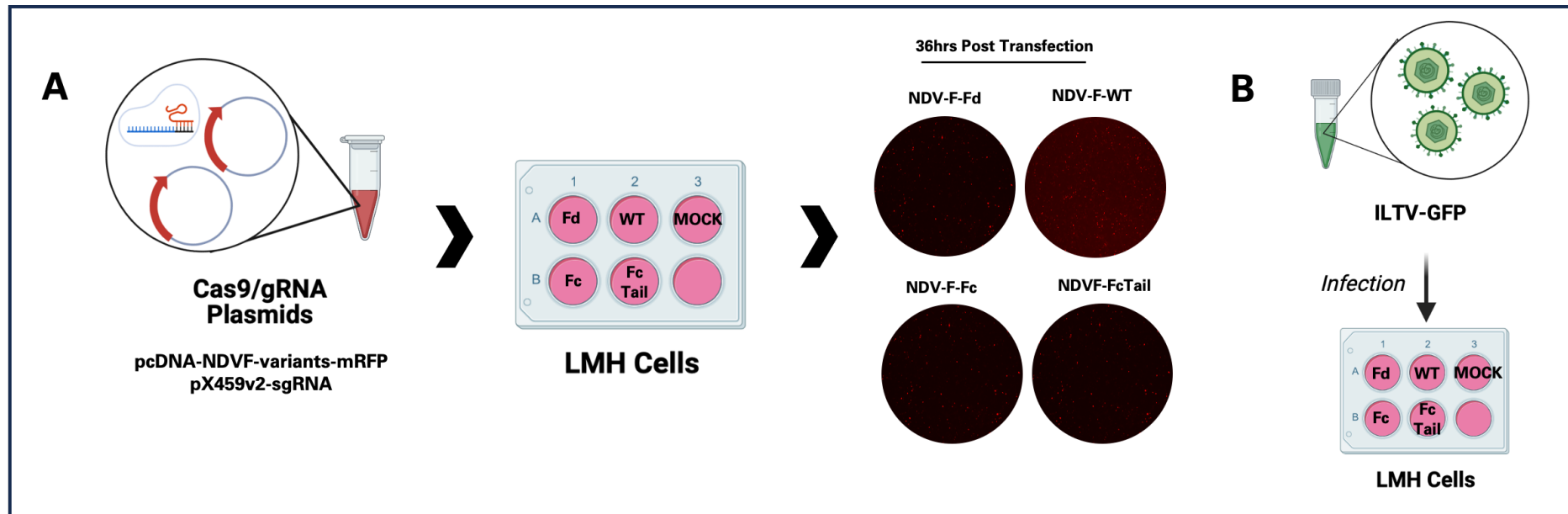


**Figure 5.4. Illustrative representation of the workflow used for the generation of recombinant ILTV-GFP-NDVF variants.** The method comprises two essential elements: **(A)** The transfection of LMH cells with pX459v2-sgRNA plasmids (plasmids containing CRISPR/Cas9-sgRNA) and pcDNA3-NDVF-variants-mRFP (donor plasmid). At the time point of 36 hours after transfection, a microscopic analysis revealed the expression of red fluorescence, indicating the detection of donor plasmids (pcDNA3-NDVF-Variants-mRFP) within LMH cells. **(B)** Following the identification of the red fluorescence in LMH cells, the cells were subsequently infected with ILTV-GFP.

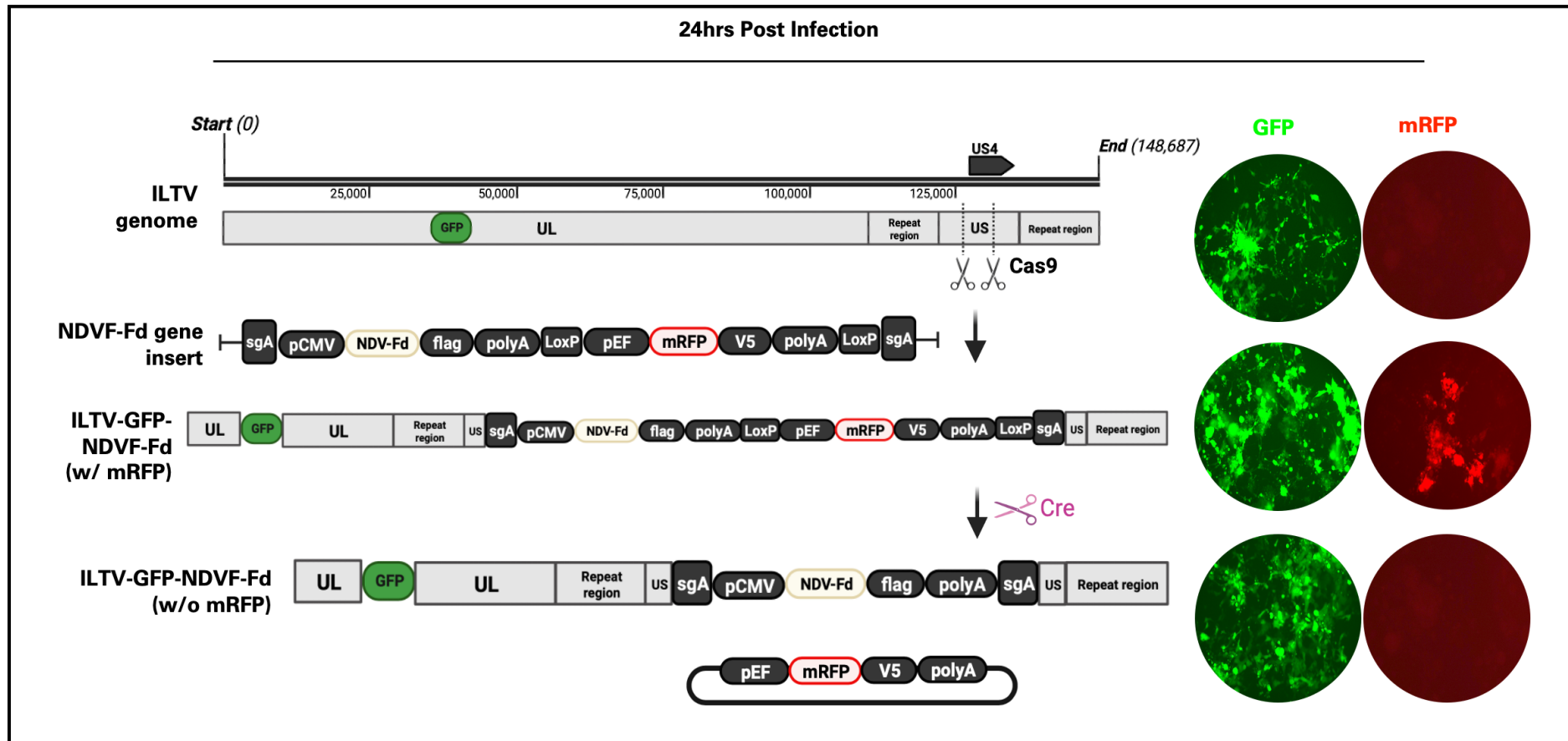


**Figure 5.5. Illustrative representation of the CRISPR/Cas9 – Cre/Lox system used to create the recombinant ILTV-GFP-NDVF-Fd.** At the 24-hour time point following infection, the CRISPR/Cas9 enzyme induces double-strand breaks at the US4 region of the ILTV-GFP genome, resulting in the insertion of the NDV-F-Fd gene insert. This genetic modification leads to the generation of the recombinant ILTV-GFP-NDVF-Fd variant, which exhibits positive GFP expression and mRFP expression. The viral progenies of ILTV-GFP-NDVF variants, which had been genetically modified by recombination, were subjected to treatment with the Cre enzyme. This enzyme recognises the LoxP region within the ILTV-GFP-NDVF variant genome and removes the surrounding area containing the mRFP gene, resulting in a permanent deletion of the gene. As a result of this deletion, the viral progenies exhibit a positive expression of GFP but lack the expression of mRFP. The Zoe Fluorescent Cell Imager (Biorad) was utilised to capture the images.



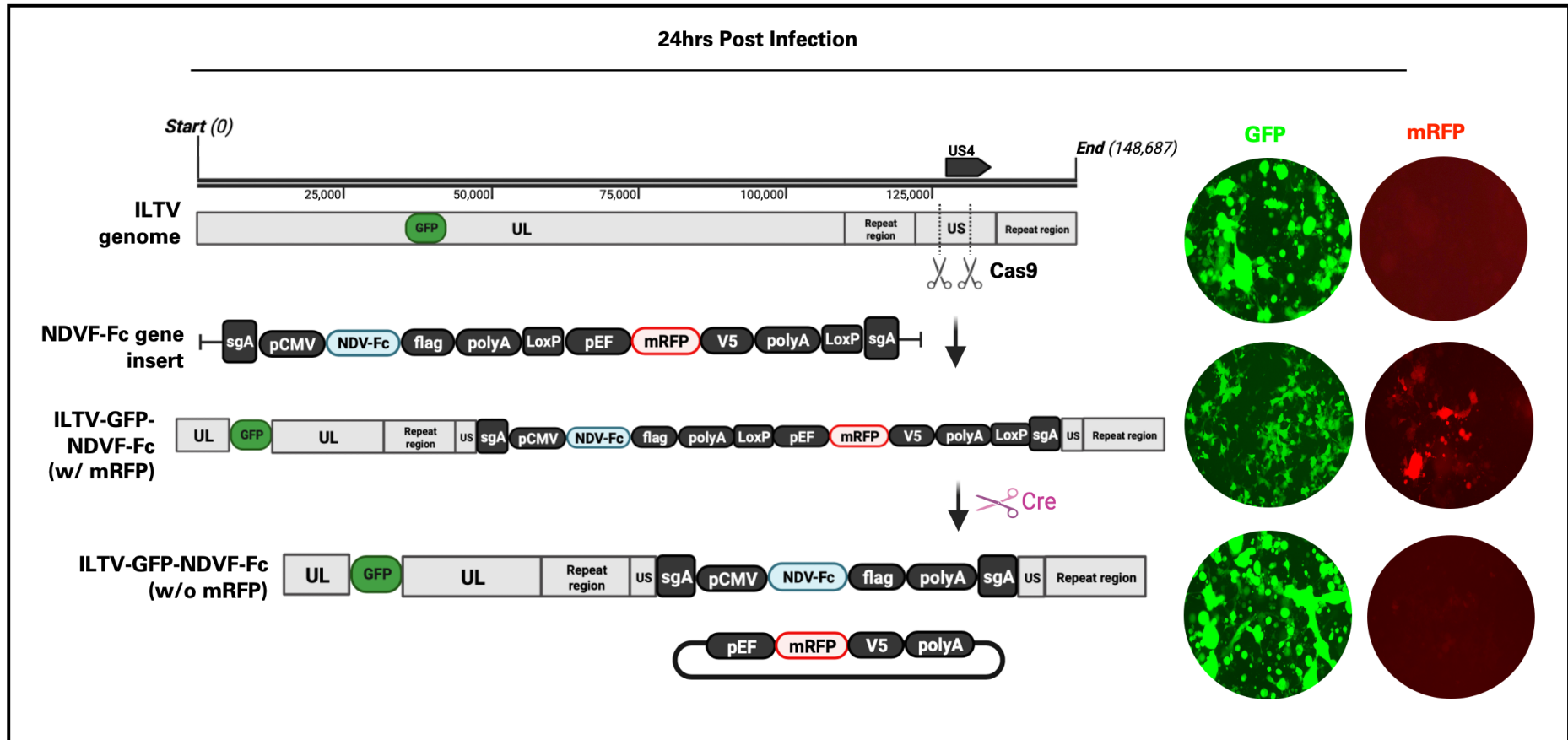


**Figure 5.6. Illustrative representation of the CRISPR/Cas9 – Cre/Lox system used to create the recombinant ILTV-GFP-NDVF-Fc.** At the 24-hour time point following infection, the CRISPR/Cas9 enzyme induces double-strand breaks at the US4 region of the ILTV-GFP genome, resulting in the insertion of the NDV-Fc gene insert. This genetic modification leads to the generation of the recombinant ILTV-GFP-NDVF-Fc variant, which exhibits positive GFP expression and mRFP expression. The viral progenies of ILTV-GFP-NDVF variants, which had been genetically modified by recombination, were subjected to treatment with the Cre enzyme. This enzyme recognises the LoxP region within the ILTV-GFP-NDVF variant genome and removes the surrounding area containing the mRFP gene, resulting in a permanent deletion of the gene. As a result of this deletion, the viral progenies exhibit a positive expression of GFP but lack the expression of mRFP. The Zoe Fluorescent Cell Imager (Biorad) was utilised to capture the images.

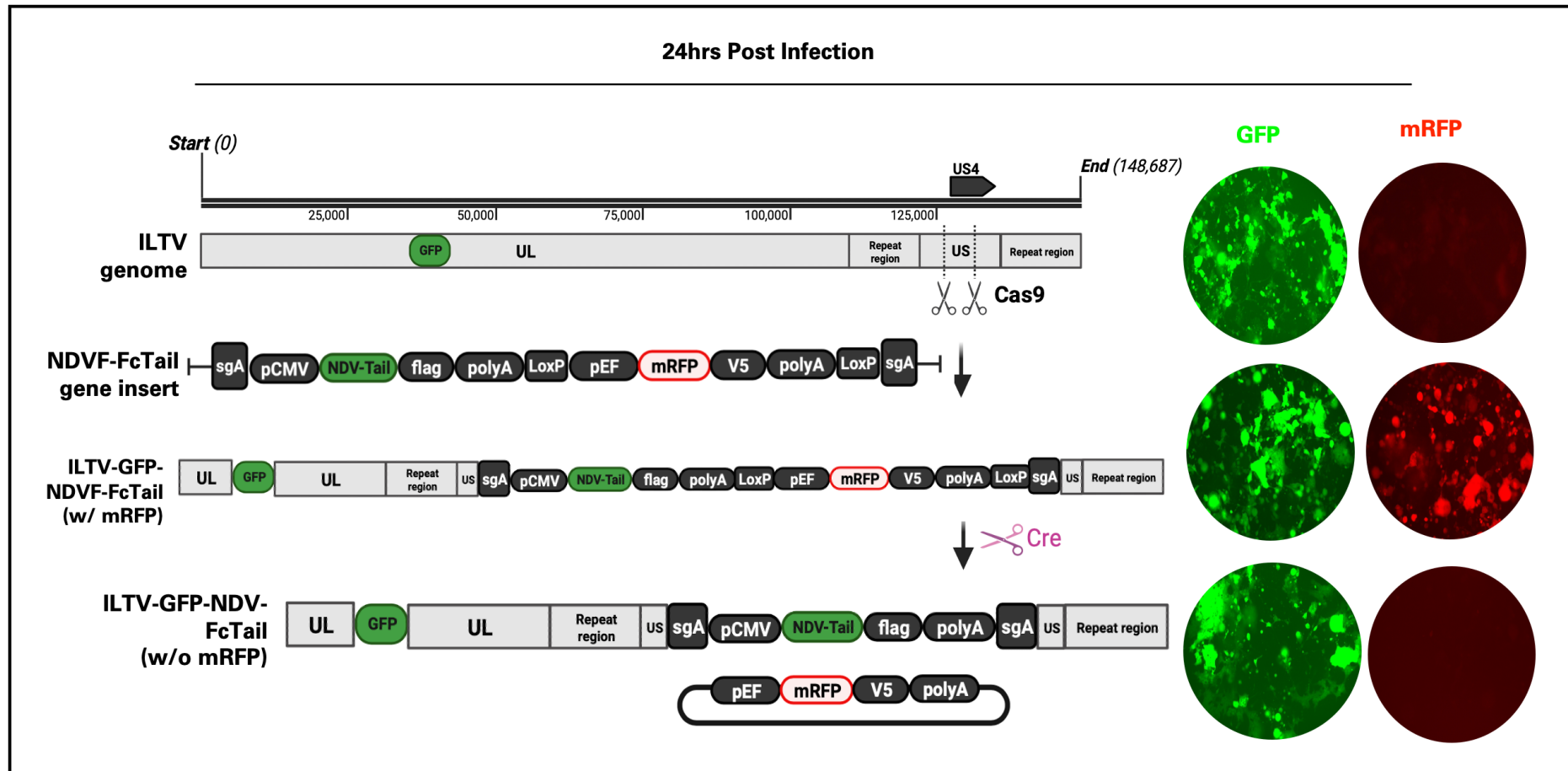


**Figure 5.7. Illustrative representation of the CRISPR/Cas9 – Cre/Lox system used to create the recombinant ILTV-GFP-NDVF-FcTail.** At the 24-hour time point following infection, the CRISPR/Cas9 enzyme induces double-strand breaks at the US4 region of the ILTV-GFP genome, resulting in the insertion of the NDVF-FcTail gene insert. This genetic modification leads to the generation of the recombinant ILTV-GFP-NDVF-FcTail variant, which exhibits positive GFP expression and mRFP expression. The viral progenies of ILTV-GFP-NDVF variants, which had been genetically modified by recombination, were subjected to treatment with the Cre enzyme. This enzyme recognises the LoxP region within the ILTV-GFP-NDVF variant genome and removes the surrounding area containing the mRFP gene, resulting in a permanent deletion of the gene. As a result of this deletion, the viral progenies exhibit a positive expression of GFP but lack the expression of mRFP. The Zoe Fluorescent Cell Imager (Biorad) was utilised to capture the images.

### 5.2.3.1. Characterisation of the Recombinant ILTV-GFP-NDVF Variants

The recombinant ILTV-GFP-NDVF variants have been subjected to validation using several molecular and imaging approaches. The LMH cell line was exposed to infection using the recombinant ILTV-GFP-NDVF variant strains. The existence of the NDVF-variant genes was initially assessed by using primers that spanned the MCS1 region of the donor plasmid. The image presented in **Figure 5.8.A** provides visual evidence supporting the existence of the NDVF variant gene fragments: NDVF-Fd, about 1.7 kb in size; NDVF-Fc, about 2.3 kb in size; and NDVF-FcTail, about 1.9 kb in size. Fragments were compared to the NDVF-WT gene amplicon, which has a size of approximately 1.6 kb and serves as the designated positive control. A Western blot study was performed to investigate the presence of the NDV-F variant proteins. The observed molecular weights of the NDV-F variants are as follows: NDVF-Fd is about 60 kDa in size, NDVF-Fc is about 81 kDa in size, and NDVF-FcTail is about 59 kDa in size. The findings of the investigation demonstrate the effective expression of NDV-F variants, as seen in **Figure 5.8.B**. The cytoplasmic location of the ILTV NDV-F variant proteins was confirmed using the results obtained from an immunofluorescence assay. The LMH cells on a 24-well plate were infected with the recombinant ILTV-GFP-NDVF variants. At the 36-hour time point following infection, the cells were subjected to fixation and subsequently labelled using anti-FLAG and Goat anti-Rabbit IgG (H+L) Cross-Adsorbed Secondary Antibody, Alexa Fluor 488. **Figure 5.8.C** illustrates the cellular localisation of the NDV-F variant protein (green) within the cytoplasm of the LMH cell, as detected using confocal microscopy imaging.

A plaque-assay-based investigation was conducted to examine the difference in viral amount (PFU/mL) between the ILTV-GFP-NDVF variants and the ILTV-WT. The

results of the one-way ANOVA suggest that there is not a statistically significant difference in viral infectivity between the recombinant ILTV-GFP-NDVF variants and the ILTV-WT, as shown in **Figure 5.9.A**. The approach used for calculating the viral quantity is illustrated in **Figure 5.9.B**, which displays images of the well containing the individual plaques.

To pursue the functional evaluation of the recombinant ILTV-GFP-NDVF variant strains, *in vitro* growth kinetics through the use of quantitative polymerase chain reaction (qPCR) was performed. The LMH cells were exposed to an infection caused by the recombinant ILTV-GFP-NDVF variant strains at a multiplicity of infection (MOI) of 1.0. Following the infection, DNA extraction was conducted at certain time intervals, namely at 6-, 12-, 24-, 48-, 72-, and 96-hours post-infection (HPI). The graph illustrates the overall pattern of viral copy number increases. The diagram depicted in **Figure 5.10** illustrates the concept under consideration.

Further analysis of the infectivity of the recombinant ILTV-GFP-NDVF-Fd was assessed by conducting flow cytometry analysis to evaluate GFP expression. LMH cells were infected with the recombinant ILTV strains. Subsequently, at 36 hours post-infection, the cells were fixed and subjected to staining. The analysis of GFP-positive cell percentages in uninfected control cells and cells infected with recombinant ILTV-GFP-NDVF-Fd, ILTV-GFP-NDVF-Fc, ILTV-GFP-NDVF-FcTail, and ILTV-GFP-NDVF-WT fails to detect statistically significant differences. However, there is an observable tendency towards an increase in GFP positivity in LMH cells following viral infection. Microscopic images illustrating the production of GFP in LMH cells infected with recombinant ILTV were also shown (**Figure 5.11.A**). A representative gating approach

is shown in **Figure 5.11.B**, providing an overview of the strategy used for the identification of GFP-positive cells in the LMH cell population. The viral particles were fluorescently marked with GFP, while the viability of the cells was determined using the live/dead staining kit.

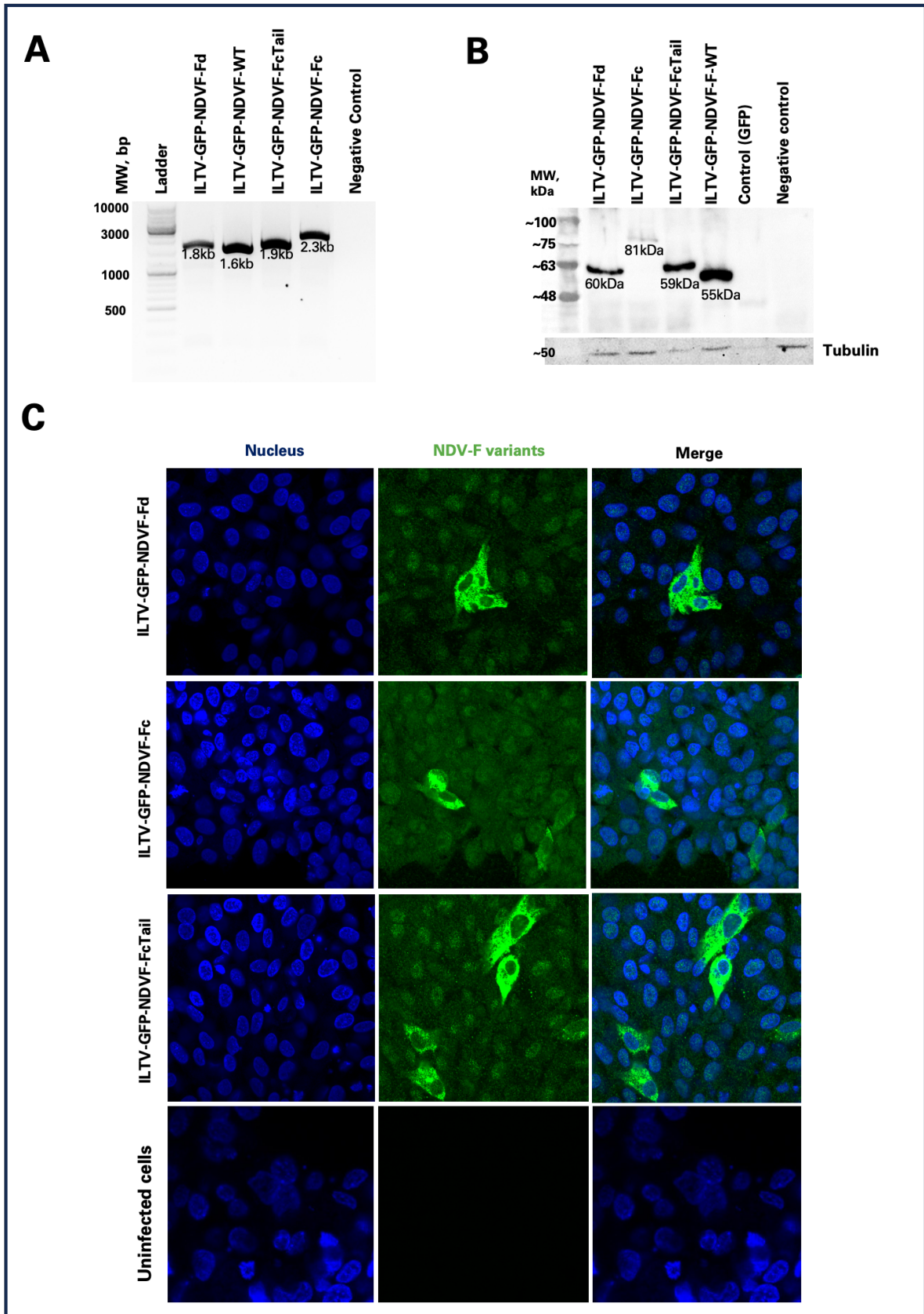


**Figure 5.8. NDV-F variants expressed at the molecular and protein-levels in LMH cells post-infection with recombinant ILTV-GFP-NDVF variants.** The LMH cell line was subjected to infection with the recombinant ILTV-GFP-NDVF variant viral vector. **(A)** An image of a gel electrophoresis is presented, depicting the amplification utilising

the primers CMV-MCS1-F (5'-AGAACCCACTGCTTACTGGCTT-3') and CMV-MCS1-R (5'- AACTAGAAGGCACAGTCGAGGC-3'). These primers flank the MCS1 region of the donor plasmid. The amplification of the NDVF variant resulted in the following fragments: NDVF-Fd, about 1.8 kb in size; NDVF-Fc, about 2.3 kb in size; and the NDVF-FcTail, about 1.9 kb in size. Throughout this chapter, the samples were compared to the NDVF-WT (~1.6 kb) gene, which was designated as the positive control. **(B)** A Western blot analysis was conducted to observe the presence of the NDVF variant proteins. The observed molecular weights of the NDVF variants are as follows: NDVF-Fd is about 60 kDa in size, NDVF-Fc is about 81 kDa in size, and the NDVF-FcTail is about 59 kDa in size. The results of the analysis indicate the successful expression of NDVF variants. **(C)** Confluent LMH cells were subjected to infection with the recombinant ILTV-GFP-NDVF variants, followed by staining to detect the presence of NDVF variant proteins (green). The confocal microscopy pictures presented in Figure C depict the localisation of the NDVF variant protein inside the cytoplasm of the LMH cells. Uninfected cells served as negative control.

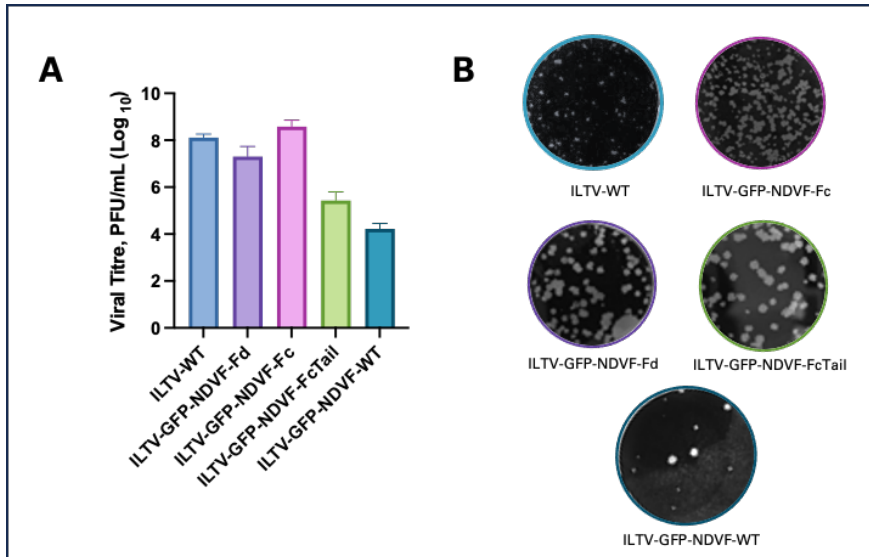


**Figure 5.9. The viral infectivity of the recombinant ILTV-NDVF variant strains is not significantly different from that of ILTV-WT.** (A) Plaque assay-based quantification of the infectious virus between the ILTV-WT and recombinant ILTVs (ILTV-GFP-NDVF-Fd, ILTV-GFP-NDVF-Fc, ILTV-GFP-NDVF-FcTail, and ILTV-GFP-NDVF-WT). The results obtained from the plaque assay-based study indicate that there is no statistically significant difference in viral infectivity between the recombinant ILTV-GFP-NDVF variant strains and the ILTV-WT. (B) Plaque images show the individual plaque-forming unit used to compute the final viral concentration. These data represent the average of three technical replicates, with SD. indicated. ns: non-significant  $p > 0.05$ , \* $p < 0.05$ , \*\*\* $p < 0.001$  using one-way ANOVA.

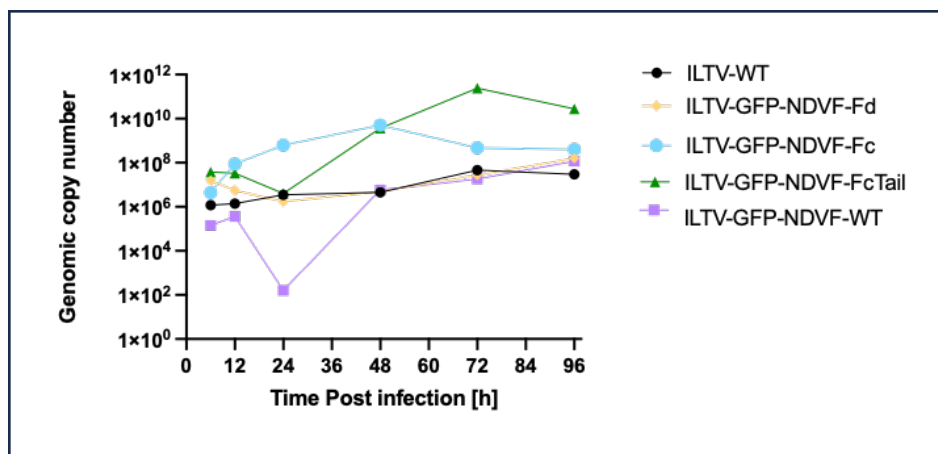


**Figure 5.10. Comparison of the replication kinetics of the ILTV-WT and recombinant ILTV-GFP-NDVF variant strains.** The quantitative polymerase chain reaction (qPCR) data analysis presented here illustrates the comparison of genomic copy number between the ILTV-WT and the recombinant ILTVs (ILTV-GFP-NDVF-Fd, ILTV-GFP-NDVF-Fc, ILTV-GFP-NDVF-FcTail, and ILTV-GFP-NDVF-WT) at various time points, with a multiplicity of infection (MOI) of 1.0. Data analysis is based on one experiment with three technical replicates.



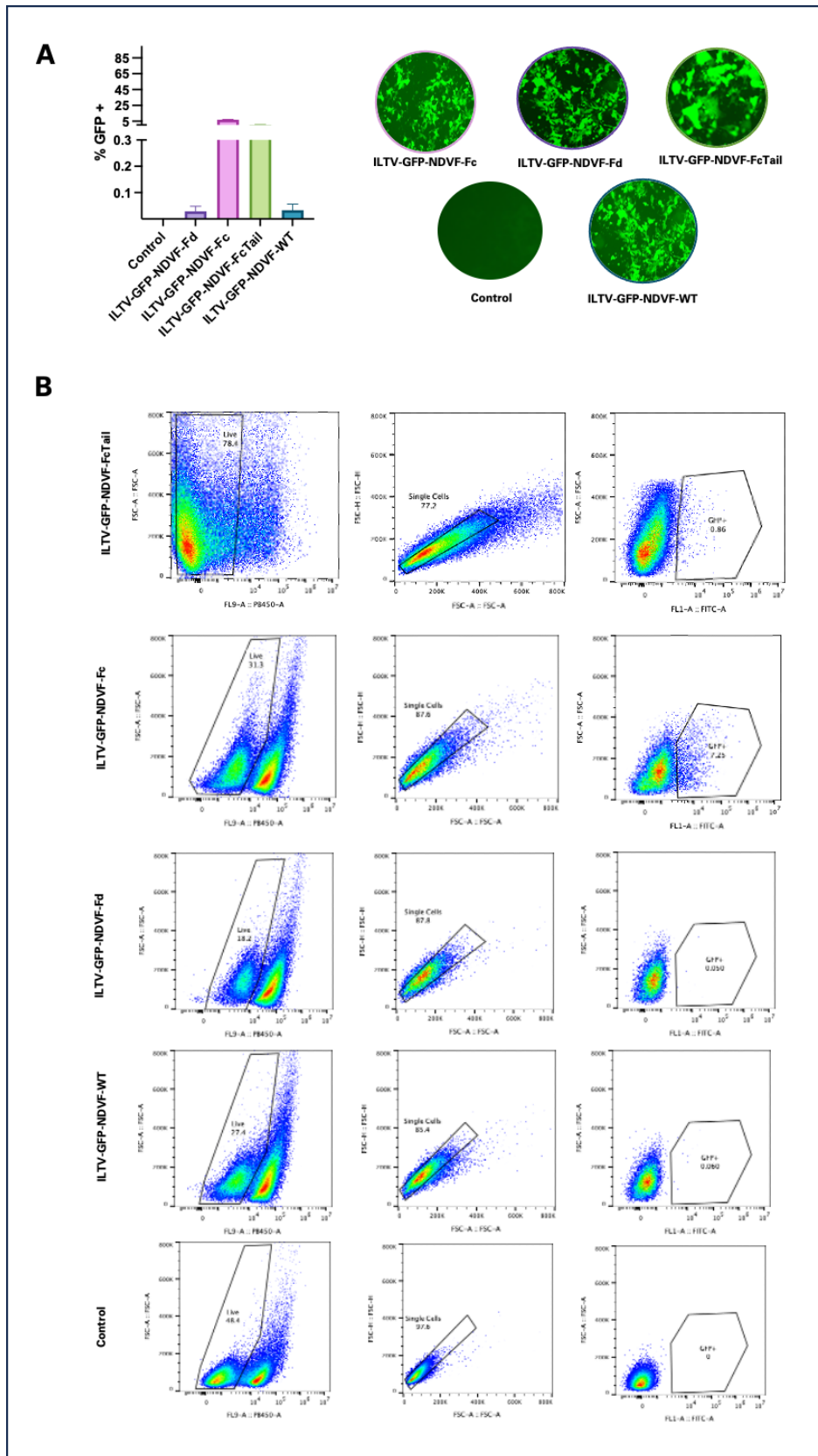


**Figure 5.11. Trend towards an increase in GFP positivity in LMH cells post-viral infection.** At 36 hours post-infection, LMH cells were infected with recombinant ILTV-GFP-NDVF variant strains. Subsequently, a flow cytometry study was conducted to

assess the infectivity and spread of the recombinant ILTVs by evaluating the expression of GFP. **(A)** The figure presents a graphical depiction of the percentage of GFP-positive cells in both uninfected control cells and cells infected with recombinant ILTV-GFP-NDVF variants. Additionally, accompanying the graph are microscopic pictures illustrating the expression of GFP in LMH cells infected with the recombinant ILTV. **(B)** The provided information represents the gating approach employed for the identification of GFP-positive cells in the LMH cell population. The viral particles were fluorescently marked with GFP, while the viability of the cells was determined using the live/dead staining kit. The process of gating was conducted via the FlowJo software. Data analysis is based on one experiment with three technical replicates.

### 5.3. Chapter Discussion

The findings obtained in Chapter 4 have provided a basis for further elucidating the capabilities of the CRISPR/Cas9 gene editing technology in the advancement of a recombinant ILTV vaccination vector that can effectively deliver foreign antigen inserts. The findings presented in Chapter 4 provide evidence of the effectiveness of CRISPR/Cas9 technology in modifying viral genomes, specifically highlighting the potential of ILTV as a preferred vector for vaccine development. This chapter delves deeper into our examination of ILTV, with a specific emphasis on ILTV's capacity to effectively transport and maintain the expression of large DNA inserts.

The development of the three NDV-F variant constructs was facilitated using *in silico* methods (Parvizpour et al., 2020). Physicochemical and antigenic properties were validated using various *in silico*-based strategies (Doytchinova & Flower, 2007; Gasteiger et al., 2005). From these results, we have provided evidence supporting the antigenicity of all the NDV-F variants as depicted through the analysis conducted

through the web-based tool VaxiJen 2.0 (Doytchinova & Flower, 2007; Salod & Mahomed, 2022). These constructs were subsequently utilised to generate recombinant ILTV-GFP-NDVF variant strains, namely ILTV-GFP-NDVF-Fd, ILTV-GFP-NDVF-Fc, and ILTV-GFP-NDVF-FcTail. These recombinant viruses were created through the insertion of the foreign gene cassettes into the US4 region of the ILTV genome.

The molecular and protein-level analyses conducted on the recombinant ILTV strains provided evidence of the expression of the NDV-F gene, therefore validating the successful use of CRISPR/Cas9 technology in modifying the ILTV genome and facilitating the integration of the NDV-F gene variants. The localisation analysis confirmed the expression of the NDV-F gene within the cytoplasm of LMH cells after being infected with the recombinant ILTV strains. The aforementioned finding aligns with previous studies that have documented the cytoplasmic accumulation and maturation of ILTV virions during the replication of ILTV within host cells, resulting in exocytosis or cell lysis (Gowthaman et al., 2020).

Numerous scientific investigations pertaining to the stability of double-stranded (ds) DNA viruses have been described (Bi et al., 2014; Borchers et al., 1994; Connolly et al., 2011; Eisenberg et al., 2012; Josefsberg & Buckland, 2012). In order to evaluate the stability and viral fitness of the genetically modified viral ILTV genome, including foreign gene insertions, a series of experiments were devised. These experiments aimed to analyse the infectivity of recombinant ILTV-GFP-NDVF variant strains in contrast to the ILTV wild-type strain. The plaque assay technique was employed to quantify viral infectivity, and the results indicated that there was no statistically

significant variation in infectivity between the wild-type ILTV strain and the recombinant ILTV strains (ILTV-GFP-NDVF-Fd, ILTV-GFP-NDVF-Fc, and ILTV-GFP-NDVF-FcTail). Nevertheless, it is important to highlight that while this discovery provides additional confirmation that the integration of the NDV-F gene into the ILTV genome did not affect its ability to infect, it should be acknowledged that the NDVF variants exhibit variations in their genomic sequence sizes. The genome of the ILTV has been expanded beyond 1.5-2.3 kb through the incorporation of isolated fragments from the NDV-F variants. These fragments include NDVF-Fd (~1.8 kb), NDVF-Fc (~2.3 kb), NDVF-FcTail (~1.9 kb), and NDVF-WT, which is approximately 1.6 kb in size. Based on the results of the plaque assay, ILTV-GFP-NDVF-Fc, which contains the largest inserted gene, exhibits a higher level of infectivity compared to the wild type of virus, providing an overview of the expandability of the ILTV genome. These results provide further evidence of the flexibility and capacity of the herpesvirus genome to integrate foreign genes of varying size without hindering the recombinant viral vector replication *in vitro* and *in vivo* (Cantello et al., 1991; Parcels et al., 1994; Sakaguchi et al., 1998). Extensive studies have been conducted in regard to the development of recombinant herpesvirus-based viral vectors (S. Liu et al., 2015; Palya et al., 2012; X. Pan et al., 2023; C. T. Rosas, König, et al., 2007; N. Tang et al., 2018). Various sizes of foreign genes, from subunit antigens to whole genic antigens, have been proven to be successfully inserted without hindering replication or infectivity. This includes recombinant viral vectors based on herpesvirus in dogs, cats, pigs, ruminants, equine, and poultry (T. Chen et al., 2019; Donofrio et al., 2013; Y. Jiang et al., 2007; Kamel & El-Sayed, 2019; M. Kit et al., 1991; Nishikawa et al., 2000; Said et al., 2013; Vermeulen, 1998). Furthermore, in the previous study conducted by Atasoy et al.

(2019), similar insertion of the NDV-F gene into the ILTV genome did not affect the capability of the recombinant virus to infect and replicate.

To further follow the potential effects of the ILTV genomic expansion, analysis of the kinetics study revealed that the recombinant ILTV-GFP-NDVF-Fc aligns with findings from other *in vitro* studies on the ILTV replication cycle. Wherein attaining the highest concentration viral genomic copy number at around 24 to 30 hours post-infection, this result is comparable to the ILTV-WT. While the NDVF variants fused with Fd and FcTail enhancers were observed to show a slight delay in the accumulation of viral particles based on the genomic copy number, the relative detection through qPCR appeared to still follow previous studies wherein viral particles are readily detectable at the earliest time point examined, and the copy number increased throughout infection (Mahmoudian et al., 2012).

The findings were also confirmed through flow cytometry analysis, which revealed an upward trend in the percentage of LMH cells expressing GFP following viral infection with the recombinant ILTV strains. The observed recombinant ILTV viruses demonstrate stability and are deemed appropriate for *in vitro* and *in vivo* imaging purposes to study ILTV replication and spread (De Baets et al., 2015; Marschall et al., 2000).

The results obtained from the recombinant ILTV-GFP-NDVF-Fc strain are particularly noteworthy. Our findings indicate that this strain exhibits a much higher level of infectivity compared to both the wild-type ILTV strain and other recombinant ILTV NDV-F variant strains. Additionally, we observed a notable pattern of enhanced

replication kinetics and viral cell-to-cell dissemination in the recombinant ILTV-GFP-NDVF-Fc strain, as shown by the early onset of the genomic copy number and the heightened expression of GFP, respectively. The Fc molecule of IgY demonstrates increased immune-enhancing effect by fusion with the epitope or immunogenic region of an antigen protein (Mancardi & Daëron, 2014; Martyn et al., 2009; Tressler & Roth, 1987; X. Zhang et al., 2017). The effectiveness of subunit vaccinations that incorporate antigens covalently linked to Fc molecules has been proven to be significant in providing protection against specific diseases (L. Chen et al., 2022; Z. Liu et al., 2020; B. Zhao et al., 2018). However, further research is necessary to explore immunological and physiological aspects, specifically focusing on the undiscovered Fc receptor found on immune cells and the structural alterations caused by the fusion of Fc molecules with antigen proteins (B.-K. Jung et al., 2022).

Furthermore, our results provide us with fundamental insights into the *in vivo* behaviour of these potential recombinant ILTV viral vectors. There have been comprehensive investigations conducted to assess the effectiveness of foldon and Fc as adjuvants or enhancers in the advancement of potential candidates for gene-to-vaccine approaches in novel vaccination strategies. These studies have focused on recombinant vaccines targeting H5N1 HA1 and have demonstrated their ability to provide cross-protection against different subtypes of H5N1. This suggests that a universal H5N1 influenza vaccine with high efficacy could be generated (Du et al., 2011). In addition, a study conducted by Yu et al. (2015) showed that the fusion of Foldon and Fc with HA1 of H5N1 resulted in a robust mucosal immune response and effectively safeguarded vaccinated mice against the potentially fatal consequences of H5N1 viral infection (F. Yu et al., 2015).

Taken together, this chapter was able to provide additional knowledge for evaluating the efficacy of Foldon and Fc domain enhancers fused with the NDV-F gene as candidate antigen inserts for the development of novel viral vectored vaccines. Furthermore, the results of the viral infectivity experiments provided insight on the elasticity and flexibility of the ILTV genome to take up large foreign gene inserts. Finally, this chapter provided us with preliminary information on the predictive behaviour of the recombinant ILTV-NDVF variants *in vitro*.

# CHAPTER 6

## Construction and Evaluation of Herpesvirus as a Multivalent Vaccine Vector Using Two Surface Glycoproteins of NDV (F and HN)

### 6.1. Introduction

The efficacy of vaccination as a disease prevention strategy and its potential to eradicate certain illnesses have been continuously demonstrated (Lauer et al., 2017). The practice of combining several vaccinations to offer broad immunity against various illnesses has been a well-established strategy in both human and poultry vaccination initiatives (Spier, 1997). Nevertheless, this approach might occasionally be complex, result in additional expenses, and incur additional costs. In recent years, notable progress has been made in the field of vaccine design technology. Vectored vaccines, a relatively recent subcategory of immunisations, are successfully overcoming challenges that conventional immunisations are unable to adequately confront (Chambers et al., 2016). The application of this technique in the field of veterinary medicine has been rapidly adopted to develop effective vaccines for domestic animals and livestock. This includes the development of targeted medications to mitigate major viral infections in poultry (Michel Bublot et al., 2021). According to Aida et al. (2021), these vaccines elicit both humoral and cellular immunological responses, possess



economic feasibility in production, exhibit safety in administration, and offer the potential to distinguish between diseased and vaccinated animals (Aida et al., 2021).

The advent of CRISPR/Cas9 genome editing technology has facilitated the generation of multivalent and multi-pathogen viral vector vaccines by making it possible to integrate multiple protective antigens into a single viral vector (Mire et al., 2015). The incorporation of several protective antigens or inserts into the genomes of large viral vectors, such as herpesviruses, has demonstrated positive outcomes in the advancement of viral vaccines. This approach has been effective in conferring protection against a wide array of diseases. The use of multivalent and multipathogen viral vectors presents a promising opportunity for the development of a potential integrated vaccine agent that may efficiently protect hosts against various prevalent infections while also providing protection against multiple serotypes or genotypes of a certain pathogen (Xiangchuan He et al., 2021; N. Tang et al., 2020).

Commercial multivalent vaccines have gained significant popularity in the poultry and animal industries. These vaccines encompass a range of formulations; some of these are HVT vectored vaccines with protection against ND-IBD, NDV vectors with protection against ILTV (CEVA Biomune), NDV vectors containing HA-NA and HA-M1 (La Sota), and HVTs containing IBD-ILT (Boehringer Ingelheim). These multivalent vaccines offer protection against highly infectious and commercially disruptive diseases that affect the poultry industry worldwide (Xiangchuan He et al., 2021; Naim, 2013; Spier, 1997).

To date, the CRISPR/Cas9 system has been effectively employed in research to develop vaccine vectors capable of carrying multiple antigens. Examples of such vectors include the herpesvirus of turkey (HVT) with three insertions: VP2 of infectious bursal disease (IBD), glycoprotein D-glycoprotein I (gDgI) of ILTV, and H9HA of H9N2 avian influenza virus (Chang et al., 2019; N. Tang et al., 2018, 2020). Additionally, the ILTV virus has been modified to include the F gene of NDV (Atasoy et al., 2019), and the DEV has been engineered to carry the HA gene of AIV (Chang et al., 2018; Zou et al., 2017).

The efficacy of clinical protection against NDV has been assessed through the use of many vaccination platforms, encompassing viral vectors and DNA vaccines (Arora et al., 2010; Ge et al., 2016; Loke et al., 2005; Morgan et al., 2019; Palya et al., 2012; Sun et al., 2008). Typically, a combined effect is shown in terms of enhanced protection when both HN and F antigens are employed in combination, as opposed to the use of either HN or F antigen alone in vaccines (Arora et al., 2010; Loke et al., 2005; Morgan et al., 2017). The efficacy of F-induced protection is often superior to that of HN alone, despite the significant role played by HN in viral attachment and fusion processes. Furthermore, the use of an NDV vaccination that exhibits antigenic similarity to the challenge virus has the potential to enhance clinical protection (Cornax et al., 2012; Ferreira et al., 2021; Miller et al., 2010).

The initial investigations conducted by Atasoy et al. (2019) regarding the effectiveness of ILTV as a potential recombinant viral vector, along with the findings from previous chapters (Chapter 4 and 5), have established an essential basis for the advancement of a potential multivalent vaccine vector targeting NDV using F and HN. This ILTV

multivalent vaccine vector would encompass not only the F gene of NDV but also the HN gene. This will further allow us to characterise the capacity of ILTV for genome expansion, stable insert and protein expression, and observe the efficacy of the recombinant multivalent vaccine vector.

### **6.1.1. Aims**

This chapter aims to utilise the CRISPR/Cas9 gene editing technology to develop a multivalent recombinant ILTV vaccine vector capable of carrying two surface glycoproteins of NDV, namely F and HN.

Specifically:

1. Demonstrate and experimentally validate the capacity of ILTV to carry antigen in another genome insertion region, specifically at UL0.
2. Evaluate the efficacy of CRISPR/Cas9 gene editing technology in the production of multivalent recombinant ILTV by introducing the NDV-HN gene insert into the genome of the recombinant ILTV that already carries the F gene of NDV.
3. Functionally validate the capability of the recombinant multivalent ILTV to behave similarly to ILTV-WT.
4. Perform *in vivo*-based analyses on recombinant ILTV viral vector strains.

## 6.2. Results

Results from previous chapters validate the capacity of ILTV to carry gene inserts as well as the effectiveness of the CRISPR/Cas9 gene editing technology to facilitate this process. This chapter will further utilise the CRISPR/Cas9 gene editing technology to create a recombinant multivalent ILTV vaccine vector.

### 6.2.1. Cloning and Validation of Gene Cassettes

The donor plasmid pCDNA3-MCS1-mRFP, which was previously created and discussed in Chapter 4, was utilised to create donor plasmids that harbour the NDV-HN gene in MCS1. **Figure 6.1.A** illustrates a schematic depiction of the donor plasmid pCDNA3-MCS1-mRFP. PCR primers were specifically designed for the amplification of the NDV-HN gene, with the inclusion of *NheI* (5'-CTAGCTAGCTCACCACCATGGACCGCGCGGTAAACAG-3') and *KpnI* (5'-GCCGGTACCCAAACTCTATCATCCTTGAGGAT-3') restriction enzyme recognition sites at the 5' and 3' ends, respectively (**Figure 6.1.B**). PCR was employed to perform positive amplification of the NDV-HN gene, resulting in the detection of a band with an estimated size of 1700 bp (**Figure 6.1.B**). In order to facilitate the insertion of the NDV-HN fragment into the multiple cloning site 1 (MCS1) of the recipient vector (pcDNA-MCS1-mRFP), both the NDV-HN insert and the recipient vector (pcDNA-MCS1-mRFP) underwent restriction enzyme digestion utilising the restriction enzymes *NheI* and *KpnI*. Subsequently, the use of DNA ligase facilitated the fusing of the NDV-F insert and the recipient vector. The donor plasmid, pcDNA-NDVHN-mRFP (**Figure 6.1.C**), obtained after ligation, was propagated by transformation into DH5 $\alpha$ -competent *E. coli* cells. Positive colonies were then subjected to a purification process

to obtain purified plasmid DNA for further examination using Sanger sequencing. The provided sequence alignment illustrates the similarity between the sequenced forward and reverse fragments of the cloned NDV-HN gene against the NDV strain ZJ1 reference genome. The Sanger sequencing outcome confirms a complete match of 100% identity between the wild-type NDV-HN gene of the NDV strain ZJ1 and pcDNA-NDVHN-mRFP (shown in pink) for both the forward and reverse fragments (**Figure 6.1.D**).

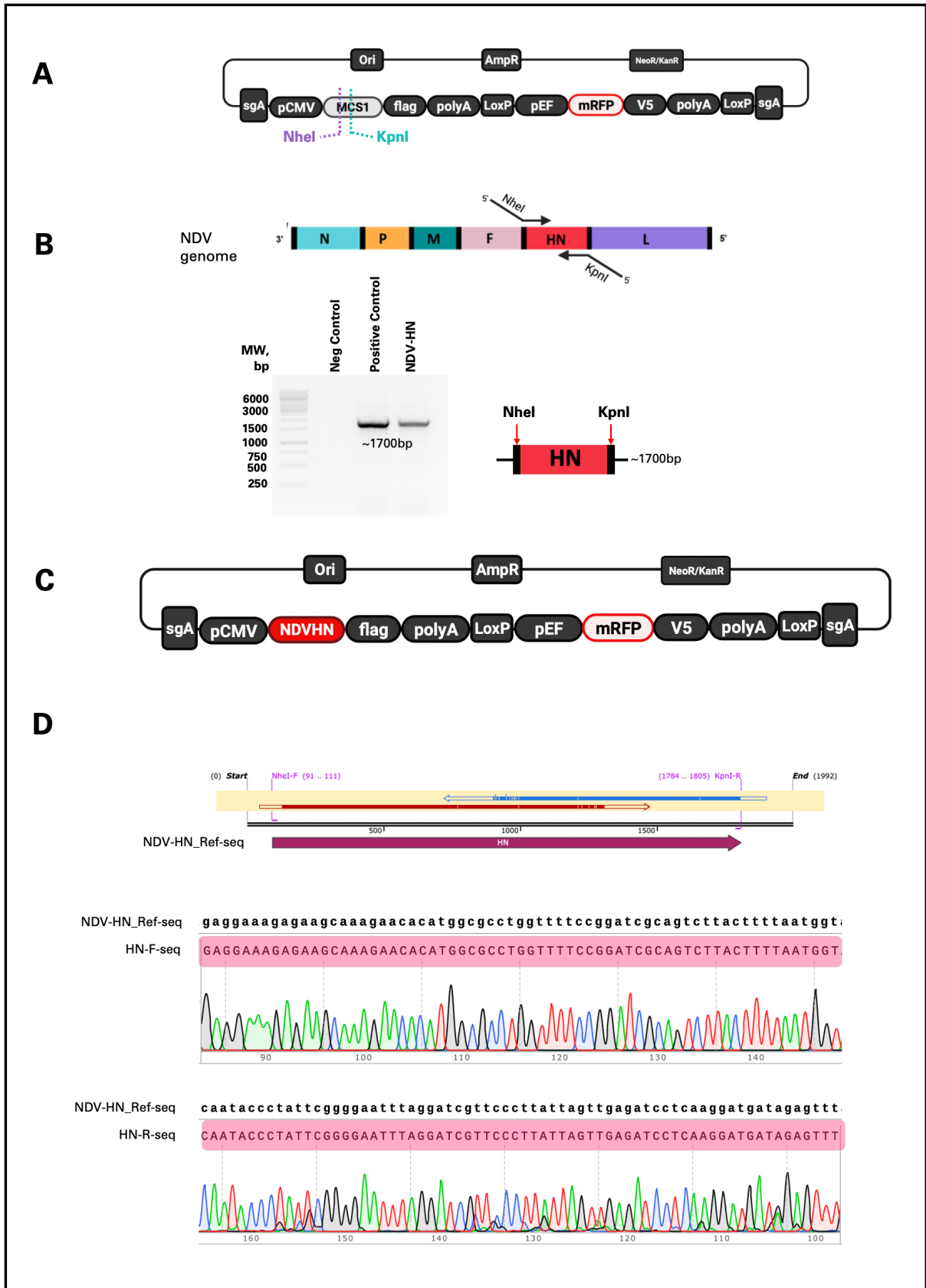


**Figure 6.1. Assembly and sequence validation of the recombinant donor plasmid pCDNA-NDVHN-mRFP.** The NDV-HN gene fragment was successfully integrated into the multiple cloning site 1 (MCS1) of the donor plasmid pCDNA-MCS1-

mRFP. **(A)** The provided figure illustrates the donor plasmid, pcDNA-MCS1-mRFP, which has specific restriction enzyme recognition sites for *NheI* and *KpnI*. **(B)** The fragment representation of the NDV genome. The primers were specifically designed for the amplification of the NDV-HN gene, with the inclusion of *NheI* and *KpnI* restriction enzyme recognition sites at the 5' and 3' ends, respectively. The gel electrophoresis picture depicts the amplified NDV-HN gene, which has an estimated size of 1700 base pairs. The amplified NDV-F gene fragment and donor plasmid pcDNA-MCS1-mRFP were cloned using restriction enzyme digestion, utilising *NheI* and *KpnI*. The process of DNA ligation was performed in order to merge the NDV-HN fragment with the recipient donor plasmid pcDNA-MCS1-mRFP, resulting in the creation of the recombinant donor vector pcDNA-NDVHN-mRFP **(C)**. **(D)** The provided sequence alignment illustrates the similarity between the sequenced forward and reverse fragments of the cloned NDV-HN gene against the NDV strain ZJ1 reference genome. The Sanger sequencing outcome confirms a complete match of 100% identity between the wild-type NDV-HN gene of the NDV strain ZJ1 and pcDNA-NDVHN-mRFP (shown in pink) for both the forward and reverse fragments.

### 6.2.2. Generation of Recombinant ILTV with the NDV-HN Gene

The process of generating the recombinant ILTV with a cassette knock-in of the NDV-HN gene required the assembly of several components. The components utilised in this study encompassed three main elements. Firstly, the recombinant ILTV-GFP construct was used, which serves as a vector for expressing the GFP gene. Secondly, the donor plasmid pcDNA-NDVHN-mRFP was employed, which contains the NDV-HN gene along with a reporter gene encoding mRFP. Lastly, the CRISPR/Cas9-sgRNA plasmids, specifically pX459v2-UL0, were utilised to induce double-strand breaks in the ILTV genome at the UL0 region.

The method encompasses two major constituents: the transfection of the donor plasmid (pcDNA-NDVHN-mRFP) and the CRISPR/Cas9-sgRNA plasmid (pX459v2-UL0) into LMH cells (**Figure 6.2.A**). During the process of incubation, the accessory guide RNA-A (pX459v2-sgRNA-A) will accurately recognise and cleave the specific

sgRNA-A site found in the donor plasmid. This action will lead to the release of the NDVFHN-mRFP gene cassette. After 36 hours of transfection, the LMH cells were infected with recombinant ILTV-GFP after the detection of red fluorescence by microscopic analysis (**Figure 6.2.B**). The CRISPR/Cas9-guideRNA (pX459v2-UL0) method is employed to facilitate the assessment of the ILTV genome and enable the targeted cleavage necessary for the insertion of the NDVHN-mRFP gene cassette into the specified UL0 genomic region of the ILTV genome. As a result, this approach leads to non-homology targeting or non-homologous end joining. At the 24-hour time point subsequent to infection, LMH cells were subjected to microscopic analysis in order to evaluate the concurrent existence of the GFP protein, which emits green fluorescence, signifying the successful infection of the ILTV-GFP, and the presence of the mRFP reporter gene within the gene cassette harboured by the donor plasmid pcDNA-NDVHN-mRFP, which emits red fluorescence as depicted in **Figure 6.2.C**.



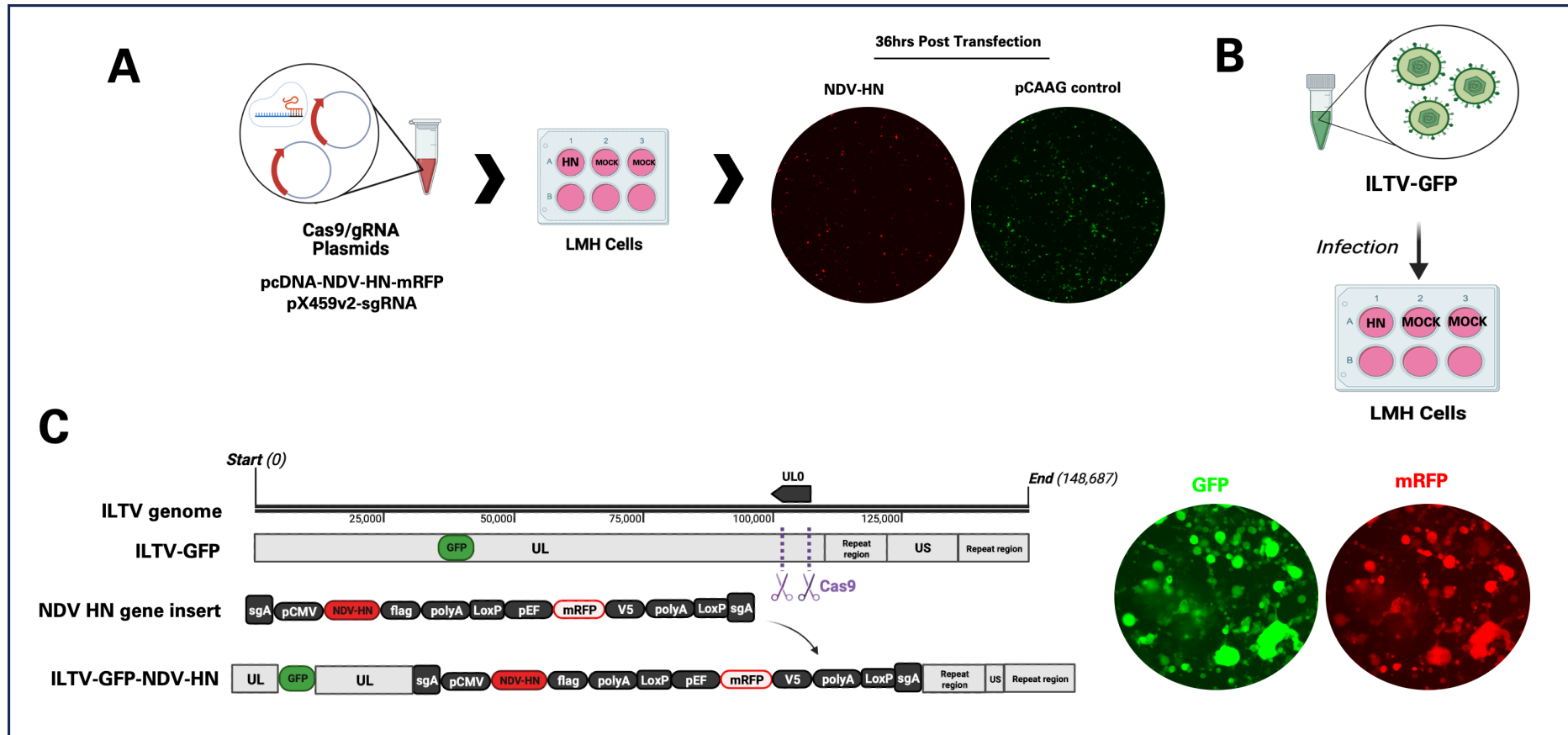


**Figure 6.2. Illustrative representation of the workflow used for the generation of recombinant ILTV-GFP-NDV-HN.** The method comprises two essential elements: **(A)** The transfection of LMH cells with pX459v2-sgRNA plasmids (plasmids containing CRISPR/Cas9-sgRNA) and pcDNA3-NDVHN-mRFP (donor plasmid). At the time point of 36 hours after transfection, a microscopic analysis revealed the expression of red fluorescence, indicating the detection of donor plasmids (pcDNA3-NDVHN-mRFP) within LMH cells. **(B)** Following the identification of the red fluorescence in LMH cells, the cells were subsequently infected with ILTV-GFP. **(C)** At the 24-hour time point following infection, the CRISPR/Cas9 enzyme induces double-strand breaks at the UL0 region of the ILTV-GFP genome, resulting in the insertion of the NDV-HN gene insert. This genetic modification leads to the generation of the

recombinant ILTV-GFP-NDV-HN, which exhibits positive GFP expression and mRFP expression. The Zoe Fluorescent Cell Imager (Biorad) was used to capture the images.

#### **6.2.2.1. Characterisation of the Recombinant ILTV-GFP-NDV-HN**

Validation of the recombinant ILTV-GFP-NDV-HN has been conducted through the use of several molecular and imaging techniques. The LMH cell line was subjected to infection through the use of the recombinant ILTV-GFP-NDV-HN strains. The presence of the NDV-HN gene was evaluated by the use of primers that included the MCS1 region of the donor plasmid. The visual representation depicted in **Figure 6.3.A** offers empirical support for the presence of the NDV-HN gene fragments, which have a size of around 1.7 kilobases. The fragments were subjected to comparison with the NDVHN-WT gene amplicon, which possesses an estimated size of 1.7 kb and functions as the designated positive control. A Western blot analysis was conducted to examine the presence of the NDV-HN protein. The detected molecular weight of the NDV-HN protein was around 75 kilodaltons. The results of the experiment illustrate the successful expression of the NDV-HN protein, as seen in **Figure 6.3.B**. The subcellular distribution of the NDV-HN protein was confirmed using the results obtained from an immunofluorescence assay. The LMH cells on a 24-well plate were infected with the recombinant ILTV strain. At 36 hours following infection, the cells were subjected to fixation and subsequent labelling using anti-FLAG and Goat anti-Rabbit IgG (H+L) Cross-Adsorbed Secondary Antibody, Alexa Fluor 594 (red). The cellular location of the NDV-HN protein (red) within the cytoplasm of the LMH cell is depicted in **Figure 6.3.C**, as observed using confocal microscope imaging.

A study was done using a plaque assay to investigate the difference in viral quantity (PFU/mL) between the ILTV-GFP-NDV-HN and the ILTV-WT. The t-test findings demonstrate a statistically significant difference in viral infectivity between the recombinant ILTV-GFP-NDV-HN strain and the ILTV-WT strain, as seen in **Figure 6.4**. The methodology employed for quantifying the viral amount is depicted adjacent to the graph, which showcases images of the wells containing the distinct plaques.

In order to investigate the functionality of the recombinant ILTV-GFP-NDV-HN strain, an *in vitro* growth kinetics study was conducted using quantitative polymerase chain reaction (qPCR). The LMH cells were subjected to an infection induced by the recombinant ILTV-GFP-NDV-HN strain, with a multiplicity of infection (MOI) of 1.0. DNA extraction was performed at certain time points, namely at 6-, 12-, 24-, 48-, 72-, and 96-hours after infection (HPI). The graph depicts the general trend of viral copy number increase. The figure presented in **Figure 6.5** provides a visual representation of the notion being discussed.

The infectivity of the recombinant ILTV-GFP-NDV-HN was further evaluated through the use of flow cytometry analysis. The LMH cell line was subjected to infection with the recombinant ILTV strain. Following this, the cells were fixed and underwent labelling 36 hours after infection. The analysis of the percentage of cells expressing GFP in both uninfected control cells and cells infected with recombinant ILTV demonstrates no statistically significant difference. However, there is an observable tendency towards a rise in GFP positivity in LMH cells following viral infection. **Figure 6.6.A** presents microscopic images that depict the production of GFP within LMH cells following infection with the recombinant ILTV. **Figure 6.6.B** illustrates the

representative gating technique employed to identify GFP-positive cells within the LMH cell population. This approach outlines the strategy utilised for this purpose. The viral particles were labelled with GFP to enable fluorescence detection, while the viability of the cells was assessed using the live/dead staining technique.

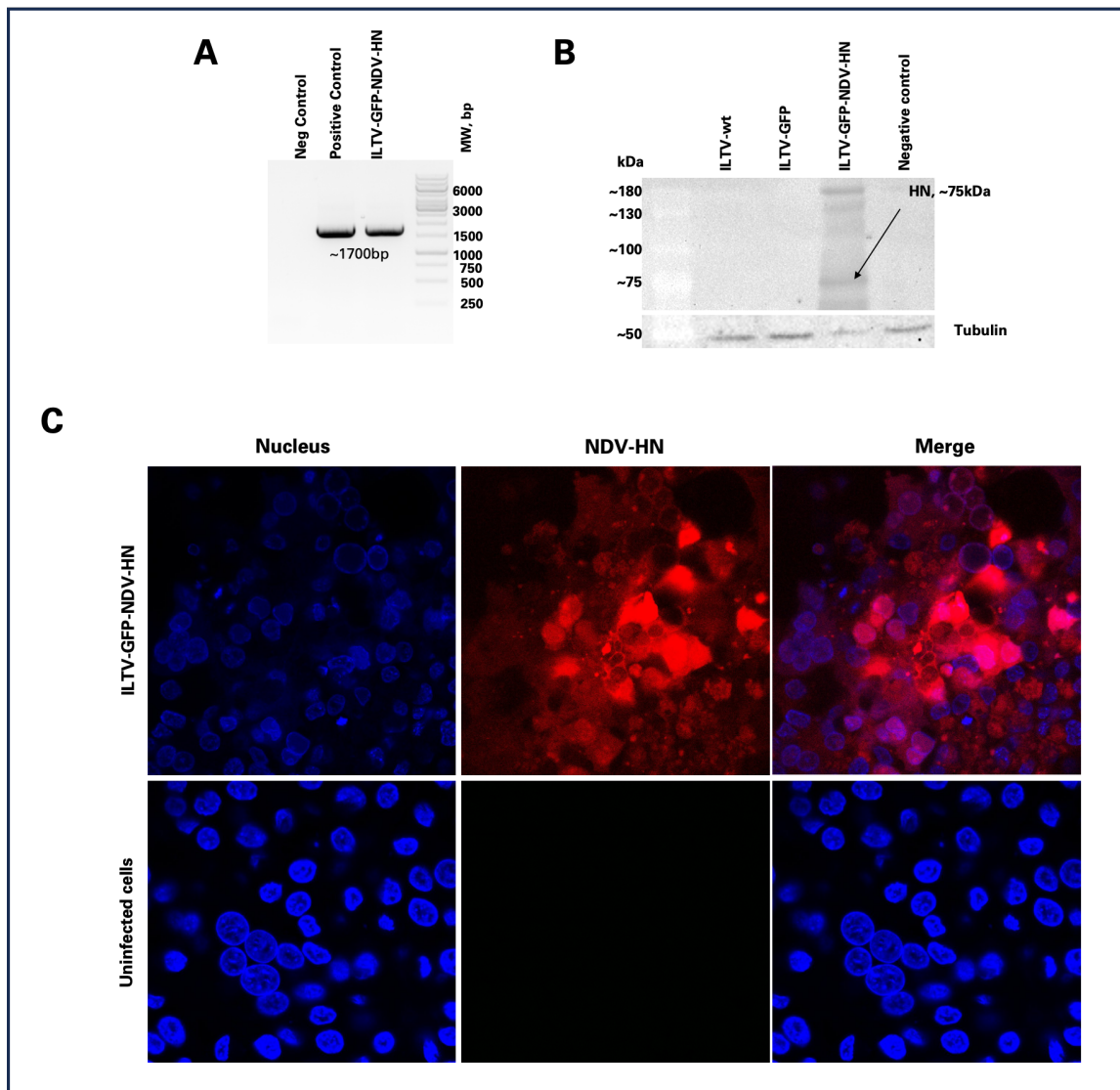


**Figure 6.3. NDV-HN is expressed at the molecular and protein-levels in LMH cells post-infection with the recombinant ILTV-GFP-NDV-HN strain.** The LMH cell line was subjected to infection using the recombinant ILTV-GFP-NDV-HN viral vector. **(A)** The gel electrophoresis depicts the amplification process using the primers CMV-MCS1-F (5'-AGAACCCACTGCTTACTGGCTT-3') and CMV-MCS1-R (5'-AACTAGAAGGCACAGTCGAGGC-3'). The primers are positioned on each side of the MCS1 region of the donor plasmid. The amplification of the NDV-HN gene yielded a DNA fragment with a length of about 1700 base pairs. In the present chapter, the samples were subjected to comparison with the NDV-HN-WT (~1.7 kb) gene, which was assigned the function of the positive control. **(B)** A Western blot analysis was performed to assess the expression of the NDV-HN protein. The detected molecular weight of the NDV-HN protein was determined to be 75 kilodaltons (kDa). The findings of the investigation demonstrate the effective expression of the NDV-HN protein. **(C)** Confluent LMH cells were exposed to infection with the recombinant ILTV-GFP-NDV-HN, thereafter undergoing staining to ascertain the presence of the NDV-HN protein. The confocal microscopy images displayed in Figure C illustrate the subcellular distribution of the NDV-HN protein throughout the cytoplasm of the LMH cells. Uninfected cells served as negative control.

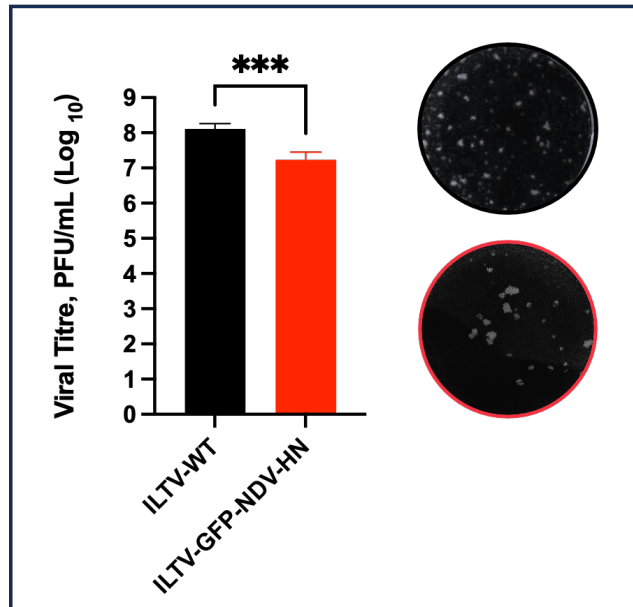


**Figure 6.4. Viral infectivity of the recombinant ILTV-GFP-NDV-HN strain is significantly different from that of ILTV-WT.** (A) Plaque assay-based quantification of the infectious virus between the ILTV-WT and recombinant ILTV-GFP-NDV-HN strains. The results obtained from the plaque assay-based study indicate that there is a strong statistically significant difference in viral infectivity between the recombinant ILTV-GFP-NDV-HN strain and the ILTV-WT. Plaque images show the individual plaque-forming units used to compute the final viral concentration. These data represent the average of three technical replicates, with indicated SD. ns: non-significant  $p > 0.05$ , \* $p < 0.05$ , \*\*\* $p < 0.001$  using the student's t-test.

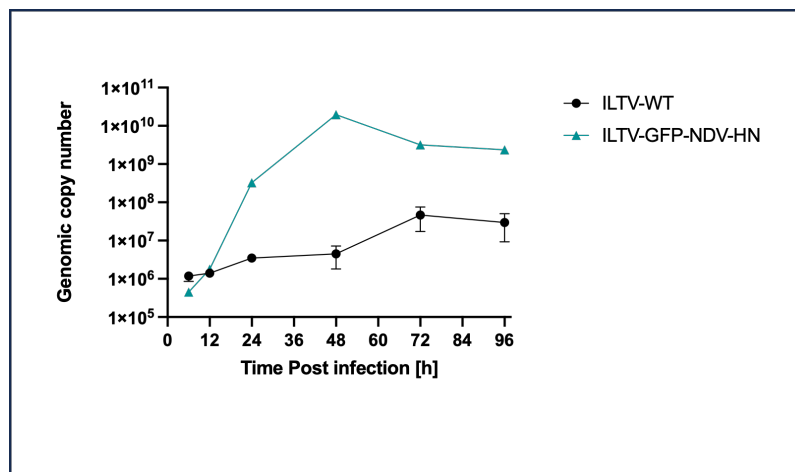


**Figure 6.5. Comparison of the replication kinetics of the ILTV-WT and recombinant ILTV-GFP-NDV-HN strains.** The quantitative polymerase chain reaction (qPCR) data analysis presented here illustrates the comparison of genomic copy numbers between the ILTV-WT and the recombinant ILTV-GFP-NDV-HN at various time periods, with a multiplicity of infection (MOI) of 1.0. Data analysis is based on one experiment with three technical replicates.

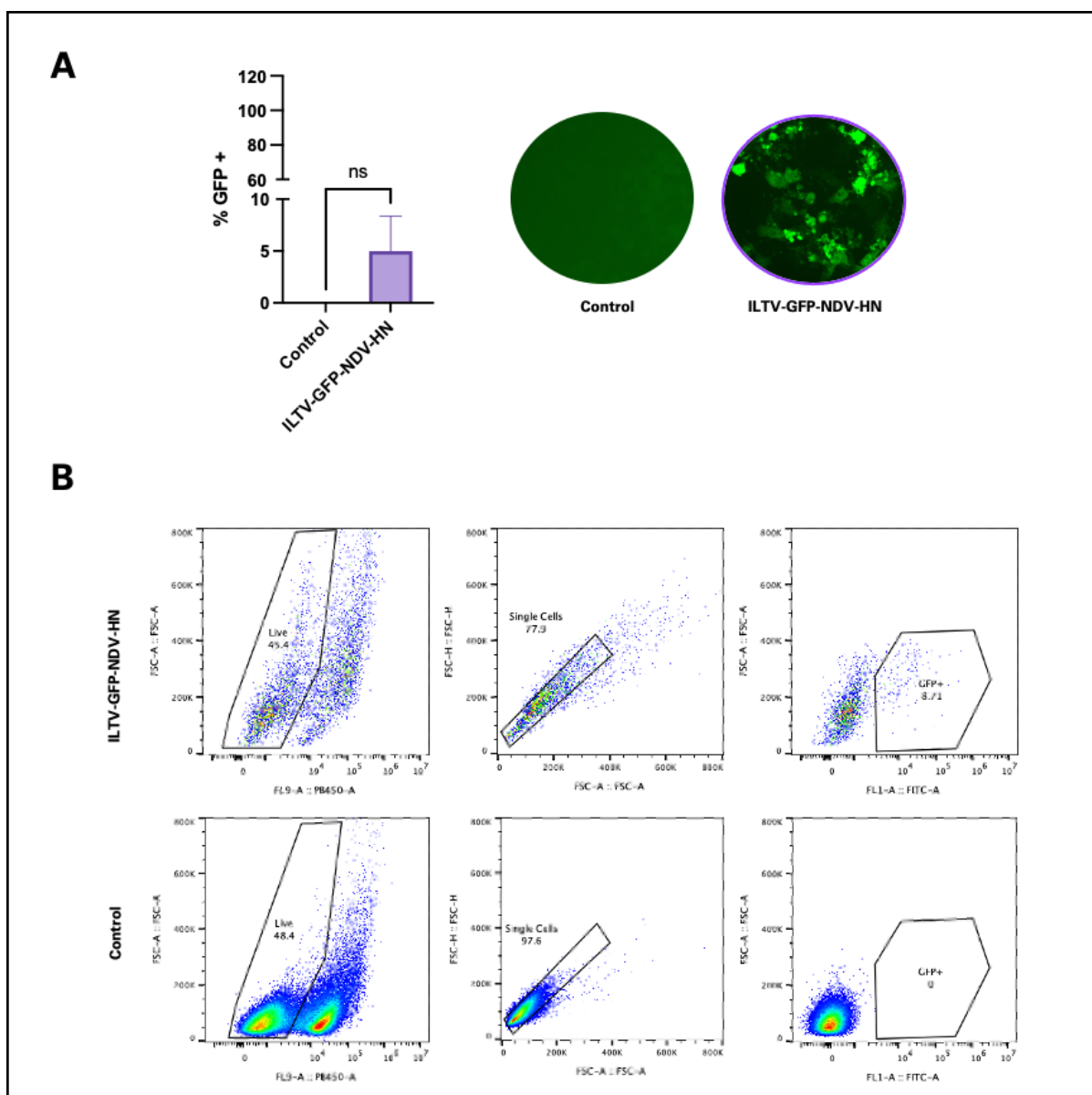


**Figure 6.6. Trend towards the increase in GFP positivity in LMH cells post-viral infection.** At 36 hours post-infection, LMH cells were infected with a recombinant ILTV-GFP-NDV-HN strain. Subsequently, a flow cytometry study was conducted to assess the infectivity of the recombinant ILTVs by evaluating the expression of GFP. **(A)** The figure presents a graphical depiction of the percentage of GFP-positive cells in both uninfected cell control and cells infected with recombinant ILTV-GFP-NDV-HN. Additionally, accompanying the graph are microscopic pictures illustrating the expression of GFP in LMH cells infected with the recombinant ILTV. **(B)** The provided information represents the gating approach employed for the identification of GFP-positive cells in the LMH cell population. The viral particles were fluorescently marked with GFP, while the viability of the cells was determined using the live/dead staining kit. The process of gating was conducted via the FlowJo software. Data analysis is based on one experiment with three technical replicates.

### **6.2.3. Generation of a Recombinant Multivalent ILTV Viral Vector with the F and HN Genes**

The generation of the recombinant multivalent ILTV viral vector, which contains two glycoproteins of NDV (F and HN), involves the transfection of CRISPR/Cas9-sgRNA, supplementary sgRNA-A, and donor plasmids, as seen in **Figure 6.7.A**. During the period of incubation, the accessory guide RNA-A (pX459v2-sgRNA-A) will accurately recognise and cleave the appropriate sgRNA-A site found in the donor plasmid, leading to the release of the NDV-HN-mRFP (Red) gene cassette. At the 36-hour time point following transfection, the presence of successful transfection was confirmed by observing the red fluorescence emitted by the NDV-HN-mRFP (Red) gene cassette under a microscope. The recombinant ILTV-GFP-NDV-F (green), which was previously developed, will serve as the backbone for incorporating the NDV-HN gene fragment into the system (refer to **Figure 6.7.B**). The recombinant ILTV-GFP-NDV-F construct underwent prior treatment with the Cre enzyme to excise the mRFP gene fused to the NDV-F gene insert. This step was used to ensure that the resulting construct emits only green fluorescence, thereby avoiding any interference with the detection of red fluorescence in later investigations.

The CRISPR/Cas9-guideRNA (pX459v2-UL0) system is employed to facilitate the screening of the ILTV genome and enable the accurate cleavage necessary for the integration of the NDV-HN-mRFP gene cassette into the ILTV genome, especially targeting the UL0 genomic region. As a result, this mechanism leads to the occurrence of non-homology targeting or non-homologous end joining. At the 24-hour time point post-infection, LMH cells were subjected to microscopic examination in order to evaluate the concurrent existence of the GFP protein, which emits green fluorescence,



signifying the successful infection of the ILTV-GFP-NDV-F, and the manifestation of the mRFP reporter gene within the gene cassette harboured by the donor plasmid pcDNA-NDVHN-mRFP, which emits red fluorescence as depicted in **Figure 6.7.C**. The developed recombinant multivalent ILTV-GFP-NDV-FHN will be subjected to further analysis.

#### **6.2.3.1. Characterisation of the Recombinant Multivalent ILTV-GFP-NDV-FHN Viral Vector**

Functional validation of the recombinant multivalent viral vector ILTV-GFP-NDV-FHN was carried out using molecular and imaging approaches. The LMH cell line was subjected to infection by the recombinant ILTV-GFP-NDV-FHN strain. At the time point of 36 hours after infection, DNA and protein samples were obtained from the LMH cells that had been infected. PCR was performed using specific primers targeting the MCS1 region of the gene insert to evaluate the presence of both NDV-F and -HN genes in the DNA recovered from the recombinant multivalent viral vaccine. The visual representation depicted in **Figure 6.8.A** offers empirical support for the presence of the NDV-F and -HN gene fragments, which exhibit approximate lengths of 1.6 kb and 1.7 kb, respectively. In order to strengthen the confidence of the integration and expression of the NDV-F and -HN genes within the recombinant multivalent viral vector, the protein obtained from this process was employed in the conduct of a western blotting analysis.

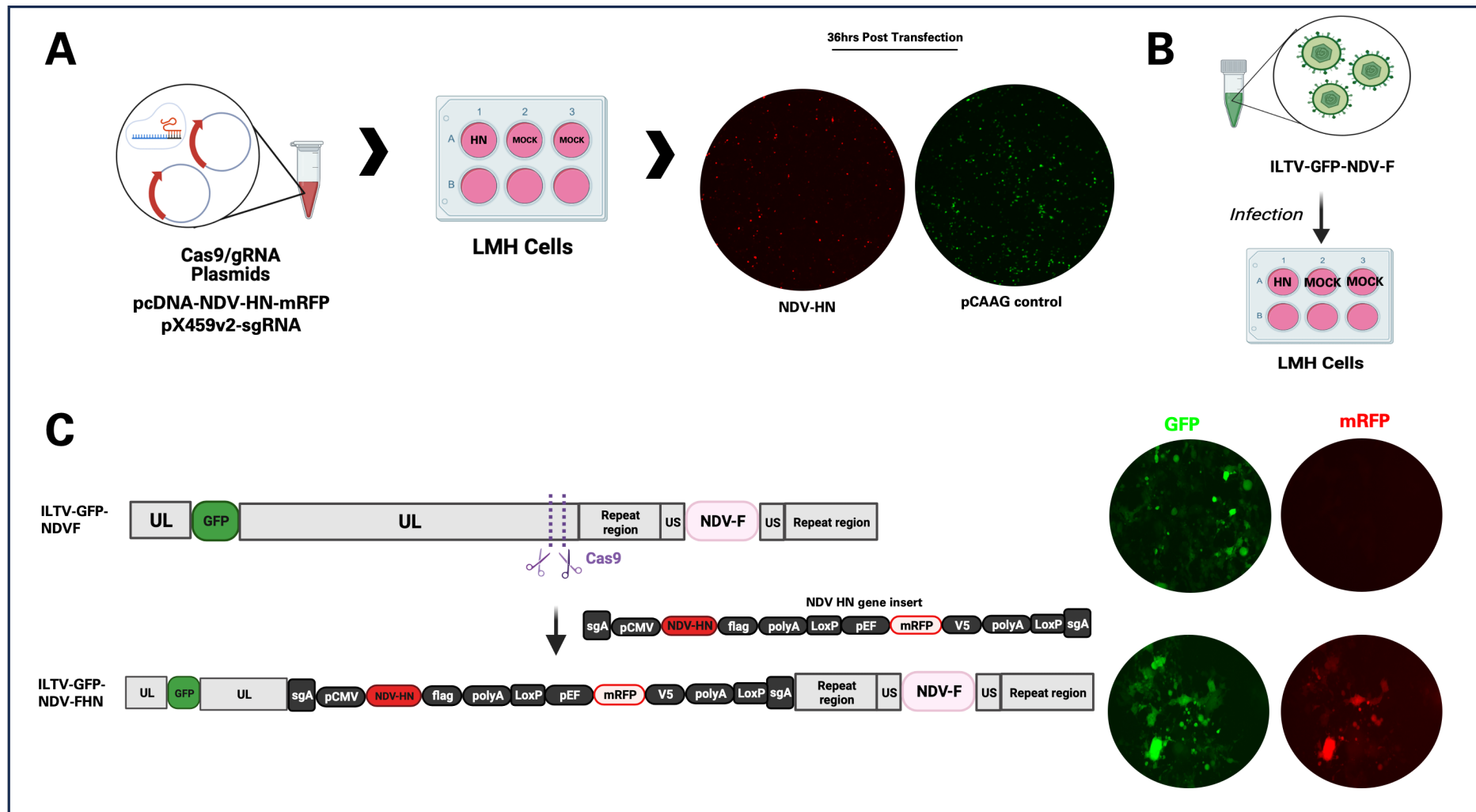


**Figure 6.7. Illustrative representation of the workflow used for the generation of a recombinant multivalent ILTV-GFP-NDV-FHN viral vector.** The method comprises two essential elements: **(A)** The transfection of LMH cells with pX459v2-sgRNA plasmids

(containing CRISPR/Cas9-sgRNA) and pcDNA3-NDVHN-mRFP (donor plasmid). At the time point of 36 hours after transfection, a microscopic analysis revealed the expression of red fluorescence, indicating the detection of donor plasmids (pcDNA3-NDVHN-mRFP) within LMH cells. **(B)** Following the identification of the red fluorescence in LMH cells, the cells were subsequently infected with the ILTV-GFP-NDV-F strain, which expresses the GFP gene but not the mRFP. **(C)** At the 24-hour time point following infection, the CRISPR/Cas9 enzyme induces double-strand breaks at the UL0 region of the ILTV-GFP-NDV-F genome, resulting in the insertion of the NDV HN gene insert. This genetic modification leads to the generation of the recombinant multivalent ILTV-GFP-NDV-FHN viral vector. Which exhibits positive GFP (GFP) expression and mRFP expression. The Zoe Fluorescent Cell Imager (Biorad) was used to capture the images.

The molecular weights of the NDV-F and -HN proteins were found to be 55 and 75 kilodaltons (kDa), respectively. The experimental findings demonstrate the effective expression of the F and HN proteins of NDV. The investigation's findings illustrate the successful expression of NDV-F and -HN, as seen in **Figure 6.8.B**. After confirming the presence and expression of NDV-F and -HN at the molecular level, we proceed to elucidate the localisation of the NDV-F and -HN proteins using an immunofluorescence experiment. The LMH cells on a 24-well plate were infected with the recombinant multivalent ILTV strain. At 36 hours following infection, the cells were subjected to fixation and subsequently labelled with anti-FLAG and Goat anti-Rabbit IgG (H+L) Cross-Adsorbed Secondary Antibody, Alexa Fluor 594 (red). The spatial arrangement of the co-expression of NDV-F and -HN protein, represented by the red colour, is illustrated in **Figure 6.8.C**, as visualised by the use of confocal microscopy imaging. In order to assess the degree of expression and cytoplasmic localisation, images depicting the individual localisation of NDV-F and -HN proteins were employed for comparative analysis.

An analysis was done using a plaque assay to investigate the difference in viral quantity (PFU/mL) between ILTV-GFP-NDV-FHN and ILTV-WT. Based on the outcomes of the one-way ANOVA, it can be inferred that there is no statistically significant difference in viral infectivity between the recombinant ILTV-GFP-NDV-FHN and the ILTV-WT, as seen in **Figure 6.9**. The methods utilised to measure the viral quantity are illustrated alongside the graph, which displays visual representations of the wells containing the individual plaques.

In order to investigate the functionality of the recombinant ILTV-GFP-NDV-FHN strain, an *in vitro* growth kinetics study was conducted using quantitative polymerase chain reaction (qPCR). The LMH cells were subjected to an infection induced by the recombinant ILTV-GFP-NDV-FHN strain at a multiplicity of infection (MOI) of 1.0. Subsequent to the infection, the process of DNA extraction was carried out at certain time points, namely at 6-, 12-, 24-, 48-, 72-, and 96-hours after the infection occurred (referred to as hours post-infection, or HPI). The graph depicts the general trend of viral copy number increase in the recombinant multivalent viral vector. The graphic presented in **Figure 6.10** portrays the concept being examined.

The infectivity of the recombinant ILTV-GFP-NDV-FHN variants was further tested by flow cytometry analysis in order to quantify the expression of GFP. The LMH cell line was subjected to infection with the recombinant multivalent ILTV strain. Following this, the cells were fixed and underwent labelling 36 hours after infection. The analysis of the percentage of GFP-positive cells in uninfected control cells and cells infected with recombinant multivalent ILTV-GFP-NDV-FHN demonstrates no statistically significant difference. However, there is an observed tendency towards an increase in GFP

positivity in LMH cells following viral infection. **Figure 6.11.A** depicts microscopic images that demonstrate the synthesis of green fluorescence protein (GFP) within LMH cells that have been subjected to infection by the recombinant ILTV. **Figure 6.11.B** illustrates a representative gating technique, which outlines the methodology employed to identify GFP-positive cells within the LMH cell population. The viral particles were labelled with GFP for visualisation, and the viability of the cells was assessed using a live/dead staining technique.

After confirming the successful integration, expression, and function of the recombinant multivalent ILTV-GFP-NDV-FHN viral vector, the stability of genome integration in subsequent generations was assessed by subjecting the vector to multiple passages. The LMH cell lines were subjected to infection with a recombinant multivalent viral vector, namely the ILTV-GFP-NDV-FHN viral vector. Subsequently, DNA extraction was performed on every succeeding generation of cells. The DNA samples were used for the amplification of the NDV-F and -HN fragments. The existence of the NDV-F and -HN fragments in the progenies from the 1<sup>st</sup> to the 5<sup>th</sup> generation is depicted in **Figure 6.12**.



NDV-FHN viral vector. **(A)** The gel electrophoresis illustrates the amplification of the NDV F and HN genes utilising the ILTV-GFP-NDV-FHN viral vector as the template. The amplification process was conducted utilising the primers CMV-MCS1-F (5'-AGAACCCACTGCTTACTGGCTT-3') and CMV-MCS1-R (5'-AACTAGAAGGCACAGTCGAGGC-3'). The primers are strategically located on both ends of the MCS1 region of the donor plasmid. The amplification of the NDV-HN gene resulted in the production of a DNA fragment of around 1700 base pairs, whereas the amplification of the NDV-F gene gave a DNA fragment of approximately 1600 base pairs. **(B)** A Western blot analysis was conducted in order to evaluate the expression levels of the F and HN proteins of the NDV. The molecular weight of the NDV-F and -HN proteins was determined to be 55 and 75 kilodaltons (kDa), respectively. The results of the experiment illustrate the successful manifestation of NDV F and HN proteins. **(C)** Confluent LMH cells were subjected to infection with the recombinant multivalent ILTV-GFP-NDV-FHN. Subsequently, these cells were stained in order to determine the presence of NDV-F and -HN proteins. The confocal microscopy pictures depicted in Figure C demonstrate the intracellular localisation of the NDV-F and -HN proteins (red) inside the cytoplasm of the LMH cells. Uninfected cells served as negative control.

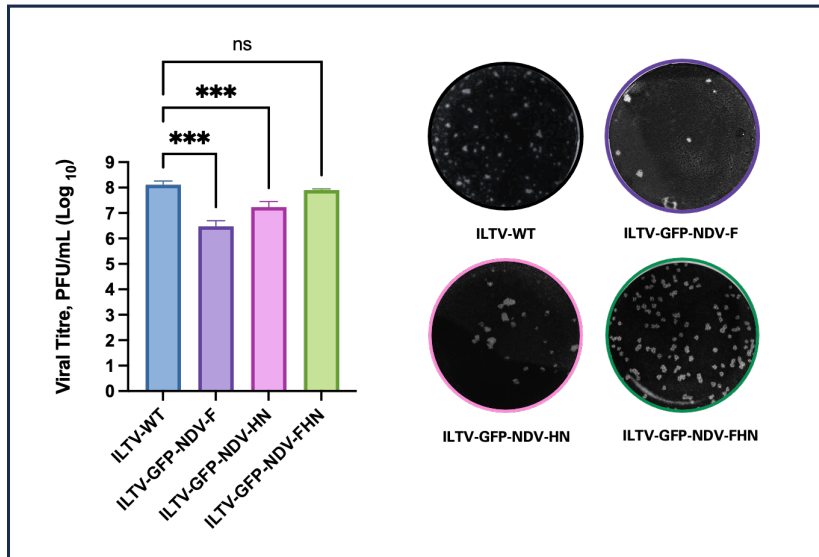


**Figure 6.9. The viral infectivity of the recombinant multivalent ILTV-NDV-FHN strain is not significantly different from that of ILTV-WT. (A)** Plaque assay-based quantification of the infectious virus between the ILTV-WT and recombinant ILTV-GFP-NDV-FHN strains. The results obtained from the plaque assay-based study indicate that there is no statistically significant difference in viral infectivity between the recombinant ILTV-GFP-NDV-FHN strain and the ILTV-WT. Plaque images show the individual plaque-forming units used to compute the final viral concentration. These data represent the average of three technical replicates, with SD indicated. Ns: non-significant  $p > 0.05$ , \* $p < 0.05$ , \*\*\* $p < 0.001$  using one-way ANOVA.

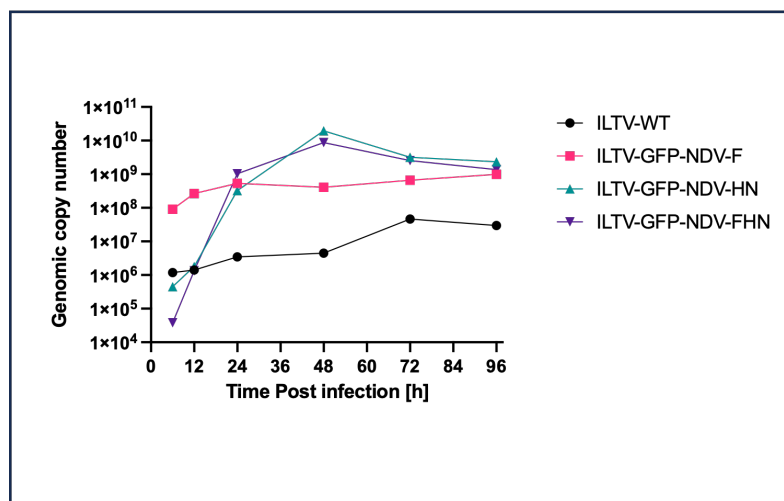


**Figure 6.10. Comparison of the replication kinetics of the ILTV-WT and recombinant multivalent ILTV-GFP-NDV-FHN strains.** The quantitative polymerase chain reaction (qPCR) data analysis presented here illustrates the comparison of genomic copy numbers between the ILTV-WT and the recombinant multivalent ILTV-GFP-NDV-FHN at various time periods, with a multiplicity of infection (MOI) of 1.0. Data analysis is based on one experiment with three technical replicates.



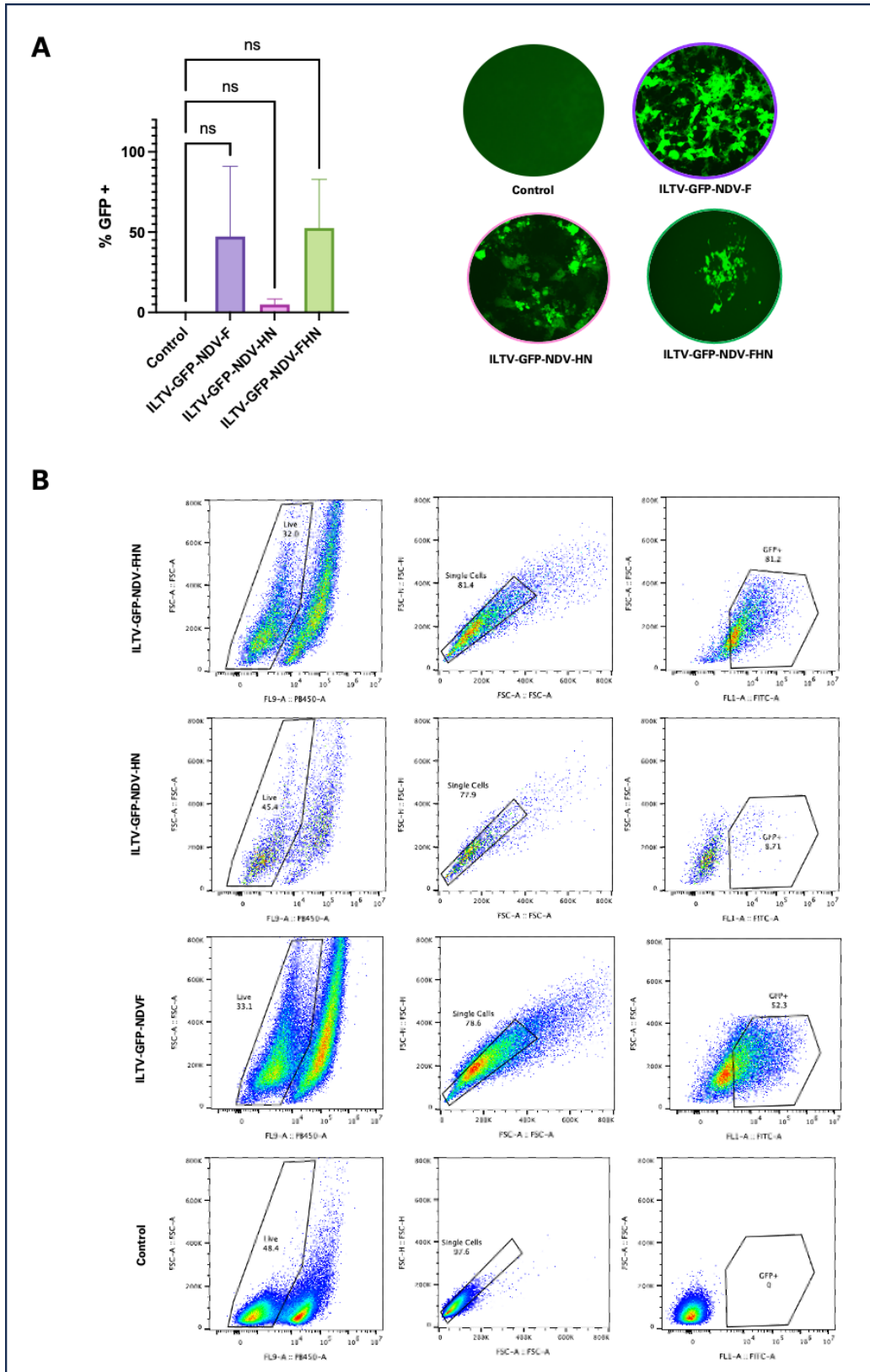


**Figure 6.11. Trend towards an increase in GFP positivity in LMH cells post-viral infection.** At 36 hours post-infection, LMH cells were infected with a recombinant multivalent ILTV-GFP-NDV-FHN strain. Subsequently, a flow cytometry study was conducted to assess the infectivity of the recombinant ILTVs by evaluating the

expression of GFP. **(A)** The figure presents a graphical depiction of the percentage of GFP-positive cells in both uninfected control cells and cells infected with recombinant ILTVs. Additionally, accompanying the graph are microscopic pictures illustrating the expression of GFP in LMH cells infected with the recombinant ILTV. **(B)** The provided information represents the gating approach employed for the identification of GFP-positive cells in the LMH cell population. The viral particles were fluorescently marked with GFP, while the viability of the cells was determined using the live/dead staining kit. The process of gating was conducted via the FlowJo software. Data analysis is based on one experiment with three technical replicates.

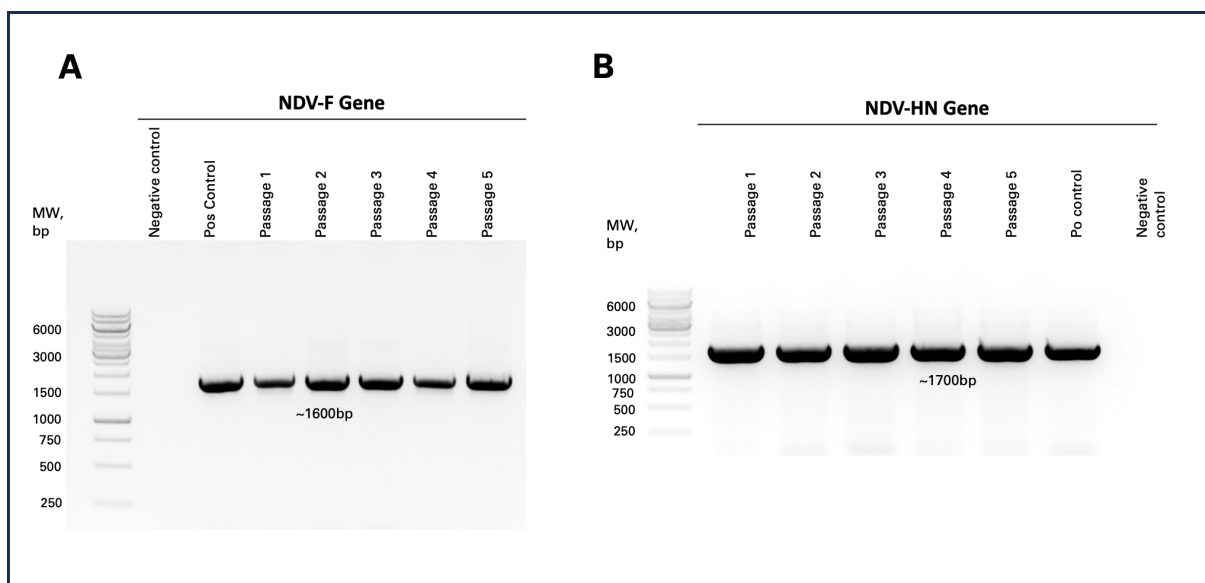


**Figure 6.12. Stable integration of the NDV-F and -HN genes into the recombinant multivalent ILTV-GFP-NDV-FHN.** The stable integration of the NDV-F gene **(A)** and NDV-HN gene **(B)** into the recombinant multivalent ILTV-GFP-NDV-FHN was confirmed by molecular investigation using PCR. This was found by amplifying gene fragments in numerous passages (Passages 1 – 5).

## 6.2.4. Immunogenicity and Protective Efficacy of the Recombinant ILTV Vaccines Against the NDV Challenge

The performance of the developed ILTV vaccine vectors was assessed using *in vitro* testing in order to gain a deeper understanding of their effectiveness. In this chapter, two putative recombinant viral vectors, namely ILTV-GFP-NDV-F and ILTV-GFP-NDV-HN, were used for analysis. The *in vivo* experiments were conducted in collaboration with the Department of Parasitology and Microbiology at the Faculty of Veterinary and Animal Sciences, Arid Agriculture University in Pakistan.

A total of 15 chicks were subjected to the administration of two doses of recombinant ILTV vaccines, namely ILTV-GFP-NDV-F and ILTV-GFP-NDV-HN, through the oculonasal route. Each treatment involved a dosage rate of 400 PFU / 20 uL. The initial administration occurred on the 18<sup>th</sup> day, with the subsequent dose being administered on the 32<sup>nd</sup> day. At 47 days, the chicks were exposed to a challenge consisting of virulent strain of the NDV. The qPCR method was utilised to determine viral shedding, utilising DNA isolated from chicken organs taken at 3-, 7-, and 10-days post-challenge. Furthermore, serological assays were performed to detect antibodies by obtaining blood samples for a duration of four weeks subsequent to the administration of the vaccine. The HI assay was run on a weekly basis, whereas the ELISA assay was performed every two weeks. The workflow is depicted in **Figure 6.13**.

### 6.2.4.1. General Workflow

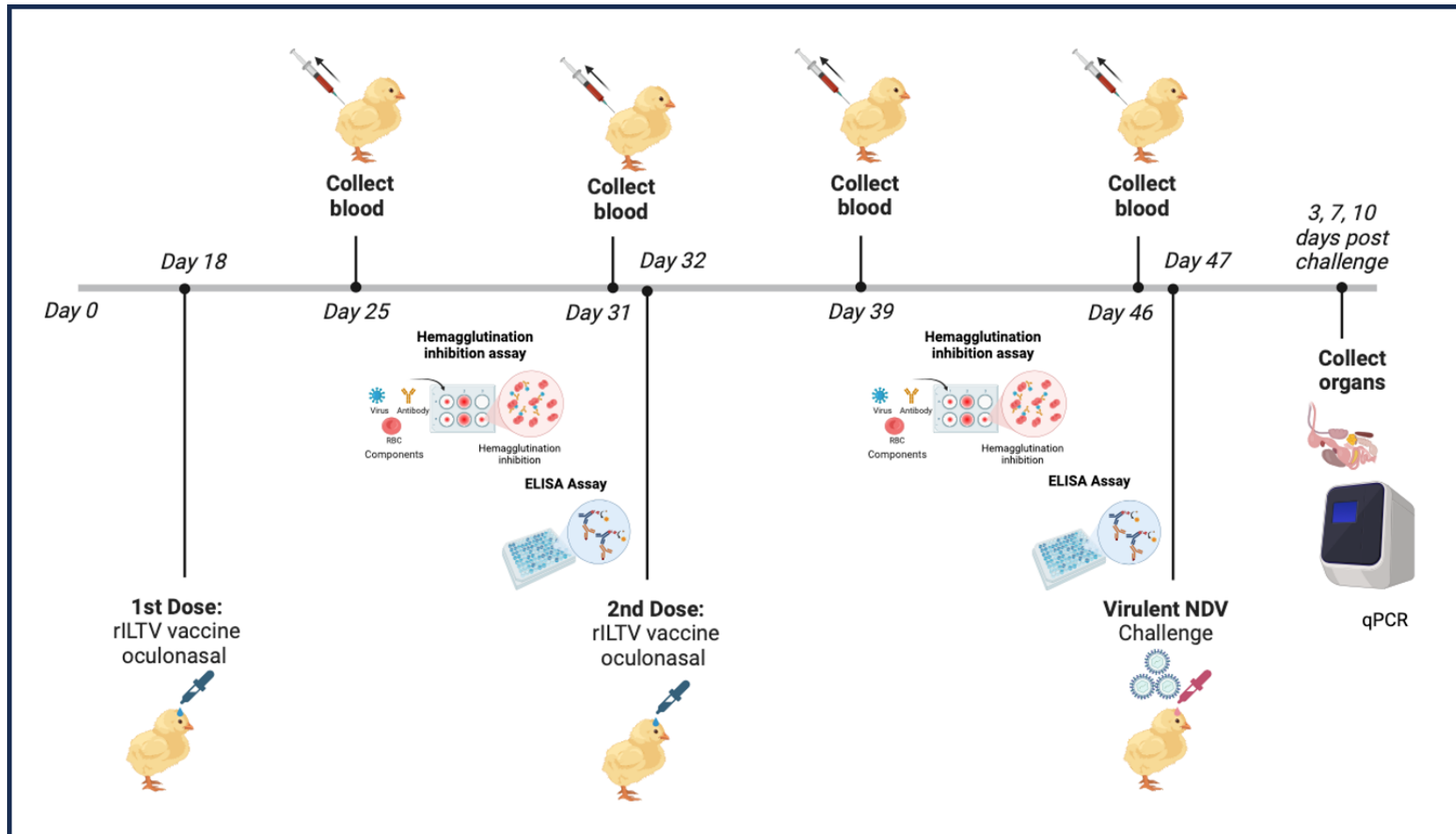


**Figure 6.13. Illustrative representation of the methods used to validate the effectiveness of the recombinant ILTV vaccines.** Two doses of recombinant ILTV vaccines, namely ILTV-GFP-NDV-F and ILTV-GFP-NDV-HN, were administered to the chicks. The first dosage was given on day 18, followed by the second dose on day 32. At 47 days, the chicks were subjected to a challenge

of an NDV virulent strain. The viral shedding was detected by employing the qPCR approach, using the extracted DNA collected from chicken organs at 3, 7, and 10 days after the challenge. In addition, serological assays were conducted to identify antibodies by collecting blood samples over a period of four weeks following the vaccination. The HI assay was performed weekly, while the ELISA assay was conducted biweekly.

#### **6.2.4.2. Serological Assays**

Blood samples were collected from the animal subjects. Antibody detection was carried out using the hemagglutination-inhibition assay (HI) and ELISA.

The chicken population was subjected to two doses of the recombinant ILTV viral vaccine strains. Subsequently, the evaluation of antibody titre was conducted over a predetermined period of time. Blood samples were collected from the chicks on day 25 post-vaccination. Analysis using the hemagglutination inhibition (HI) test failed to reveal any statistically significant distinctions between the positive control and the recombinant ILTV strain. However, a noticeable difference may be detected between the positive control and the recombinant ILTV viral vaccination strain during the 31-day period. An evident increase in the detection of antibodies may be observed over a period of time, as evidenced by the comparison of observations conducted on days 25 and 31 (**Figure 6.14.A.B**). Analysis performed by ELISA yields complementary evidence of a statistically significant difference and an increase in the production of antibodies when comparing the positive control and recombinant ILTV viral vaccine strains (**Figure 6.15.A**). The administration of the second dose of the vaccine was conducted on day 32, followed by the subsequent completion of the HI test on both days 39 and 46. The findings demonstrated a steady increasing trajectory in the generation of antibodies, with a substantial difference observed in antibody production

between the positive control and the recombinant ILTV viral vaccine strains (**Figure 6.14.C.D.**). On the 46<sup>th</sup> day, Elisa presents empirical data that substantiates the observed positive pattern, illustrating a significant difference in the generation of antibodies between the positive control and recombinant ILTV strains, as seen in **Figure 6.15.B.**

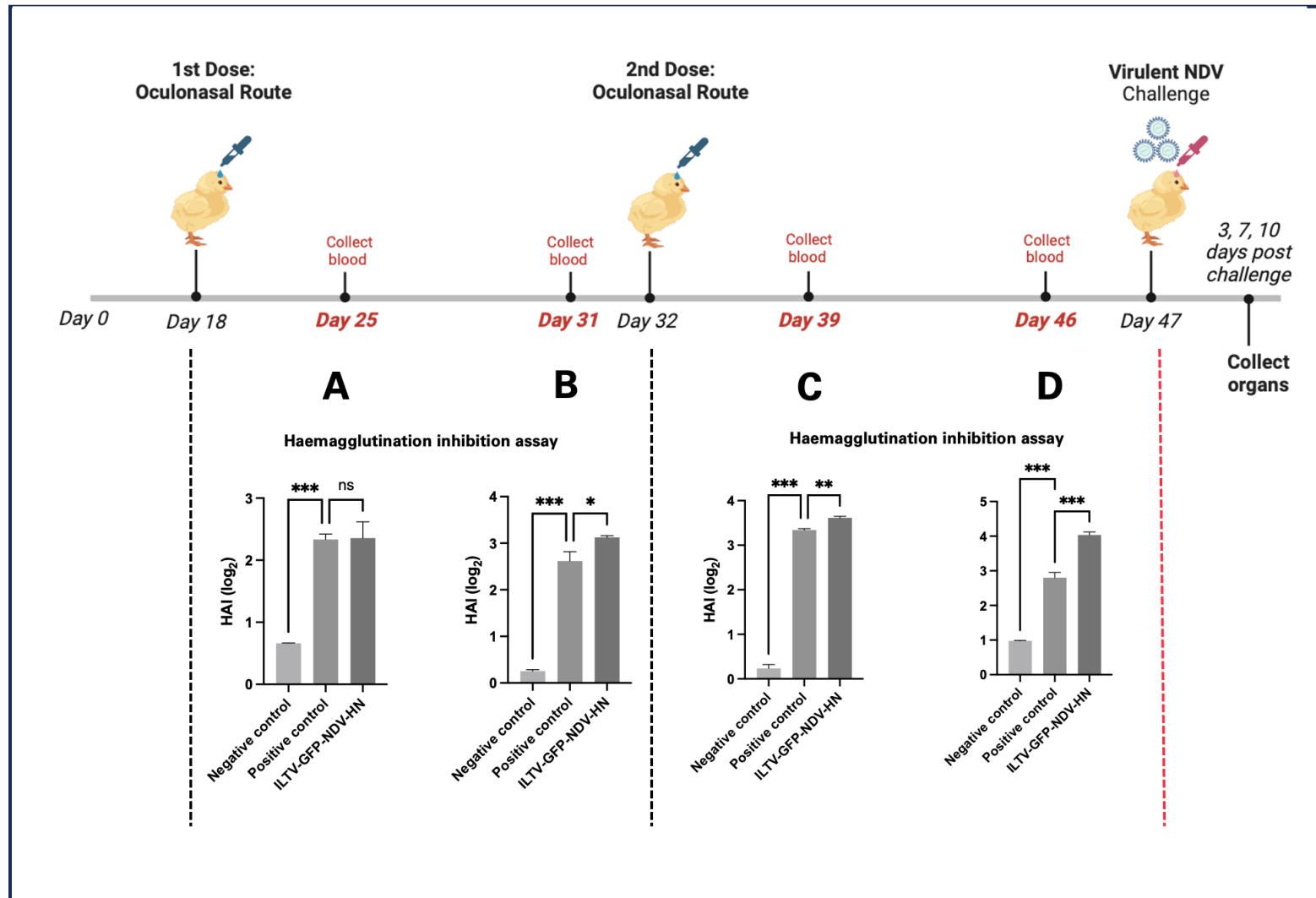


**Figure 6.14. Increasing trend in antibody production over time post-recombinant ILTV vaccination.** The samples were administered two doses of the recombinant ILTV viral vaccine strains, following which the assessment of antibody titre was carried out over a specified duration. **(A)** At day 25 after vaccination, the hemagglutination inhibition (HI) assay does not reveal any

statistically significant differences between the positive control and the recombinant ILTV strain. **(B)** However, at the 31-day time point, a significant difference may be noticed between the positive control and the recombinant ILTV viral vaccine strain. There is an observable upward trend in antibody detection over time, as seen by the comparison of observations made on days 25 and 31. The administration of the second dose of vaccination occurred on day 32, followed by the performance of the **(C)** HI test on day 39 and **(D)** on day 46. The results revealed a consistent upward trend in antibody production and a notable difference in antibody production between the positive control and the recombinant ILTV viral vaccine strains. The provided data is the mean value derived from 15 biological replicates, with the standard error of the mean (SEM) noted. The statistical analysis employed a one-way ANOVA to determine the significance of the observed results. The notation used to denote the level of significance was as follows: a p-value greater than 0.05 was considered non-significant (ns), a p-value less than 0.05 was denoted by a single asterisk (\*), and a p-value less than 0.001 was indicated by three asterisks (\*\*\*)



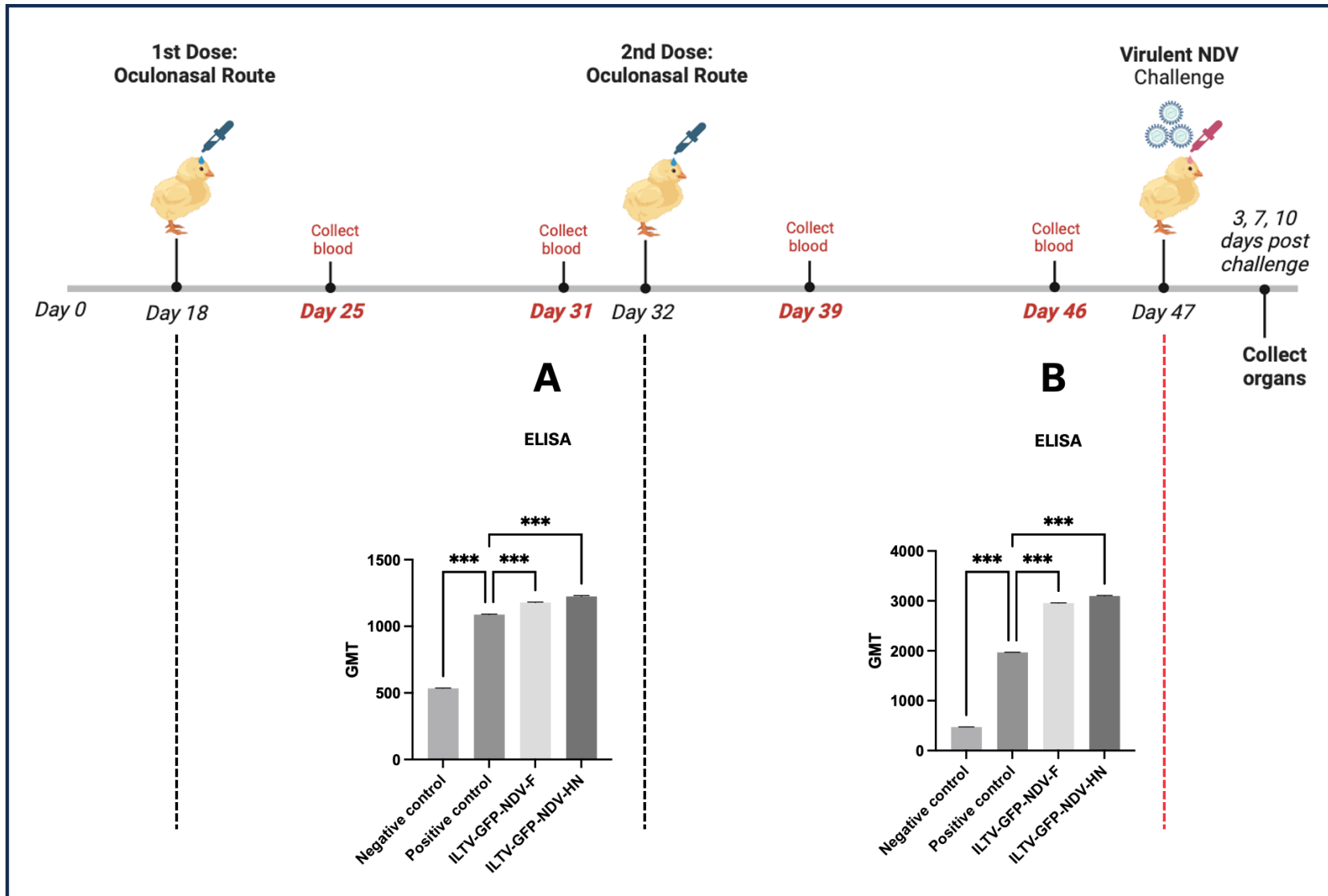


**Figure 6.15. Observed upward trend in antibody production after the administration of recombinant ILTV vaccine strains. (A)** The analysis conducted by ELISA provides additional evidence of a statistically significant difference and an increase in the

production of antibodies when comparing the positive control and recombinant ILTV viral vaccination strains. The administration of the second dose of vaccination occurred on day 32. **(B)** At day 46, Elisa provides further evidence in support of the observed positive trend, demonstrating a notable difference in antibody production between the positive control and recombinant ILTV strains. The provided data is the mean value derived from 15 biological replicates, with the standard error of the mean (SEM) noted. The statistical analysis employed a one-way ANOVA to determine the significance of the observed results. The notation used to denote the level of significance was as follows: a p-value greater than 0.05 was considered non-significant (ns), a p-value less than 0.05 was denoted by a single asterisk (\*), and a p-value less than 0.001 was indicated by three asterisks (\*\*\*)

## 6.3. Chapter Discussion

This chapter focuses on the development of a recombinant multivalent viral vaccine vector carrying the F and HN genes of NDV. Furthermore, this chapter aims to present substantial data supporting the notion that these recombinant vaccine viral vectors offer heightened protection against virulent NDV strains.

Recombinant vector vaccines have gained significant popularity in the poultry sector due to their ability to provide immunity against a variety of illnesses and their potential for the implementation of the differentiating infected from vaccinated animals (DIVA) method in practical settings (Suarez, 2012). The development of recombinant vector vaccines for NDV used the herpesvirus of turkeys and fowlpox as vectors. These vaccines were designed to express the F or HN proteins of the NDV (Bournnell et al., 1990; Ferreira et al., 2021; Morgan et al., 2017, 2019).

In order to provide a basis for comparison of the properties and functionality of a recombinant ILTV with an NDV-HN insert at the UL0 region of the ILTV genome, we have successfully generated the recombinant ILTV-GFP-NDV-HN strain using the CRISPR/Cas9 gene editing technique. We have designed guide RNAs with specificity to target and cleave the UL0 region of the ILTV genome, resulting in the targeted insertion of the NDV-HN gene by a targeted non-homologous mechanism. The molecular and protein-level investigation of the recombinant ILTV-GFP-NDV-HN strain demonstrated the effective integration of the HN gene. Additionally, protein expression analysis and imaging techniques confirmed the presence of the HN protein and its localisation within the cytoplasm. The results obtained from the plaque assay-based study indicate a notable decrease in viral infectivity of the recombinant ILTV with the

HN insert in comparison to the wild type of virus. However, these findings do not suggest that the recombinant virus is incapable of infecting LMH cells and undergoing replication. This concept was further substantiated by conducting a kinetics study using the quantitative polymerase chain reaction (qPCR) technique. The observed slight delay in viral development may suggest a potentially advantageous role of UL0 in the first stages of virus replication (Veits et al., 2003). Moreover, the slight delay of the recombinant ILTV with HN insert viral development still followed the pattern of replication cycle as observed in other herpesviruses, showing that the peak concentration of viral genomic copy number occurs approximately 24 to 30 hours after infection (Bagust & Johnson, 1995).

Having functionally characterised and proven the effectivity and efficacy of the insertion of the NDV-HN gene into the ILTV genome, we have carried out the generation of a recombinant multivalent vaccine vector with NDV-F and -HN inserts. In the previous chapter (Chapter 4), we have already created a recombinant viral vector with the NDV-F gene insert, the ILTV-GFP-NDV-F. The recombinant ILTV-GFP-NDV-F served as the vector backbone for the integration of the NDV-HN gene, resulting in the creation of a potential multivalent recombinant viral vector known as ILTV-GFP-NDV-FHN. Prior to conducting stability testing on animal trials, the existence of the NDV-F and -HN genes in the genome of the ILTV-GFP-NDV-FHN was confirmed using molecular and protein-level investigations as well as localisation analyses. Additional stability testing was conducted by *in vitro* passaging up to the fifth generation, revealing the continued presence of the NDV-F and -HN inserts through the fifth passage. While several publications raise concerns regarding the potential instability of the insert resulting from the engineering of the dsDNA viral genome and

subsequent genome expansion, our current findings indicate that the inserts of NDV-F and -HN are stable and actively produced (Elde et al., 2012).

Based on the results obtained from the viral infectivity experiment, it is noteworthy to mention that the multivalent recombinant ILTV exhibited superior performance compared to both ILTV-GFP-NDV-F and ILTV-GFP-NDV-HN. The multivalent recombinant ILTV with both F and HN was found to be more infective compared to the wild type and the recombinant ILTV with only F or HN inserted. Additionally, in terms of kinetics, the multivalent recombinant ILTV exhibited an early onset of replication, suggesting that the disruption of the TK, UL0, and US4 regions of the ILTV genome did not affect the replication efficacy of the recombinant viral vector (Veits et al., 2003; Willemsen & Zwart, 2019). The results of our study provide additional support for prior research that has demonstrated the dispensability of the UL0 protein for *in vitro* replication. Additionally, our findings confirm that deletion mutants of UL0 only display minimal growth abnormalities in cultured cells, consistent with the observations made by Veits et al. (2003). Furthermore, the deletion of TK and US4 (gG), which are virulence-related factors, provided the baseline for the attenuation of the recombinant ILTV using knockout techniques (Devlin et al., 2006; Han et al., 2002). And finally, by modifying these three regions of the ILTV genome, we have developed a candidate multivalent recombinant ILTV vaccine vector against NDV.

The effectiveness of these putative vaccination vectors was assessed by serological and molecular analysis. In order to investigate the impact of dosage on antibody formation, a study was carried out on chicks. These chicks were administered two doses of the recombinant ILTV-GFP-NDV-F and ILTV-GFP-NDV-HN candidate viral

vectored vaccines, with a 14-day interval between doses. During the interval between doses, haemagglutination inhibition tests and ELISA were conducted to assess the immune response. The hemagglutination inhibition (HI) experiments conducted at 7 and 14 days after the initial dosage demonstrated a notable upward trajectory in antibody levels when comparing the recombinant ILTV with HN insert to the positive control (i.e., the commercially available vaccine). The levels of antibodies showed a significant rise subsequent to the administration of a booster vaccine on day 32. Nevertheless, it is noteworthy that the antibody levels demonstrated variability depending on the specific type of booster vaccine employed. The groups that received the recombinant ILTV-GFP-NDV-HN vaccine had the greatest mean titre for hemagglutination inhibition (HI) in all HI assay timepoints, both after the first dose and the booster dose. After receiving a booster vaccination, it was shown that both the recombinant vaccines (ILTV-GFP-NDV-F and ILTV-GFP-NDV-HN) elicited considerably elevated levels of antibody titres in comparison to those generated by immunisation with the control vaccine.

Although there were variations in the level of antibody response, the recombinant vaccination regimens provided complete clinical protection against a velogenic NDV field strain of genotype VII. The study conducted by Allan and Gough in 1976 has revealed that NDV protection can be observed even with minimal levels of antibody or in the presence of detectable antibody when conventional live attenuated vaccines are administered (Allan & Gough, 1976; Boursnell et al., 1990). In contrast, it was observed that all avian subjects who had not received vaccinations exhibited symptoms of respiratory distress, along with diarrhoea, conjunctivitis, and indicators

of nervous system impairment, ultimately resulting in death within four days following the challenge.

Subsequently, an assessment was conducted to determine the extent of protection provided by the recombinant viral vaccination vectors against the highly pathogenic NDV challenge. The viral shedding outcomes, as evaluated by RT-qPCR, exhibited negative findings, as indicated by the cycle threshold (C<sub>q</sub>) values. The findings of this study indicate that the use of recombinant viral vectors containing the F or HN insert, derived from a strain that is genotypically compatible with the challenge strain, may exhibit enhanced efficacy in mitigating virus shedding (Arora et al., 2010; Ferreira et al., 2021; Palya et al., 2012).

According to previous studies, it has been proposed that the F and HN glycoproteins have a mutual interaction that enhances fusion activity (Stone-Hulslander & Morrison, 1997). Therefore, it was hypothesised that the immunisation involving both genes may potentially elicit a more comprehensive immune response, targeting a wider range of epitopes present in two distinct antigens (Loke et al., 2005). Hence, we hypothesised based on the serological results discussed above that the administration of a recombinant multivalent vaccine vector, which expresses the F and HN proteins, would yield superior results compared to the individual administration of either component.

Collectively, this chapter successfully demonstrated the generation and confirmation of the stability of a multivalent recombinant ILTV viral vector harbouring the F and HN genes of the NDV *in vitro*. The potential of this novel multivalent candidate vaccine lies

in its ability to address immunisation needs in places where various genotypes of virulent NDV are prevalent. Furthermore, this chapter included an examination of the processes by which recombinant candidate vaccines may potentially confer heightened protection against a highly pathogenic strain of NDV *in vivo*.



# CHAPTER 7

## **Construction of a Herpesvirus-Based Vaccine Against Economically Important Poultry Viruses (Infectious Bronchitis Virus and Avian Influenza)**

### **7.1. Introduction**

Various methodologies have been employed to modify viral vectors in order to develop recombinant vaccine candidates targeting avian viruses (Baron et al., 2018). The existing techniques for altering viral vectored vaccines are characterised by inefficiency, time consumption, and labour intensiveness, particularly in relation to purifying protocols (Zou et al., 2017). Therefore, there is a critical need for the development of a more efficient and dependable genome editing method in order to enhance the development of viral vectored vaccines. The CRISPR/Cas9 genome editing methodology is considered very advantageous due to its ability to offer a more convenient and straightforward option compared to traditional approaches.

In general, viruses can serve as vectors for the expression of exogenous genes. According to Marín-López and Ortego (2016), the poxvirus (derived from both the orthopoxvirus and parapoxvirus genera), herpesvirus, adenovirus, and baculovirus are the DNA viruses that are most commonly employed for the purpose of delivering

vaccine antigens. The primary advantages of DNA viruses, as opposed to RNA viruses, are their genomic stability, accessibility of various insertion sites, and the availability of BAC-DNA clones for the purpose of creating and rescuing recombinant viruses within laboratory settings. In general, an optimal viral vector should possess several key characteristics. Firstly, it should be safe and capable of facilitating effective expression of the desired antigen. Secondly, it should have little inherent immunogenicity, therefore permitting repeated injections and serving as a suitable platform for booster vaccinations. Lastly, it must satisfy specific requirements that facilitate its large-scale production (Haut et al., 2005). The application of CRISPR/Cas9 technology in the production of viral vectors has been extensively utilised in several viral vectors, including adenovirus, herpesvirus, and poxvirus (Marín-López & Ortego, 2016).

The principal approach for the control of the H9N2 AIV in poultry is vaccination. The efficacy of existing H9N2 inactivated vaccines is constrained by their failure to elicit cellular immunity, despite their capacity to provide protection against clinical manifestations and reduce viral shedding (X. Cheng et al., 2013). The recombinant herpesvirus of turkeys (HVT) has been shown to elicit a robust immune response, encompassing both humoral and cellular components, hence offering effective protection (L. Liu et al., 2019). Other recombinant herpesvirus-based viral vaccine vectors were also developed to overcome maternal-derived antibodies (MDA), generating a new rHVT-H9 vaccine that stimulated strong humoral and cellular immunity, reducing virus shedding and transmission of H9N2 AIV even in the presence of passively transferred antibodies (PTAs) in chickens (X. Pan et al., 2023).

Live-attenuated vaccinations have demonstrated efficacy in the management of infectious bronchitis (IB). However, it is important to note that while these vaccines provide cross-protection against certain variants of the IBV, it may not confer protection against other forms (De Wit et al., 2011; Gelb Jr et al., 2005; Terregino et al., 2008). Furthermore, there is a possibility of the emergence of variant strains of IBV due to genetic mutations or genetic recombination events (Abozeid et al., 2017; Toro et al., 2012). Viral vectored vaccinations offer an alternate strategy in comparison to live-attenuated IBV vaccines (Abozeid et al., 2019).

The focus of this chapter is on the flexibility of the proposed CRISPR/Cas9 methodology in the production of recombinant viral vectors. The CRISPR/Cas9 system has been previously evaluated using the F and HN antigens of NDV. This chapter aims to extend and assess the efficacy of the CRISPR/Cas9 workflow and ILTV in producing recombinant viral vectors containing gene inserts from other economically significant poultry viruses, such as IBV-S and AIV-HA (H9N2).

### **7.1.1. Aims**

The objective of this chapter is to employ the CRISPR/Cas9 gene editing technology in order to develop a recombinant ILTV vaccine vector that has the ability to carry antigens associated with various avian diseases that hold economic significance.

Specifically:

1. Demonstrate and experimentally validate the capacity of ILTV to carry the S gene of the IBV.
2. Demonstrate and experimentally validate the capacity of ILTV to carry the HA (H9N2) gene of the AIV.
3. Functionally validate the capability of the recombinant ILTV viral vectors to behave similarly to ILTV-WT.
4. Provide evidence of the flexibility and efficacy of the CRISPR/Cas9 system developed in this research study.

## 7.2. Results

The preceding chapters produced crucial findings that are relevant to this chapter. These findings include: (1) the efficacy of the CRISPR/Cas9 gene editing technology as a promising approach to developing functional recombinant ILTV viral vectors; (2) the ability of the ILTV genome to accommodate large gene inserts at different genomic locations; and (3) the potential of ILTV as a preferred viral vector for the development of multivalent vaccine vectors. Ultimately, this chapter will explore deeper into the effectiveness of CRISPR/Cas9 gene editing technology in the development of recombinant ILTV vaccine vectors that carry antigen inserts from economically important poultry viruses, such as the infectious bronchitis virus and the avian influenza virus.

### 7.2.1. Spike Gene of the Infectious Bronchitis Virus

#### 7.2.1.1. Cloning and Validation of Gene Cassettes

The donor plasmid pCDNA3-MCS1-mRFP, which was previously created and discussed in Chapter 4, was utilised to create donor plasmids that harbour the IBV-S gene in MCS1. **Figure 7.1.A** illustrates a schematic depiction of the donor plasmid pCDNA3-MCS1-mRFP. PCR primers were specifically designed for the amplification of the IBV-S gene, with the inclusion of *HindIII* (5'-CTAAAGCTTCCACCATGCTGGGCAAGAGCCTG-3') and *KpnI* (5'-GCCGGTACCTCAGGTGCTGTCCAGGCCCA-3') restriction enzyme recognition sites at the 5' and 3' ends, respectively (**Figure 7.1.B**). PCR was employed to perform positive amplification of the IBV-S gene, resulting in the detection of a band with an

estimated size of 3400 bp (**Figure 7.1.B**). In order to facilitate the insertion of the IBV-S fragment into the multiple cloning site 1 (MCS1) of the recipient vector (pcDNA-MCS1-mRFP), both the IBV-S insert and the recipient vector (pcDNA-MCS1-mRFP) underwent restriction enzyme digestion utilising the restriction enzymes *HindIII* and *KpnI*. Subsequently, the use of DNA ligase facilitated the fusion of the IBV-S insert and the recipient vector. The donor plasmid, pcDNA-IBVS-mRFP (**Figure 7.1.C**), obtained after ligation, was propagated by transformation into DH5 $\alpha$  competent *E. coli* cells. Positive colonies were then subjected to a purification process to obtain purified plasmid DNA for further examination using Sanger sequencing. The provided sequence alignment illustrates the similarity between the sequenced forward fragment of the cloned IBV-S gene and the IBV reference genome. The Sanger sequencing outcome confirms a complete match of 100% identity between the reference genome IBV and pcDNA-IBVS-mRFP (shown in pink) for the forward fragment (**Figure 7.1.D**).

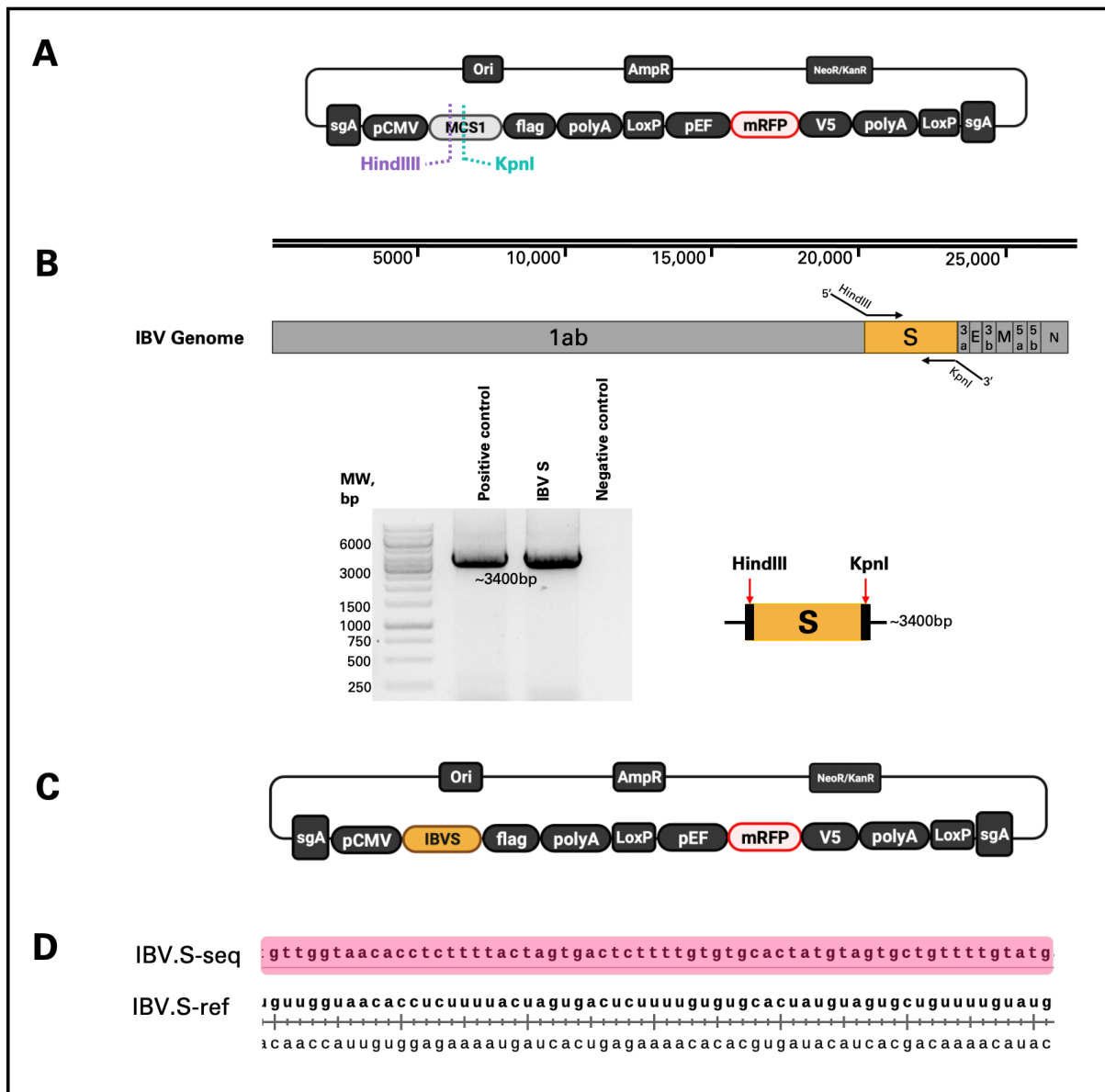


**Figure 7.1. Assembly and sequence validation of the recombinant donor plasmid pCDNA-IBVS-mRFP.** The integration of the IBV-S gene fragment was accomplished at multiple cloning site 1 (MCS1) of the donor plasmid pcDNA-MCS1-mRFP. **(A)** The image presented depicts the donor plasmid, pcDNA-MCS1-mRFP, which possesses distinct recognition sites for the restriction enzymes *HindIII* and *KpnI*. **(B)** The following is the fragment representation of the genome of the IBV. The primers were created with the particular purpose of amplifying the IBV-S gene. These primers were strategically constructed to include *HindIII* and *KpnI* restriction enzyme recognition sites at the 5' and 3' ends, respectively. The gel electrophoresis image illustrates the amplified IBV-S gene, with an approximate length of 3400 base pairs. The process involved in this study consisted of cloning the amplified IBV-S gene fragment and the donor plasmid pcDNA-MCS1-mRFP. This was achieved by the use of restriction enzyme digestion, specifically employing *HindIII* and *KpnI*. **(C)** The DNA ligation procedure was conducted to facilitate the fusion of the IBV-S fragment with the recipient donor plasmid pcDNA-MCS1-mRFP, therefore generating the recombinant

donor vector pcDNA-IBVS-mRFP. **(D)** The presented sequence alignment demonstrates the similarity between the sequenced forward portion of the cloned IBV-S gene and the reference IBV genome (NCBI accession number AJ311317). The results of Sanger sequencing demonstrate a 100% identical match between the wild-type S gene of the IBV and pcDNA-IBVS-mRFP, as indicated by the forward fragment. The colour pink highlight is used to represent the pcDNA-IBVS-mRFP sequence.

#### **7.2.1.2. Generation of Recombinant ILTV Strains**

The process of generating the recombinant ILTV with a cassette knock-in of the IBV-S gene required the assembly of several components. The components utilised in this study encompassed three main elements. Firstly, the recombinant ILTV-GFP construct was used, which serves as a vector for expressing the GFP gene. Secondly, the donor plasmid pcDNA-IBVS-mRFP was employed, which contains the IBV-S gene along with a reporter gene encoding mRFP. Lastly, the CRISPR/Cas9-sgRNA plasmids, specifically pX459v2-UL0, were utilised to induce double-strand breaks in the ILTV genome at the UL0 region.

The method encompasses two major constituents: the transfection of the donor plasmid (pcDNA-IBVS-mRFP) and the CRISPR/Cas9-sgRNA plasmid (pX459v2-UL0) into LMH cells (**Figure 7.2.A**). During the process of incubation, the accessory guide RNA-A (pX459v2-sgRNA-A) will accurately recognise and cleave the specific sgRNA-A site found in the donor plasmid. This action will lead to the release of the IBVS-mRFP gene cassette. After 36 hours of transfection, the LMH cells were infected with recombinant ILTV-GFP after the detection of red fluorescence by microscopic analysis (**Figure 7.2.B**). The CRISPR/Cas9-guideRNA (pX459v2-UL0) method is employed to facilitate the assessment of the ILTV genome and enable the targeted cleavage



necessary for the insertion of the IBVS-mRFP gene cassette into the specified UL0 genomic region of the ILTV genome. As a result, this approach leads to non-homology targeting or non-homologous end joining. At the 24-hour time point subsequent to infection, LMH cells were subjected to microscopic analysis in order to evaluate the concurrent existence of the GFP protein, which emits green fluorescence, signifying the successful infection of the ILTV-GFP, and the presence of the mRFP reporter gene within the gene cassette harboured by the donor plasmid pcDNA-IBVS-mRFP, which emits red fluorescence as depicted in **Figure 7.2.C**.

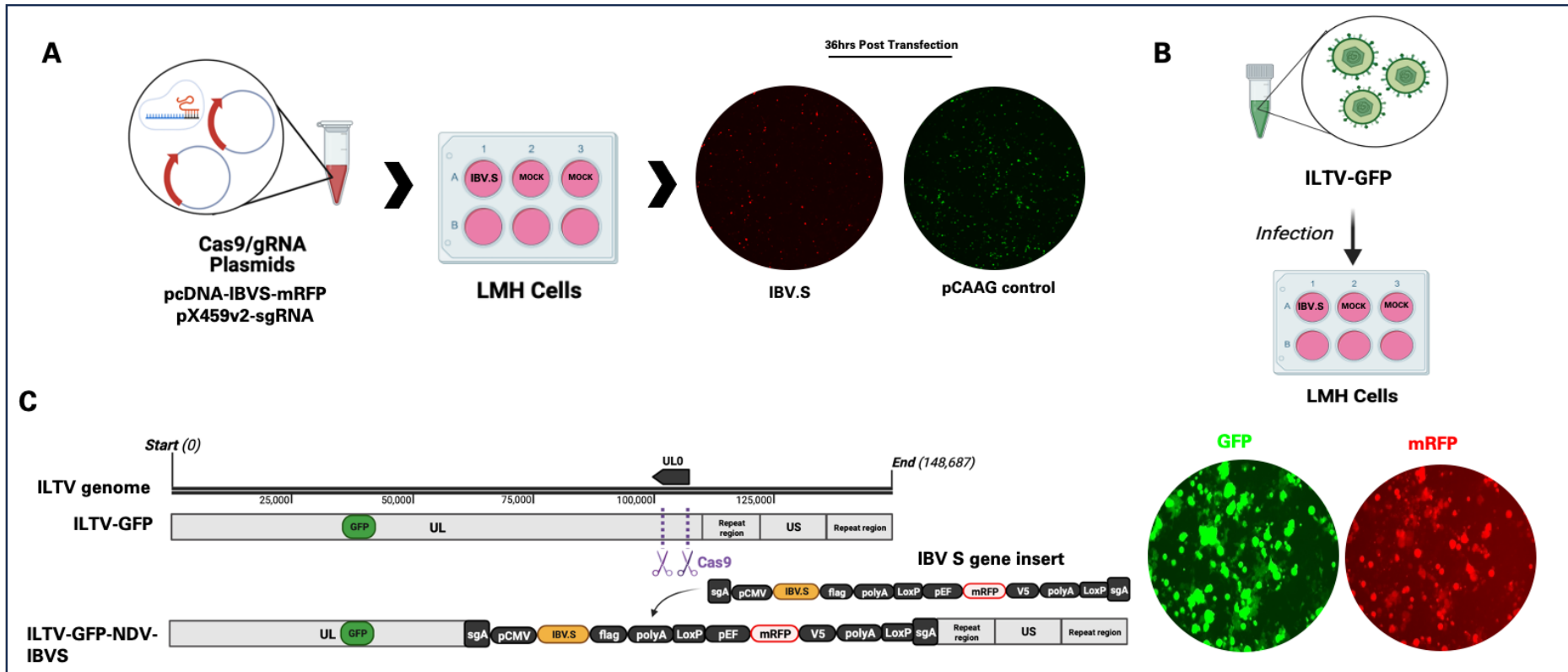


**Figure 7.2. Illustrative representation of the workflow used for the generation of recombinant ILTV-GFP-IBVS.** The methodology consists of two fundamental components: **(A)** The introduction of pX459v2-sgRNA plasmids (plasmids carrying CRISPR/Cas9-sgRNA) and pcDNA3-IBVS-mRFP (donor plasmid) into LMH cells using transfection. At the 36-hour time point following transfection, a microscopic examination demonstrated the presence of red fluorescence, which signifies the successful identification of donor plasmids (pcDNA3-IBVS-mRFP) within LMH cells. **(B)** After the red fluorescence was observed in LMH cells, the cells were infected with ILTV-GFP. **(C)** At the 24-hour time point subsequent to infection, the CRISPR/Cas9 enzyme induces the formation of double-strand breaks at the UL0 region of the ILTV-GFP genome, leading to the incorporation of the IBV-S gene insert.

The genetic alteration results in the production of the recombinant ILTV-GFP-IBVS, which demonstrates the presence of GFP and mRFP by observable fluorescence. The Zoe Fluorescent Cell Imager, manufactured by Biorad, was employed for image acquisition.

#### **7.2.1.2.1. Characterisation of the Recombinant ILTV-GFP-IBVS**

Validation of the recombinant ILTV-GFP-IBVS has been conducted through the use of several molecular and imaging techniques. The LMH cell line was subjected to infection through the use of the recombinant ILTV-GFP-IBVS strains. The presence of the IBV-S gene was originally evaluated by the use of primers that included the MCS1 region of the donor plasmid. The visual representation depicted in **Figure 7.3.A** offers empirical support for the presence of the IBV-S gene fragment, which has a size of around 3.4 kilobases. The fragment was subjected to comparison with the IBVS-WT gene amplicon, which possesses an estimated size of 3.4 kb and functions as the designated positive control. A Western blot analysis was conducted to examine the presence of the IBV-S protein. The detected molecular weight of the IBV-S protein was around 170 kilodaltons. Fragments S1 or S2 may also be detected at an estimated molecular weight of 110 kDa. The results of the experiment illustrate the successful expression of the IBV-S protein, as seen in **Figure 7.3.B**. The subcellular distribution of the IBV-S protein was confirmed using the results obtained from an immunofluorescence assay. The LMH cells on a 24-well plate were infected with the recombinant ILTV strain. At 36 hours following infection, the cells were subjected to fixation and subsequent labelling using anti-FLAG and Goat anti-Rabbit IgG (H+L) Cross-Adsorbed Secondary Antibody, Alexa Fluor 594 (red). The cellular location of the IBV-S protein (red) within the cytoplasm of the LMH cell is depicted in **Figure 7.3.C**, as observed using confocal microscope imaging.

A study was done using a plaque assay to investigate the difference in viral quantity (PFU/mL) between the ILTV-GFP-IBVS and the ILTV-WT. The t-test findings demonstrate a significant difference in viral infectivity between the recombinant ILTV-GFP-IBVS strain and the ILTV-WT strain, as seen in **Figure 7.4**. The methodology employed for quantifying the viral amount is depicted adjacent to the graph, which showcases images of the wells containing the distinct plaques.

In order to investigate the functionality of the recombinant ILTV-GFP-IBVS strain, an *in vitro* growth kinetics study was conducted using quantitative polymerase chain reaction (qPCR). The LMH cells were subjected to an infection induced by the recombinant ILTV-GFP-IBVS strain, with a multiplicity of infection (MOI) of 1.0. DNA extraction was performed at certain time points, namely at 6-, 12-, 24-, 48-, 72-, and 96-hours after infection (HPI). The graph depicts the general trend of viral copy number increase. The figure presented in **Figure 7.5** provides a visual representation of the notion being discussed.

The infectivity of the recombinant ILTV-GFP-IBVS was further evaluated through the use of flow cytometry analysis. The LMH cell line was subjected to infection with the recombinant ILTV strain. Following this, the cells were fixed and underwent labelling 36 hours after infection. The analysis of the percentage of cells expressing GFP in both uninfected control cells and cells infected with recombinant ILTV demonstrates no statistically significant difference. However, there is an observable tendency towards a rise in GFP positivity in LMH cells following viral infection. **Figure 7.6.A** presents microscopic images that depict the production of GFP within LMH cells following infection with the recombinant ILTV. **Figure 7.6.B** illustrates the

representative gating technique employed to identify GFP-positive cells within the LMH cell population. This approach outlines the strategy utilised for this purpose. The viral particles were labelled with GFP to enable fluorescence detection, while the viability of the cells was assessed using the live/dead staining technique.

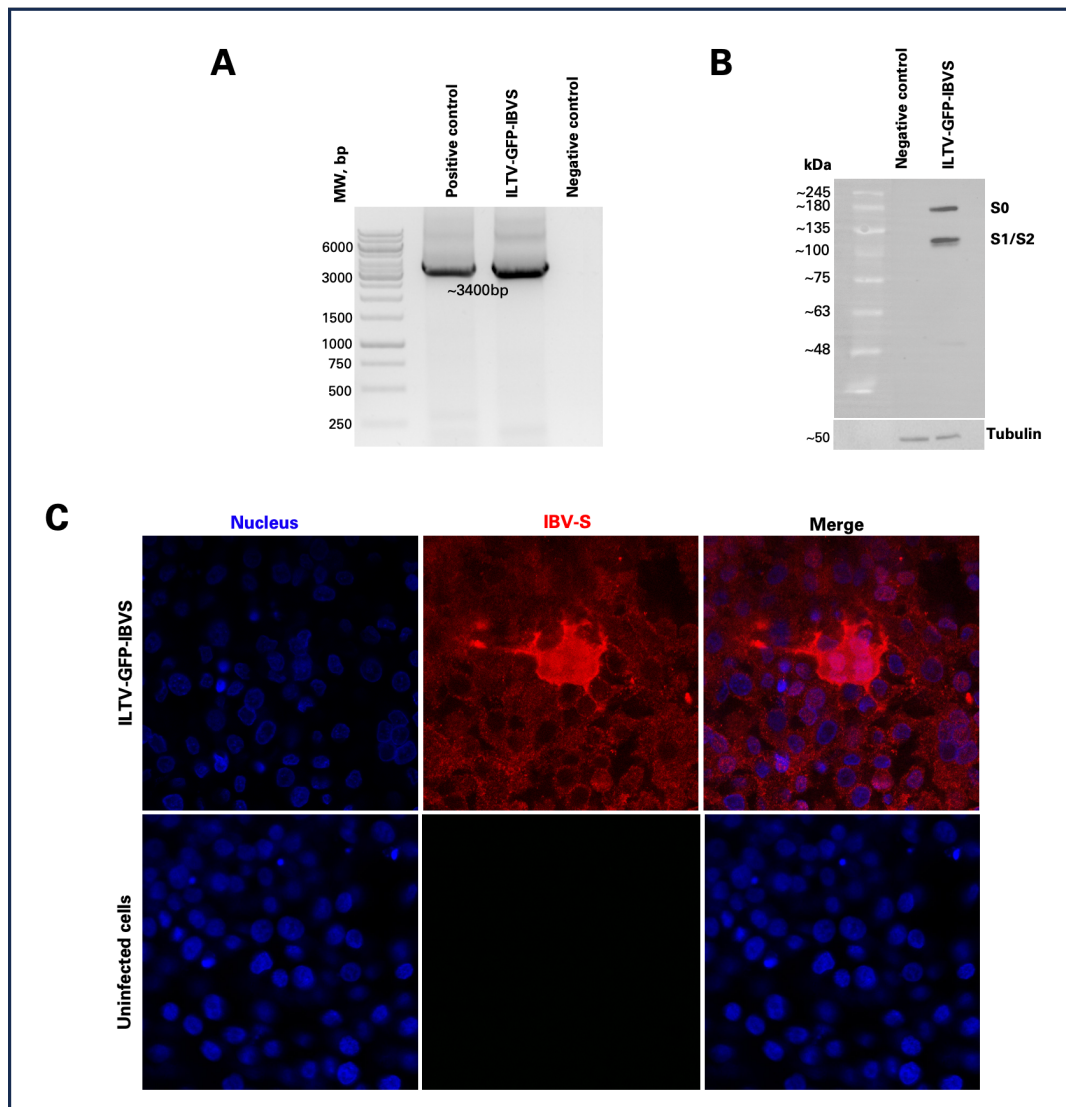


**Figure 7.3. IBV-S expression at the molecular and protein-levels in LMH cells post-infection with the recombinant ILTV-GFP-IBVS strain.** The LMH cell line was subjected to infection by the use of the recombinant ILTV-GFP-IBVS viral vector. **(A)** The gel electrophoresis illustrates the amplification process utilising the primers CMV-MCS1-F (5'-AGAACCCACTGCTTACTGGCTT-3') and CMV-MCS1-R (5'-AACTAGAAGGCACAGTCGAGGC-3'). The primers are strategically located on both ends of the MCS1 region of the donor plasmid. The polymerase chain reaction (PCR) was employed to amplify the IBV-S gene, resulting in the production of a DNA fragment of about 3400 base pairs in length. In the current chapter, the samples underwent a comparison with the IBVS-WT (~3.4 kb) gene, which was designated as the positive control for the experiment. **(B)** A Western blot analysis was conducted in order to evaluate the expression of the IBV-S protein. The molecular weight of the IBV-S protein was confirmed to be 170 kilodaltons (kDa) by detection methods. Fragments S1 or S2 may also be detected at an estimated molecular weight of 110 kDa. The results of the experiment illustrate the successful manifestation of the IBV-S protein. **(C)** Confluent LMH cells were subjected to infection with the recombinant ILTV-GFP-IBVS, followed by staining to determine the presence of the IBV-S protein. The confocal microscopy images depicted in **Figure C** provide a visual representation of the intracellular localisation of the IBV-S protein (red) inside the cytoplasm of the LMH cells. Uninfected cells served as negative control.

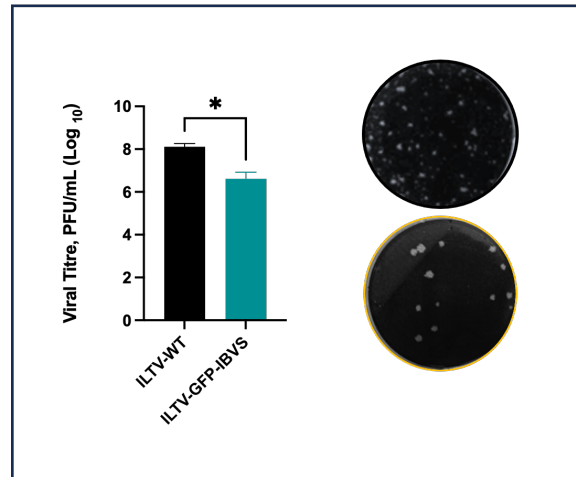


**Figure 7.4. Viral infectivity of the recombinant ILTV-GFP-IBVS strain is significantly different from that of ILTV-WT.** The quantification of infectious virus between the ILTV-WT and recombinant ILTV-GFP-IBVS strains was performed using a plaque assay-based analysis. The findings derived from the study utilising the plaque assay method demonstrate that there is significant difference in viral infectivity between the recombinant ILTV-GFP-IBVS strain and the ILTV-WT strain. The photos of plaques depict the discrete units responsible for plaque formation, which are then utilised in the calculation of the final viral concentration. The provided data is the mean value derived from three technical replicates, with SD reported. The statistical analysis conducted in this study utilised the student's t-test to determine the significance of the observed results. The notation used to indicate the level of significance was as follows: a p-value greater than 0.05 was considered non-significant (ns), a p-value less than 0.05 was denoted as significant (\*), and a p-value less than 0.001 was indicated as very significant (\*\*\*)

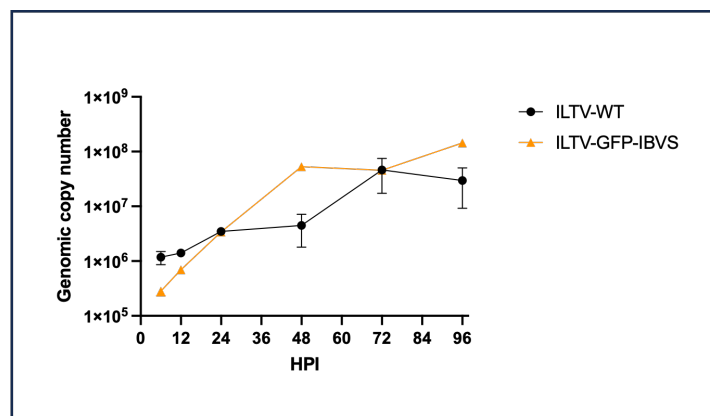


**Figure 7.5. Comparison of the replication kinetics of the ILTV-WT and recombinant ILTV-GFP-IBVS strains.** The present experiment demonstrates the utilisation of quantitative polymerase chain reaction (qPCR) for the analysis of the kinetics data. Specifically, the study focuses on comparing the genomic copy number of two strains of ILTV: the wild-type strain (ILTV-WT) and the recombinant strain (ILTV-GFP-IBVS). This comparison is conducted at different time intervals, while maintaining a multiplicity of infection (MOI) of 1.0. Data analysis is based on one experiment with three technical replicates.

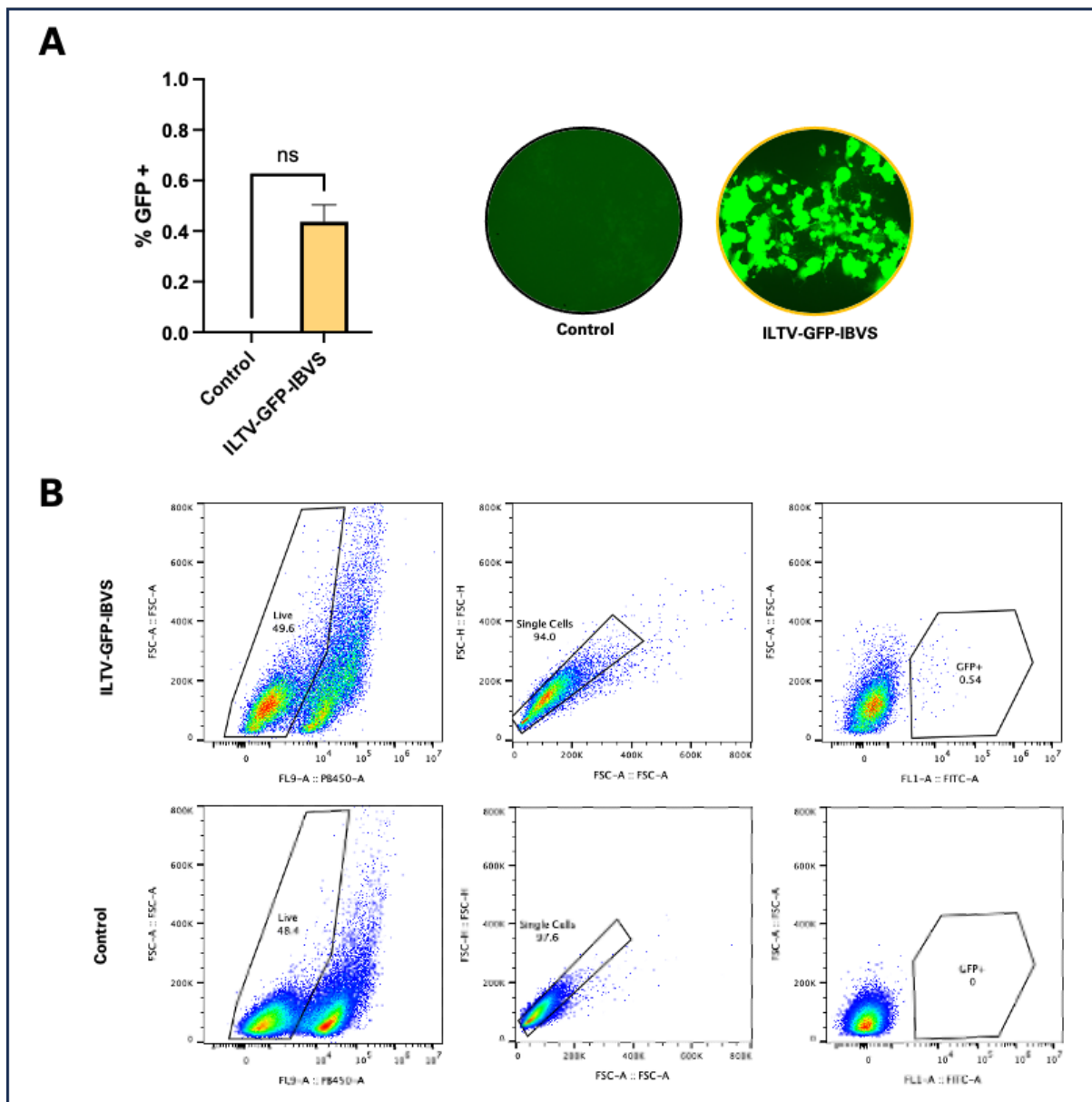


**Figure 7.6. Trend towards the increase in GFP positivity in LMH cells post-viral infection.** At the time point of 36 hours after infection, LMH cells were subjected to infection with the recombinant ILTV-GFP-IBVS strain. Following this, a flow cytometry analysis was performed to evaluate the infectivity of the recombinant ILTV by analysing the expression of GFP. **(A)** The diagram illustrates the percentage of cells expressing GFP in two different set-up, namely infected control cells and cells infected with recombinant ILTV-GFP-IBVS. In addition, the graph is accompanied by microscopic images that depict the expression of GFP in LMH cells that have been infected with the recombinant ILTV. **(B)** The information provided describes the gating methodology used to identify cells expressing GFP within the LMH cell population. The viral particles were labelled with GFP to enable fluorescence detection, while the viability of the cells was assessed using the live/dead staining technique. The gating procedure was performed using the FlowJo programme. Data analysis is based on one experiment with three technical replicates.



## 7.2.2. HA (H9N2) Gene of the Avian Influenza Virus

### 7.2.2.1. Cloning and Validation of Gene Cassettes

The donor plasmid pCDNA3-MCS1-mRFP, which was previously created and discussed in Chapter 4, was utilised to create donor plasmids that harbour the AIV-HA gene in MCS1. **Figure 7.7.A** illustrates a schematic depiction of the donor plasmid pCDNA3-MCS1-mRFP. PCR primers were specifically designed for the amplification of the AIV-HA gene, with the inclusion of *NheI* (5'-CTAGCTAGCCCACCATGGAGATTATCCCCCTGATGGC-3') and *KpnI* (5'-GCCGGTACCTCAGGTGCTATCCAGTCCCAGC-3') restriction enzyme recognition sites at the 5' and 3' ends, respectively (**Figure 7.7.B**). PCR was employed to perform positive amplification of the AIV-HA gene, resulting in the detection of a band with an estimated size of 1700 bp (**Figure 7.7.B**). In order to facilitate the insertion of the AIV-HA fragment into the multiple cloning site 1 (MCS1) of the recipient vector (pcDNA-MCS1-mRFP), both the AIV-HA insert and the recipient vector (pcDNA-MCS1-mRFP) underwent restriction enzyme digestion utilising the restriction enzymes *NheI* and *KpnI*. Subsequently, the use of DNA ligase facilitated the fusion of the AIV-HA insert and the recipient vector. The donor plasmid, pcDNA-HAH9N2-mRFP (**Figure 7.7.C**), obtained after ligation, was propagated by transformation into DH5 $\alpha$  competent *E. coli* cells. Positive colonies were then subjected to a purification process to obtain purified plasmid DNA for further examination using Sanger sequencing. The provided sequence alignment illustrates the similarity between the sequenced forward fragment of the cloned AIV-HA gene and the AIV reference genome. The Sanger sequencing outcome confirms a complete match of 100% identity between the reference genome AIV and pcDNA-HAH9n2-mRFP (shown in pink) for the forward fragment (**Figure 7.7.D**).

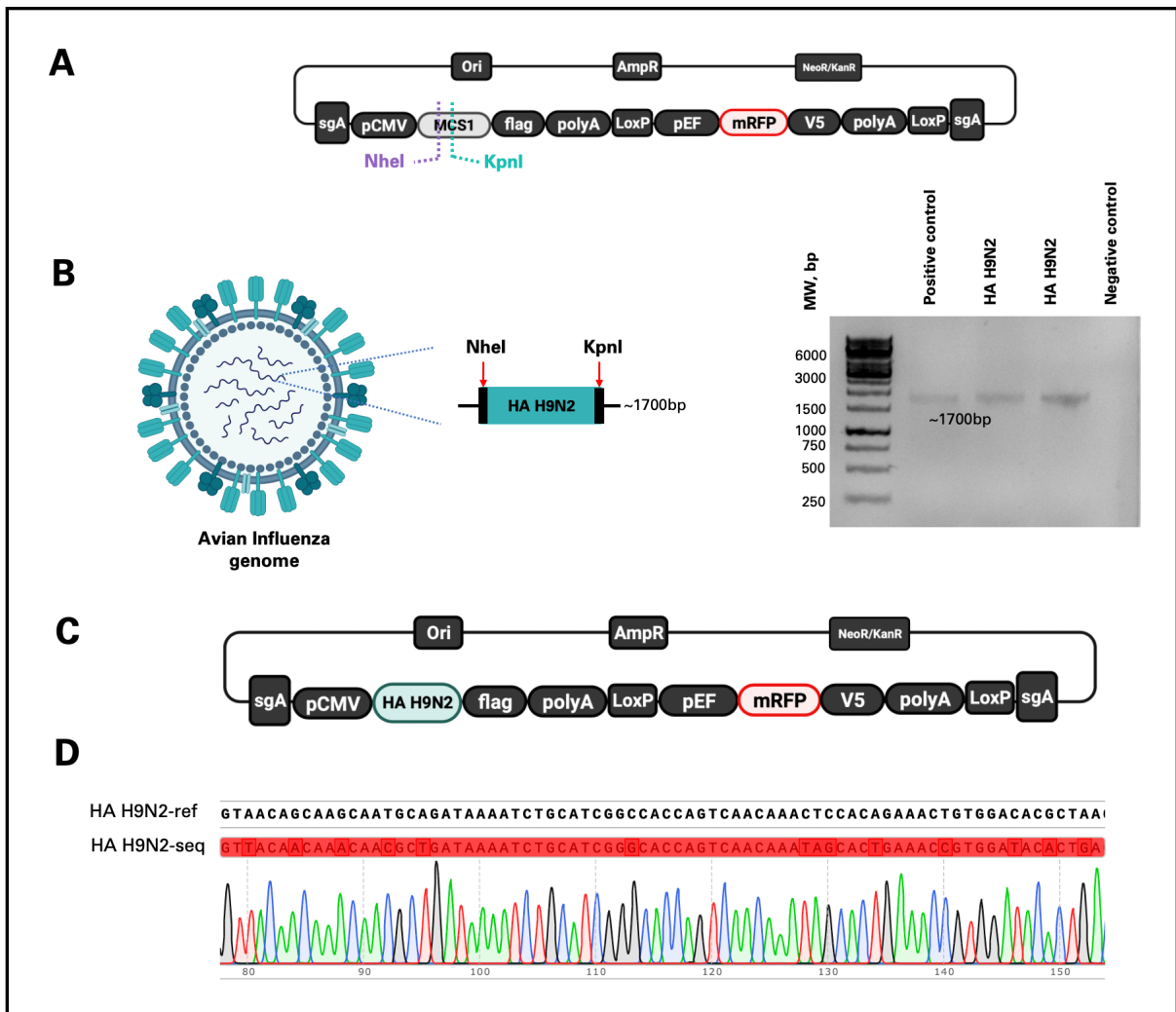


**Figure 7.7. Assembly and sequence validation of the recombinant donor plasmid pCDNA-HAH9N2-mRFP.** The successful insertion of the AIV-HA (H9N2) gene fragment was effectively achieved within the multiple cloning site 1 (MCS1) of the donor plasmid pcDNA-MCS1-mRFP. **(A)** The image presented depicts the donor plasmid, pcDNA-MCS1-mRFP, which possesses distinct recognition sites for the restriction enzymes *NheI* and *KpnI*. **(B)** The illustrative depiction shows the genome of Avian Influenza (AI). The primers were created with the particular purpose of amplifying the AIV-HA (H9N2) gene. These primers were constructed to include recognition sites for the *NheI* and *KpnI* restriction enzymes at the 5' and 3' ends, respectively. The gel electrophoresis image illustrates the amplified AIV-HA gene, with an approximate length of 1700 base pairs. The amplified gene segment of the HA gene and the donor plasmid pcDNA-MCS1-mRFP were successfully cloned by the process of restriction enzyme digestion, specifically employing *NheI* and *KpnI*. **(C)** The DNA ligation procedure was conducted to facilitate the fusion of the AIV-HA fragment with the recipient donor plasmid pcDNA-MCS1-mRFP, therefore generating the recombinant donor vector pcDNA-HAH9N2-mRFP. **(D)** The sequence alignment presented demonstrates the degree of similarity between the forward portion of the cloned AIV-HA gene and the reference Avian Influenza genome (NCBI Accession NC\_004908). The results of Sanger sequencing validate a perfect match of 100% similarity between the wild-type HA gene of the Avian Influenza (AI) and pcDNA-HAH9N2-mRFP (highlighted in red) for both the forward fragment.

#### 7.2.2.2. Generation of Recombinant ILTV Strains

The process of generating the recombinant ILTV with a cassette knock-in of the AIV-HA gene required the assembly of several components. The components utilised in this study encompassed three main elements. Firstly, the recombinant ILTV-GFP construct was used, which serves as a vector for expressing the GFP gene. Secondly, the donor plasmid pcDNA-HAH9N2-mRFP was employed, which contains the AIV-HA (H9N2) gene along with a reporter gene encoding mRFP. Lastly, the CRISPR/Cas9-sgRNA plasmids, specifically pX459v2-UL0, were utilised to induce double-strand breaks in the ILTV genome at the UL0 region.

The method encompasses two major constituents: the transfection of the donor plasmid (pcDNA-HAH9N2-mRFP) and the CRISPR/Cas9-sgRNA plasmid (pX459v2-UL0) into LMH cells (**Figure 7.8.A**). During the process of incubation, the accessory guide RNA A (pX459v2-sgRNA-A) will accurately recognise and cleave the specific sgRNA A site found in the donor plasmid. This action will lead to the release of the HAH9N2-mRFP gene cassette. After 36 hours of transfection, the LMH cells were infected with recombinant ILTV-GFP after the detection of red fluorescence by microscopic analysis (**Figure 7.8.B**). The CRISPR/Cas9-guideRNA (pX459v2-UL0) method is employed to facilitate the assessment of the ILTV genome and enable the targeted cleavage necessary for the insertion of the HAH9N2-mRFP gene cassette into the specified UL0 genomic region of the ILTV genome. As a result, this approach leads to non-homology targeting or non-homologous end joining. At the 24-hour time point subsequent to infection, LMH cells were subjected to microscopic analysis in order to evaluate the concurrent existence of the GFP protein, which emits green fluorescence, signifying the successful infection of the ILTV-GFP, and the presence of

the mRFP reporter gene within the gene cassette harboured by the donor plasmid pcDNA-HAH9N2-mRFP, which emits red fluorescence as depicted in **Figure 7.8.C**.

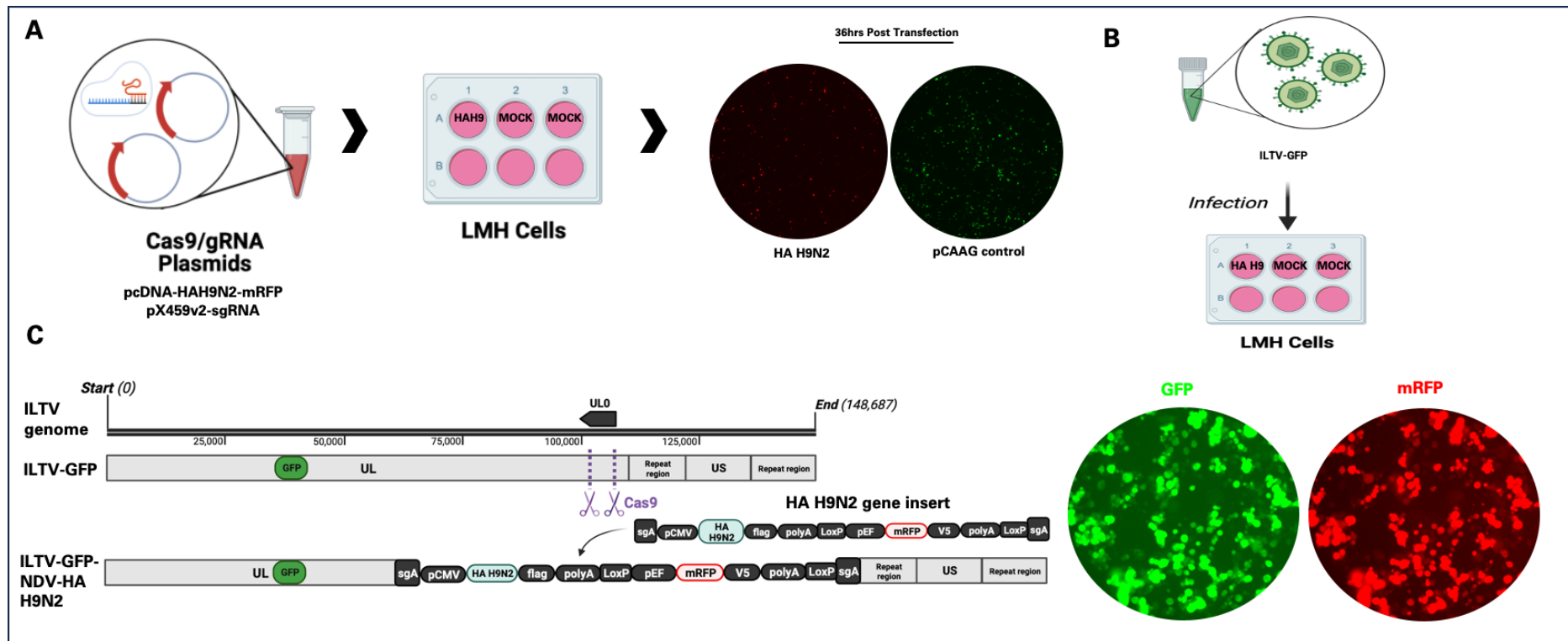


**Figure 7.8. Illustrative representation of the workflow used for the generation of recombinant ILTV-GFP-HA H9N2.** The methodology consists of two fundamental components: **(A)** The introduction of pX459v2-sgRNA plasmids (plasmids containing CRISPR/Cas9-sgRNA) and pcDNA3-HAH9N2-mRFP (donor plasmid) into LMH cells by transfection. At the 36-hour time point following transfection, a microscopic examination demonstrated the presence of red fluorescence, suggesting the successful identification of donor plasmids (pcDNA3-HAH9N2-mRFP) within LMH cells. **(B)** Subsequent to the detection of red fluorescence in LMH cells, the cells were further subjected to infection with ILTV-GFP. **(C)** At the 24-hour time period post-infection, the CRISPR/Cas9 enzyme initiates double-strand breaks at the UL0 region of the ILTV-GFP genome, leading to the incorporation of the AIV HA (H9N2) gene insert. The genetic modifications result in the production of the recombinant ILTV-GFP-HA H9N2, which demonstrates the presence of GFP and mRFP expression. The Zoe Fluorescent Cell Imager, manufactured by Biorad, was employed for image acquisition.

#### 7.2.2.2.1. Characterisation of the Recombinant ILTV-GFP-HAH9N2

Validation of the recombinant ILTV-GFP-HAH9N2 has been conducted through the use of several molecular and imaging techniques. The LMH cell line was subjected to infection through the use of the recombinant ILTV-GFP-HAH9N2 strains. The presence of the AIV-HA gene was originally evaluated by the use of primers that included the MCS1 region of the donor plasmid. The visual representation depicted in **Figure 7.9.A** offers empirical support for the presence of the AIV-HA gene fragment, which has a size of around 1.7 kilobases. The fragment was subjected to comparison with the HAH9N2-WT gene amplicon, which possesses an estimated size of 1.7 kb and functions as the designated positive control. A Western blot analysis was conducted to examine the presence of the AIV-HA protein. The detected molecular weight of the AIV-HA protein was around 70 kilodaltons. The results of the experiment illustrate the successful expression of AIV-HA protein, as seen in **Figure 7.9.B**. The subcellular distribution of the ILTV AIV-HA protein was confirmed using the results obtained from an immunofluorescence assay. The LMH cells on a 24-well plate were infected with the recombinant ILTV strain. At 36 hours following infection, the cells were subjected to fixation and subsequent labelling using anti-FLAG and Goat anti-Rabbit IgG (H+L) Cross-Adsorbed Secondary Antibody, Alexa Fluor 594 (red). The cellular location of the AIV-HA protein (red) within the cytoplasm and nucleus of the LMH cell is depicted in **Figure 7.9.C.**, as observed using confocal microscope imaging.

A study was done using a plaque assay to investigate the difference in viral quantity (PFU/mL) between the ILTV-GFP-HAH9N2 and the ILTV-WT. The t-test findings demonstrate a very significant difference in viral infectivity between the recombinant ILTV-GFP-HAH9N2 strain and the ILTV-WT strain, as seen in **Figure 7.10**. The

methodology employed for quantifying the viral amount is depicted adjacent to the graph, which showcases images of the wells containing the distinct plaques.

In order to investigate the functionality of the recombinant ILTV-GFP-HAH9N2 strain, an *in vitro* growth kinetics study was conducted using quantitative polymerase chain reaction (qPCR). The LMH cells were subjected to an infection induced by the recombinant ILTV-GFP-IBVS strain, with a multiplicity of infection (MOI) of 1.0. DNA extraction was performed at certain time points, namely at 6-, 12-, 24-, 48-, 72-, and 96-hours after infection (HPI). The graph depicts the general trend of viral copy number increase. The figure presented in **Figure 7.11** provides a visual representation of the notion being discussed.

The infectivity of the recombinant ILTV-GFP-HAH9N2 was further evaluated through the use of flow cytometry analysis. The LMH cell line was subjected to infection with the recombinant ILTV strain. Following this, the cells were fixed and underwent labelling 36 hours after infection. The analysis of the percentage of cells expressing GFP in both uninfected control cells and cells infected with recombinant ILTV demonstrates no statistically significant difference. However, there is an observable tendency towards a rise in GFP positivity in LMH cells following viral infection. **Figure 7.12.A** presents microscopic images that depict the production of GFP within LMH cells following infection with the recombinant ILTV. **Figure 7.12.B** illustrates the representative gating technique employed to identify GFP-positive cells within the LMH cell population. This approach outlines the strategy utilised for this purpose. The viral particles were labelled with GFP to enable fluorescence detection, while the viability of the cells was assessed using the live/dead staining technique.

Further cellular imaging analysis was done through the cytopathogenicity of Leghorn Male Hepatoma (LMH) cells to recombinant ILTV-GFP-HAH9N2 infection at 36 hours after infection. **Figure 7.13** shows the comparison of the infected and non-infected cells.



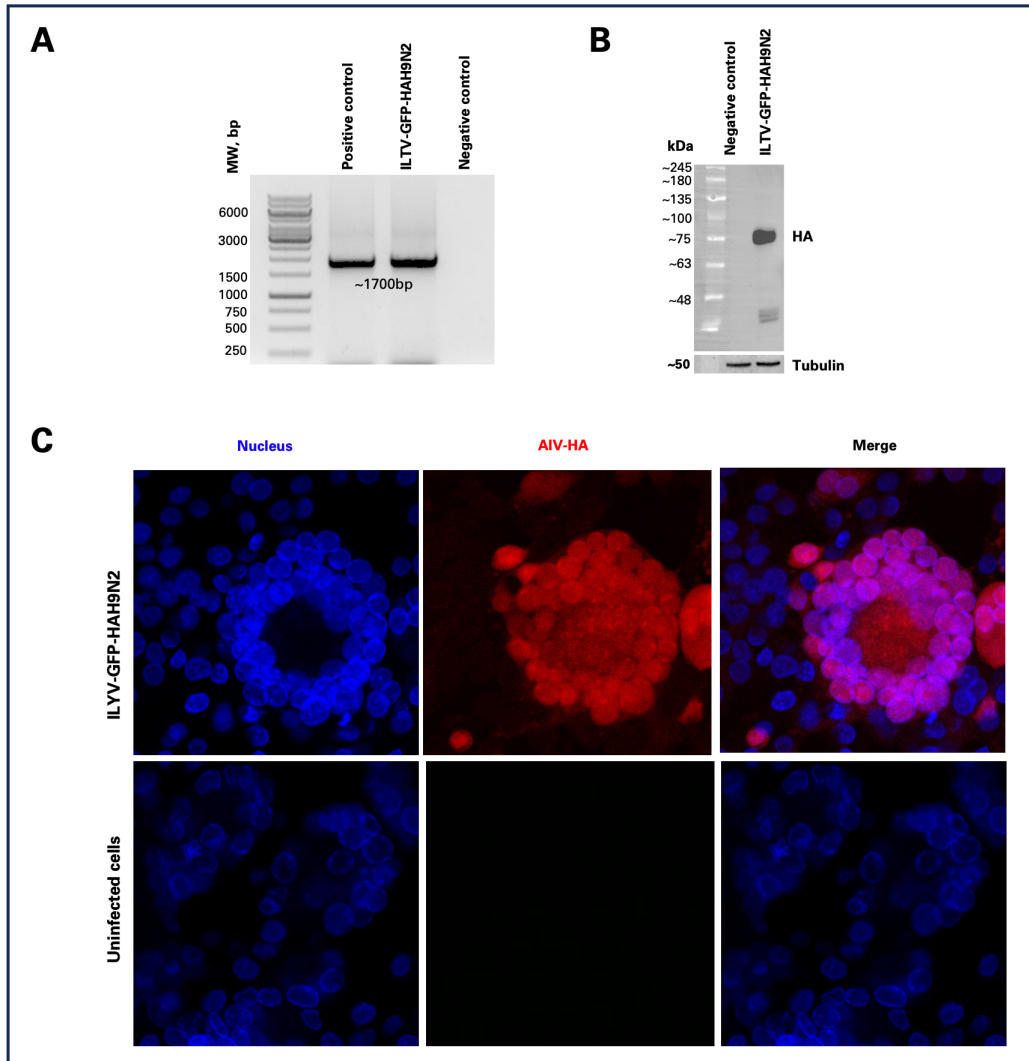


**Figure 7.9. AIV-HA is expressed at the molecular and protein-levels in LMH cells post-infection with the recombinant ILTV-GFP-HAH9N2 strain.** The LMH cell line was subjected to infection using the recombinant ILTV-GFP-HAH9N2 viral vector. **(A)** The gel electrophoresis depicts the amplification process using the primers CMV-MCS1-F (5'-AGAACCCACTGCTTACTGGCTT-3') and CMV-MCS1-R (5'-AACTAGAAGGCACAGTCGAGGC-3'). The primers are positioned on each side of the MCS1 region of the donor plasmid. The amplification of the AIV-HA (H9N2) gene yielded a DNA fragment with a length of about 1700 base pairs. In the present chapter, the samples were subjected to comparison with the HA-WT (~1.7 kb) gene, which was assigned the function of the positive control. **(B)** A Western blot analysis was performed to assess the expression of the AIV-HA (H9N2) protein. The detected molecular weight of the AIV-HA (H9N2) protein was determined to be approximately 70 kilodaltons (kDa). The findings of the investigation demonstrate the effective expression of the HA H9N2 protein. **(C)** Confluent LMH cells were exposed to infection with the recombinant ILTV-GFP-HAH9N2, thereafter undergoing staining to ascertain the presence of the AIV-HA (H9N2) protein. The confocal microscopy images displayed in Figure C illustrate the subcellular distribution of the AIV-HA (H9N2) (red) protein throughout the cytoplasm and nucleus of the LMH cells. Uninfected cells served as negative control.

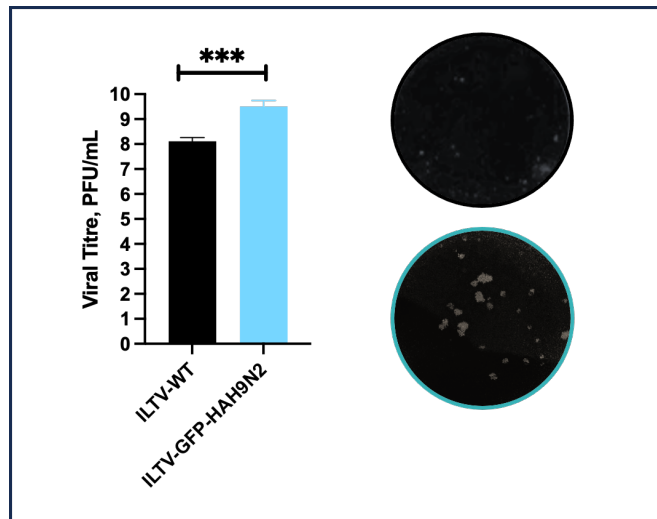


**Figure 7.10. The viral infectivity of the recombinant ILTV-GFP-HAH9N2 strain is significantly different from that of ILTV-WT. (A)** Plaque assay-based quantification of the infectious virus between the ILTV-WT and recombinant ILTV-GFP-HAH9N2 strains. The results obtained from the plaque assay-based study indicate that there is a strong statistically significant difference in viral infectivity between the recombinant ILTV-GFP-HAH9N2 strain and the ILTV-WT. Plaque images show the individual plaque-forming units used to compute the final viral concentration. These data represent the average of three technical replicates, with SD. indicated. ns: non-significant  $p > 0.05$ , \* $p < 0.05$ , \*\*\* $p < 0.001$  using the student's t-test.

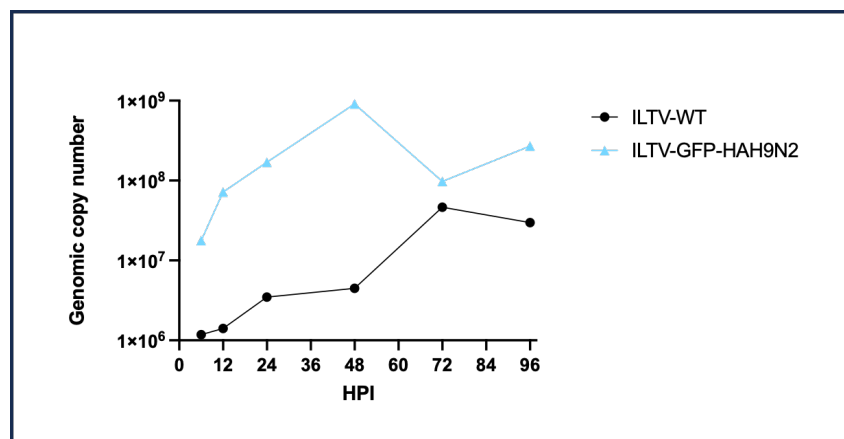


**Figure 7.11. Comparison of the replication kinetics of the ILTV-WT and recombinant ILTV-GFP-HAH9N2 strains.** The quantitative polymerase chain reaction (qPCR) data analysis presented here illustrates the comparison of genomic copy numbers between the ILTV-WT and the recombinant ILTV-GFP-HAH9N2 at various time periods, with a multiplicity of infection (MOI) of 1.0. Data analysis is based on one experiment with three technical replicates.

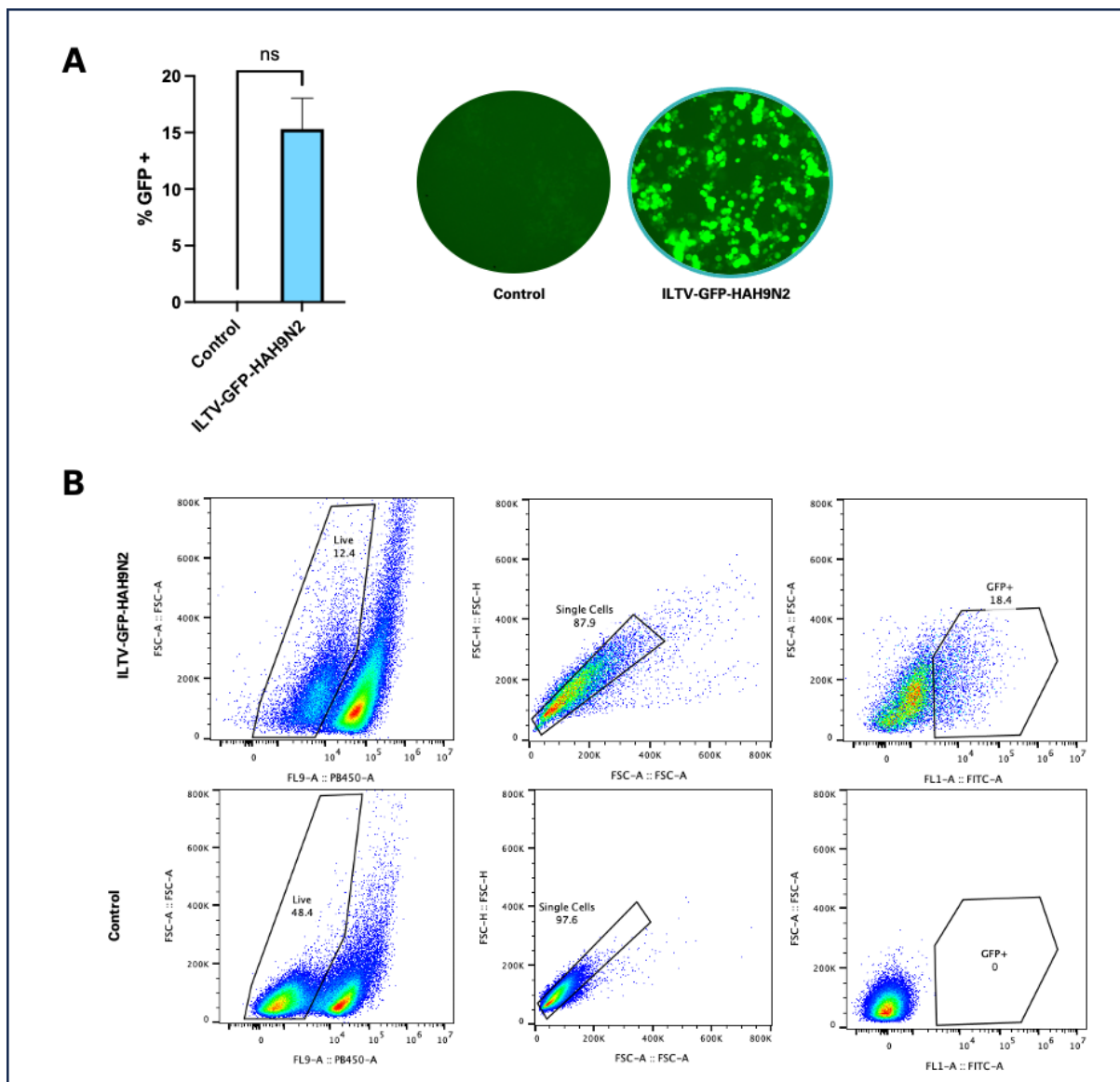


**Figure 7.12. Trend towards an increase in GFP positivity in LMH cells post-viral infection.** At 36 hours post-infection, LMH cells were infected with a recombinant ILTV-GFP-HAH9N2 strain. Subsequently, a flow cytometry study was conducted to assess the infectivity of the recombinant ILTVs by evaluating the expression of GFP. **(A)** The figure presents a graphical depiction of the percentage of GFP-positive cells in both uninfected control cells and cells infected with recombinant ILTV-GFP-HAH9N2. Additionally, accompanying the graph are microscopic pictures illustrating the expression of GFP in LMH cells infected with the recombinant ILTV. **(B)** The provided information represents the gating approach employed for the identification of GFP-positive cells in the LMH cell population. The viral particles were fluorescently marked with GFP, while the viability of the cells was determined using the live/dead staining kit. The process of gating was conducted via the FlowJo software. Data analysis is based on one experiment with three technical replicates.

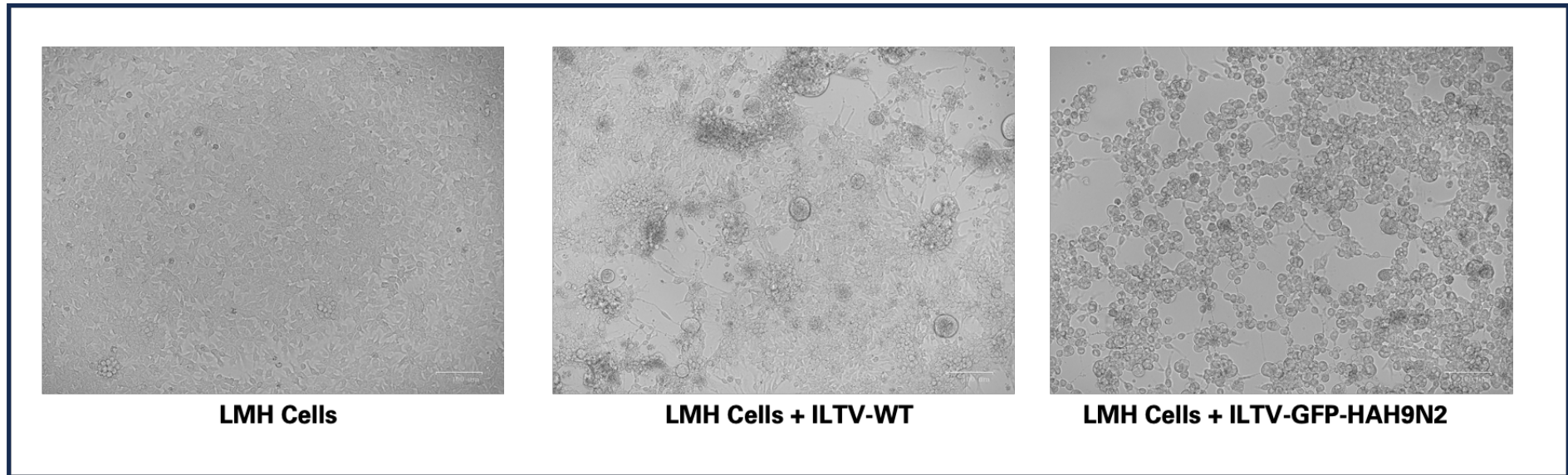


**Figure 7.13. The cytopathogenicity of Leghorn Male Hepatoma (LMH) Cells.** The cytopathogenicity of Leghorn Male Hepatoma (LMH) cells was evaluated in relation to the infection of recombinant ILTV-GFP-HAH9N2 at a post-infection time point of 36 hours. The images provide a comparative analysis between LMH cells and LMH cells that have been infected with ILTV-WT and the recombinant ILTV-GFP-HAH9N2. The Zoe Fluorescent Cell Imager, manufactured by Biorad, was employed for image acquisition.

## 7.3. Chapter Discussion

This chapter offers a comprehensive analysis of the efficacy of CRISPR/Cas9 gene editing technology in the creation of recombinant ILTV vaccine vectors. These vectors contain antigen gene fragments derived from the S gene of the IBV and the HA gene (H9N2) of the AIV (Legnardi et al., 2020; Wilks et al., 2012).

The main aim of this chapter is to provide more evidence on the efficacy and efficiency of the CRISPR/Cas9 gene editing technology that has been established, specifically in generating recombinant viral vectors for addressing economically important avian diseases.

In order to assess and empirically verify the efficacy of CRISPR/Cas9 in generating recombinant ILTV viral vectors containing the S gene of IBV and the HA H9N2 gene of AIV, we designed guide RNAs that exhibit specificity to selectively target and cleave the UL0 region of the ILTV genome. This process leads to the deliberate insertion of the IBV-S and AIV-HA (H9N2) gene inserts through a targeted, non-homologous mechanism. According to a study conducted by Veits et al. (2003), it has been demonstrated that the UL0 region of the ILTV does not play a crucial role in viral replication (Veits et al., 2003). Thus, we hypothesised that the recombinant ILTV strains created through the knockout of the UL0 region of the ILTV genome will behave and perform similarly to the ILTV wild type. The recombinant ILTV-GFP-IBVS and ILTV-GFP-HAH9N2 viral vectors were generated. Analysis at the molecular and protein levels of the recombinant strains ILTV-GFP-IBVS and ILTV-GFP-HAH9N2 provided evidence of successful integration of the IBVS and HAH9N2 genes into the UL0 region of the ILTV genome. Demonstrating the efficacy of the CRISPR/Cas9 gene

editing methodology. Furthermore, the expression of the S and HA proteins was validated using protein expression analysis and imaging methods.

To assess the presence of sub-lethal abnormalities, a comparative analysis was conducted on the plaque formation and growth kinetics of two recombinant strains, ILTV-GFP-IBVS and ILTV-GFP-HAH9N2, in comparison to the ILTV wild-type strain. The findings derived from the study utilising the plaque assay method indicate that the maximum viral titres of both the ILTV wild-type and the recombinant ILTV-GFP-IBVS virus are highly comparable, measuring at  $1.3 \times 10^8$  and  $4.0 \times 10^6$ , respectively. A notable difference in the quantification of infectious virus has been observed between ILTV-WT and ILTV-GFP-IBVS, as determined by plaque assay. The infectivity of the recombinant ILTV-GFP-IBVS appears to be lower in comparison to that of the ILTV wild-type. One potential explanation for this behaviour might be attributed to the size of the foreign DNA, which, in the instance of IBV-S, is estimated to be around 3.4 kilobases (kb). The preceding chapters have provided evidence to support the notion that the genome of the herpesvirus has flexibility, enabling it to tolerate substantial quantities of foreign gene inserts (N. Tang et al., 2019). However, the increase of transgene size often results in genetic instability and a decline in viral productivity throughout the process of production (Holman et al., 2009). On the other hand, it was shown that the maximum viral titre of ILTV-GFP-HAH9N2 ( $3.2 \times 10^9$ ) was significantly higher in comparison to the ILTV wild type ( $1.3 \times 10^8$ ), showing that the recombinant ILTV with AIV-HA (H9N2) is performing better than the ILTV wild type. The validity of this assumption was further supported by the implementation of kinetics research utilising quantitative polymerase chain reaction (qPCR) technology. By 48 hours post-infection (hpi), the replication of the recombinant ILTV-GFP-IBVS in LMH cells resulted

in a maximum genomic copy number of  $5.3 \times 10^7$ . In comparison, the recombinant ILTV-GFP-HAH9N2 obtained a maximum genomic copy number of  $4.1 \times 10^8$  by the same time point, again higher than the ILTV wild-type genomic copy number of  $4.4 \times 10^6$ . The results of this work have validated the similarity between the recombinant ILTVs containing IBVS and HAH9N2 inserts and prior *in vitro* investigations on the ILTV replication cycle (Bagust & Johnson, 1995; Prideaux et al., 1992). The recombinant ILTV strains were sequentially passaged for five times for genetic stability analysis. There was no observed variation in the size and quantity of the IBV-S and AIV-HA (H9N2) gene product after five passages of the virus in cultured LMH cells, suggesting that the IBV-S and AIV-HA (H9N2) gene incorporated into the ILTV genome remained stable following previous observations in other herpesvirus-based recombinant viral vectors (Abozeid et al., 2019; X. Pan et al., 2023; N. Tang et al., 2020). Hence, no empirical support was found to substantiate the presence of non-lethal abnormalities resulting from the integration of the IBV-S or AIV-HA (H9N2) gene into the UL0 region of the ILTV genome.

In order to gain a deeper understanding of the behaviour of the recombinant ILTV viral vector strains, an analysis based on cytopathogenicity was conducted. The present investigation revealed noteworthy observations regarding the behaviour shown by the LMH cells infected with ILTV-GFP-HAH9N2. At the 36-hour time point following infection, microscopic examination revealed cytoplasmic shrinkage and condensation, resulting in apoptosis of LMH cells that were infected with the recombinant ILTV containing the HA gene insert in comparison to LMH cells infected with ILTV-WT. This phenomenon is also evident in the immunofluorescence assay (IFA) images, whereby there is a notable reduction in the size of the cytoplasm of the LMH cells, accompanied

by the predominant localisation of the HA protein within the nucleus. The behaviour in question has been previously documented to be associated with AIV infection (Fesq et al., 1994; Hinshaw et al., 1994; Mori et al., 1995; Takizawa et al., 1993). It is evident that the recombinant ILTV, although just containing the HA particle of the AIV, displays a possible direct influence on the induction of apoptosis in LMH cells that are infected. The aforementioned phenomenon has been previously documented, indicating that some viral proteins have the ability to directly regulate apoptosis. Nevertheless, the precise mechanism of this process remains unclear (Schultz-Cherry et al., 2001).

Previous studies have proven the efficiency of the CRISPR/Cas9 strategy in the development of herpesvirus-based viral vectors. A CRISPR/Cas9 HVT-based recombinant viral vector carrying the H9N2 of Avian Influenza was created. Liu et al., (2019) showed that there were no discernible differences seen between the recombinant rHVT-H9 and the wild-type HVT in terms of plaque morphology and viral replication kinetics (L. Liu et al., 2019). Which was also in agreement with our results. Moreover, the administration of rHVT-H9 has been shown to elicit strong humoral and cellular immune responses in avian species. The findings indicate that the administration of rHVT-H9 is efficacious in safeguarding chickens against the H9N2 AIV (L. Liu et al., 2019). This observation prompts us to develop the hypothesis that the *in vitro* behaviour of recombinant ILTV viral vector strains may correspond to the immunological response observed *in vivo*, as demonstrated in prior literature (L. Liu et al., 2019). Furthermore, the studies conducted by Tang et al., (2020) effectively utilised CRISPR/Cas9 in generating a recombinant HVT with triple insertion of foreign genic antigens ILTV gDgl, AIV H9HA, and IBDV VP2 (N. Tang et al., 2018, 2020). The observation showed that recombinant viruses with three foreign gene insertions



exhibited comparable growth to the wild-type virus, providing additional evidence supporting the stability of the recombinant viral vector.

Collectively, the final part of this research successfully demonstrated and empirically confirmed the ability of ILTV to carry antigens from other economically significant avian viruses, such as the S gene from the IBV and the HA H9N2 gene from the AIV. This enabled the development of a potential recombinant ILTV vaccine vector. This chapter further presented comprehensive data about the versatility and effectiveness of the CRISPR/Cas9 workflow in the integration of foreign genes into a recombinant viral vector, as well as the capability to monitor the viral vector using fluorescent markers. In this chapter, we have examined a potential method by which the AIV-HA protein particle could induce cellular death and apoptosis. A thorough understanding of the molecular processes and regulatory networks through which Influenza A viruses (IAVs) elicit cellular death might potentially enhance the generation of more efficacious antiviral therapies.

# CHAPTER 8

## General Discussion

To date, vaccinations continue to serve as the predominant method for disease prevention in the poultry industry through the implementation of immunisation regimens (Chambers et al., 2016; Vilela et al., 2020). Given the ongoing arms race against rapidly changing viruses, there is an urgent unmet need for novel advancements in vaccine research to effectively combat the emergence and re-emergence of new viral strains (S. Khan et al., 2016; Nadeem et al., 2020; Swayne et al., 2013; Vilela et al., 2020). Recombinant viral vaccine vectors have been essential in the advancement of novel vaccine development (Kamel & El-Sayed, 2019). Advantages over conventional vaccine strategies encompass not only the ability to transport foreign genes to target cells with a higher degree of specificity and efficiency but also the capacity to induce strong immune responses and enhance cellular immunity (Ewer et al., 2016; Kamel & El-Sayed, 2019; Schultz & Chamberlain, 2008). Advances in pathogen biology and recombinant DNA technology are laying the foundations for providing novel approaches to overcome the problems encountered with conventional vaccine design (Khan et al., 2016; Nadeem et al., 2020). Most recently, CRISPR/Cas9 genome editing technology has been utilised for the development of novel recombinant viral vectors (Vilela et al., 2020; D. Wang et al., 2018). The CRISPR/Cas9 genome editing technique paved a platform that will enable the advancement of the field of vaccine development. Therefore, the overarching aim of this PhD was to develop a recombinant herpesvirus-based viral vector using the CRISPR/Cas9 genome editing technology.

The key aims were to:

1. Identify potential antigenic proteins and epitopes for vaccine design and profile the existing field strains of NDV, IBV, and AIV in the Philippines through *in silico*-based techniques.
2. Provide comprehensive characterisation of the herpesvirus-based viral vector (ILTV) and proof-of-concept validation of the suitability of CRISPR/Cas9 genome editing technology through knock-in and knockout experiments.
3. Demonstrate the effectiveness of CRISPR/Cas9 genome editing technology to create a herpesvirus-based viral vector carrying foreign genes fused with adjuvants.
4. Demonstrate the effectiveness of CRISPR/Cas9 genome editing technology to create a herpesvirus-based multivalent viral vector.
5. Demonstrate the effectiveness and flexibility of the CRISPR/Cas9 gene editing system in combination with a herpesvirus-based viral vector for the development of candidate vaccines against various poultry diseases that hold significant economic importance.

## 8.1. Overview of Thesis Findings

In **Chapter 3**, we were able to identify potential antigenic proteins and epitopes that may be utilised for the creation of putative vaccine candidates or serological tests through the application of *in silico* approaches (Can, Köseoğlu, et al., 2020; Dangi et al., 2018; Parvizpour et al., 2020). Additionally, through molecular pathotyping, we were able to identify the genotypic profile of the key antigens of circulating field strains of NDV (i.e., F and HN), IBV (S), and AIV H9N2 (HA) in the Philippines.

In **Chapter 4**, we have generated the following important findings: (1) a versatile and flexible donor plasmid encoding two multiple cloning sites, allowing simultaneous insertion of multiple genes (Atasoy et al., 2019); (2) an approach to visualising the virus and qualitative selection of recombinant viruses. This system provides a fast-screening method when selecting a putative recombinant virus; and (3) successful proof-of-concept knock-in and knockout experiments utilising the CRISPR/Cas9 gene editing technology. We were able to prove that the CRISPR/Cas9 technology can effectively cleave specific regions of the ILTV genome for the facilitation of either the integration of desired gene cassettes or gene knockout. Furthermore, we were able to screen the ILTV genome for regions viable for gene insertion (Lüschoew et al., 2001; Mahmoudian et al., 2012; Veits et al., 2003). Providing the necessary baseline data for the succeeding chapters.

Vaccines based on the herpesvirus have been the subject of extensive research in the past (Kamel & El-Sayed, 2019). We endeavoured to formulate a novel approach to vaccine development by integrating critical components of vaccine design: (1) an antigenic gene cassette containing the F gene of NDV fused with immune enhancers

(Fc and Foldon); (2) recombinant ILTV tagged with a GFP marker; and (3) the cutting-edge genome editing technology, CRISPR/Cas9. By utilising these components, we have generated ILTV-based recombinant viral vector strains that exhibit comparable or, in certain instances, enhanced performance in comparison to the ILTV wild-type. The findings from our viral infectivity assays have yielded valuable insights into the capacity of the ILTV genome to accommodate substantial foreign gene insertion, highlighting its elasticity and flexibility. **Chapter 5** presented findings about the *in vitro* predictive behaviour of the recombinant ILTV-NDVF variants.

The primary emphasis of **Chapter 6** is to further advance our understanding of recombinant viral vectors and integrate our previous results into ultimately creating a multivalent vaccine vector harbouring two or more foreign genes (Spier, 1997; N. Tang et al., 2020). Our molecular and protein level results showed a successful integration and expression of the two NDV genes, F and HN, into the ILTV genome. Furthermore, we have assessed the effectiveness of the candidate recombinant vaccine vectors through serological and molecular analysis. Our results showed enhanced immunity conferred by the recombinant ILTV strains against a highly pathogenic strain of NDV *in vivo*.

Finally, **Chapter 7** offers a comprehensive analysis of the efficacy of the strategy we have devised throughout this whole research endeavour, specifically in generating recombinant viral vectors for addressing economically important avian diseases such as IBV and AIV (Atasoy et al., 2019; Legnardi et al., 2020; L. Liu et al., 2019). The findings of our study demonstrate significant achievements in utilising our own CRISPR/Cas9 approach to generate recombinant ILTV strains. This is evidenced by

the successful manipulation of the ILTV genome and the subsequent observation of recombinant viral production over several passages. The stability findings shown in our study provide additional confirmation of the appropriateness of ILTV as a potential recombinant vaccine vector.

The objective of this chapter is to compile and consolidate all the findings obtained from the preceding chapters that presented the results. This synthesis has the potential to yield both valid conclusions and potential inquiries that may be addressed in further research.

## **8.2. CRISPR/Cas9 Gene Editing Technology as a Tool in the Development of Novel Avian Recombinant Vaccine Vectors**

The use of the CRISPR/Cas9 system in the field of virology research has experienced a substantial rise over the past decade, as evidenced by the findings of Teng et al. (2021). Although several recombinant vaccine vectors have been produced through CRISPR/Cas9 gene editing technology, it is worth noting that there is a lack of information demonstrating the effectiveness of this approach in the production of poultry viral vector vaccines. In **Chapter 4**, our study aimed to establish baseline data on the behaviour of CRISPR/Cas9 *in vitro*. This was done with the intention of conducting gene knock-in and gene knockout studies.

The outcomes of our knock-in experiments demonstrated the efficacy of the CRISPR/Cas9 genome editing technique in precisely screening specific regions of the ILTV genome and inducing the required cleavage, thereby facilitating the integration of foreign gene cassettes into the ILTV genome at UL0, UL50, and US4 regions.

Consequently, this process resulted in non-homology targeting or non-homologous end joining (**Chapter 4, Section 4.3.3**). The stability of the recombinant ILTV strains generated using this approach was evaluated *in vitro*. **Chapters 5, 6, and 7** demonstrate that comparable outcomes were achieved when employing CRISPR/Cas9 for the development of recombinant ILTV strains.

In the same way, the outcomes of our knockout experiment provided confirmation of the deliberate disruption of the ILTV ICP4 gene, resulting in a noteworthy decrease in ILTV viral replication (**Chapter 4, Section 4.3.4**).

### **8.3. ILTV as a Candidate Viral Vector in the Development of Novel Avian Recombinant Vaccine Vectors**

It is worth noting that the genome of ILTV consists of diverse sections that have been identified as non-essential for viral replication, along with genomic regions that have the potential to induce attenuation, as demonstrated in **Chapter 4**. The recombinant strains of ILTV that have been generated in this study have been attenuated by modifying the Thymidine Kinase (TK) area. Additionally, our findings indicate that the UL0, UL50, and US4 regions of ILTV are not crucial for replication, suggesting that they might serve as sites for inserting foreign genes (**Chapters 4, 5, 6, and 7**).

Moreover, we successfully demonstrated the efficacy of the recombinant viral vaccine vector based on the ILTV through serological tests. This recombinant ILTV vaccine vector exhibited the ability to provide heightened immunity against a particularly virulent strain of NDV in an *in vivo* setting (**Chapter 6, Section 6.2.4.1**).

It is important to highlight that several instances within this research investigation revealed the superior performance of recombinant ILTV strains in comparison to wild-type ILTV. This discovery prompts further inquiry into the intricate interplay between the genomic regions of ILTV and the host-virus interaction in an *in vitro* setting.

#### **8.4. Immunoenhancement of the Recombinant Viral Vector through the Addition of Enhancers or Adjuvants**

Antigens are essential components for the development of effective vaccines, which is also true in the development of recombinant viral vector vaccines. In **Chapter 5**, we have developed a strategy to putatively enhance the immune response of the recombinant ILTV strain through the fusion of known adjuvants or enhancers, Foldon and IgY Fc, with the F gene of the NDV (**Chapter 5**).

As demonstrated through our results, the integration of Foldon and IgY Fc into the NDV-F gene cassette, followed by the successful expression of these gene variants using the recombinant ILTV viral vectors, provides us with fundamental insights into the *in vitro* behaviour of these potential recombinant viral vectors.

Additionally, our findings indicate that the ILTV-GFP-NDVF-Fc strain had a greater degree of infectivity, improved replication kinetics, and better viral cell-to-cell spread. This finding, however innovative, has also prompted inquiries into the underlying mechanism of this occurrence.



## **8.5. ILTV as a Potential Multivalent or Polyvalent Broad-Spectrum Recombinant Viral Vector**

In **Chapter 6**, our objective was to construct a recombinant multivalent viral vector using ILTV as the backbone. As demonstrated in **Chapter 4**, it has been established that the genome of ILTV features numerous regions that are favourable for the insertion of foreign genes. This finding has led us to hypothesise that it is possible to introduce more than two NDV glycoproteins, specifically F and HN, into the ILTV genome. Our hypothesis postulated that the integration of the NDV-F and -HN into a single recombinant viral vector would provide more favourable outcomes in comparison to the separate delivery of each component.

A potential multivalent recombinant ILTV vaccine vector against NDV has been produced by modifying the ILTV regions TK (GFP insertion region), UL0 (HN insertion region), and US4 (F insertion region) (**Chapter 6, Section 6.2.3**). The findings of our study indicate that the NDV-F and -HN inserts were consistently present and expressed throughout the fifth passage. The recombinant ILTV harbouring the three modifications exhibited comparable or perhaps superior performance in comparison to the ILTV wild type. Through this result, we were able to confirm the potential of ILTV as a multivalent recombinant viral vector.

## **8.6. ILTV as a Potential Multivalent or Polyvalent Recombinant Viral Vector Against Economically Important Avian Diseases**

After successfully demonstrating the efficacy of our CRISPR/Cas9-based approach in the generation of stable recombinant ILTV-based viral vectors, we proceeded to

generate recombinant ILTV strains harbouring gene inserts derived from AIV and IBV (**Chapter 7**). The findings of our study align with the previous chapters, indicating that the recombinant ILTV strains exhibit stability and equivalent performance to the wild-type ILTV.

## **8.7. Future Work**

Throughout the conduct of this PhD, we have provided preliminary data that can be utilised for future research. This includes (1) a recombinant ILTV strain that can serve as a potential reference point for the creation of a rapid, high-throughput approach for infectious virus titration and GFP-based flow cytometry antiviral assays, and (2) the investigation employing the CRISPR/Cas9 system to gain a more comprehensive understanding of the molecular mechanisms through which a viral protein modulates apoptosis and other cellular responses that are linked to the process of infection.

Furthermore, in the last phase of our investigation, we carried out *in vivo* experiments to comprehensively evaluate the effectiveness of the recombinant ILTV vaccine vector strains. Nevertheless, the logistical challenges associated with conducting animal testing on all six recombinant ILTV vaccine vector strains developed in the context of this PhD study are evident.

Finally, it is our aspiration to create a unique recombinant strain of ILTV that incorporates the F gene of NDV, the HA gene of AIV, and the S gene of IBV. In future *in vivo* experiments, we expect to acquire significant information that will contribute to the development of a comprehensive vaccination strategy capable of protecting poultry against multiple viral infections using a single dose.

# CHAPTER 9

## Appendices

### Annex 1. NDV, IBV, and AIV reference sequence and genotypes.

NDV Isolate (F)	Genotype	Accession number
Tyva_14	I	KX352834
NIE08_121	I	HG326605
Ishi	I	AB465607
Lasota	II	AF077761
TX_GB	II	GU978777
Hitchner_B1	II	JN872151
Mukteswar	III	EF201805
SPVC_Karachi_1	III	GU182327
Novo_Selo_1161	III	MH996904
Herts	IV	AY741404
Plovdiv_1153	IV	MH996900
Coast_8278	V	JN872189
498109_15	V	JN872194
Estado_de_Mexico_466	V	EU518684
Ningxia_2068	VI	MG840654.1
sms12	VI	JX094510
PA_810	VI	JX901367
B2_Isiolo	VI	JX518532

100	VI	JX244794
TX_209682	VI	JN872180
S_1	VI	FJ865434
152608_ancestral	VII	JN986837
Behshahr	VII	KX268351
A7	VII	AY028995
Trenque_Lauquen	VIII	AY734534
AF2240	VIII	JX012096
ZJ_1	IX	FJ436303
FJ_1	IX	AF458009
99_376	X	FJ705466
ndv42_AI09_4117	X	KX857716
MGMNJ	XI	JX518882
MG_725	XI	HQ266602
Apurimac_50009	XII	KU594615
GD_12	XII	JN627504
Polashbari	XIII	KT734767
SPVC_Karachi_43	XIII	GU182323
EMM_7	XIII	JQ267579
47385_11	XIII	JN942043
NIE08_453	XIV	HF969187
VIR_1377_7	XIV	JN872165
28138_4	XVI	JX915242
Queretaro_452_1947	XVI	JX915243
NIE10_310	XVII	HF969176

NIE08_2199	XVII	HF969194
ML57051T	XVIII	JX518885
CIV08_42	XVIII	HF969218
WI_272409	XIX	JN942024
MN_92_40140	XIX	FJ705456
88_M	XX	KY042142
ZhJ_2	XX	AF458016
Vladimir_687	XXI	JF824032
Jallo_Lahore_221B	XXI	KY042141
10VIR7155	XXI	KU377533
ETHMG1C	XXI	KC205479

<b>NDV Strain (HN)</b>	<b>Genotype</b>	<b>Accession number</b>
Chicken/Guizhou/1032/2012	VII	KT760568
Goose/Yunnan/1200/2013	VII	KT760569
Chicken/Yunnan/1027/2016	VII	KX765879
Egret/China/Guangxi/2011	VII	JX193074
Turkey/South_Africa/N2057/2013	VII	KR815908
I-2	I	AY935499
La_Sota	II	AF077761
Mukteswar	III	EF201805
Herts/33	IV	AY741404
Anhinga/U.S.(FI)/44083/93	V	AY288989
Pigeon/China/SDLC/2011	VI	JQ979176
QH1	VIII	FJ751918

F48E8	IX	AF163440
Mallard/US(MN)/MN00-39/2000	X	GQ288392
MG_1992	XI	HQ266603
NDV/peacock/Peru/2011	XII	KR732614
JKT1997	XIII	JX393313
Mali_ML029_07	XIV	JF966386
Chicken/Dominican Republic (Juan-Lopez)/499-31/2008	XVI	JX119193
Duck/Nigeria/903/KUDU-113/1992	XVII	KU058680
2009_Mali_ML008	XVIII	JF966387

<b>Virus Name (S)</b>	<b>Genotype</b>	<b>Accession number</b>
Infectious bronchitis virus strain H12	GI-1	FJ888351
Avian infectious bronchitis virus strain M41	GI-1	AY561711
Infectious bronchitis virus serotype Holte	GI-2	GU393336
Infectious bronchitis virus strain SDW	GI-2	DQ070840
Avian infectious bronchitis virus (clone G13-1)	GI-3	L14069
Avian infectious bronchitis virus (clone J2)	GI-3	L14070
Avian infectious bronchitis virus surface glycoprotein Holte USA	GI-4	L18988
Avian infectious bronchitis virus isolate GX2-98	GI-4	AY251816
Infectious bronchitis virus strain V2-02	GI-5	DQ490215
Avian infectious bronchitis virus strain Vic S	GI-5	U29519
Infectious bronchitis virus strain J9	GI-6	DQ515802
Avian infectious bronchitis virus isolate TP/64	GI-7	AY606320

Infectious bronchitis virus isolate TW2575/98	GI-7	DQ646405
Avian infectious bronchitis virus (strain SE 17)	GI-8	M99484
Infectious bronchitis virus Ark DPI	GI-9	AF006624
Infectious bronchitis virus strain CAL99	GI-9	DQ912831
Avian infectious bronchitis virus strain K87	GI-10	AF151959
Avian infectious bronchitis virus strain T6	GI-10	AF151960
Infectious bronchitis virus isolate IBV/Brasil/351/1984	GI-11	GU393339
Infectious bronchitis virus isolate UFMG/1141	GI-11	JX182783
Infectious bronchitis virus D3896	GI-12	X52084
Infectious bronchitis virus D274	GI-12	X15832
Avian infectious bronchitis virus UK/7/91	GI-13	Z83975
Infectious bronchitis virus isolate Moroccan- G/83	GI-13	EU914938
Infectious bronchitis virus Belgian isolate B1648	GI-14	X87238
Infectious bronchitis virus strain NGA/324/2006	GI-14	FN182277
Infectious bronchitis virus isolate B4	GI-15	FJ807932
Infectious bronchitis virus isolate K620/02	GI-15	FJ807944
Avian infectious bronchitis virus isolate Q1	GI-16	AF286302
Infectious bronchitis virus strain IZO 28/86	GI-16	KJ941019
Avian infectious bronchitis virus isolate AL/6609/98	GI-17	AF510656
Avian infectious bronchitis virus CV-56b	GI-17	AF027509
Avian infectious bronchitis virus strain JP8127	GI-18	AY296744
Infectious bronchitis virus isolate 53XJ-99II	GI-18	KC577391

Infectious bronchitis virus QXIBV	GI-19	AF193423
Avian infectious bronchitis virus isolate LX4	GI-19	AY189157
Avian infectious bronchitis virus strain Qu16	GI-20	AF349620
Avian infectious bronchitis virus strain Qu_mv	GI-20	AF349621
Avian infectious bronchitis virus isolate Italy-02	GI-21	AJ457137
Infectious bronchitis virus isolate Spain/98/313	GI-21	DQ064808
Infectious bronchitis virus strain HN08	GI-22	GQ265940
Infectious bronchitis virus isolate CK/CH/LSC/99I	GI-22	DQ167147
Infectious bronchitis virus isolate IBV/Ck/EG/CU/4/2014	GI-23	KY805846
Avian infectious bronchitis virus isolate variant 2	GI-23	AF093796
Infectious bronchitis virus isolate V13	GI-24	KF757447
Infectious bronchitis virus isolate IBV506	GI-24	KF809796
Infectious bronchitis virus isolate GA/10216/2010	GI-25	KM660636
Infectious bronchitis virus isolate GA/12274/2012	GI-25	KP085595
Infectious bronchitis virus strain NGA/BP61/2007	GI-26	FN182268
Infectious bronchitis virus strain NGA/N545/2006	GI-26	FN182270
Infectious bronchitis virus isolate Georgia 08	GI-27	GU301925
Infectious bronchitis virus isolate GA/12341/2012	GI-27	KM660634



Infectious bronchitis virus strain GX-NN-13	GI-28	JX291989
Infectious bronchitis virus strain ck/CH/LGX/111119	GI-28	KX640829
Infectious bronchitis virus strain gammaCoV/ck/China/I0114/14	GI-29	KY407556
Infectious bronchitis virus strain gammaCoV/ck/China/I0118/14	GI-29	KY407558
Avian infectious bronchitis virus (strain D1466)	GII-1	M21971
Avian infectious bronchitis virus (strain V1397)	GII-1	M21968
Avian infectious bronchitis virus N1/88	GIII-1	U29450
Avian infectious bronchitis virus strain V18/91	GIII-1	U29521
Infectious bronchitis virus DE/072/92	GIV-1	U77298
Avian infectious bronchitis virus AR/6386/97	GIV-1	AF274436
Infectious bronchitis virus isolate N1/03	GV-1	FJ235194
Infectious bronchitis virus strain 018	GV-1	JX018208
Infectious bronchitis virus strain SDIB781/2012	GVI-1	KF007209
Infectious bronchitis virus strain TC07-2	GVI-1	GQ265948
Infectious bronchitis virus strain gammaCoV/ck/China/I0636/16	GVII-1	MH924835
Infectious bronchitis virus strain GX-NN130021	GVII-1	KM365468
<b>Virus Name (HA)</b>	<b>Genotype</b>	<b>Accession number</b>
A/chicken/Hongkong/NT16/1999	A0	AF222608
A/Hongkong/1074/1999	A0	AJ404627

A/Parakeet/Narita/92A/98	A0	AB049160
A/chicken/Germany/R45/98	A1	AJ781822
A/chicken/Iran/11T/99	A2	AF508558
A/chicken/Saudi Arabia/532/99	A3	AF508559
A/chicken/Israel/90658/2000	A3	EF492221
A/turkey/Israel/1013/2002	A3	EF492237
A/quail/Shantou/1912/2001	A4	EF154922
A/quail/Shantou/1235/2001	A4	EF154917
A/quail/Shantou/1555/2001	A4	EF154921
A/quail/Dubai/301/2000	A5	EF063510
A/chicken/Dubai/338/2001	A5	EF063513
A/chicken/Pakistan/UDL-03/2008	A5	CY038474
A/quail/Shantou/1242/2001	A6	EF154918
A/quail/Shantou/1475/2004	A7	EF154959
A/quail/Shantou/4203/2002	A7	EF154938
A/quail/Shantou/21605/2005	A7	EF154979
A/chukkar/Shantou/22116/2005	A8	CY024552
A/chicken/Israel/1525/2006	A9	FJ464728
A/chicken/Israel/1638/2006	A9	FJ464714
A/chicken/Israel/524/2008	A9	FJ464723

---

A/chicken/Guangdong/5/97	B0	DQ064360
A/chicken/Hong kong/739/94	B0	AF156379
A/chicken/Osaka/aq48/97	B0	AB256666
A/chicken/Hongkong/G9/97	B1	AF156373
A/chicken/Guangdong/6/97	B1	DQ064362
A/Pigeon/Hong Kong/Y233/97	B1	AF156375
A/chicken/Sichuan/5/97	B2	AF508569
A/Guangzhou/333/99	B2	AY043028
A/Duck/Shantou/1043/00	B2	AF523382
A/chicken/Shanghai/F/98	B3	AY743216
A/chicken/Jiangsu/2/2001	B3	FJ793396
A/chicken/Osaka/aq69/2001	B3	AB256698
A/chicken/Henan/nd/1998	B4	DQ997448
A/chicken/Beijing/ne/1999	B5	DQ997505
A/chicken/HongKong/BD90/03	B5	AY664662
A/Gf/HK/NT101/2003	B5	DQ226116
A/chicken/Jiangsu/1/1999	B6	AF461509
A/chicken/Guangxi/4/1999	B7	EU081869
A/chicken/Guangxi/9/99	B8	DQ064364
A/chicken/Guangxi/10/99	B9	DQ064363

A/chicken/Guangdong/10/00	B10	DQ064356
A/chicken/Yokohama/aq120/2001	B10	AB256730
A/swine/Jiangxi/wx2/2004	B10	EU502901
A/chicken/Henan/26/00	B11	DQ064368
A/chicken/Henan/62/00	B12	AF508567
A/chicken/china/Guangxi1/2000	B13	DQ485208
A/quail/Nanchang/2-0460/2000	B14	CY006018
A/duck/Shantou/2102/00	B15	AF523378
A/chicken/Shantou/94/2000	B16	CY024568
A/chicken/Shantou/212/2000	B16	CY024576
A/chicken/Shantou/859/2000	B16	CY024584
A/duck/Shantou/830/00	B17	AF523377
A/chicken/Shantou/1610/2001	B17	CY024664
A/quail/Shantou/1158/2001	B17	EF154916
A/quail/Shantou/1318/2000	B18	EF154910
A/silky chicken/Shantou/1818/2000	B19	CY024616
A/duck/Shantou/1881/2000	B19	AF523373
A/chicken/Shantou/2098/2000	B19	CY024624
A/Partridge/Shantou/5692/2000	B20	CY024384
A/pheasant/Shantou/511/2003	B20	CY024072

A/Partridge/Shantou/3987/2003	B20	CY024144
A/chicken/Guangxi/6/2000	B21	EU086237
A/chicken/china/Guangxi14/2000	B22	DQ485216
A/chicken/china/Guangxi17/2000	B23	DQ485224
A/Partridge/Shantou/24/2000	B24	CY023091
A/duck/Shantou/2134/2000	B24	AF523380
A/Partridge/Shantou/2158/2000	B24	CY024296
A/Partridge/Shantou/2063/2000	B25	CY024208
A/Partridge/Shantou/1800/2000	B25	CY024120
A/duck/Shantou/1042/2000	B25	AF523383
A/chicken/Osaka/aq58/2001	B26	AB256690
A/chicken/Shantou/2686/2003	B26	CY023208
A/chicken/Osaka/aq19/2001	B27	AB256738
A/chicken/YoKohama/aq55/2001	B27	AB256674
A/chicken/YoKohama/aq135/2001	B27	AB256722
A/chicken/Guangdong/56/01	B28	DQ064361
A/chicken/Kobe/aq26/2001	B29	AB256682
A/chicken/YoKohama/aq134/2002	B29	AB256714
A/chicken/Jiangsu/ng/2001	B30	DQ997460
A/quail/Shantou/5663/2001	B31	EF154928

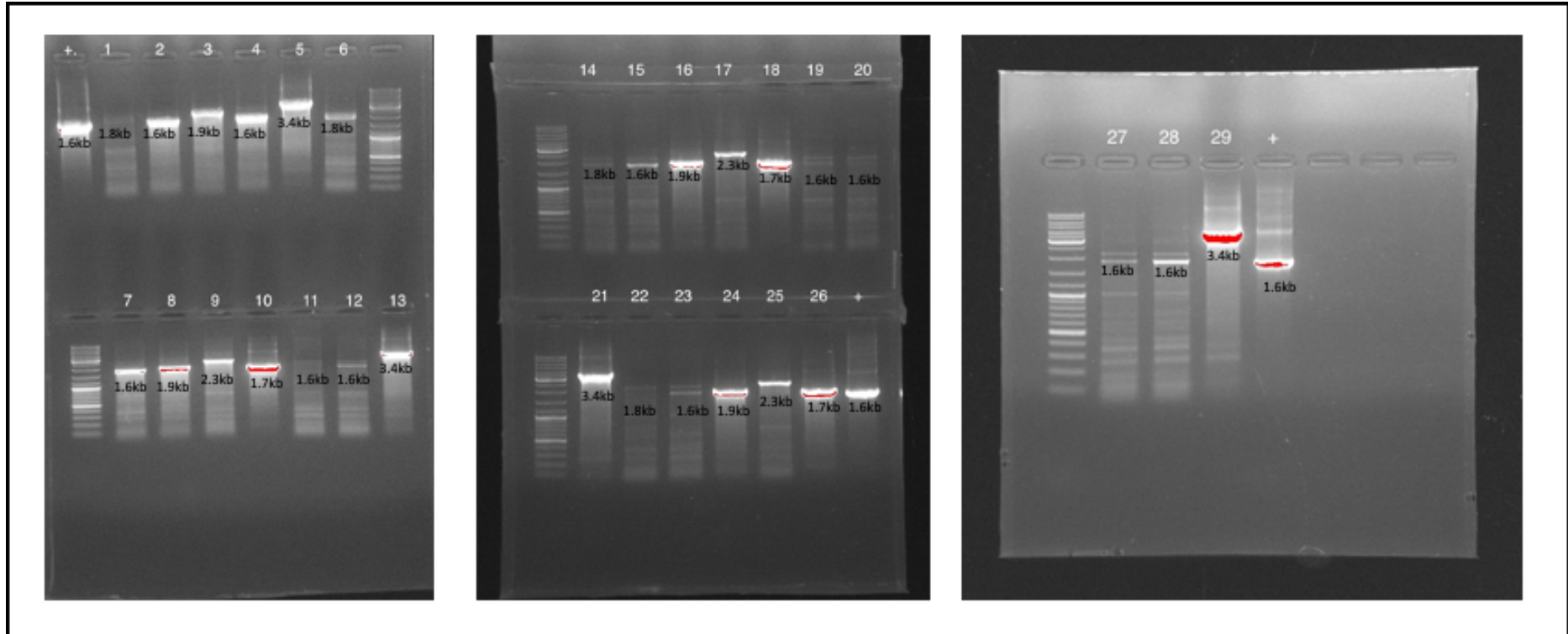
A/quail/Shantou/4762/2001	B32	EF154927
A/chicken/Yunnan/401/2002	B33	CY023848
A/duck/Shantou/4359/2002	B34	CY023960
A/chicken/Jiangsu/7/2002	B35	FJ384751
A/chukkar/Shantou/338/2002	B36	CY023536
A/quail/Shantou/1038/2002	B37	EF154935
A/quail/Shantou/2615/2003	B38	EF154947
A/chicken/Shantou/3040/2003	B39	CY023216
A/chicken/Shantou/4101/2003	B40	CY023232
A/quail/Shantou/4038/2003	B41	EF154954
A/guineafowl/HongKong/NT184/03	B42	AY664674
A/quail/Shantou/1780/2003	B43	EF154944
A/swine/Guangdong/WXI/2004	B44	EU516312
A/chicken/Shantou/4726/2004	B45	CY023344
A/chicken/Guangxi/1857/2004	B46	CY023696
A/Partridge/Shantou/4648/2004	B47	CY024328
A/pheasant/Shantou/45/2004	B48	CY024240
A/chicken/Henan/01/2004	B49	AY950230
A/swine/Guangxi/FS2/2005	B50	EU086302
A/swine/Guangxi/S15/2005	B51	EU086318

A/chicken/Guangxi/521/2005	B52	CY023728
A/swine/Guangxi/58/2005	B53	EF612742
A/chicken/Guangxi/1428/2005	B54	CY023744
A/chicken/Hunan/6108/2005	B55	CY023840
A/chicken/Guangxi/55/2005	B56	EU086245
A/chicken/Shantou/19465/2005	B57	CY023504
A/chicken/Hunan/4246/2005	B58	CY023808
A/bird/Guangxi/A1/2006	B59	EU086284
A/chicken/Shandong/B2/2007	B60	EU935071
A/chicken/Zhejiang/Hj/2007	B61	FJ581431
<hr/>		
A/chicken/Korea/38349-p96323/96	C0	AF156384
A/Korea/KBNP-0028/2000	C1	EF620900
A/chicken/Korea/S16/03	C2	AY862605
A/swine/Korea/S190/2004	C3	AY790297
<hr/>		
A/Duck/Germany/113/95	D1	AF508557
A/ostrich/South Africa/9508103/95	D2	AF508554
A/pheasant/Ireland/PV18/97	D3	AF508560
A/duck/Hongkong/Y439/97	D4	AF156377
A/duck/Hokkaido/49/98	D5	AB125928
A/duck/Hokkaido/9/99	D6	AB262463

<i>A/duck/Shantou/163/2004</i>	D7	CY024016
<i>A/duck/Shantou/7488/2004</i>	D8	CY024032
<i>A/Eurasian wigeon/Netherlands/3/2005</i>	D9	CY043856
<i>A/Gadwall/Netherlands/1/2006</i>	D10	CY043864
<i>A/laughing gull/Delaware/12/2006</i>	D11	CY041426
<i>A/Bewick swan/Netherlands/5/2007</i>	D12	CY041274
<hr/>		
<i>A/duck/Hongkong/289/78</i>	E0	AF523384
<i>A/duck/Hongkong/366/78</i>	E1	AY206674
<i>A/duck/Hk/784/1979</i>	E2	CY005632
<i>A/duck/Hongkong/552/79</i>	E3	AY206679
<i>A/goose/MN/5733-1/1980</i>	E4	CY006042
<i>A/mallard/Alberta/11/1991</i>	E5	CY005990
<hr/>		
<i>A/quail/Hongkong/AF157/92</i>	F	AF156381
<hr/>		
<i>A/turkey/Wisconsin/1/1966</i>	G0	GQ247858
<i>A/turkey/California/189/66</i>	G1	AF156390
<i>A/chicken/Heilongjiang/35/00</i>	G2	DQ064366
<hr/>		



**Annex 2. Stability testing.** DNA samples from recombinant ILTVs were tested for stability through PCR amplification up to the 5<sup>th</sup> passage.



Legend for Annex 2 Stability testing

Lane	Passage	Fragment amplicon
1	2	P2-DNA-ILTV-NDVF-Fd
2	2	P2-DNA-ILTV-NDVF-WT
3	2	P2-DNA-ILTV-NDVF-FcTail
4	2	P2-DNA-ILTV-UL0
5	2	P2-DNA-ILTV-IBVS
6	3	P3-DNA-ILTV-NDVF-Fd
7	3	P3-DNA-ILTV-NDVF-WT
8	3	P3-DNA-ILTV-NDVF-FcTail
9	3	P3-DNA-ILTV-NDVF-Fc
10	3	P3-DNA-ILTV-HA
11	3	P3-DNA-ILTV-UL50
12	3	P3-DNA-ILTV-UL0
13	3	P3-DNA-ILTV-IBVS
14	4	P4-DNA-ILTV-NDVF-Fd
15	4	P4-DNA-ILTV-NDVF-WT
16	4	P4-DNA-ILTV-NDVF-FcTail
17	4	P4-DNA-ILTV-NDVF-Fc
18	4	P4-DNA-ILTV-HA
19	4	P4-DNA-ILTV-UL50
20	4	P4-DNA-ILTV-UL0
21	4	P4-DNA-ILTV-IBVS
22	5	P5-DNA-ILTV-NDVF-Fd
23	5	P5-DNA-ILTV-NDVF-WT
24	5	P5-DNA-ILTV-NDVF-FcTail
25	5	P5-DNA-ILTV-NDVF-Fc
26	5	P5-DNA-ILTV-H9
27	5	P5-DNA-ILTV-UL50
28	5	P5-DNA-ILTV-UL0
29	5	P5-DNA-ILTV-IBVS
positive		pDNA-Fgene in MCS1



### Annex 3. qPCR standard curve.

Sample computation for the standard curve:

#### Calculation of the copy number of interest.

	n	1.096E-21 g/bp	m
m=	3956	1.10E-21	4.34E-18
copy #s of interest	4.34E-18	300000	1.30E-12

#### Calculating the dilution's copy number

Copy #	m	Mass of plasmid DNA g	Final concn of Plasmid DNA g/μl
300000	4.34E-18	1.30E-12	2.60E-13
30000	4.34E-18	1.30E-13	2.60E-14
3000	4.34E-18	1.30E-14	2.60E-15
300	4.34E-18	1.30E-15	2.60E-16
30	4.34E-18	1.30E-16	2.60E-17

#### Dilution computation

Dilution #	Source of plasmid DNA for Dilution	C1 Initial concn, g/μl	V1 Volume of plasmid DNA, μl	Volume of diluent, μl	V2 Final Volume, μl	C2 Final coc. In g/μl	Resulting copy #
1	Stock	2.80E-07	10	990	1000	2.80E-09	N/A
2	Dilution 1	2.80E-09	10	990	1000	2.80E-11	N/A
3	Dilution 2	2.80E-11	0.464286	99.53571	100	1.30E-13	300000
4	Dilution 3	1.30E-13	10	90	100	1.30E-14	30000
5	Dilution 4	1.30E-14	10	90	100	1.30E-15	3000
6	Dilution 5	1.30E-15	10	90	100	1.30E-16	300
7	Dilution 6	1.30E-16	10	90	100	1.30E-17	30
8	Dilution 7	1.30E-17	10	90	100	1.30E-18	3
9	Dilution 8	1.30E-18	10	90	100	1.30E-19	0

# CHAPTER 10

## References

- Aamir, U. B., Wernery, U., Ilyushina, N., & Webster, R. G. (2007). Characterization of avian H9N2 influenza viruses from United Arab Emirates 2000 to 2003. *Virology*, *361*(1), 45–55.
- Abozeid, H. H., Paldurai, A., Khattar, S. K., Afifi, M. A., El-Kady, M. F., El-Deeb, A. H., & Samal, S. K. (2017). Complete genome sequences of two avian infectious bronchitis viruses isolated in Egypt: Evidence for genetic drift and genetic recombination in the circulating viruses. *Infection, Genetics and Evolution*, *53*, 7–14. <https://doi.org/https://doi.org/10.1016/j.meegid.2017.05.006>
- Abozeid, H. H., Paldurai, A., Varghese, B. P., Khattar, S. K., Afifi, M. A., Zouelfakkar, S., El-Deeb, A. H., El-Kady, M. F., & Samal, S. K. (2019). Development of a recombinant Newcastle disease virus-vectored vaccine for infectious bronchitis virus variant strains circulating in Egypt. *Veterinary Research*, *50*(1), 1–13. <https://doi.org/10.1186/s13567-019-0631-5>
- Acheson, N. H. (2011). Fundamentals of Molecular Virology. In *John Wiley & Sons, Inc* (2nd ed.). <https://doi.org/10.1002/pauz.200790112>
- Afonso, C. L., Tulman, E. R., Lu, Z., Zsak, L., Rock, D. L., & Kutish, G. F. (2001). The Genome of Turkey Herpesvirus. *Journal of Virology*, *75*(2), 971–978. <https://doi.org/10.1128/jvi.75.2.971-978.2001>
- Aida, V., Pliasis, V. C., Neasham, P. J., North, J. F., McWhorter, K. L., Glover, S. R., & Kyriakis, C. S. (2021). Novel Vaccine Technologies in Veterinary Medicine: A Herald to Human Medicine Vaccines. *Frontiers in Veterinary Science*, *8*(April),

1–20. <https://doi.org/10.3389/fvets.2021.654289>

Alexander, D. J. (2001). Newcastle disease. *British Poultry Science*, 42(1), 5–22.

<https://doi.org/10.1080/713655022>

Allan, W. H., & Gough, R. E. (1976). A comparison between the haemagglutination inhibition and complement fixation tests for Newcastle disease. *Research in Veterinary Science*, 20(1), 101–103.

[https://doi.org/https://doi.org/10.1016/S0034-5288\(18\)33487-8](https://doi.org/https://doi.org/10.1016/S0034-5288(18)33487-8)

Antos, A., Miroslaw, P., Rola, J., & Polak, M. P. (2021). Vaccination Failure in Eradication and Control Programs for Bovine Viral Diarrhea Infection. *Frontiers in Veterinary Science*, 8(June), 1–11. <https://doi.org/10.3389/fvets.2021.688911>

Arora, P., Lakhchaura, B. D., & Garg, S. K. (2010). Evaluation of immunogenic potential of 75kDa and 56kDa proteins of newcastle disease virus (NDV). *Indian Journal of Experimental Biology*, 48(9), 889–895.

Arstila, T. P., Vainio, O., & Lassila, O. (1994). Central role of CD4+ T cells in avian immune response. *Poultry Science*, 73(7), 1019–1026.

<https://doi.org/10.3382/ps.0731019>

Atasoy, M. O., Rohaim, M. A., & Munir, M. (2019). Simultaneous deletion of virulence factors and insertion of antigens into the infectious laryngotracheitis virus using NHEJ-CRISPR/Cas9 and cre-lox system for construction of a stable vaccine vector. *Vaccines*, 7(4). <https://doi.org/10.3390/vaccines7040207>

Awate, S., Babiuk, L., & Mutwiri, G. (2013). Mechanisms of Action of Adjuvants. In *Frontiers in Immunology* (Vol. 4, p. 114).

<https://www.frontiersin.org/article/10.3389/fimmu.2013.00114>

Bae, S., Park, J., & Kim, J. S. (2014). Cas-OFFinder: A fast and versatile algorithm that searches for potential off-target sites of Cas9 RNA-guided endonucleases.

- Bioinformatics*, 30(10), 1473–1475. <https://doi.org/10.1093/bioinformatics/btu048>
- Bagust, T. J., & Johnson, M. A. (1995). Avian infectious laryngotracheitis: virus-host interactions in relation to prospects for eradication. *Avian Pathology: Journal of the W.V.P.A*, 24(3), 373–391. <https://doi.org/10.1080/03079459508419079>
- Bakhrebah, M. A., Nassar, M. S., Alsuabeyl, M. S., Zaher, W. A., & Meo, S. A. (2018). CRISPR technology: new paradigm to target the infectious disease pathogens. *European Review for Medical and Pharmacological Sciences*, 22(11), 3448–3452. [https://doi.org/10.26355/eurrev\\_201806\\_15169](https://doi.org/10.26355/eurrev_201806_15169)
- Baron, M. D., Iqbal, M., & Nair, V. (2018). Recent advances in viral vectors in veterinary vaccinology. *Current Opinion in Virology*, 29, 1–7. <https://doi.org/10.1016/j.coviro.2018.02.002>
- Barrangou, R., & Marraffini, L. A. (2014). CRISPR-Cas systems: Prokaryotes upgrade to adaptive immunity. *Molecular Cell*, 54(2), 234–244. <https://doi.org/10.1016/j.molcel.2014.03.011>
- Batra, S. A., Shanthalingam, S., Donofrio, G., Haldorson, G. J., Chowdhury, S., White, S. N., & Srikumaran, S. (2017). Immunization of bighorn sheep against *Mannheimia haemolytica* with a bovine herpesvirus 1-vectored vaccine. *Vaccine*, 35(12), 1630–1636. <https://doi.org/https://doi.org/10.1016/j.vaccine.2017.02.006>
- Bayat, H., Naderi, F., Khan, A. H., Memarnejadian, A., & Rahimpour, A. (2018). The impact of CRISPR-Cas system on antiviral therapy. *Advanced Pharmaceutical Bulletin*, 8(4), 591–597. <https://doi.org/10.15171/apb.2018.067>
- Belouzard, S., Millet, J. K., Licitra, B. N., & Whittaker, G. R. (2012). Mechanisms of Coronavirus Cell Entry Mediated by the Viral Spike Protein. In *Viruses* (Vol. 4, Issue 6). <https://doi.org/10.3390/v4061011>

- Bi, Y., Sun, L., Gao, D., Ding, C., Li, Z., Li, Y., Cun, W., & Li, Q. (2014). High-Efficiency Targeted Editing of Large Viral Genomes by RNA-Guided Nucleases. *PLOS Pathogens*, *10*(5), e1004090. <https://doi.org/10.1371/journal.ppat.1004090>
- Bierle, C. J., Anderholm, K. M., Wang, J. Ben, McVoy, M. A., & Schleiss, M. R. (2016). Targeted Mutagenesis of Guinea Pig Cytomegalovirus Using CRISPR/Cas9-Mediated Gene Editing. *Journal of Virology*, *90*(15), 6989 LP – 6998. <https://doi.org/10.1128/JVI.00139-16>
- Bogs, J., Veits, J., Gohrbandt, S., Hundt, J., Stech, O., Breithaupt, A., Teifke, J. P., Mettenleiter, T. C., & Stech, J. (2010). Highly Pathogenic H5N1 Influenza Viruses Carry Virulence Determinants beyond the Polybasic Hemagglutinin Cleavage Site. *PLOS ONE*, *5*(7), e11826. <https://doi.org/10.1371/journal.pone.0011826>
- Borca, M. V., Holinka, L. G., Berggren, K. A., & Gladue, D. P. (2018). CRISPR-Cas9, a tool to efficiently increase the development of recombinant African swine fever viruses. *Scientific Reports*, *8*(1), 3154. <https://doi.org/10.1038/s41598-018-21575-8>
- Borchers, K., Goltz, M., & Ludwig, H. (1994). Genome organization of the herpesviruses: minireview. *Acta Veterinaria Hungarica*, *42*(2–3), 217–225. <http://europepmc.org/abstract/MED/7810416>
- Bortnik, V., Wu, M., Julcher, B., Salinas, A., Nikolic, I., Simpson, K. J., McMillan, N. A., & Idris, A. (2021). Loss of HPV type 16 E7 restores cGAS-STING responses in human papilloma virus-positive oropharyngeal squamous cell carcinomas cells. *Journal of Microbiology, Immunology, and Infection = Wei Mian Yu Gan Ran Za Zhi*, *54*(4), 733–739. <https://doi.org/10.1016/j.jmii.2020.07.010>



- Bosch, B. J., Bodewes, R., de Vries, R. P., Kreijtz, J. H. C. M., Willem, B., Geert, van A., Rimmelzwaan, G. F., de Haan, C. A. M., Osterhaus, A. D. M. E., & Rottier, P. J. M. (2010). Recombinant Soluble, Multimeric HA and NA Exhibit Distinctive Types of Protection against Pandemic Swine-Origin 2009 A(H1N1) Influenza Virus Infection in Ferrets. *Journal of Virology*, *84*(19), 10366–10374. <https://doi.org/10.1128/JVI.01035-10>
- Bournsnell, M. E. G., Green, P. F., Samson, A. C. R., Campbell, J. I. A., Deuter, A., Peters, R. W., Millar, N. S., Emmerson, P. T., & Binns, M. M. (1990). A recombinant fowlpox virus expressing the hemagglutinin-neuraminidase gene of Newcastle disease virus (NDV) protects chickens against challenge NDV. *Virology*, *178*(1), 297–300. [https://doi.org/https://doi.org/10.1016/0042-6822\(90\)90408-J](https://doi.org/https://doi.org/10.1016/0042-6822(90)90408-J)
- Brun, A., Albina, E., Barret, T., Chapman, D. A. G., Czub, M., Dixon, L. K., Keil, G. M., Klonjowski, B., Le Potier, M. F., Libeau, G., Ortego, J., Richardson, J., & Takamatsu, H. H. (2008). Antigen delivery systems for veterinary vaccine development. Viral-vector based delivery systems. *Vaccine*, *26*(51), 6508–6528. <https://doi.org/10.1016/j.vaccine.2008.09.044>
- Bublout, M., Pritchard, N., Le Gros, F.-X., & Goutebroze, S. (2007). Use of a Vectored Vaccine against Infectious Bursal Disease of Chickens in the Face of High-Titred Maternally Derived Antibody. *Journal of Comparative Pathology*, *137*, S81–S84. <https://doi.org/https://doi.org/10.1016/j.jcpa.2007.04.017>
- Bublout, Michel, Woerly, V., Wang, Q., & King, H. (2021). *Regulatory Strategies and Factors Affecting Veterinary Viral Vector Development BT - Viral Vectors in Veterinary Vaccine Development: A Textbook* (T. Vanniasinkam, S. K. Tikoo, & S. K. Samal (eds.); pp. 201–215). Springer International Publishing.

[https://doi.org/10.1007/978-3-030-51927-8\\_13](https://doi.org/10.1007/978-3-030-51927-8_13)

Bukreyev, A., & Collins, P. L. (2008). Newcastle disease virus as a vaccine vector for humans. *Current Opinion in Molecular Therapeutics*, *10*(1), 46–55.

Cáceres, C. J., Rajao, D. S., & Perez, D. R. (2021). Airborne Transmission of Avian Origin H9N2 Influenza A Viruses in Mammals. *Viruses*, *13*(10).

<https://doi.org/10.3390/v13101919>

Can, H., Alak, S. E., Köseoğlu, A. E., Döşkaya, M., & Ün, C. (2020). Do *Toxoplasma gondii* apicoplast proteins have antigenic potential? An in silico study. *Computational Biology and Chemistry*, *84*, 107158.

Can, H., Köseoğlu, A. E., Erkunt Alak, S., Güvendi, M., Döşkaya, M., Karakavuk, M., Gürüz, A. Y., & Ün, C. (2020). In silico discovery of antigenic proteins and epitopes of SARS-CoV-2 for the development of a vaccine or a diagnostic approach for COVID-19. *Scientific Reports*, *10*(1), 1–16.

<https://doi.org/10.1038/s41598-020-79645-9>

Cantello, J. L., Anderson, A. S., Francesconi, A., & Morgan, R. W. (1991). Isolation of a Marek's disease virus (MDV) recombinant containing the lacZ gene of *Escherichia coli* stably inserted within the MDV US2 gene. *Journal of Virology*, *65*(3), 1584–1588. <https://doi.org/10.1128/jvi.65.3.1584-1588.1991>

Capua, I., Terregino, C., Cattoli, G., Mutinelli, F., & Rodriguez, J. F. (2003). Development of a DIVA (Differentiating Infected from Vaccinated Animals) strategy using a vaccine containing a heterologous neuraminidase for the control of avian influenza. *Avian Pathology: Journal of the W.V.P.A.*, *32*(1), 47–55. <https://doi.org/10.1080/0307945021000070714>

Cardone, G., Winkler, D. C., Trus, B. L., Cheng, N., Heuser, J. E., Newcomb, W. W., Brown, J. C., & Steven, A. C. (2007). Visualization of the herpes simplex virus

portal in situ by cryo-electron tomography. *Virology*, 361(2), 426–434.

<https://doi.org/10.1016/j.virol.2006.10.047>

Cattoli, G., Fusaro, A., Monne, I., Molia, S., Le Menach, A., Maregeya, B., Nchare, A., Bangana, I., Maina, A. G., Koffi, J.-N. N., Thiam, H., Bezeid, O. E. M. A., Salviato, A., Nisi, R., Terregino, C., & Capua, I. (2010). Emergence of a new genetic lineage of Newcastle disease virus in West and Central Africa-- implications for diagnosis and control. *Veterinary Microbiology*, 142(3–4), 168–176. <https://doi.org/10.1016/j.vetmic.2009.09.063>

Cavanagh, D., Davis, P. J., & Mockett, A. P. A. (1988). Amino acids within hypervariable region 1 of avian coronavirus IBV (Massachusetts serotype) spike glycoprotein are associated with neutralization epitopes. *Virus Research*, 11(2), 141–150.

Chambers, M. A., Graham, S. P., & La Ragione, R. M. (2016). Challenges in Veterinary Vaccine Development and Immunization. *Methods in Molecular Biology (Clifton, N.J.)*, 1404, 3–35. [https://doi.org/10.1007/978-1-4939-3389-1\\_1](https://doi.org/10.1007/978-1-4939-3389-1_1)

Chang, P., Ameen, F., Sealy, J. E., Sadeyen, J., Bhat, S., Li, Y., & Iqbal, M. (2019). *Application of HDR-CRISPR / Cas9 and Erythrocyte Binding for Rapid Generation of Recombinant Turkey Herpesvirus-Vectored Avian Influenza Virus Vaccines*. 1–11.

Chang, P., Yao, Y., Tang, N., Sadeyen, J. R., Sealy, J., Clements, A., Bhat, S., Munir, M., Bryant, J. E., & Iqbal, M. (2018). The application of NHEJ-CRISPR/Cas9 and cre-lox system in the generation of bivalent duck enteritis virus vaccine against avian influenza virus. *Viruses*, 10(2), 1–11.

<https://doi.org/10.3390/v10020081>

Chen, J., Lee, K. H., Steinhauer, D. A., Stevens, D. J., Skehel, J. J., & Wiley, D. C.

- (1998). Structure of the hemagglutinin precursor cleavage site, a determinant of influenza pathogenicity and the origin of the labile conformation. *Cell*, 95(3), 409–417. [https://doi.org/10.1016/s0092-8674\(00\)81771-7](https://doi.org/10.1016/s0092-8674(00)81771-7)
- Chen, L., Qi, X., Liang, D., Li, G., Peng, X., Li, X., Ke, B., Zheng, H., Liu, Z., Ke, C., Liao, G., Liu, L., & Feng, Q. (2022). Human Fc-Conjugated Receptor Binding Domain-Based Recombinant Subunit Vaccines with Short Linker Induce Potent Neutralizing Antibodies against Multiple SARS-CoV-2 Variants. In *Vaccines* (Vol. 10, Issue 9). <https://doi.org/10.3390/vaccines10091502>
- Chen, M., Payne, W. S., Hunt, H., Zhang, H., Holmen, S. L., & Dodgson, J. B. (2008). Inhibition of Marek's disease virus replication by retroviral vector-based RNA interference. *Virology*, 377(2), 265–272. <https://doi.org/10.1016/j.virol.2008.03.019>
- Chen, T., Zhou, X., Qi, Y., Mi, L., Sun, X., Zhang, S., Liu, Y., Olson, V., Qiu, W., Wu, X., & Hu, R. (2019). Feline herpesvirus vectored-rabies vaccine in cats: A dual protection. *Vaccine*, 37(16), 2224–2231. <https://doi.org/https://doi.org/10.1016/j.vaccine.2019.03.008>
- Chen, Yang, Guo, W., Xu, Z., Yan, Q., Luo, Y., Shi, Q., Chen, D., Zhu, L., & Wang, X. (2011). A novel recombinant pseudorabies virus expressing parvovirus VP2 gene: Immunogenicity and protective efficacy in swine. *Virology Journal*, 8(1), 307. <https://doi.org/10.1186/1743-422X-8-307>
- Chen, Yuqiu, Jiang, L., Zhao, W., Liu, L., Zhao, Y., Shao, Y., Li, H., Han, Z., & Liu, S. (2017). Identification and molecular characterization of a novel serotype infectious bronchitis virus (GI-28) in China. *Veterinary Microbiology*, 198, 108–115. <https://doi.org/10.1016/j.vetmic.2016.12.017>
- Cheng, J., Randall, A. Z., Sweredoski, M. J., & Baldi, P. (2005). SCRATCH: a protein

- structure and structural feature prediction server. *Nucleic Acids Research*, 33(suppl\_2), W72–W76. <https://doi.org/10.1093/nar/gki396>
- Cheng, X., Zengel, J. R., Suguitan Jr, A. L., Xu, Q., Wang, W., Lin, J., & Jin, H. (2013). Evaluation of the Humoral and Cellular Immune Responses Elicited by the Live Attenuated and Inactivated Influenza Vaccines and Their Roles in Heterologous Protection in Ferrets. *The Journal of Infectious Diseases*, 208(4), 594–602. <https://doi.org/10.1093/infdis/jit207>
- Chrzastek, K., Lee, D., Gharaibeh, S., Zsak, A., & Kapczynski, D. R. (2018). Characterization of H9N2 avian influenza viruses from the Middle East demonstrates heterogeneity at amino acid position 226 in the hemagglutinin and potential for transmission to mammals. *Virology*, 518, 195–201.
- Cid, R., & Bolívar, J. (2021). Platforms for Production of Protein-Based Vaccines: From Classical to Next-Generation Strategies. *Biomolecules*, 11(8). <https://doi.org/10.3390/biom11081072>
- Collett, S. R., Smith, J. A., Boulianne, M., Owen, R. L., Gingerich, E., Singer, R. S., Johnson, T. J., Hofacre, C. L., Berghaus, R. D., & Stewart-Brown, B. (2020). Principles of Disease Prevention, Diagnosis, and Control. In *Diseases of Poultry* (pp. 1–78). <https://doi.org/doi:10.1002/9781119371199.ch1>
- Cong, L., Ran, F. A., Cox, D., Lin, S., Barretto, R., Habib, N., Hsu, P. D., Wu, X., Jiang, W., Marraffini, L. A., & Zhang, F. (2013). Multiplex Genome Engineering Using CRISPR/Cas Systems. *Science*, 339(6121), 819 LP – 823. <https://doi.org/10.1126/science.1231143>
- Connolly, S. A., Jackson, J. O., Jardetzky, T. S., & Longnecker, R. (2011). Fusing structure and function: a structural view of the herpesvirus entry machinery. *Nature Reviews Microbiology*, 9(5), 369–381.

<https://doi.org/10.1038/nrmicro2548>

Coppo, M. J. C., Noormohammadi, A. H., Browning, G. F., & Devlin, J. M. (2013).

Challenges and recent advancements in infectious laryngotracheitis virus vaccines. *Avian Pathology*, 42(3), 195–205.

<https://doi.org/10.1080/03079457.2013.800634>

Cornax, I., Miller, P. J., & Afonso, C. L. (2012). Characterization of Live LaSota

Vaccine Strain–Induced Protection in Chickens upon Early Challenge with a Virulent Newcastle Disease Virus of Heterologous Genotype. *Avian Diseases*, 56(3), 464–470. <https://doi.org/10.1637/10043-122011-Reg.1>

Crosby, A. W. (1976). *Epidemic and peace, 1918 / Alfred W. Crosby, Jr.* Greenwood Press.

Cruickshank, J. G., Berry, D. M., & Hay, B. (1963). The fine structure of infectious laryngotracheitis virus. *Virology*, 20(2), 376–378.

[https://doi.org/https://doi.org/10.1016/0042-6822\(63\)90129-6](https://doi.org/https://doi.org/10.1016/0042-6822(63)90129-6)

Dangi, M., Kumari, R., Singh, B., & Chhillar, A. K. (2018). Advanced In Silico Tools for Designing of Antigenic Epitope as Potential Vaccine Candidates Against Corona virus. *Bioinformatics: Sequences, Structures, Phylogeny*, 329–357.

Darteil, R., Bublot, M., Laplace, E., Bouquet, J. F., Audonnet, J. C., & Rivière, M.

(1995). Herpesvirus of turkey recombinant viruses expressing infectious bursal disease virus (IBDV) VP2 immunogen induce protection against an IBDV virulent challenge in chickens. *Virology*, 211(2), 481–490.

<https://doi.org/10.1006/viro.1995.1430>

De Baets, S., Verhelst, J., Van den Hoecke, S., Smet, A., Schotsaert, M., Job, E. R.,

Roose, K., Schepens, B., Fiers, W., & Saelens, X. (2015). A GFP Expressing

Influenza A Virus to Report In Vivo Tropism and Protection by a Matrix Protein 2

Ectodomain-Specific Monoclonal Antibody. *PLOS ONE*, 10(3), e0121491.

<https://doi.org/10.1371/journal.pone.0121491>

- De Wit, J. J., Nieuwenhuisen-van Wilgen, J., Hoogkamer, A., van de Sande, H., Zuidam, G. J., & Fabri, T. H. F. (2011). Induction of cystic oviducts and protection against early challenge with infectious bronchitis virus serotype D388 (genotype QX) by maternally derived antibodies and by early vaccination. *Avian Pathology*, 40(5), 463–471. <https://doi.org/10.1080/03079457.2011.599060>
- Devaux, C. A. (2012). Emerging and re-emerging viruses: A global challenge illustrated by Chikungunya virus outbreaks. *World Journal of Virology*, 1(1), 11–22. <https://doi.org/10.5501/wjv.v1.i1.11>
- Devlin, J. M., Browning, G. F., Hartley, C. A., Kirkpatrick, N. C., Mahmoudian, A., Noormohammadi, A. H., & Gilkerson, J. R. (2006). Glycoprotein G is a virulence factor in infectious laryngotracheitis virus. *Journal of General Virology*, 87(10), 2839–2847. <https://doi.org/10.1099/vir.0.82194-0>
- Di Giovine, P., Settembre, E. C., Bhargava, A. K., Luftig, M. A., Lou, H., Cohen, G. H., Eisenberg, R. J., Krummenacher, C., & Carfi, A. (2011). Structure of Herpes Simplex Virus Glycoprotein D Bound to the Human Receptor Nectin-1. *PLOS Pathogens*, 7(9), e1002277. <https://doi.org/10.1371/journal.ppat.1002277>
- Dimitrov, K. M., Abolnik, C., Afonso, C. L., Albina, E., Bahl, J., Berg, M., Briand, F. X., Brown, I. H., Choi, K. S., Chvala, I., Diel, D. G., Durr, P. A., Ferreira, H. L., Fusaro, A., Gil, P., Goujgoulova, G. V., Grund, C., Hicks, J. T., Joannis, T. M., ... Wong, F. Y. K. (2019). Updated unified phylogenetic classification system and revised nomenclature for Newcastle disease virus. *Infection, Genetics and Evolution*, 74(June), 103917. <https://doi.org/10.1016/j.meegid.2019.103917>
- DiNapoli, J. M., Kotelkin, A., Yang, L., Elankumaran, S., Murphy, B. R., Samal, S. K.,

- Collins, P. L., & Bukreyev, A. (2007). Newcastle disease virus, a host range-restricted virus, as a vaccine vector for intranasal immunization against emerging pathogens. *Proceedings of the National Academy of Sciences of the United States of America*, *104*(23), 9788–9793.  
<https://doi.org/10.1073/pnas.0703584104>
- Dong, G., Luo, J., Zhang, H., Wang, C., Duan, M., Deliberto, T. J., Nolte, D. L., Ji, G., & He, H. (2011). Phylogenetic Diversity and Genotypical Complexity of H9N2 Influenza A Viruses Revealed by Genomic Sequence Analysis. *PLOS ONE*, *6*(2), e17212. <https://doi.org/10.1371/journal.pone.0017212>
- Dong, W., Zhang, H., Huang, H., Zhou, J., Hu, L., Lian, A., Zhu, L., Ma, N., Yang, P., Wei, K., & Zhu, R. (2016). Chicken IgY Fc linked to bordetella avium ompA and taishan Pinus massoniana pollen polysaccharide adjuvant enhances macrophage function and specific immune responses. *Frontiers in Microbiology*, *7*(NOV), 1–11. <https://doi.org/10.3389/fmicb.2016.01708>
- Donofrio, G., Franceschi, V., Lovero, A., Capocéfalo, A., Camero, M., Losurdo, M., Cavarani, S., Marinaro, M., Grandolfo, E., Buonavoglia, C., & Tempesta, M. (2013). Clinical Protection of Goats against CpHV-1 Induced Genital Disease with a BoHV-4-Based Vector Expressing CpHV-1 gD. *PLOS ONE*, *8*(1), e52758. <https://doi.org/10.1371/journal.pone.0052758>
- Donofrio, G., Sartori, C., Ravanetti, L., Cavarani, S., Gillet, L., Vanderplasschen, A., Taddei, S., & Flammini, C. F. (2007). Establishment of a Bovine Herpesvirus 4 based vector expressing a secreted form of the Bovine Viral Diarrhoea Virus structural glycoprotein E2 for immunization purposes. *BMC Biotechnology*, *7*(1), 68. <https://doi.org/10.1186/1472-6750-7-68>
- Doudna, J. A., & Charpentier, E. (2014). The new frontier of genome engineering



with CRISPR-Cas9. *Science*, 346(6213).

<https://doi.org/10.1126/science.1258096>

Doytchinova, I. A., & Flower, D. R. (2007). VaxiJen: a server for prediction of protective antigens, tumour antigens and subunit vaccines. *BMC Bioinformatics*, 8(1), 4. <https://doi.org/10.1186/1471-2105-8-4>

Droppa-Almeida, D., Franceschi, E., & Padilha, F. F. (2018). Immune-Informatic Analysis and Design of Peptide Vaccine From Multi-epitopes Against *Corynebacterium pseudotuberculosis*. *Bioinformatics and Biology Insights*, 12, 1177932218755337. <https://doi.org/10.1177/1177932218755337>

Du, L., Leung, V. H.-C., Zhang, X., Zhou, J., Chen, M., He, W., Zhang, H.-Y., Chan, C. C. S., Poon, V. K.-M., Zhao, G., Sun, S., Cai, L., Zhou, Y., Zheng, B.-J., & Jiang, S. (2011). A Recombinant Vaccine of H5N1 HA1 Fused with Foldon and Human IgG Fc Induced Complete Cross-Clade Protection against Divergent H5N1 Viruses. *PLOS ONE*, 6(1), e16555.

<https://doi.org/10.1371/journal.pone.0016555>

Dunaevskaia, G. N. (1988). [Pains and the lumbosacral area]. *Fel'dsher i akusherka*, 53(6), 33–37.

Dutta, S. K., & Langenburg, T. (2023). A Perspective on Current Flavivirus Vaccine Development: A Brief Review. *Viruses*, 15(4). <https://doi.org/10.3390/v15040860>

Ebina, H., Misawa, N., Kanemura, Y., & Koyanagi, Y. (2013). Harnessing the CRISPR/Cas9 system to disrupt latent HIV-1 provirus. *Scientific Reports*, 3, 2510. <https://doi.org/10.1038/srep02510>

Eisenberg, R. J., Atanasiu, D., Cairns, T. M., Gallagher, J. R., Krummenacher, C., & Cohen, G. H. (2012). Herpes Virus Fusion and Entry: A Story with Many Characters. In *Viruses* (Vol. 4, Issue 5). <https://doi.org/10.3390/v4050800>

- Elde, N. C., Child, S. J., Eickbush, M. T., Kitzman, J. O., Rogers, K. S., Shendure, J., Geballe, A. P., & Malik, H. S. (2012). Poxviruses deploy genomic accordions to adapt rapidly against host antiviral defenses. *Cell*, *150*(4), 831–841.  
<https://doi.org/10.1016/j.cell.2012.05.049>
- Elias, T., Diamond, B., Bjarne, B., Kristian, A. T., & Gunnveig, G. (2023). Trimeric, APC-Targeted Subunit Vaccines Protect Mice against Seasonal and Pandemic Influenza. *Journal of Virology*, *97*(2), e01694-22.  
<https://doi.org/10.1128/jvi.01694-22>
- Erdem, A. E., & Sareyyupoglu, B. (2022). DIVA (Differentiating Infected from Vaccinated Animals) Vaccines and Strategies. *Etlik Veteriner Mikrobiyoloji Dergisi*, *33*(1), 102–109. <https://doi.org/10.35864/evmd.932993>
- Esaki, M., Godoy, A., Rosenberger, J. K., Rosenberger, S. C., Gardin, Y., Yasuda, A., & Dorsey, K. M. (2013). Protection and antibody response caused by turkey herpesvirus vector Newcastle disease vaccine. *Avian Diseases*, *57*(4), 750–755. <https://doi.org/10.1637/10540-032613-Reg.1>
- Esaki, M., Noland, L., Eddins, T., Godoy, A., Saeki, S., Saitoh, S., Yasuda, A., & Dorsey, K. M. (2013). Safety and Efficacy of a Turkey Herpesvirus Vector Laryngotracheitis Vaccine for Chickens. *Avian Diseases*, *57*(2), 192–198.  
<https://doi.org/10.1637/10383-092412-Reg.1>
- Ewer, K. J., Lambe, T., Rollier, C. S., Spencer, A. J., Hill, A. V. S., & Dorrell, L. (2016). Viral vectors as vaccine platforms: from immunogenicity to impact. *Current Opinion in Immunology*, *41*, 47–54.  
<https://doi.org/https://doi.org/10.1016/j.coi.2016.05.014>
- Fauci, A. S. (2005). Emerging and reemerging infectious diseases: The perpetual challenge. *Academic Medicine*, *80*(12), 1079–1085.

<https://doi.org/10.1097/00001888-200512000-00002>

Felsenstein, J. (1985). Confidence Limits on Phylogenies: An Approach Using the Bootstrap. *Evolution*, 39(4), 783–791. <https://doi.org/10.2307/2408678>

Ferreira, H. L., Miller, P. J., & Suarez, D. L. (2021). Protection against different genotypes of newcastle disease viruses (Ndv) afforded by an adenovirus-vectored fusion protein and live ndv vaccines in chickens. *Vaccines*, 9(2), 1–18. <https://doi.org/10.3390/vaccines9020182>

Ferreira Júnior, Á., Dos Santos, J. P., Sousa, I. de O., Martin, I., Alves, E. G. L., & Rosado, I. R. (2018). Gallus gallus domesticus: Immune system and its potential for generation of immunobiologics. *Ciencia Rural*, 48(8). <https://doi.org/10.1590/0103-8478cr20180250>

Fesq, H., Bacher, M., Nain, M., & Gemsa, D. (1994). Programmed cell death (apoptosis) in human monocytes infected by influenza A virus. *Immunobiology*, 190(1–2), 175–182. [https://doi.org/10.1016/S0171-2985\(11\)80292-5](https://doi.org/10.1016/S0171-2985(11)80292-5)

Ficken, M. D., Ellsworth, M. A., Tucker, C. M., & Cortese, V. S. (2006). Effects of modified-live bovine viral diarrhea virus vaccines containing either type 1 or types 1 and 2 BVDV on heifers and their offspring after challenge with noncytopathic type 2 BVDV during gestation. *Journal of the American Veterinary Medical Association*, 228(10), 1559–1564. <https://doi.org/10.2460/javma.228.10.1559>

Field, H. J., & Wildy, P. (1978). The pathogenicity of thymidine kinase-deficient mutants of herpes simplex virus in mice. *Journal of Hygiene*, 81(2), 267–277. <https://doi.org/DOI:10.1017/S0022172400025109>

Fleury, D., Barrère, B., Bizebard, T., Daniels, R. S., Skehel, J. J., & Knossow, M. (1999). A complex of influenza hemagglutinin with a neutralizing antibody that

- binds outside the virus receptor binding site. *Nature Structural Biology*, 6(6), 530–534. <https://doi.org/10.1038/9299>
- Franceschi, V., Capocefalo, A., Calvo-Pinilla, E., Redaelli, M., Mucignat-Caretta, C., Mertens, P., Ortego, J., & Donofrio, G. (2011). Immunization of knock-out  $\alpha/\beta$  interferon receptor mice against lethal bluetongue infection with a BoHV-4-based vector expressing BTV-8 VP2 antigen. *Vaccine*, 29(16), 3074–3082. <https://doi.org/https://doi.org/10.1016/j.vaccine.2011.01.075>
- Franceschi, V., Parker, S., Jacca, S., Crump, R. W., Doronin, K., Hembrador, E., Pompilio, D., Tebaldi, G., Estep, R. D., Wong, S. W., Buller, M. R., & Donofrio, G. (2015). BoHV-4-Based Vector Single Heterologous Antigen Delivery Protects STAT1(-/-) Mice from Monkeypoxvirus Lethal Challenge. *PLoS Neglected Tropical Diseases*, 9(6), e0003850. <https://doi.org/10.1371/journal.pntd.0003850>
- Franzo, G., Legnardi, M., Tucciarone, C. M., Drigo, M., Martini, M., & Cecchinato, M. (2019). Evolution of infectious bronchitis virus in the field after homologous vaccination introduction. *Veterinary Research*, 50(1), 92. <https://doi.org/10.1186/s13567-019-0713-4>
- Fuchs, W., Veits, J., Helferich, D., Granzow, H., Teifke, J. P., & Mettenleiter, T. C. (2007). Molecular biology of avian infectious laryngotracheitis virus. *Veterinary Research*, 38(2), 261–279. <https://doi.org/10.1051/vetres:200657>
- Fuchs, W., Veits, J., & Mettenleiter, T. C. (2006). Recombinant viruses of poultry as vector vaccines against fowl plague. *Berliner und Munchener tierarztliche Wochenschrift*, 119(3–4), 160–166.
- Fuchs, W., Ziemann, K., Teifke, J. P., Werner, O., & Mettenleiter, T. C. (2000). The non-essential UL50 gene of avian infectious laryngotracheitis virus encodes a functional dUTPase which is not a virulence factor. *Journal of General Virology*,

81(3), 627–638. <https://doi.org/10.1099/0022-1317-81-3-627>

Ganar, K., Das, M., Sinha, S., & Kumar, S. (2014). Newcastle disease virus: Current status and our understanding. *Virus Research*, 184, 71–81.

<https://doi.org/10.1016/j.virusres.2014.02.016>

Garcia, P., Wang, Y., Viallet, J., & Macek Jilkova, Z. (2021). The Chicken Embryo Model: A Novel and Relevant Model for Immune-Based Studies. *Frontiers in Immunology*, 12(November), 1–16. <https://doi.org/10.3389/fimmu.2021.791081>

Garnier, J., Gibrat, J.-F., & Robson, B. (1996). GOR method for predicting protein secondary structure from amino acid sequence. In *Computer Methods for Macromolecular Sequence Analysis* (Vol. 266, pp. 540–553). Academic Press.

[https://doi.org/https://doi.org/10.1016/S0076-6879\(96\)66034-0](https://doi.org/https://doi.org/10.1016/S0076-6879(96)66034-0)

Gasiunas, G., Barrangou, R., Horvath, P., & Siksnys, V. (2012). Cas9-crRNA ribonucleoprotein complex mediates specific DNA cleavage for adaptive immunity in bacteria. *Proceedings of the National Academy of Sciences of the United States of America*, 109(39), 2579–2586.

<https://doi.org/10.1073/pnas.1208507109>

Gasteiger, E., Hoogland, C., Gattiker, A., Duvaud, S., Wilkins, M. R., Appel, R. D., & Bairoch, A. (2005). *Protein Identification and Analysis Tools on the ExPASy Server BT - The Proteomics Protocols Handbook* (J. M. Walker (ed.); pp. 571–607). Humana Press. <https://doi.org/10.1385/1-59259-890-0:571>

Ge, J., Liu, Y., Jin, L., Gao, D., Bai, C., & Ping, W. (2016). Construction of recombinant baculovirus vaccines for Newcastle disease virus and an assessment of their immunogenicity. *Journal of Biotechnology*, 231, 201–211.

<https://doi.org/https://doi.org/10.1016/j.jbiotec.2016.03.037>

Gelb Jr, J., Weisman, Y., Ladman, B. S., & Meir, R. (2005). S1 gene characteristics

- and efficacy of vaccination against infectious bronchitis virus field isolates from the United States and Israel (1996 to 2000). *Avian Pathology*, 34(3), 194–203. <https://doi.org/10.1080/03079450500096539>
- Genzel, Y. (2015). Designing cell lines for viral vaccine production: Where do we stand? *Biotechnology Journal*, 10(5), 728–740. <https://doi.org/10.1002/biot.201400388>
- Gerdt, V., Wilson, H. L., Meurens, F., van Drunen Littel - van den Hurk, S., Wilson, D., Walker, S., Wheler, C., Townsend, H., & Potter, A. A. (2015). Large Animal Models for Vaccine Development and Testing. *ILAR Journal*, 56(1), 53–62. <https://doi.org/10.1093/ilar/ilv009>
- Gergen, L., Cook, S., Ledesma, B., Cress, W., Higuchi, D., Counts, D., Cruz-Coy, J., Crouch, C., Davis, P., Tarpey, I., & Morsey, M. (2019). A double recombinant herpes virus of turkeys for the protection of chickens against Newcastle, infectious laryngotracheitis and Marek's diseases. *Avian Pathology: Journal of the W.V.P.A.*, 48(1), 45–56. <https://doi.org/10.1080/03079457.2018.1546376>
- Ghorbani, A., Moosakhani, F., & Marandi, M. V. (2016). Phylogenetic analysis of the hemagglutinin gene of recent H9N2 avian influenza viruses isolated from broiler flocks in Iran. *Veterinarski Arhiv*, 86(1), 95–109.
- Glick, B., Chang, T. S., & Jaap, R. G. (1956). The Bursa of Fabricius and Antibody Production. *Poultry Science*, 35(1), 224–225. <https://doi.org/https://doi.org/10.3382/ps.0350224>
- Godoy, A., Icard, A., Martinez, M., Mashchenko, A., García, M., & El-Attrache, J. (2013). Detection of Infectious Laryngotracheitis Virus Antibodies by Glycoprotein-Specific ELISAs in Chickens Vaccinated with Viral Vector Vaccines. *Avian Diseases*, 57(2s1), 432–436. <https://doi.org/10.1637/10345->

090312-Reg.1

Gong, Y., Chen, T., Feng, N., Meng, X., Sun, W., Wang, T., Zhao, Y., Yang, S., Song, X., Li, W., Dong, H., Wang, H., He, H., Wang, J., Zhang, L., Gao, Y., & Xia, X. (2020). A highly efficient recombinant canarypox virus-based vaccine against canine distemper virus constructed using the CRISPR/Cas9 gene editing method. *Veterinary Microbiology*, *251*, 108920.

<https://doi.org/10.1016/j.vetmic.2020.108920>

Gowthaman, V., Kumar, S., Koul, M., Dave, U., Murthy, T. R. G. K., Munuswamy, P., Tiwari, R., Karthik, K., Dhama, K., Michalak, I., & Joshi, S. K. (2020). Infectious laryngotracheitis: Etiology, epidemiology, pathobiology, and advances in diagnosis and control - a comprehensive review. *The Veterinary Quarterly*, *40*(1), 140–161. <https://doi.org/10.1080/01652176.2020.1759845>

Grigorov, B., Rabilloud, J., Lawrence, P., & Gerlier, D. (2011). Rapid titration of measles and other viruses: optimization with determination of replication cycle length. *PloS One*, *6*(9), e24135.

Gruffat, H., Marchione, R., & Manet, E. (2016). Herpesvirus Late Gene Expression: A Viral-Specific Pre-initiation Complex Is Key . In *Frontiers in Microbiology* (Vol. 7). <https://www.frontiersin.org/articles/10.3389/fmicb.2016.00869>

Gummow, B. (2010). Challenges posed by new and re-emerging infectious diseases in livestock production, wildlife and humans. *Livestock Science*, *130*(1–3), 41–46. <https://doi.org/10.1016/j.livsci.2010.02.009>

Guo, P., Scholz, E., Turek, J., Nodgreen, R., & Maloney, B. (1993). Assembly pathway of avian infectious laryngotracheitis virus. *American Journal of Veterinary Research*, *54*(12), 2031–2039.

Haeussler, M., Schönig, K., Eckert, H., Eschstruth, A., Mianné, J., Renaud, J. B.,

- Schneider-Maunoury, S., Shkumatava, A., Teboul, L., Kent, J., Joly, J. S., & Concordet, J. P. (2016). Evaluation of off-target and on-target scoring algorithms and integration into the guide RNA selection tool CRISPOR. *Genome Biology*, 17(1), 1–12. <https://doi.org/10.1186/s13059-016-1012-2>
- Han, M. G., Kweon, C. H., Mo, I. P., & Kim, S. J. (2002). Pathogenicity and vaccine efficacy of a thymidine kinase gene deleted infectious laryngotracheitis virus expressing the green fluorescent protein gene. *Archives of Virology*, 147(5), 1017–1031. <https://doi.org/10.1007/s00705-001-0794-y>
- Hansson, M., Nygren, P.-A., & Staahl, S. (2000). Design and production of recombinant subunit vaccines. *Biotechnology and Applied Biochemistry*, 32(2), 95–107. <https://doi.org/https://doi.org/10.1042/BA20000034>
- Hatcher, E. L., Zhdanov, S. A., Bao, Y., Blinkova, O., Nawrocki, E. P., Ostapchuck, Y., Schaffer, A. A., & Rodney Brister, J. (2017). Virus Variation Resource-improved response to emergent viral outbreaks. *Nucleic Acids Research*, 45(D1), D482–D490. <https://doi.org/10.1093/nar/gkw1065>
- Haut, L., Pinto, A. R., Federal, U., Catarina, D. S., & Drive, R. (2005). *Recombinant viruses as vaccines against viral diseases*. 38, 509–522.
- He, Xiangchuan, Zhang, M., Zhao, C., Zheng, P., Zhang, X., & Xu, J. (2021). From Monovalent to Multivalent Vaccines, the Exploration for Potential Preventive Strategies Against Hand, Foot, and Mouth Disease (HFMD). *Virologica Sinica*, 36(2), 167–175. <https://doi.org/10.1007/s12250-020-00294-3>
- He, Xiangjun, Tan, C., Wang, F., Wang, Y., Zhou, R., Cui, D., You, W., Zhao, H., Ren, J., & Feng, B. (2016). Knock-in of large reporter genes in human cells via CRISPR/Cas9-induced homology-dependent and independent DNA repair. *Nucleic Acids Research*, 44(9), e85. <https://doi.org/10.1093/nar/gkw064>



- He, Y., Qian, P., Zhang, K., Yao, Q., Wang, D., Xu, Z., Wu, B., Jin, M., Xiao, S., & Chen, H. (2008). Construction and immune response characterization of a recombinant pseudorabies virus co-expressing capsid precursor protein (P1) and a multiepitope peptide of foot-and-mouth disease virus in swine. *Virus Genes*, 36(2), 393–400. <https://doi.org/10.1007/s11262-008-0204-6>
- Heidary, M., Kaviar, V. H., Shirani, M., Ghanavati, R., Motahar, M., Sholeh, M., Ghahramanpour, H., & Khoshnood, S. (2022). A Comprehensive Review of the Protein Subunit Vaccines Against COVID-19 . In *Frontiers in Microbiology* (Vol. 13). <https://www.frontiersin.org/articles/10.3389/fmicb.2022.927306>
- Hinshaw, V. S., Olsen, C. W., Dybdahl-Sissoko, N., & Evans, D. (1994). Apoptosis: a mechanism of cell killing by influenza A and B viruses. *Journal of Virology*, 68(6), 3667–3673. <https://doi.org/10.1128/jvi.68.6.3667-3673.1994>
- Holman, D. H., Wang, D., Woraratanadharm, J., & Dong, J. Y. (2009). Viral Vectors. In *Vaccines for Biodefense and Emerging and Neglected Diseases* (pp. 77–91). <https://doi.org/10.1016/B978-0-12-369408-9.00007-X>
- Honess, R. W. (1984). Herpes Simplex and “The Herpes Complex”: Diverse Observations and A Unifying Hypothesis. *Journal of General Virology*, 65(12), 2077–2107. <https://doi.org/10.1099/0022-1317-65-12-2077>
- Honess, R. W., Buchan, A., Halliburton, I. W., & Watson, D. H. (1980). Recombination and linkage between structural and regulatory genes of herpes simplex virus type 1: study of the functional organization of the genome. *Journal of Virology*, 34(3), 716–742. <https://doi.org/10.1128/jvi.34.3.716-742.1980>
- Hong, Q., Qian, P., Li, X.-M., Yu, X.-L., & Chen, H.-C. (2007). A recombinant pseudorabies virus co-expressing capsid proteins precursor P1-2A of FMDV and VP2 protein of porcine parvovirus: a trivalent vaccine candidate.

*Biotechnology Letters*, 29(11), 1677–1683. <https://doi.org/10.1007/s10529-007-9459-6>

Horimoto, T., & Kawaoka, Y. (1994). Reverse genetics provides direct evidence for a correlation of hemagglutinin cleavability and virulence of an avian influenza A virus. *Journal of Virology*, 68(5), 3120–3128.

<https://doi.org/10.1128/JVI.68.5.3120-3128.1994>

Houta, M. H., Hassan, K. E., El-Sawah, A. A., Elkady, M. F., Kilany, W. H., Ali, A., & Abdel-Moneim, A. S. (2021). The emergence, evolution and spread of infectious bronchitis virus genotype GI-23. *Archives of Virology*, 166(1), 9–26.

<https://doi.org/10.1007/s00705-020-04920-z>

Hsu, P. D., Lander, E. S., & Zhang, F. (2014). *Development and Applications of CRISPR-Cas9 for Genome Engineering*. 157(6), 1262–1278.

<https://doi.org/10.1016/j.cell.2014.05.010.Development>

Hu, W., Kaminski, R., Yang, F., Zhang, Y., Cosentino, L., Li, F., Luo, B., Alvarez-Carbonell, D., Garcia-Mesa, Y., Karn, J., Mo, X., & Khalili, K. (2014). RNA-directed gene editing specifically eradicates latent and prevents new HIV-1 infection. *Proceedings of the National Academy of Sciences*, 111(31), 11461–11466. <https://doi.org/10.1073/pnas.1405186111>

Hu, Zenglei, He, X., Deng, J., Hu, J., & Liu, X. (2022). Current situation and future direction of Newcastle disease vaccines. *Veterinary Research*, 53(1), 99.

<https://doi.org/10.1186/s13567-022-01118-w>

Hu, Zenglei, Ni, J., Cao, Y., & Liu, X. (2020). Newcastle disease virus as a vaccine vector for 20 years: A focus on maternally derived antibody interference.

*Vaccines*, 8(2). <https://doi.org/10.3390/vaccines8020222>

Hu, Zheng, Yu, L., Zhu, D., Ding, W., Wang, X., Zhang, C., Wang, L., Jiang, X.,

- Shen, H., He, D., Li, K., Xi, L., Ma, D., & Wang, H. (2014). Disruption of HPV16-E7 by CRISPR/Cas system induces apoptosis and growth inhibition in HPV16 positive human cervical cancer cells. *BioMed Research International*, 2014, 612823. <https://doi.org/10.1155/2014/612823>
- Hulo, C., de Castro, E., Masson, P., Bougueleret, L., Bairoch, A., Xenarios, I., & Le Mercier, P. (2011). ViralZone: a knowledge resource to understand virus diversity. *Nucleic Acids Research*, 39(Database issue), D576-82. <https://doi.org/10.1093/nar/gkq901>
- Ibba, G., Piu, C., Uleri, E., Serra, C., & Dolei, A. (2018). Disruption by SaCas9 Endonuclease of HERV-Kenv, a Retroviral Gene with Oncogenic and Neuropathogenic Potential, Inhibits Molecules Involved in Cancer and Amyotrophic Lateral Sclerosis. *Viruses*, 10(8). <https://doi.org/10.3390/v10080412>
- Imran, M. S., Aslam, A., Yasin, M., Yaqoob, T., & Zahid, B. (2020). A Comparative Assessment of Efficacy of Currently Applied Vaccines in Broiler Chicken against Individual and Co-Infection with Field Prevailing Newcastle Disease and Infectious Bronchitis Viruses. *Pakistan Journal of Zoology*, 52(5), 1895–1901. <https://doi.org/10.17582/journal.pjz/20190424090449>
- Iorio, R. M., & Mahon, P. J. (2008). Paramyxoviruses: different receptors - different mechanisms of fusion. *Trends in Microbiology*, 16(4), 135–137. <https://doi.org/10.1016/j.tim.2008.01.006>
- Jackwood, M. W., Hall, D., & Handel, A. (2012). Molecular evolution and emergence of avian gammacoronaviruses. *Infection, Genetics and Evolution*, 12(6), 1305–1311. <https://doi.org/https://doi.org/10.1016/j.meegid.2012.05.003>
- Jefferis, R. (2009). Recombinant antibody therapeutics: the impact of glycosylation

- on mechanisms of action. *Trends in Pharmacological Sciences*, 30(7), 356–362. <https://doi.org/10.1016/j.tips.2009.04.007>
- Jegaskanda, S. (2018). The potential role of fc-receptor functions in the development of a universal influenza vaccine. *Vaccines*, 6(2). <https://doi.org/10.3390/vaccines6020027>
- Jiang, L., Zhao, W., Han, Z., Chen, Y., Zhao, Y., Sun, J., Li, H., Shao, Y., Liu, L., & Liu, S. (2017). Genome characterization, antigenicity and pathogenicity of a novel infectious bronchitis virus type isolated from south China. *Infection, Genetics and Evolution*, 54, 437–446. <https://doi.org/https://doi.org/10.1016/j.meegid.2017.08.006>
- Jiang, Y., Fang, L., Xiao, S., Zhang, H., Pan, Y., Luo, R., Li, B., & Chen, H. (2007). Immunogenicity and protective efficacy of recombinant pseudorabies virus expressing the two major membrane-associated proteins of porcine reproductive and respiratory syndrome virus. *Vaccine*, 25(3), 547–560. <https://doi.org/https://doi.org/10.1016/j.vaccine.2006.07.032>
- Jinek, M., Chylinski, K., Fonfara, I., Hauer, M., Doudna, J. A., & Charpentier, E. (2012). A programmable dual-RNA-guided DNA endonuclease in adaptive bacterial immunity. *Science*, 337(6096), 816–821. <https://doi.org/10.1126/science.1225829>
- Jinek, M., East, A., Cheng, A., Lin, S., Ma, E., & Doudna, J. (2013). RNA-programmed genome editing in human cells. *ELife*, 2, e00471. <https://doi.org/10.7554/eLife.00471>
- Johnson, M. A., Prideaux, C. T., Kongsuwan, K., Sheppard, M., & Fahey, K. J. (1991). Gallid herpesvirus 1 (infectious laryngotracheitis virus): cloning and physical maps of the SA-2 strain. *Archives of Virology*, 119(3), 181–198.

<https://doi.org/10.1007/BF01310669>

Jones, D. T., Taylor, W. R., & Thornton, J. M. (1992). The rapid generation of mutation data matrices from protein sequences. *Computer Applications in the Biosciences : CABIOS*, 8(3), 275–282.

<https://doi.org/10.1093/bioinformatics/8.3.275>

Josefsberg, J. O., & Buckland, B. (2012). Vaccine process technology.

*Biotechnology and Bioengineering*, 109(6), 1443–1460.

<https://doi.org/10.1002/bit.24493>

Ju, C., Fan, H., Tan, Y., Liu, Z., Xi, X., Cao, S., Wu, B., & Chen, H. (2005).

Immunogenicity of a recombinant pseudorabies virus expressing ORF1–ORF2 fusion protein of porcine circovirus type 2. *Veterinary Microbiology*, 109(3), 179–190. <https://doi.org/https://doi.org/10.1016/j.vetmic.2005.06.001>

Jung, B.-K., An, Y., Park, J.-E., Chang, K.-S., & Jang, H. (2022). Development of a recombinant vaccine containing a spike S1-Fc fusion protein induced protection against MERS-CoV in human DPP4 knockin transgenic mice. *Journal of Virological Methods*, 299, 114347.

<https://doi.org/10.1016/j.jviromet.2021.114347>

Jung, H. E., & Lee, H. K. (2020). Host Protective Immune Responses against Influenza A Virus Infection. In *Viruses* (Vol. 12, Issue 5).

<https://doi.org/10.3390/v12050504>

Kamel, M., & El-Sayed, A. (2019). Utilization of herpesviridae as recombinant viral vectors in vaccine development against animal pathogens. *Virus Research*, 270(January), 197648. <https://doi.org/10.1016/j.virusres.2019.197648>

Kanabagatte Basavarajappa, M., Kumar, S., Khattar, S. K., Gebreluul, G. T.,

Paldurai, A., & Samal, S. K. (2014). A recombinant Newcastle disease virus

- (NDV) expressing infectious laryngotracheitis virus (ILTV) surface glycoprotein D protects against highly virulent ILTV and NDV challenges in chickens. *Vaccine*, 32(28), 3555–3563. <https://doi.org/10.1016/j.vaccine.2014.04.068>
- Kanekiyo, M., Ellis, D., & King, N. P. (2019). New Vaccine Design and Delivery Technologies. *Journal of Infectious Diseases*, 219(Suppl 1), S88–S96. <https://doi.org/10.1093/infdis/jiy745>
- Kant, A., Koch, G., Van Roozelaar, D. J., Kusters, J. G., Poelwijk, F. A. J., & Van der Zeijst, B. A. M. (1992). Location of antigenic sites defined by neutralizing monoclonal antibodies on the S1 avian infectious bronchitis virus glycopolyptide. *Journal of General Virology*, 73(3), 591–596.
- Kapczynski, D. R., Esaki, M., Dorsey, K. M., Jiang, H., Jackwood, M., Moraes, M., & Gardin, Y. (2015). Vaccine protection of chickens against antigenically diverse H5 highly pathogenic avian influenza isolates with a live HVT vector vaccine expressing the influenza hemagglutinin gene derived from a clade 2.2 avian influenza virus. *Vaccine*, 33(9), 1197–1205. <https://doi.org/https://doi.org/10.1016/j.vaccine.2014.12.028>
- Karlsson, M., Kollberg, H., & Larsson, A. (2004). Chicken IgY: utilizing the evolutionary advantage. *World's Poultry Science Journal*, 60(3), 341–348. <https://doi.org/10.1079/WPS200422>
- Kawaguchi, T., Nomura, K., Hirayama, Y., & Kitagawa, T. (1987). Establishment and characterization of a chicken hepatocellular carcinoma cell line, LMH. *Cancer Research*, 47(16), 4460–4464.
- Kennedy, E. M., Kornepati, A. V. R., & Cullen, B. R. (2015). Targeting hepatitis B virus cccDNA using CRISPR/Cas9. *Antiviral Research*, 123, 188–192. <https://doi.org/https://doi.org/10.1016/j.antiviral.2015.10.004>

- Khan, S., Ullah, M. W., Siddique, R., Nabi, G., Manan, S., Yousaf, M., & Hou, H. (2016). Role of recombinant DNA technology to improve life. *International Journal of Genomics*, 2016. <https://doi.org/10.1155/2016/2405954>
- Khan, T. A., Rue, C. A., Rehmani, S. F., Ahmed, A., Wasilenko, J. L., Miller, P. J., & Afonso, C. L. (2010). Phylogenetic and biological characterization of Newcastle disease virus isolates from Pakistan. *Journal of Clinical Microbiology*, 48(5), 1892–1894. <https://doi.org/10.1128/JCM.00148-10>
- Kim, S.-H., & Samal, S. K. (2016). Newcastle Disease Virus as a Vaccine Vector for Development of Human and Veterinary Vaccines. *Viruses*, 8(7). <https://doi.org/10.3390/v8070183>
- Kingsley, D. H., Hazel, J. W., & Keeler, C. L. J. (1994). Identification and characterization of the infectious laryngotracheitis virus glycoprotein C gene. *Virology*, 203(2), 336–343. <https://doi.org/10.1006/viro.1994.1492>
- Kingsley, D. H., & Keeler, C. L. J. (1999). Infectious laryngotracheitis virus, an alpha herpesvirus that does not interact with cell surface heparan sulfate. *Virology*, 256(2), 213–219. <https://doi.org/10.1006/viro.1999.9609>
- Kirkpatrick, N. C., Mahmoudian, A., Colson, C. A., Devlin, J. M., & Noormohammadi, A. H. (2006). Relationship between mortality, clinical signs and tracheal pathology in infectious laryngotracheitis. *Avian Pathology: Journal of the W.V.P.A.*, 35(6), 449–453. <https://doi.org/10.1080/03079450601028803>
- Kit, M., Kit, S., Little, S. P., Di Marchi, R. D., & Gale, C. (1991). Bovine herpesvirus-1 (infectious bovine rhinotracheitis virus)-based viral vector which expresses foot-and-mouth disease epitopes. *Vaccine*, 9(8), 564–572. [https://doi.org/https://doi.org/10.1016/0264-410X\(91\)90243-Y](https://doi.org/https://doi.org/10.1016/0264-410X(91)90243-Y)
- Kit, S., Kit, M., & Pirtle, E. C. (1985). Attenuated properties of thymidine kinase-

- negative deletion mutant of pseudorabies virus. *American Journal of Veterinary Research*, 46(6), 1359–1367. <http://europepmc.org/abstract/MED/2992322>
- Klenk, H. D., Rott, R., Orlich, M., & Blödorn, J. (1975). Activation of influenza A viruses by trypsin treatment. *Virology*, 68(2), 426–439.  
[https://doi.org/10.1016/0042-6822\(75\)90284-6](https://doi.org/10.1016/0042-6822(75)90284-6)
- Klingbeil, K., Lange, E., Blohm, U., Teifke, J. P., Mettenleiter, T. C., & Fuchs, W. (2015). Protection of pigs against pandemic swine origin H1N1 influenza A virus infection by hemagglutinin- or neuraminidase-expressing attenuated pseudorabies virus recombinants. *Virus Research*, 199, 20–30.  
<https://doi.org/https://doi.org/10.1016/j.virusres.2015.01.009>
- Klingbeil, K., Lange, E., Teifke, J. P., Mettenleiter, T. C., & Fuchs, W. (2014). Immunization of pigs with an attenuated pseudorabies virus recombinant expressing the haemagglutinin of pandemic swine origin H1N1 influenza A virus. *Journal of General Virology*, 95(4), 948–959.  
<https://doi.org/10.1099/vir.0.059253-0>
- Klupp, B. G., Hengartner, C. J., Mettenleiter, T. C., & Enquist, L. W. (2004). Complete, Annotated Sequence of the Pseudorabies Virus Genome. *Journal of Virology*, 78(4), 2166–2166. <https://doi.org/10.1128/jvi.78.4.2166.2004>
- Krogh, A., Larsson, B., Von Heijne, G., & Sonnhammer, E. L. L. (2001). Predicting transmembrane protein topology with a hidden Markov model: application to complete genomes. *Journal of Molecular Biology*, 305(3), 567–580.
- Kusters, J. G., Niesters, H. G. M., Lenstra, J. A., Horzinek, M. C., & Van Der Zeijst, B. A. M. (1989). Phylogeny of antigenic variants of avian coronavirus IBV. *Virology*, 169(1), 217–221.
- Labun, K., Montague, T. G., Gagnon, J. A., Thyme, S. B., & Valen, E. (2016).



CHOPCHOP v2: a web tool for the next generation of CRISPR genome engineering. *Nucleic Acids Research*, 44(W1), W272–W276.

<https://doi.org/10.1093/nar/gkw398>

Lambeth, L. S., Zhao, Y., Smith, L. P., Kgosana, L., & Nair, V. (2009). Targeting Marek's disease virus by RNA interference delivered from a herpesvirus vaccine. *Vaccine*, 27(2), 298–306.

<https://doi.org/https://doi.org/10.1016/j.vaccine.2008.10.023>

Lauer, K. B., Borrow, R., & Blanchard, T. J. (2017). Multivalent and multipathogen viral vector vaccines. In *Clinical and Vaccine Immunology* (Vol. 24, Issue 1).

<https://doi.org/10.1128/CVI.00298-16>

Lauring, A. S., Jones, J. O., & Andino, R. (2010). Rationalizing the development of live attenuated virus vaccines. *Nature Biotechnology*, 28(6), 573–579.

<https://doi.org/10.1038/nbt.1635>

Lazear, E., Whitbeck, J. C., Ponce-de-Leon, M., Cairns, T. M., Willis, S. H., Zuo, Y., Krummenacher, C., Cohen, G. H., & Roselyn, E. J. (2012). Antibody-Induced Conformational Changes in Herpes Simplex Virus Glycoprotein gD Reveal New Targets for Virus Neutralization. *Journal of Virology*, 86(3), 1563–1576.

<https://doi.org/10.1128/JVI.06480-11>

Lebbink, R. J., de Jong, D. C. M., Wolters, F., Kruse, E. M., van Ham, P. M., Wiertz, E. J. H. J., & Nijhuis, M. (2017). A combinational CRISPR/Cas9 gene-editing approach can halt HIV replication and prevent viral escape. *Scientific Reports*, 7(1), 41968. <https://doi.org/10.1038/srep41968>

Lee, H. J., Lee, K. Y., Jung, K. M., Park, K. J., Lee, K. O., Suh, J. Y., Yao, Y., Nair, V., & Han, J. Y. (2017). Precise gene editing of chicken Na<sup>+</sup>/H<sup>+</sup> exchange type 1 (chNHE1) confers resistance to avian leukosis virus subgroup J (ALV-J).

*Developmental and Comparative Immunology*, 77, 340–349.

<https://doi.org/10.1016/j.dci.2017.09.006>

Lee, S.-W., Hartley, C. A., Coppo, M. J. C., Vaz, P. K., Legione, A. R., Quinteros, J. A., Noormohammadi, A. H., Markham, P. F., Browning, G. F., & Devlin, J. M. (2015). Growth kinetics and transmission potential of existing and emerging field strains of infectious laryngotracheitis virus. *PloS One*, 10(3), e0120282–e0120282. <https://doi.org/10.1371/journal.pone.0120282>

Lee, S.-W., Markham, P. F., Markham, J. F., Petermann, I., Noormohammadi, A. H., Browning, G. F., Ficorilli, N. P., Hartley, C. A., & Devlin, J. M. (2011). First complete genome sequence of infectious laryngotracheitis virus. *BMC Genomics*, 12, 197. <https://doi.org/10.1186/1471-2164-12-197>

Lee, W., Syed Atif, A., Tan, S. C., & Leow, C. H. (2017). Insights into the chicken IgY with emphasis on the generation and applications of chicken recombinant monoclonal antibodies. *Journal of Immunological Methods*, 447, 71–85. <https://doi.org/10.1016/j.jim.2017.05.001>

Legnardi, M., Tucciarone, C. M., Franzo, G., & Cecchinato, M. (2020). Infectious bronchitis virus evolution, diagnosis and control. *Veterinary Sciences*, 7(2), 1–18. <https://doi.org/10.3390/vetsci7020079>

Leib, D. A., Bradbury, J. M., Hart, C. A., & McCarthy, K. (1987). Genome isomerism in two alphaherpesviruses: Herpesvirus saimiri-1 (Herpesvirus tamarinus) and avian infectious laryngotracheitis virus. *Archives of Virology*, 93(3), 287–294. <https://doi.org/10.1007/BF01310982>

Li, F. (2016). Structure, Function, and Evolution of Coronavirus Spike Proteins. *Annual Review of Virology*, 3(1), 237–261. <https://doi.org/10.1146/annurev-virology-110615-042301>

- Li, J., Ulitzky, L., Silberstein, E., Taylor, D. R., & Viscidi, R. (2013). Immunogenicity and protection efficacy of monomeric and trimeric recombinant SARS coronavirus spike protein subunit vaccine candidates. *Viral Immunology*, *26*(2), 126–132. <https://doi.org/10.1089/vim.2012.0076>
- Li, L., Kang, H., Liu, P., Makkinje, N., Williamson, S. T., Leibowitz, J. L., & Giedroc, D. P. (2008). Structural Lability in Stem–Loop 1 Drives a 5' UTR–3' UTR Interaction in Coronavirus Replication. *Journal of Molecular Biology*, *377*(3), 790–803. <https://doi.org/https://doi.org/10.1016/j.jmb.2008.01.068>
- Li, X., Liu, R., Tang, H., Jin, M., Chen, H., & Qian, P. (2008). Induction of protective immunity in swine by immunization with live attenuated recombinant pseudorabies virus expressing the capsid precursor encoding regions of foot-and-mouth disease virus. *Vaccine*, *26*(22), 2714–2722. <https://doi.org/https://doi.org/10.1016/j.vaccine.2008.03.020>
- Li, Yonghua, Rehman, Z. U., Li, M., Manzoor, Z., Liu, W., Qiu, X., Sun, Y., Liao, Y., Tan, L., Song, C., Liu, W., Yu, S., Ding, C., & Meng, C. (2021). Comparison of the protective antigen variabilities of prevalent Newcastle disease viruses in response to homologous/heterologous genotype vaccines. *Poultry Science*, *100*(8), 101267. <https://doi.org/10.1016/j.psj.2021.101267>
- Li, Yongqing, Reddy, K., Reid, S. M., Cox, W. J., Brown, I. H., Britton, P., Nair, V., & Iqbal, M. (2011). Recombinant herpesvirus of turkeys as a vector-based vaccine against highly pathogenic H7N1 avian influenza and Marek's disease. *Vaccine*, *29*(46), 8257–8266. <https://doi.org/10.1016/j.vaccine.2011.08.115>
- Li, Z., Ling, L., Liu, X., Laus, R., & Delcayre, A. (2010). A flow cytometry-based immuno-titration assay for rapid and accurate titer determination of modified vaccinia Ankara virus vectors. *Journal of Virological Methods*, *169*(1), 87–94.

- Liang, X., Sun, L., Yu, T., Pan, Y., Wang, D., Hu, X., Fu, Z., He, Q., & Cao, G. (2016). A CRISPR/Cas9 and Cre/Lox system-based express vaccine development strategy against re-emerging Pseudorabies virus. *Scientific Reports*, 6(December 2015), 1–10. <https://doi.org/10.1038/srep19176>
- Liao, H.-K., Gu, Y., Diaz, A., Marlett, J., Takahashi, Y., Li, M., Suzuki, K., Xu, R., Hishida, T., Chang, C.-J., Esteban, C. R., Young, J., & Belmonte, J. C. I. (2015). Use of the CRISPR/Cas9 system as an intracellular defense against HIV-1 infection in human cells. *Nature Communications*, 6(1), 6413. <https://doi.org/10.1038/ncomms7413>
- Liao, Y., Bajwa, K., Reddy, S. M., & Lupiani, B. (2021). Methods for the Manipulation of Herpesvirus Genome and the Application to Marek's Disease Virus Research. In *Microorganisms* (Vol. 9, Issue 6). <https://doi.org/10.3390/microorganisms9061260>
- Lin, H., Li, G., Peng, X., Deng, A., Ye, L., Shi, L., Wang, T., & He, J. (2021). The Use of CRISPR/Cas9 as a Tool to Study Human Infectious Viruses. *Frontiers in Cellular and Infection Microbiology*, 11(August), 1–14. <https://doi.org/10.3389/fcimb.2021.590989>
- Lin, S. R., Yang, H. C., Kuo, Y. T., Liu, C. J., Yang, T. Y., Sung, K. C., Lin, Y. Y., Wang, H. Y., Wang, C. C., Shen, Y. C., Wu, F. Y., Kao, J. H., Chen, D. S., & Chen, P. J. (2014). The CRISPR/Cas9 system facilitates clearance of the intrahepatic HBV templates in vivo. *Molecular Therapy - Nucleic Acids*, 3(June), e186. <https://doi.org/10.1038/mtna.2014.38>
- Linden, C. D., & Roth, T. F. (1978). IgG receptors on foetal chick yolk sac. *Journal of Cell Science*, 33, 317–328. <https://doi.org/10.1242/jcs.33.1.317>
- Lino, C. A., Harper, J. C., Carney, J. P., & Timlin, J. A. (2018). Delivering crispr: A

review of the challenges and approaches. *Drug Delivery*, 25(1), 1234–1257.

<https://doi.org/10.1080/10717544.2018.1474964>

Liu, J.-H., Okazaki, K., Mweene, A., Shi, W.-M., Wu, Q.-M., Su, J.-L., Zhang, G.-Z., Bai, G.-R., & Kida, H. (2004). Genetic conservation of hemagglutinin gene of H9 influenza virus in chicken population in Mainland China. *Virus Genes*, 29, 329–334.

Liu, L., Wang, T., Wang, M., Tong, Q., Sun, Y., Pu, J., Sun, H., & Liu, J. (2019).

Recombinant turkey herpesvirus expressing H9 hemagglutinin providing protection against H9N2 avian influenza. *Virology*, 529(January), 7–15.

<https://doi.org/10.1016/j.virol.2019.01.004>

Liu, Q., Gao, S., Jiang, L., Shang, L., Men, J., Wang, Z., Zhai, Y., Xia, Z., Hu, R.,

Zhang, X., & Zhu, X.-Q. (2008). A recombinant pseudorabies virus expressing TgSAG1 protects against challenge with the virulent *Toxoplasma gondii* RH strain and pseudorabies in BALB/c mice. *Microbes and Infection*, 10(12), 1355–

1362. <https://doi.org/https://doi.org/10.1016/j.micinf.2008.08.002>

Liu, S., Sun, W., Chu, J., Huang, X., Wu, Z., Yan, M., Zhang, Q., Zhao, P.,

Igietseme, J. U., Black, C. M., He, C., & Li, Y. (2015). Construction of Recombinant HVT Expressing PmpD, and Immunological Evaluation against *Chlamydia psittaci* and Marek's Disease Virus. *PLOS ONE*, 10(4), e0124992.

<https://doi.org/10.1371/journal.pone.0124992>

Liu, Y., Xu, Z., Zhang, Y., Yu, M., Wang, S., Gao, Y., Liu, C., Zhang, Y., Gao, L., Qi,

X., Cui, H., Pan, Q., Li, K., & Wang, X. (2020). Marek's disease virus as a CRISPR/Cas9 delivery system to defend against avian leukosis virus infection in chickens. *Veterinary Microbiology*, 242(January), 108589.

<https://doi.org/10.1016/j.vetmic.2020.108589>

- Liu, Z., Xu, W., Xia, S., Gu, C., Wang, X., Wang, Q., Zhou, J., Wu, Y., Cai, X., Qu, D., Ying, T., Xie, Y., Lu, L., Yuan, Z., & Jiang, S. (2020). RBD-Fc-based COVID-19 vaccine candidate induces highly potent SARS-CoV-2 neutralizing antibody response. *Signal Transduction and Targeted Therapy*, 5(1), 282.  
<https://doi.org/10.1038/s41392-020-00402-5>
- Liverani, M., Waage, J., Barnett, T., Pfeiffer, D. U., Rushton, J., Rudge, J. W., Loevinsohn, M. E., Scoones, I., Smith, R. D., Cooper, B. S., White, L. J., Goh, S., Horby, P., Wren, B., Gundogdu, O., Woods, A., & Coker, R. J. (2013). Understanding and managing zoonotic risk in the new livestock industries. *Environmental Health Perspectives*, 121(8), 873–877.  
<https://doi.org/10.1289/ehp.1206001>
- Loera-Muro, A., & Angulo, C. (2018). New trends in innovative vaccine development against *Actinobacillus pleuropneumoniae*. *Veterinary Microbiology*, 217, 66–75.  
<https://doi.org/https://doi.org/10.1016/j.vetmic.2018.02.028>
- Logan, M., Manalil, J., Notte, C., Kearse, C., George, S., Zeiser, A., Farrell, P., & Aucoin, M. G. (2019). A flow cytometric granularity assay for the quantification of infectious virus. *Vaccine*, 37(47), 7090–7099.  
<https://doi.org/https://doi.org/10.1016/j.vaccine.2019.02.059>
- Loke, C. F., Omar, A. R., Raha, A. R., & Yusoff, K. (2005). Improved protection from velogenic Newcastle disease virus challenge following multiple immunizations with plasmid DNA encoding for F and HN genes. *Veterinary Immunology and Immunopathology*, 106(3), 259–267.  
<https://doi.org/https://doi.org/10.1016/j.vetimm.2005.03.005>
- Lonsdale, R., Pau, M. G., Oerlemans, M., Ophorst, C., Vooy, A., Havenga, M., Goudsmit, J., UytdeHaag, F., & Marzio, G. (2003). A rapid method for

immunotitration of influenza viruses using flow cytometry. *Journal of Virological Methods*, 110(1), 67–71.

Loureiro, S., Ren, J., Phapugrangkul, P., Colaco, C. A., Bailey, C. R., Shelton, H., Molesti, E., Temperton, N. J., Barclay, W. S., & Jones, I. M. (2011). Adjuvant-Free Immunization with Hemagglutinin-Fc Fusion Proteins as an Approach to Influenza Vaccines. *Journal of Virology*, 85(6), 3010–3014.

<https://doi.org/10.1128/jvi.01241-10>

Lu, Z., Yu, S., Wang, W., Chen, W., Wang, X., Wu, K., Li, X., Fan, S., Ding, H., Yi, L., & Chen, J. (2022). Development of Foot-and-Mouth Disease Vaccines in Recent Years. *Vaccines*, 10(11). <https://doi.org/10.3390/vaccines10111817>

Lundstrom, K. (2014). Alphavirus-based vaccines. *Viruses*, 6(6), 2392–2415.

<https://doi.org/10.3390/v6062392>

Lüschow, D., Werner, O., Mettenleiter, T. C., & Fuchs, W. (2001). Protection of chickens from lethal avian influenza A virus infection by live-virus vaccination with infectious laryngotracheitis virus recombinants expressing the hemagglutinin (H5) gene. *Vaccine*, 19(30), 4249–4259.

[https://doi.org/10.1016/s0264-410x\(01\)00167-0](https://doi.org/10.1016/s0264-410x(01)00167-0)

Ma, G., Eschbaumer, M., Said, A., Hoffmann, B., Beer, M., & Osterrieder, N. (2012). An Equine Herpesvirus Type 1 (EHV-1) Expressing VP2 and VP5 of Serotype 8 Bluetongue Virus (BTV-8) Induces Protection in a Murine Infection Model. *PLOS ONE*, 7(4), e34425. <https://doi.org/10.1371/journal.pone.0034425>

Ma, Y., Zhang, X., Shen, B., Lu, Y., Chen, W., Ma, J., Bai, L., Huang, X., & Zhang, L. (2014). Generating rats with conditional alleles using CRISPR/Cas9. *Cell Research*, 24(1), 122–125. <https://doi.org/10.1038/cr.2013.157>

Macchi, F., Rojas, J. M., Verna, A. E., Sevilla, N., Franceschi, V., Tebaldi, G.,

- Cavirani, S., Martín, V., & Donofrio, G. (2018). Bovine Herpesvirus-4-Based Vector Delivering Peste des Petits Ruminants Virus Hemagglutinin ORF Induces both Neutralizing Antibodies and Cytotoxic T Cell Responses . In *Frontiers in Immunology* (Vol. 9).  
<https://www.frontiersin.org/articles/10.3389/fimmu.2018.00421>
- Mahmoudian, A., Markham, P. F., Noormohammadi, A. H., & Browning, G. F. (2012). Kinetics of transcription of infectious laryngotracheitis virus genes. *Comparative Immunology, Microbiology and Infectious Diseases*, 35(2), 103–115.  
<https://doi.org/https://doi.org/10.1016/j.cimid.2011.11.001>
- Mali, P., Esvelt, K. M., & Church, G. M. (2013). Cas9 for engineering biology. *Nat Methods*, 10(10), 957–963. <https://doi.org/10.1038/nmeth.2649.Cas9>
- Mali, P., Yang, L., Esvelt, K. M., Aach, J., Guell, M., DiCarlo, J. E., Norville, J. E., & Church, G. M. (2013). RNA-guided human genome engineering via Cas9. *Science (New York, N.Y.)*, 339(6121), 823–826.  
<https://doi.org/10.1126/science.1232033>
- Mancardi, D., & Daëron, M. (2014). Fc Receptors in Immune Responses. In *Reference Module in Biomedical Sciences*. <https://doi.org/10.1016/B978-0-12-801238-3.00119-7>
- Marín-López, A., & Ortego, J. (2016). Vaccine Technologies for Veterinary Viral Diseases. In *Methods in Molecular Biology* (Vol. 1349).  
<https://doi.org/10.1007/978-1-4939-3008-1>
- Marschall, M., Freitag, M., Weiler, S., Sorg, G., & Stamminger, T. (2000). Recombinant green fluorescent protein-expressing human cytomegalovirus as a tool for screening antiviral agents. *Antimicrobial Agents and Chemotherapy*, 44(6), 1588–1597. <https://doi.org/10.1128/AAC.44.6.1588-1597.2000>



- Martínez-Flores, D., Zepeda-Cervantes, J., Cruz-Reséndiz, A., Aguirre-Sampieri, S., Sampieri, A., & Vaca, L. (2021). SARS-CoV-2 Vaccines Based on the Spike Glycoprotein and Implications of New Viral Variants . In *Frontiers in Immunology* (Vol. 12, p. 2774).  
<https://www.frontiersin.org/article/10.3389/fimmu.2021.701501>
- Martyn, J. C., Cardin, A. J., Wines, B. D., Cendron, A., Li, S., Mackenzie, J., Powell, M., & Gowans, E. J. (2009). Surface display of IgG Fc on baculovirus vectors enhances binding to antigen-presenting cells and cell lines expressing Fc receptors. *Archives of Virology*, *154*(7), 1129–1138.  
<https://doi.org/10.1007/s00705-009-0423-8>
- Matunis, M. J. (2016). *Vaccines for Veterinary Diseases* (Vol. 1).  
<https://doi.org/10.1007/978-1-4939-2687-9>
- Mayo-Muñoz, D., He, F., Jørgensen, J. B., Madsen, P. K., Bhoobalan-Chitty, Y., & Peng, X. (2018). Anti-crispr-based and crispr-based genome editing of *Sulfolobus islandicus* rod-shaped virus 2. *Viruses*, *10*(12).  
<https://doi.org/10.3390/v10120695>
- McGinnes, L. W., Sergel, T., Chen, H., Hamo, L., Schwertz, S., Li, D., & Morrison, T. G. (2001). Mutational analysis of the membrane proximal heptad repeat of the newcastle disease virus fusion protein. *Virology*, *289*(2), 343–352.  
<https://doi.org/10.1006/viro.2001.1123>
- McKee, A. S., Munks, M. W., & Marrack, P. (2007). How do adjuvants work? Important considerations for new generation adjuvants. *Immunity*, *27*(5), 687–690. <https://doi.org/10.1016/j.immuni.2007.11.003>
- Mefferd, A. L., Bogerd, H. P., Irwan, I. D., & Cullen, B. R. (2018). Insights into the mechanisms underlying the inactivation of HIV-1 proviruses by CRISPR/Cas.

- Virology*, 520, 116–126. <https://doi.org/https://doi.org/10.1016/j.virol.2018.05.016>
- Meng, C., Rehman, Z. U., Liu, K., Qiu, X., Tan, L., Sun, Y., Liao, Y., Song, C., Yu, S., Ding, Z., Nair, V., Munir, M., & Ding, C. (2018). Potential of genotype VII Newcastle disease viruses to cause differential infections in chickens and ducks. *Transboundary and Emerging Diseases*, 65(6), 1851–1862. <https://doi.org/https://doi.org/10.1111/tbed.12965>
- Meng, X. J. (2000). Heterogeneity of porcine reproductive and respiratory syndrome virus: Implications for current vaccine efficacy and future vaccine development. *Veterinary Microbiology*, 74(4), 309–329. [https://doi.org/10.1016/S0378-1135\(00\)00196-6](https://doi.org/10.1016/S0378-1135(00)00196-6)
- Meunier, M., Guyard-Nicodème, M., Hirchaud, E., Parra, A., Chemaly, M., & Dory, D. (2016). Identification of Novel Vaccine Candidates against *Campylobacter* through Reverse Vaccinology. *Journal of Immunology Research*, 2016, 5715790. <https://doi.org/10.1155/2016/5715790>
- Miller, P. J., Decanini, E. L., & Afonso, C. L. (2010). Newcastle disease: evolution of genotypes and the related diagnostic challenges. *Infection, Genetics and Evolution: Journal of Molecular Epidemiology and Evolutionary Genetics in Infectious Diseases*, 10(1), 26–35. <https://doi.org/10.1016/j.meegid.2009.09.012>
- Minor, P. D. (2015). Live attenuated vaccines: Historical successes and current challenges. *Virology*, 479–480, 379–392. <https://doi.org/10.1016/j.virol.2015.03.032>
- Mire, C. E., Geisbert, J. B., Versteeg, K. M., Mamaeva, N., Agans, K. N., Geisbert, T. W., & Connor, J. H. (2015). A Single-Vector, Single-Injection Trivalent Filovirus Vaccine: Proof of Concept Study in Outbred Guinea Pigs. *The Journal of Infectious Diseases*, 212 Suppl(Suppl 2), S384-8.

<https://doi.org/10.1093/infdis/jiv126>

- Mishima, M., Xuan, X., Yokoyama, N., Igarashi, I., Fujisaki, K., Nagasawa, H., & Mikami, T. (2002). Recombinant feline herpesvirus type 1 expressing *Toxoplasma gondii* ROP2 antigen inducible protective immunity in cats. *Parasitology Research*, *88*(2), 144–149. <https://doi.org/10.1007/s004360100429>
- Montague, T. G., Cruz, J. M., Gagnon, J. A., Church, G. M., & Valen, E. (2014). CHOPCHOP: A CRISPR/Cas9 and TALEN web tool for genome editing. *Nucleic Acids Research*, *42*(W1), 401–407. <https://doi.org/10.1093/nar/gku410>
- Morgan, R. W., Gelb, J. J., Pope, C. R., & Sondermeijer, P. J. A. (2017). *Efficacy in Chickens of a Herpesvirus of Turkeys Recombinant Vaccine Containing the Fusion Gene of Newcastle Disease Virus: Onset of Protection and Effect of Maternal Antibodies*. *37*(4), 1032–1040.
- Morgan, R. W., Gelb, J., Schreurs, C. S., Lütticken, D., Rosenberger, K., Sondermeijer, P. J. A., Liitticken, D., Rosenberger, B. J. K., & Sondern, P. J. A. (2019). *Protection of Chickens from Newcastle and Marek ' s Diseases with a Recombinant Herpesvirus of Turkeys Vaccine Expressing the Newcastle Disease Virus Fusion Protein Published by : American Association of Avian Pathologists Stable URL : <https://www.jstor.o>* *36*(4), 858–870.
- Mori, I., Komatsu, T., Takeuchi, K., Nakakuki, K., Sudo, M., & Kimura, Y. (1995). In vivo induction of apoptosis by influenza virus. *The Journal of General Virology*, *76* ( Pt 11, 2869–2873. <https://doi.org/10.1099/0022-1317-76-11-2869>
- Moyle, P. M., & Toth, I. (2013). Modern Subunit Vaccines: Development, Components, and Research Opportunities. *ChemMedChem*, *8*(3), 360–376. <https://doi.org/https://doi.org/10.1002/cmdc.201200487>
- Murr, M., Hoffmann, B., Grund, C., Römer-Oberdörfer, A., & Mettenleiter, T. C.

- (2020). A novel recombinant Newcastle disease virus vectored DIVA vaccine against peste des petits ruminants in goats. *Vaccines*, 8(2), 1–25.  
<https://doi.org/10.3390/vaccines8020205>
- Nadeem, S. M., Khan, M. U. R., Aslam, A., Sheikh, A. A., Ahmad, A., & Anees, M. (2020). Molecular characterization and phylogeny of chicken anemia virus detected in broiler poultry flocks in Punjab, Pakistan. *Pakistan Journal of Zoology*, 52(1), 421–424.  
<https://doi.org/10.17582/JOURNAL.PJZ/2020.52.1.SC14>
- Naim, H. Y. (2013). Applications and challenges of multivalent recombinant vaccines. *Human Vaccines and Immunotherapeutics*, 9(3), 457–461.  
<https://doi.org/10.4161/hv.23220>
- Nascimento, I. P., & Leite, L. (2012). Recombinant vaccines and the development of new vaccine strategies. *Brazilian Journal of Medical and Biological Research*, 45, 1102–1111.
- Nishikawa, Y., Ikeda, H., Fukumoto, S., Xuan, X., Nagasawa, H., Otsuka, H., & Mikami, T. (2000). Immunisation of dogs with a canine herpesvirus vector expressing Neospora caninum surface protein, NcSRS2. *International Journal for Parasitology*, 30(11), 1167–1171.  
[https://doi.org/https://doi.org/10.1016/S0020-7519\(00\)00111-9](https://doi.org/https://doi.org/10.1016/S0020-7519(00)00111-9)
- Okoli, A., Okeke, M. I., Tryland, M., & Moens, U. (2018). CRISPR/Cas9—Advancing orthopoxvirus genome editing for vaccine and vector development. *Viruses*, 10(1), 1–27. <https://doi.org/10.3390/v10010050>
- Olsen, L. M., Ch'ng, T. H., Card, J. P., & Enquist, L. W. (2006). Role of Pseudorabies Virus Us3 Protein Kinase during Neuronal Infection. *Journal of Virology*, 80(13), 6387–6398. <https://doi.org/10.1128/jvi.00352-06>

- Ou, S.-C., & Giambone, J. J. (2012). Infectious laryngotracheitis virus in chickens. *World Journal of Virology*, 1(5), 142–149. <https://doi.org/10.5501/wjv.v1.i5.142>
- Paldurai, A., Kim, S.-H., Nayak, B., Xiao, S., Shive, H., Collins, P. L., & Samal, S. K. (2014). Evaluation of the Contributions of Individual Viral Genes to Newcastle Disease Virus Virulence and Pathogenesis. *Journal of Virology*, 88(15), 8579 LP – 8596. <https://doi.org/10.1128/JVI.00666-14>
- Palmer, G. A., Brogdon, J. L., Constant, S. L., & Tattersall, P. (2004). A nonproliferating parvovirus vaccine vector elicits sustained, protective humoral immunity following a single intravenous or intranasal inoculation. *Journal of Virology*, 78(3), 1101–1108. <https://doi.org/10.1128/jvi.78.3.1101-1108.2004>
- Palya, V., Kiss, I., Tatár-Kis, T., Mató, T., Felföldi, B., & Gardin, Y. (2012). Advancement in Vaccination Against Newcastle Disease: Recombinant HVT NDV Provides High Clinical Protection and Reduces Challenge Virus Shedding with the Absence of Vaccine Reactions. *Avian Diseases*, 56(2), 282–287. <https://doi.org/10.1637/9935-091511-Reg.1>
- Pan, X., Liu, Q., Niu, S., Huang, D., Yan, D., Teng, Q., Li, X., Beerens, N., Forlenza, M., de Jong, M. C. M., & Li, Z. (2023). Efficacy of a recombinant turkey herpesvirus (H9) vaccine against H9N2 avian influenza virus in chickens with maternal-derived antibodies . In *Frontiers in Microbiology* (Vol. 13). <https://www.frontiersin.org/articles/10.3389/fmicb.2022.1107975>
- Pan, Z., Liu, J., Ma, J., Jin, Q., Yao, H., & Osterrieder, N. (2017). The recombinant EHV-1 vector producing CDV hemagglutinin as potential vaccine against canine distemper. *Microbial Pathogenesis*, 111, 388–394. <https://doi.org/https://doi.org/10.1016/j.micpath.2017.09.006>
- Panda, A., Huang, Z., Elankumaran, S., Rockemann, D. D., & Samal, S. K. (2004).

- Role of fusion protein cleavage site in the virulence of Newcastle disease virus. *Microbial Pathogenesis*, 36(1), 1–10.  
<https://doi.org/10.1016/j.micpath.2003.07.003>
- Parcells, M. S., Anderson, A. S., Cantello, J. L., & Morgan, R. W. (1994). Characterization of Marek's disease virus insertion and deletion mutants that lack US1 (ICP22 homolog), US10, and/or US2 and neighboring short-component open reading frames. *Journal of Virology*, 68(12), 8239–8253.  
<https://doi.org/10.1128/jvi.68.12.8239-8253.1994>
- Parvizpour, S., Pourseif, M. M., Razmara, J., Rafi, M. A., & Omid, Y. (2020). Epitope-based vaccine design: a comprehensive overview of bioinformatics approaches. *Drug Discovery Today*, 25(6), 1034–1042.  
<https://doi.org/https://doi.org/10.1016/j.drudis.2020.03.006>
- Pastoret, P.-P., & Vanderplasschen, A. (2003). Poxviruses as vaccine vectors. *Comparative Immunology, Microbiology and Infectious Diseases*, 26(5), 343–355. [https://doi.org/https://doi.org/10.1016/S0147-9571\(03\)00019-5](https://doi.org/https://doi.org/10.1016/S0147-9571(03)00019-5)
- Peeters, B. P., de Leeuw, O. S., Koch, G., & Gielkens, A. L. (1999). Rescue of Newcastle disease virus from cloned cDNA: evidence that cleavability of the fusion protein is a major determinant for virulence. *Journal of Virology*, 73(6), 5001–5009. <https://doi.org/10.1128/JVI.73.6.5001-5009.1999>
- Peiris, J. S. M., de Jong, M. D., & Guan, Y. (2007). Avian Influenza Virus (H5N1): a Threat to Human Health. *Clinical Microbiology Reviews*, 20(2), 243 LP – 267.  
<https://doi.org/10.1128/CMR.00037-06>
- Pellett, P. E., & Roizman, B. (2013). Herpesviridae. *Fields Virology*, 2(6), 1802–1822.
- Peng, Z., Ouyang, T., Pang, D., Ma, T., Chen, X., Guo, N., Chen, F., Yuan, L.,

- Ouyang, H., & Ren, L. (2016). Pseudorabies virus can escape from CRISPR-Cas9-mediated inhibition. *Virus Research*, 223, 197–205.  
<https://doi.org/10.1016/j.virusres.2016.08.001>
- Pereira, L. (1994). Function of glycoprotein B homologues of the family herpesviridae. *Infectious Agents and Disease*, 3(1), 9–28.
- Pickar-Oliver, A., & Gersbach, C. A. (2019). The next generation of CRISPR–Cas technologies and applications. *Nature Reviews Molecular Cell Biology*, 20(8), 490–507. <https://doi.org/10.1038/s41580-019-0131-5>
- Pollard, A. J., & Bijker, E. M. (2021). A guide to vaccinology: from basic principles to new developments. *Nature Reviews Immunology*, 21(2), 83–100.  
<https://doi.org/10.1038/s41577-020-00479-7>
- Prideaux, C. T., Kongsuwan, K., Johnson, M. A., Sheppard, M., & Fahey, K. J. (1992). Infectious laryngotracheitis virus growth, DNA replication, and protein synthesis. *Archives of Virology*, 123(1–2), 181–192.  
<https://doi.org/10.1007/BF01317148>
- Promkuntod, N., van Eijndhoven, R. E. W., de Vriese, G., Gröne, A., & Verheije, M. H. (2014). Mapping of the receptor-binding domain and amino acids critical for attachment in the spike protein of avian coronavirus infectious bronchitis virus. *Virology*, 448, 26–32. <https://doi.org/https://doi.org/10.1016/j.virol.2013.09.018>
- Promkuntod, N., Wickramasinghe, I. N. A., de Vriese, G., Gröne, A., & Verheije, M. H. (2013). Contributions of the S2 spike ectodomain to attachment and host range of infectious bronchitis virus. *Virus Research*, 177(2), 127–137.  
<https://doi.org/https://doi.org/10.1016/j.virusres.2013.09.006>
- Qi, Z., Pan, C., Lu, H., Shui, Y., Li, L., Li, X., Xu, X., Liu, S., & Jiang, S. (2010). A recombinant mimetics of the HIV-1 gp41 prehairpin fusion intermediate fused

- with human IgG Fc fragment elicits neutralizing antibody response in the vaccinated mice. *Biochemical and Biophysical Research Communications*, 398(3), 506–512. <https://doi.org/https://doi.org/10.1016/j.bbrc.2010.06.109>
- Qian, P., Li, X.-M., Jin, M.-L., Peng, G.-Q., & Chen, H.-C. (2004). An approach to a FMD vaccine based on genetic engineered attenuated pseudorabies virus: one experiment using VP1 gene alone generates an antibody responds on FMD and pseudorabies in swine. *Vaccine*, 22(17), 2129–2136. <https://doi.org/https://doi.org/10.1016/j.vaccine.2003.12.005>
- Qian, P., Zhi, X., Wang, B., Zhang, H., Chen, H., & Li, X. (2015). Construction and immune efficacy of recombinant pseudorabies virus expressing PrM-E proteins of Japanese encephalitis virus genotype I. *Virology Journal*, 12(1), 214. <https://doi.org/10.1186/s12985-015-0449-3>
- Rajão, D. S., & Pérez, D. R. (2018). Universal Vaccines and Vaccine Platforms to Protect against Influenza Viruses in Humans and Agriculture . In *Frontiers in Microbiology* (Vol. 9, p. 123). <https://www.frontiersin.org/article/10.3389/fmicb.2018.00123>
- Ran, F. A., Hsu, P. D., Wright, J., Agarwala, V., Scott, D. A., & Zhang, F. (2013). Genome engineering using the CRISPR-Cas9 system. *Nature Protocols*, 8(11), 2281–2308. <https://doi.org/10.1038/nprot.2013.143>
- Rauch, S., Jasny, E., Schmidt, K. E., & Petsch, B. (2018). New Vaccine Technologies to Combat Outbreak Situations . In *Frontiers in Immunology* (Vol. 9, p. 1963). <https://www.frontiersin.org/article/10.3389/fimmu.2018.01963>
- Ravikumar, R., Chan, J., & Prabakaran, M. (2022). Vaccines against Major Poultry Viral Diseases: Strategies to Improve the Breadth and Protective Efficacy. *Viruses*, 14(6). <https://doi.org/10.3390/v14061195>



- Rechenchoski, D. Z., Faccin-Galhardi, L. C., Linhares, R. E. C., & Nozawa, C. (2017). Herpesvirus: an underestimated virus. *Folia Microbiologica*, 62(2), 151–156. <https://doi.org/10.1007/s12223-016-0482-7>
- Reed, S. G., Orr, M. T., & Fox, C. B. (2013). Key roles of adjuvants in modern vaccines. *Nature Medicine*, 19(12), 1597–1608. <https://doi.org/10.1038/nm.3409>
- Ren, X.-G., Xue, F., Zhu, Y.-M., Tong, G.-Z., Wang, Y.-H., Feng, J.-K., Shi, H.-F., & Gao, Y.-R. (2009). Construction of a recombinant BHV-1 expressing the VP1 gene of foot and mouth disease virus and its immunogenicity in a rabbit model. *Biotechnology Letters*, 31(8), 1159–1165. <https://doi.org/10.1007/s10529-009-9988-2>
- Rocha-Martins, M., Cavalheiro, G. R., Matos-Rodrigues, G. E., & Martins, R. A. P. (2015). From gene targeting to genome editing: Transgenic animals applications and beyond. *Anais Da Academia Brasileira de Ciencias*, 87(2), 1323–1348. <https://doi.org/10.1590/0001-3765201520140710>
- Roeder, P., Mariner, J., & Kock, R. (2013). Rinderpest: the veterinary perspective on eradication. *Philosophical Transactions of the Royal Society of London. Series B, Biological Sciences*, 368(1623), 20120139. <https://doi.org/10.1098/rstb.2012.0139>
- Roehm, P. C., Shekarabi, M., Wollebo, H. S., Bellizzi, A., He, L., Salkind, J., & Khalili, K. (2016). Inhibition of HSV-1 Replication by Gene Editing Strategy. *Scientific Reports*, 6(October 2015), 1–11. <https://doi.org/10.1038/srep23146>
- Roizman, B., Carmichael, L. E., Deinhardt, F., De-The, G., Nahmias, A. J., Plowright, W., Rapp, F., Sheldrick, P., Takahashi, M., & Wolf, K. (1981). Herpesviridae: Definition, Provisional Nomenclature, and Taxonomy. *Intervirology*, 16(4), 201–217. <https://doi.org/10.1159/000149269>

- Rosamilia, A., Jacca, S., Tebaldi, G., Tiberti, S., Franceschi, V., Macchi, F., Cavirani, S., Kobinger, G., Knowles, D. P., & Donofrio, G. (2016). BoHV-4-based vector delivering Ebola virus surface glycoprotein. *Journal of Translational Medicine*, *14*(1), 325. <https://doi.org/10.1186/s12967-016-1084-5>
- Rosas, C. T., König, P., Beer, M., Dubovi, E. J., Tischer, B. K., & Osterrieder, N. (2007). Evaluation of the vaccine potential of an equine herpesvirus type 1 vector expressing bovine viral diarrhoea virus structural proteins. *Journal of General Virology*, *88*(3), 748–757. <https://doi.org/10.1099/vir.0.82528-0>
- Rosas, C. T., Paessler, S., Ni, H., & Osterrieder, N. (2008). Protection of mice by equine herpesvirus type 1-based experimental vaccine against lethal Venezuelan equine encephalitis virus infection in the absence of neutralizing antibodies. *American Journal of Tropical Medicine and Hygiene*, *78*(1), 83–92. <https://doi.org/10.4269/ajtmh.2008.78.83>
- Rosas, C. T., Tischer, B. K., Perkins, G. A., Wagner, B., Goodman, L. B., & Osterrieder, N. (2007). Live-attenuated recombinant equine herpesvirus type 1 (EHV-1) induces a neutralizing antibody response against West Nile virus (WNV). *Virus Research*, *125*(1), 69–78. <https://doi.org/https://doi.org/10.1016/j.virusres.2006.12.009>
- Rosas, C., Van de Walle, G. R., Metzger, S. M., Hoelzer, K., Dubovi, E. J., Kim, S. G., Parrish, C. R., & Osterrieder, N. (2008). Evaluation of a vectored equine herpesvirus type 1 (EHV-1) vaccine expressing H3 haemagglutinin in the protection of dogs against canine influenza. *Vaccine*, *26*(19), 2335–2343. <https://doi.org/https://doi.org/10.1016/j.vaccine.2008.02.064>
- Rouet, P, Smih, F., & Jasin, M. (1994). Introduction of double-strand breaks into the genome of mouse cells by expression of a rare-cutting endonuclease. *Molecular*

*and Cellular Biology*, 14(12), 8096–8106.

<https://doi.org/10.1128/mcb.14.12.8096>

- Rouet, Philippe, Smih, F., & Jasin, M. (1994). Expression of a site-specific endonuclease stimulates homologous recombination in mammalian cells. *Proceedings of the National Academy of Sciences of the United States of America*, 91(13), 6064–6068. <https://doi.org/10.1073/pnas.91.13.6064>
- Rouse, B. T., & Kaistha, S. D. (2006). A Tale of Two  $\alpha$ -Herpesviruses: Lessons for Vaccinologists. *Clinical Infectious Diseases*, 42(6), 810–817. <https://doi.org/10.1086/500141>
- Rudin, N., Sugarman, E., & Haber, J. E. (1989). Genetic and physical analysis of double-strand break repair and recombination in *Saccharomyces cerevisiae*. *Genetics*, 122(3), 519–534.
- Said, A., Elmanzalawy, M., Ma, G., Damiani, A. M., & Osterrieder, N. (2017). An equine herpesvirus type 1 (EHV-1) vector expressing Rift Valley fever virus (RVFV) Gn and Gc induces neutralizing antibodies in sheep. *Virology Journal*, 14(1), 154. <https://doi.org/10.1186/s12985-017-0811-8>
- Said, A., Lange, E., Beer, M., Damiani, A., & Osterrieder, N. (2013). Recombinant equine herpesvirus 1 (EHV-1) vaccine protects pigs against challenge with influenza A(H1N1)pmd09. *Virus Research*, 173(2), 371–376. <https://doi.org/https://doi.org/10.1016/j.virusres.2013.01.004>
- Saitou, N., & Nei, M. (1987). The neighbor-joining method: a new method for reconstructing phylogenetic trees. *Molecular Biology and Evolution*, 4(4), 406–425. <https://doi.org/10.1093/oxfordjournals.molbev.a040454>
- Sakaguchi, M., Nakamura, H., Sonoda, K., Okamura, H., Yokogawa, K., Matsuo, K., & Hira, K. (1998). Protection of chickens with or without maternal antibodies

- against both Marek's and Newcastle diseases by one-time vaccination with recombinant vaccine of Marek's disease virus type 1. *Vaccine*, 16(5), 472–479. [https://doi.org/https://doi.org/10.1016/S0264-410X\(97\)80001-1](https://doi.org/https://doi.org/10.1016/S0264-410X(97)80001-1)
- Salameh, S., Sheth, U., & Shukla, D. (2012). Early events in herpes simplex virus lifecycle with implications for an infection of lifetime. *The Open Virology Journal*, 6, 1–6. <https://doi.org/10.2174/1874357901206010001>
- Salod, Z., & Mahomed, O. (2022). Mapping Potential Vaccine Candidates Predicted by VaxiJen for Different Viral Pathogens between 2017–2021—A Scoping Review. *Vaccines*, 10(11). <https://doi.org/10.3390/vaccines10111785>
- Salvatori, G., Luberto, L., Maffei, M., Aurisicchio, L., Roscilli, G., Palombo, F., & Marra, E. (2020). SARS-CoV-2 SPIKE PROTEIN: an optimal immunological target for vaccines. *Journal of Translational Medicine*, 18(1), 222. <https://doi.org/10.1186/s12967-020-02392-y>
- Samal, S., Kumar, S., Khattar, S. K., & Samal, S. K. (2011). A single amino acid change, Q114R, in the cleavage-site sequence of Newcastle disease virus fusion protein attenuates viral replication and pathogenicity. *Journal of General Virology*, 92(10), 2333–2338. <https://doi.org/10.1099/vir.0.033399-0>
- Sander, J. D., & Joung, J. K. (2014). CRISPR-Cas systems for genome editing, regulation and targeting. *Nature Biotechnology*, 32(4), 347–355. <https://doi.org/10.1038/nbt.2842.CRISPR-Cas>
- Sanders, B., Koldijk, M., & Schuitemaker, H. (2014). Inactivated Viral Vaccines. In *Vaccine Analysis: Strategies, Principles, and Control* (pp. 45–80). [https://doi.org/10.1007/978-3-662-45024-6\\_2](https://doi.org/10.1007/978-3-662-45024-6_2)
- Santos, M. P. de M., Morais, M. P. L. de A., Fonseca, D. D. D., Faria, A. B. S. de, Silva, I. H. M., Carvalho, A. A. T., & Leão, J. C. (2012). Herpesvírus humano:

- tipos, manifestações orais e tratamento. *Odontologia Clínico-Científica (Online)*, 11(3), 191–196.
- Sato, E., Miyazawa, T., Nishimura, Y., Ikeda, Y., Kawakami, K., Mochizuki, M., Yokoyama, N., Maeda, K., Fujita, K., Kohmoto, M., Takahashi, E., & Mikami, T. (2001). Further development of a recombinant feline herpesvirus type 1 expressing the Gag protein of feline immunodeficiency virus. *Archives of Virology*, 146(2), 379–387. <https://doi.org/10.1007/s007050170182>
- Schmidt, S. R. (2009). Fusion-proteins as biopharmaceuticals - Applications and challenges. *Current Opinion in Drug Discovery and Development*, 12(2), 284–295.
- Schmitt, J., Becher, P., Thiel, H.-J., & Keil, G. M. (1999). Expression of bovine viral diarrhoea virus glycoprotein E2 by bovine herpesvirus-1 from a synthetic ORF and incorporation of E2 into recombinant virions. *Journal of General Virology*, 80(11), 2839–2848. <https://doi.org/10.1099/0022-1317-80-11-2839>
- Schnitzlein, W. M., Radzevicius, J., & Tripathy, D. N. (1994). *Propagation of Infectious Laryngotracheitis Virus in an Avian Liver Cell Line*. 38(2), 211–217.
- Schnitzlein, W. M., Winans, R., Ellsworth, S., & Tripathy, D. N. (1995). Generation of Thymidine Kinase-Deficient Mutants of Infectious Laryngotracheitis Virus. *Virology*, 209(2), 304–314. <https://doi.org/https://doi.org/10.1006/viro.1995.1262>
- Schultz-Cherry, S., Dybdahl-Sissoko, N., Neumann, G., Kawaoka, Y., & Hinshaw, V. S. (2001). Influenza Virus NS1 Protein Induces Apoptosis in Cultured Cells. *Journal of Virology*, 75(17), 7875–7881. <https://doi.org/10.1128/jvi.75.17.7875-7881.2001>
- Schultz, B. R., & Chamberlain, J. S. (2008). Recombinant Adeno-associated Virus Transduction and Integration. *Current Opinion in Immunology*, 16(7), 47–54.

<https://doi.org/https://doi.org/10.1038/mt.2008.103>

- Schwab, I., & Nimmerjahn, F. (2013). Intravenous immunoglobulin therapy: how does IgG modulate the immune system? *Nature Reviews. Immunology*, *13*(3), 176–189. <https://doi.org/10.1038/nri3401>
- Selim, K. M., Selim, A., Arafa, A., Hussein, H. A., & Elsanousi, A. A. (2018). Molecular characterization of full fusion protein (F) of Newcastle disease virus genotype VIId isolated from Egypt during 2012-2016. *Veterinary World*, *11*(7), 930–938. <https://doi.org/10.14202/vetworld.2018.930-938>
- Shaddel, M., Ebrahimi, M., & Tabandeh, M. R. (2018). Bioinformatics analysis of single and multi-hybrid epitopes of GRA-1, GRA-4, GRA-6 and GRA-7 proteins to improve DNA vaccine design against *Toxoplasma gondii*. *Journal of Parasitic Diseases*, *42*(2), 269–276. <https://doi.org/10.1007/s12639-018-0996-9>
- Shafer, A. L., Katz, J. B., & Eernisse, K. A. (1998). Development and validation of a competitive enzyme-linked immunosorbent assay for detection of type A influenza antibodies in avian sera. *Avian Diseases*, *42*(1), 28–34.
- Shang, J., Zheng, Y., Yang, Y., Liu, C., Geng, Q., Luo, C., Zhang, W., & Li, F. (2018). Cryo-EM structure of infectious bronchitis coronavirus spike protein reveals structural and functional evolution of coronavirus spike proteins. *PLOS Pathogens*, *14*(4), e1007009. <https://doi.org/10.1371/journal.ppat.1007009>
- Sharma, J. M. (1999). Introduction to poultry vaccines and immunity. *Advances in Veterinary Medicine*, *41*(C), 481–494. [https://doi.org/10.1016/S0065-3519\(99\)80036-6](https://doi.org/10.1016/S0065-3519(99)80036-6)
- Shen, H.-B., & Chou, K.-C. (2010). Virus-mPLoc: a fusion classifier for viral protein subcellular location prediction by incorporating multiple sites. *Journal of Biomolecular Structure and Dynamics*, *28*(2), 175–186.

- Shey, R. A., Ghogomu, S. M., Esoh, K. K., Nebangwa, N. D., Shintouo, C. M., Nongley, N. F., Asa, B. F., Ngale, F. N., Vanhamme, L., & Souopgui, J. (2019). In-silico design of a multi-epitope vaccine candidate against onchocerciasis and related filarial diseases. *Scientific Reports*, 9(1), 4409. <https://doi.org/10.1038/s41598-019-40833-x>
- Skehel, J. J., & Wiley, D. C. (2000). Receptor binding and membrane fusion in virus entry: the influenza hemagglutinin. *Annual Review of Biochemistry*, 69, 531–569. <https://doi.org/10.1146/annurev.biochem.69.1.531>
- Slater, J. D., Gibson, J. S., & Field, H. J. (1993). Pathogenicity of a thymidine kinase-deficient mutant of equine herpesvirus 1 in mice and specific pathogen-free foals. *Journal of General Virology*, 74(5), 819–828. <https://doi.org/10.1099/0022-1317-74-5-819>
- Sno, M., Cox, E., Holtslag, H., Nell, T., Pel, S., Segers, R., Fachinger, V., & Witvliet, M. (2016). Efficacy and safety of a new intradermal PCV2 vaccine in pigs. *Trials in Vaccinology*, 5, 24–31. <https://doi.org/https://doi.org/10.1016/j.trivac.2016.01.002>
- Soda, K., Asakura, S., Okamatsu, M., Sakoda, Y., & Kida, H. (2011). H9N2 influenza virus acquires intravenous pathogenicity on the introduction of a pair of di-basic amino acid residues at the cleavage site of the hemagglutinin and consecutive passages in chickens. *Virology Journal*, 8, 1–9.
- Solana, J. C., Moreno, J., Iborra, S., Soto, M., & Requena, J. M. (2022). Live attenuated vaccines, a favorable strategy to provide long-term immunity against protozoan diseases. *Trends in Parasitology*, 38(4), 316–334. <https://doi.org/10.1016/j.pt.2021.11.004>
- Song, Y., Jin, M., Zhang, S., Xu, X., Xiao, S., Cao, S., & Chen, H. (2007). Generation

- and immunogenicity of a recombinant pseudorabies virus expressing cap protein of porcine circovirus type 2. *Veterinary Microbiology*, 119(2), 97–104.  
<https://doi.org/https://doi.org/10.1016/j.vetmic.2006.08.026>
- Spear, P. G., Eisenberg, R. J., & Cohen, G. H. (2000). Three Classes of Cell Surface Receptors for Alpha herpesvirus Entry. *Virology*, 275(1), 1–8.  
<https://doi.org/https://doi.org/10.1006/viro.2000.0529>
- Speedy, A. W. (2003). Global Production and Consumption of Animal Source Foods. *J. Nutr*, 133, 4048S–4053S.
- Spier, R. E. (1997). Multivalent Vaccines: Prospects and Challenges. *Folia Microbiologica*, 42(2), 105–112. <https://doi.org/10.1007/BF02898716>
- Stanberry, L. R., Spruance, S. L., Cunningham, A. L., Bernstein, D. I., Mindel, A., Sacks, S., Tyring, S., Aoki, F. Y., Slaoui, M., Denis, M., Vandepapeliere, P., & Dubin, G. (2002). Glycoprotein-D–Adjuvant Vaccine to Prevent Genital Herpes. *New England Journal of Medicine*, 347(21), 1652–1661.  
<https://doi.org/10.1056/NEJMoa011915>
- Stear, M. J. (2005). OIE Manual of Diagnostic Tests and Vaccines for Terrestrial Animals (Mammals, Birds and Bees) 5th Edn. Volumes 1 & 2. World Organization for Animal Health 2004. ISBN 92 9044 622 6.€ 140. *Parasitology*, 130(6), 727.
- Stech, O., Veits, J., Abdelwhab, E.-S. M., Wessels, U., Mettenleiter, T. C., & Stech, J. (2015). The Neuraminidase Stalk Deletion Serves as Major Virulence Determinant of H5N1 Highly Pathogenic Avian Influenza Viruses in Chicken. *Scientific Reports*, 5, 13493. <https://doi.org/10.1038/srep13493>
- Stone-Hulslander, J., & Morrison, T. G. (1997). Detection of an interaction between the HN and F proteins in Newcastle disease virus-infected cells. *Journal of*



- Virology*, 71(9), 6287–6295. <https://doi.org/10.1128/JVI.71.9.6287-6295.1997>
- Suarez, D. L. (2012). DIVA Vaccination Strategies for Avian Influenza Virus. *Avian Diseases*, 56(4s1), 836–844. <https://doi.org/10.1637/10207-041512-Review.1>
- Suenaga, T., Kohyama, M., Hirayasu, K., & Arase, H. (2014). Engineering large viral DNA genomes using the CRISPR-Cas9 system. *Microbiology and Immunology*, 58(9), 513–522. <https://doi.org/10.1111/1348-0421.12180>
- Sultan, H. A., Elfeil, W. K., Nour, A. A., Tantawy, L., Kamel, E. G., Eed, E. M., El Askary, A., & Talaat, S. (2021). Efficacy of the Newcastle Disease Virus Genotype VII.1.1-Matched Vaccines in Commercial Broilers. *Vaccines*, 10(1). <https://doi.org/10.3390/vaccines10010029>
- Sun, H.-L., Wang, Y.-F., Tong, G.-Z., Zhang, P.-J., Miao, D.-Y., Zhi, H.-D., Wang, M., & Wang, M. (2008). Protection of Chickens from Newcastle Disease and Infectious Laryngotracheitis with a Recombinant Fowlpox Virus Co-Expressing the F, HN Genes of Newcastle Disease Virus and gB Gene of Infectious Laryngotracheitis Virus. *Avian Diseases*, 52(1), 111–117. <https://doi.org/10.1637/7998-041807-Reg>
- Swayne, D. E., Glisson, J. R., McDougald, L. R., Nolan, L. K., Suarez, D. L., & Nair, V. (2013). *Diseases of Poultry*. <https://doi.org/10.1016/B978-1-4557-0297-8.00402-X>
- Takizawa, T., Matsukawa, S., Higuchi, Y., Nakamura, S., Nakanishi, Y., & Fukuda, R. (1993). Induction of programmed cell death (apoptosis) by influenza virus infection in tissue culture cells. *The Journal of General Virology*, 74 ( Pt 11, 2347–2355. <https://doi.org/10.1099/0022-1317-74-11-2347>
- Tamura, K., Stecher, G., & Kumar, S. (2021). MEGA11: Molecular Evolutionary Genetics Analysis Version 11. *Molecular Biology and Evolution*, 38(7), 3022–

3027. <https://doi.org/10.1093/molbev/msab120>

Tan, L., Zhang, Y., Liu, F., Yuan, Y., Zhan, Y., Sun, Y., Qiu, X., Meng, C., Song, C., & Ding, C. (2016). Infectious bronchitis virus poly-epitope-based vaccine protects chickens from acute infection. *Vaccine*, *34*(44), 5209–5216.

<https://doi.org/10.1016/j.vaccine.2016.09.022>

Tang, N., Zhang, Y., Pedrera, M., Chang, P., Baigent, S., Moffat, K., Shen, Z., Nair, V., & Yao, Y. (2018). A simple and rapid approach to develop recombinant avian herpesvirus vectored vaccines using CRISPR/Cas9 system. *Vaccine*, *36*(5), 716–722. <https://doi.org/10.1016/j.vaccine.2017.12.025>

Tang, N., Zhang, Y., Pedrera, M., Chang, P., Baigent, S., Moffat, K., Shen, Z., Nair, V., & Yao, Y. (2019). Generating recombinant avian herpesvirus vectors with CRISPR/Cas9 Gene Editing. *Journal of Visualized Experiments*, *2019*(143), 1–7. <https://doi.org/10.3791/58193>

Tang, N., Zhang, Y., Sadigh, Y., Moffat, K., Shen, Z., Nair, V., & Yao, Y. (2020). Generation of a triple insert live avian herpesvirus vectored vaccine using crispr/cas9-based gene editing. *Vaccines*, *8*(1).

<https://doi.org/10.3390/vaccines8010097>

Tang, N., Zhang, Y., Shen, Z., Yao, Y., & Nair, V. (2021). Application of CRISPR-Cas9 Editing for Virus Engineering and the Development of Recombinant Viral Vaccines. *The CRISPR Journal*, *4*(4), 477–490.

<https://doi.org/10.1089/crispr.2021.0017>

Tang, Y. D., Liu, J. T., Wang, T. Y., An, T. Q., Sun, M. X., Wang, S. J., Fang, Q. Q., Hou, L. lin, Tian, Z. J., & Cai, X. H. (2016). Live attenuated pseudorabies virus developed using the CRISPR/Cas9 system. *Virus Research*, *225*, 33–39.

<https://doi.org/10.1016/j.virusres.2016.09.004>

- Tatsis, N., & Ertl, H. C. J. (2004). Adenoviruses as vaccine vectors. *Molecular Therapy: The Journal of the American Society of Gene Therapy*, 10(4), 616–629. <https://doi.org/10.1016/j.ymthe.2004.07.013>
- Taylor, G., Rijsewijk, F. A. M., Thomas, L. H., Wyld, S. G., Gaddum, R. M., Cook, R. S., Morrison, W. I., Hensen, E., Van Oirschot, J. T., & Keil, G. (1998). Resistance to bovine respiratory syncytial virus (BRSV) induced in calves by a recombinant bovine herpesvirus-1 expressing the attachment glycoprotein of BRSV. *Journal of General Virology*, 79(7), 1759–1767. <https://doi.org/10.1099/0022-1317-79-7-1759>
- Teng, M., Yao, Y., Nair, V., & Luo, J. (2021). Latest advances of virology research using crispr/cas9-based gene-editing technology and its application to vaccine development. *Viruses*, 13(5). <https://doi.org/10.3390/v13050779>
- Tenser, R. B., Ressel, S. J., Fralish, F. A., & Jones, J. C. (1983). The role of pseudorabies virus thymidine kinase expression in trigeminal ganglion infection. *Journal of General Virology*, 64(6), 1369–1373. <https://doi.org/10.1099/0022-1317-64-6-1369>
- Terregino, C., Toffan, A., Serena Beato, M., De Nardi, R., Vascellari, M., Meini, A., Ortali, G., Mancin, M., & Capua, I. (2008). Pathogenicity of a QX strain of infectious bronchitis virus in specific pathogen free and commercial broiler chickens, and evaluation of protection induced by a vaccination programme based on the Ma5 and 4/91 serotypes. *Avian Pathology*, 37(5), 487–493. <https://doi.org/10.1080/03079450802356938>
- Thomas, S. (2000). Vaccine Design Methods Methods and Protocols, Volume 2: Vaccines for Veterinary Diseases. In *Science And Technology*. [https://doi.org/10.1016/S1570-002X\(07\)00016-X](https://doi.org/10.1016/S1570-002X(07)00016-X)

- Tian, Z.-J., Zhou, G.-H., Zheng, B.-L., Qiu, H.-J., Ni, J.-Q., Yang, H.-L., Yin, X.-N., Hu, S.-P., & Tong, G.-Z. (2006). A recombinant pseudorabies virus encoding the HA gene from H3N2 subtype swine influenza virus protects mice from virulent challenge. *Veterinary Immunology and Immunopathology*, *111*(3), 211–218.  
<https://doi.org/https://doi.org/10.1016/j.vetimm.2006.01.015>
- Tizard, I. R. (2021). Adverse consequences of vaccination. In *Vaccines for Veterinarians* (pp. 115-130.e1). <https://doi.org/10.1016/B978-0-323-68299-2.00019-8>
- Tombari, W., Nsiri, J., Larbi, I., Guerin, J. L., & Ghram, A. (2011). Genetic evolution of low pathogenicity H9N2 Avian influenza viruses in Tunisia: acquisition of new mutations. *Virology Journal*, *8*, 1–12.
- Toro, H., Pennington, D., Gallardo, R. A., van Santen, V. L., van Ginkel, F. W., Zhang, J., & Joiner, K. S. (2012). Infectious Bronchitis Virus Subpopulations in Vaccinated Chickens After Challenge. *Avian Diseases*, *56*(3), 501–508.  
<https://doi.org/10.1637/9982-110811-Reg.1>
- Travis, J. (2015). Making the cut. *Science*, *350*(6267), 1456 LP – 1457.  
<https://doi.org/10.1126/science.350.6267.1456>
- Tressler, R. L., & Roth, T. F. (1987). IgG receptors on the embryonic chick yolk sac. *The Journal of Biological Chemistry*, *262*(32), 15406–15412.
- Trus, B. L., Cheng, N., Newcomb, W. W., Homa, F. L., Brown, J. C., & Steven, A. C. (2004). Structure and polymorphism of the UL6 portal protein of herpes simplex virus type 1. *Journal of Virology*, *78*(22), 12668–12671.  
<https://doi.org/10.1128/JVI.78.22.12668-12671.2004>
- Vagnozzi, A., Riblet, S. M., Williams, S. M., Zavala, G., & García, M. (2015). Infection of Broilers with Two Virulent Strains of Infectious Laryngotracheitis

- Virus: Criteria for Evaluation of Experimental Infections. *Avian Diseases*, 59(3), 394–399. <https://doi.org/10.1637/11075-033115-Reg.1>
- Valastro, V., Holmes, E. C., Britton, P., Fusaro, A., Jackwood, M. W., Cattoli, G., & Monne, I. (2016). S1 gene-based phylogeny of infectious bronchitis virus: An attempt to harmonize virus classification. *Infection, Genetics and Evolution*, 39, 349–364. <https://doi.org/https://doi.org/10.1016/j.meegid.2016.02.015>
- Van Diemen, F. R., Kruse, E. M., Hooykaas, M. J. G., Bruggeling, C. E., Schürch, A. C., van Ham, P. M., Imhof, S. M., Nijhuis, M., Wiertz, E. J. H. J., & Lebbink, R. J. (2016). CRISPR/Cas9-Mediated Genome Editing of Herpesviruses Limits Productive and Latent Infections. *PLoS Pathogens*, 12(6), 1–29. <https://doi.org/10.1371/journal.ppat.1005701>
- van Diemen, F. R., & Lebbink, R. J. (2017). CRISPR/Cas9, a powerful tool to target human herpesviruses. *Cellular Microbiology*, 19(2). <https://doi.org/10.1111/cmi.12694>
- Veits, J., Lüschow, D., Kindermann, K., Werner, O., Teifke, J. P., Mettenleiter, T. C., & Fuchs, W. (2003). Deletion of the non-essential UL0 gene of infectious laryngotracheitis (ILT) virus leads to attenuation in chickens, and UL0 mutants expressing influenza virus haemagglutinin (H7) protect against ILT and fowl plague. *The Journal of General Virology*, 84(Pt 12), 3343–3352. <https://doi.org/10.1099/vir.0.19570-0>
- Veits, J., Wiesner, D., Fuchs, W., Hoffmann, B., Granzow, H., Starick, E., Mundt, E., Schirmeier, H., Mebatsion, T., Mettenleiter, T. C., & Römer-Oberdörfer, A. (2006). Newcastle disease virus expressing H5 hemagglutinin gene protects chickens against Newcastle disease and avian influenza. *Proceedings of the National Academy of Sciences of the United States of America*, 103(21), 8197–

8202. <https://doi.org/10.1073/pnas.0602461103>

Vermeulen, A. N. (1998). Progress in recombinant vaccine development against coccidiosis A review and prospects into the next millennium. *International Journal for Parasitology*, 28(7), 1121–1130.

[https://doi.org/https://doi.org/10.1016/S0020-7519\(98\)00080-0](https://doi.org/https://doi.org/10.1016/S0020-7519(98)00080-0)

Vetter, V., Denizer, G., Friedland, L. R., Krishnan, J., & Shapiro, M. (2018). Understanding modern-day vaccines: what you need to know. *Annals of Medicine*, 50(2), 110–120. <https://doi.org/10.1080/07853890.2017.1407035>

Vilela, J., Rohaim, M. A., & Munir, M. (2020). Application of CRISPR/Cas9 in Understanding Avian Viruses and Developing Poultry Vaccines . In *Frontiers in Cellular and Infection Microbiology* (Vol. 10, p. 631).

<https://www.frontiersin.org/article/10.3389/fcimb.2020.581504>

Vilela, J., Rohaim, M. A., & Munir, M. (2022). Avian Orthoavulavirus Type-1 as Vaccine Vector against Respiratory Viral Pathogens in Animal and Human. *Vaccines*, 10(2), 1–19. <https://doi.org/10.3390/vaccines10020259>

Vita, R., Mahajan, S., Overton, J. A., Dhanda, S. K., Martini, S., Cantrell, J. R., Wheeler, D. K., Sette, A., & Peters, B. (2019). The immune epitope database (IEDB): 2018 update. *Nucleic Acids Research*, 47(D1), D339–D343.

Walls, A. C., Park, Y.-J., Tortorici, M. A., Wall, A., McGuire, A. T., & Veerler, D. (2020). Structure, Function, and Antigenicity of the SARS-CoV-2 Spike Glycoprotein. *Cell*, 181(2), 281-292.e6. <https://doi.org/10.1016/j.cell.2020.02.058>

Wang, D., Wang, X.-W., Peng, X.-C., Xiang, Y., Song, S.-B., Wang, Y.-Y., Chen, L., Xin, V. W., Lyu, Y.-N., Ji, J., Ma, Z.-W., Li, C.-B., & Xin, H.-W. (2018). CRISPR/Cas9 genome editing technology significantly accelerated herpes simplex virus research. *Cancer Gene Therapy*, 25(5–6), 93–105.

<https://doi.org/10.1038/s41417-018-0016-3>

- Wang, Jianbin, & Quake, S. R. (2014). RNA-guided endonuclease provides a therapeutic strategy to cure latent herpesviridae infection. *Proceedings of the National Academy of Sciences of the United States of America*, 111(36), 13157–13162. <https://doi.org/10.1073/pnas.1410785111>
- Wang, Jie, Xu, Z.-W., Liu, S., Zhang, R.-Y., Ding, S.-L., Xie, X.-M., Long, L., Chen, X.-M., Zhuang, H., & Lu, F.-M. (2015). Dual gRNAs guided CRISPR/Cas9 system inhibits hepatitis B virus replication. *World Journal of Gastroenterology*, 21(32), 9554–9565. <https://doi.org/10.3748/wjg.v21.i32.9554>
- Wang, Y., Yuan, J., Cong, X., Qin, H.-Y., Wang, C.-H., Li, Y., Li, S., Luo, Y., Sun, Y., & Qiu, H.-J. (2015). Generation and Efficacy Evaluation of a Recombinant Pseudorabies Virus Variant Expressing the E2 Protein of Classical Swine Fever Virus in Pigs. *Clinical and Vaccine Immunology*, 22(10), 1121–1129. <https://doi.org/10.1128/CVI.00383-15>
- Watrach, A. M., Hanson, L. E., & Watrach, M. A. (1963). The structure of infectious laryngotracheitis virus. *Virology*, 21, 601–608. [https://doi.org/10.1016/0042-6822\(63\)90233-2](https://doi.org/10.1016/0042-6822(63)90233-2)
- Webster, R. G., Bean, W. J., Gorman, O. T., Chambers, T. M., & Kawaoka, Y. (1992). Evolution and ecology of influenza A viruses. *Microbiological Reviews*, 56(1), 152–179. <https://doi.org/10.1128/mr.56.1.152-179.1992>
- Webster, R. G., & Rott, R. (1987). Influenza virus A pathogenicity: the pivotal role of hemagglutinin. *Cell*, 50(5), 665–666. [https://doi.org/10.1016/0092-8674\(87\)90321-7](https://doi.org/10.1016/0092-8674(87)90321-7)
- Wei, C.-J., Xu, L., Kong, W.-P., Shi, W., Canis, K., Stevens, J., Yang, Z.-Y., Dell, A., Haslam, S., Wilson, I., & Nabel, G. (2008). Comparative Efficacy of Neutralizing

Antibodies Elicited by Recombinant Hemagglutinin Proteins from Avian H5N1 Influenza Virus. *Journal of Virology*, 82(13), 6200–6208.

<https://doi.org/10.1128/JVI.00187-08>

Wei, F., Zhai, Y., Jin, H., Shang, L., Men, J., Lin, J., Fu, Z., Shi, Y., Zhu, X.-Q., Liu, Q., & Gao, H. (2010). Development and immunogenicity of a recombinant pseudorabies virus expressing Sj26GST and SjFABP from *Schistosoma japonicum*. *Vaccine*, 28(32), 5161–5166.

<https://doi.org/https://doi.org/10.1016/j.vaccine.2010.06.012>

Weldon, W. C., Wang, B.-Z., Martin, M. P., Koutsonanos, D. G., Skountzou, I., & Compans, R. W. (2010). Enhanced Immunogenicity of Stabilized Trimeric Soluble Influenza Hemagglutinin. *PLOS ONE*, 5(9), e12466.

<https://doi.org/10.1371/journal.pone.0012466>

Wernike, K., Mundt, A., Link, E. K., Aebischer, A., Schlotthauer, F., Sutter, G., Fux, R., & Beer, M. (2018). N-terminal domain of Schmallenberg virus envelope protein Gc delivered by recombinant equine herpesvirus type 1 and modified vaccinia virus Ankara: Immunogenicity and protective efficacy in cattle. *Vaccine*, 36(34), 5116–5123. <https://doi.org/https://doi.org/10.1016/j.vaccine.2018.07.047>

Wickramasinghe, I. N. A., van Beurden, S. J., Weerts, E. A. W. S., & Verheije, M. H. (2014). The avian coronavirus spike protein. *Virus Research*, 194, 37–48.

<https://doi.org/https://doi.org/10.1016/j.virusres.2014.10.009>

Wilhelm, J., Pingoud, A., & Hahn, M. (2003). Real-time PCR-based method for the estimation of genome sizes. *Nucleic Acids Research*, 31(10), e56.

<https://doi.org/10.1093/nar/gng056>

Wilks, S., de Graaf, M., Smith, D. J., & Burke, D. F. (2012). A review of influenza haemagglutinin receptor binding as it relates to pandemic properties. *Vaccine*,



30(29), 4369–4376. <https://doi.org/10.1016/j.vaccine.2012.02.076>

Willemse, M. J., van Schooneveld, S. H., Chalmers, W. S., & Sondermeijer, P. J. (1996). Vaccination against feline leukaemia using a new feline herpesvirus type 1 vector. *Vaccine*, *14*(16), 1511–1516. [https://doi.org/10.1016/s0264-410x\(96\)00108-9](https://doi.org/10.1016/s0264-410x(96)00108-9)

Willemsen, A., & Zwart, M. P. (2019). On the stability of sequences inserted into viral genomes. *Virus Evolution*, *5*(2), vez045. <https://doi.org/10.1093/ve/vez045>

Wright, A. V., Nuñez, J. K., & Doudna, J. A. (2016). Biology and Applications of CRISPR Systems: Harnessing Nature's Toolbox for Genome Engineering. *Cell*, *164*(1), 29–44. <https://doi.org/https://doi.org/10.1016/j.cell.2015.12.035>

Wu, A., Su, C., Wang, D., Peng, Y., Liu, M., Hua, S., Li, T., Gao, G. F., Tang, H., Chen, J., Liu, X., Shu, Y., Peng, D., & Jiang, T. (2013). Sequential reassortments underlie diverse influenza H7N9 genotypes in China. *Cell Host and Microbe*, *14*(4), 446–452. <https://doi.org/10.1016/j.chom.2013.09.001>

Xiao, A., Cheng, Z., Kong, L., Zhu, Z., Lin, S., Gao, G., & Zhang, B. (2014). CasOT: A genome-wide Cas9/gRNA off-target searching tool. *Bioinformatics*, *30*(8), 1180–1182. <https://doi.org/10.1093/bioinformatics/btt764>

Xu, A., Qin, C., Lang, Y., Wang, M., Lin, M., Li, C., Zhang, R., & Tang, J. (2015). A simple and rapid approach to manipulate pseudorabies virus genome by CRISPR/Cas9 system. *Biotechnology Letters*, *37*(6), 1265–1272. <https://doi.org/10.1007/s10529-015-1796-2>

Xu, G., Xu, X., Li, Z., He, Q., Wu, B., Sun, S., & Chen, H. (2004). Construction of recombinant pseudorabies virus expressing NS1 protein of Japanese encephalitis (SA14-14-2) virus and its safety and immunogenicity. *Vaccine*, *22*(15), 1846–1853. <https://doi.org/https://doi.org/10.1016/j.vaccine.2003.09.015>

- Xu, X., Fan, S., Zhou, J., Zhang, Y., Che, Y., Cai, H., Wang, L., Guo, L., Liu, L., & Li, Q. (2016). The mutated tegument protein UL7 attenuates the virulence of herpes simplex virus 1 by reducing the modulation of  $\alpha$ -4 gene transcription. *Virology Journal*, *13*(1), 152. <https://doi.org/10.1186/s12985-016-0600-9>
- Xuan, X., Tuchiya, K., Sato, I., Nishikawa, Y., Onoderaz, Y., Takashima, Y., Yamamoto, A., Katsumata, A., Iwata, A., Ueda, S., Mikami, T., & Otsuka, H. (1998). Biological and immunogenic properties of rabies virus glycoprotein expressed by canine herpesvirus vector. *Vaccine*, *16*(9), 969–976. [https://doi.org/https://doi.org/10.1016/S0264-410X\(97\)00285-5](https://doi.org/https://doi.org/10.1016/S0264-410X(97)00285-5)
- Yajima, M., Ikuta, K., & Kanda, T. (2018). Rapid CRISPR/cas9-mediated cloning of full-length epstein-barr virus genomes from latently infected cells. *Viruses*, *10*(4), 1–13. <https://doi.org/10.3390/v10040171>
- Yan, W., Qiu, R., Wang, F., Fu, X., Li, H., Cui, P., Zhai, Y., Li, C., Zhang, L., Gu, K., Zuo, L., Lei, C., Wang, H., & Yang, X. (2021). Genetic and pathogenic characterization of a novel recombinant avian infectious bronchitis virus derived from GI-1, GI-13, GI-28, and GI-19 strains in Southwestern China. *Poultry Science*, *100*(7), 101210. <https://doi.org/10.1016/j.psj.2021.101210>
- Yang, D., & Leibowitz, J. L. (2015). The structure and functions of coronavirus genomic 3' and 5' ends. *Virus Research*, *206*, 120–133. <https://doi.org/https://doi.org/10.1016/j.virusres.2015.02.025>
- Yin, J., Ren, X., Tian, Z., & Li, Y. (2007). Assembly of pseudorabies virus genome-based transfer vehicle carrying major antigen sites of S gene of transmissible gastroenteritis virus: Potential perspective for developing live vector vaccines. *Biologicals*, *35*(1), 55–61. <https://doi.org/https://doi.org/10.1016/j.biologicals.2006.02.001>

- Yokoyama, N., Fujita, K., Damiani, A., Sato, E., Kurosawa, K., Miyazawa, T., Ishiguro, S., Mochizuki, M., Maeda, K., & Mikami, T. (1998). Further Development of a Recombinant Feline Herpesvirus Type 1 Vector Expressing Feline Calicivirus Immunogenic Antigen. *Journal of Veterinary Medical Science*, 60(6), 717–723. <https://doi.org/10.1292/jvms.60.717>
- Yokoyama, N., Maeda, K., & Mikami, T. (1997). Recombinant Viral Vector Vaccines for the Veterinary Use. *Journal of Veterinary Medical Science*, 59(5), 311–322. <https://doi.org/10.1292/jvms.59.311>
- York, J. J., Sonza, S., Brandon, M. R., & Fahey, K. J. (1990). Antigens of infectious laryngotracheitis herpesvirus defined by monoclonal antibodies. *Archives of Virology*, 115(3), 147–162. <https://doi.org/10.1007/BF01310527>
- York, J. J., Sonza, S., & Fahey, K. J. (1987). Immunogenic glycoproteins of infectious laryngotracheitis herpesvirus. *Virology*, 161(2), 340–347. [https://doi.org/https://doi.org/10.1016/0042-6822\(87\)90126-7](https://doi.org/https://doi.org/10.1016/0042-6822(87)90126-7)
- You, Y., Cheng, A.-C., Wang, M.-S., Jia, R.-Y., Sun, K.-F., Yang, Q., Wu, Y., Zhu, D., Chen, S., Liu, M.-F., Zhao, X.-X., & Chen, X.-Y. (2017). The suppression of apoptosis by  $\alpha$ -herpesvirus. *Cell Death & Disease*, 8(4), e2749–e2749. <https://doi.org/10.1038/cddis.2017.139>
- Yu, F., Li, Y., Guo, Y., Wang, L., Yang, J., Zhao, G., Zhou, Y., Du, L., & Jiang, S. (2015). Intranasal vaccination of recombinant H5N1 HA1 proteins fused with foldon and Fc induces strong mucosal immune responses with neutralizing activity: Implication for developing novel mucosal influenza vaccines. *Human Vaccines and Immunotherapeutics*, 11(12), 2831–2838. <https://doi.org/10.1080/21645515.2015.1074363>
- Yu, Y., Lee, C., Kim, J., & Hwang, S. (2005). Group-specific primer and probe sets to

detect methanogenic communities using quantitative real-time polymerase chain reaction. *Biotechnology and Bioengineering*, 89(6), 670–679.

<https://doi.org/10.1002/bit.20347>

Yuan, M., Gao, X., Chard, L. S., Ali, Z., Ahmed, J., Li, Y., Liu, P., Lemoine, N. R., & Wang, Y. (2015). A marker-free system for highly efficient construction of

vaccinia virus vectors using CRISPR Cas9. *Molecular Therapy - Methods and Clinical Development*, 2(June), 15035. <https://doi.org/10.1038/mtm.2015.35>

Yuan, X., Wang, Y., Yang, J., Xu, H., Zhang, Y., Qin, Z., Ai, H., & Wang, J. (2012).

Genetic and biological characterizations of a Newcastle disease virus from swine in china. *Virology Journal*, 9, 9–11. <https://doi.org/10.1186/1743-422X-9-129>

Yuan, Z., Zhang, S., Liu, Y., Zhang, F., Fooks, A. R., Li, Q., & Hu, R. (2008). A

recombinant pseudorabies virus expressing rabies virus glycoprotein: Safety and immunogenicity in dogs. *Vaccine*, 26(10), 1314–1321.

<https://doi.org/https://doi.org/10.1016/j.vaccine.2007.12.050>

Yuen, K.-S., Chan, C.-P., Kok, K.-H., & Jin, D.-Y. (2017). Mutagenesis and Genome Engineering of Epstein-Barr Virus in Cultured Human Cells by CRISPR/Cas9.

*Methods in Molecular Biology (Clifton, N.J.)*, 1498, 23–31.

[https://doi.org/10.1007/978-1-4939-6472-7\\_2](https://doi.org/10.1007/978-1-4939-6472-7_2)

Yuen, K. S., Wang, Z. M., Wong, N. H. M., Zhang, Z. Q., Cheng, T. F., Lui, W. Y.,

Chan, C. P., & Jin, D. Y. (2018). Suppression of Epstein-Barr virus DNA load in latently infected nasopharyngeal carcinoma cells by CRISPR/Cas9. *Virus*

*Research*, 244(April 2017), 296–303.

<https://doi.org/10.1016/j.virusres.2017.04.019>

Yusoff, K., & Wen Siang Tan. (2001). Newcastle disease virus: Macromolecules and

opportunities. *Avian Pathology*, 30(5), 439–455.

<https://doi.org/10.1080/03079450120078626>

Zahid, B., Qazi, J. I., Zohaib, A., Aslam, A., Akhter, R., Sadia, H., Ul Ain, Q., Sultana, R., Irshad, I., & Alyas, S. (2020). Detection and molecular characterization of virulent newcastle disease virus in ducks (*Anas platyrhynchos domesticus*).

*Pakistan Journal of Zoology*, 52(1), 369–372.

<https://doi.org/10.17582/journal.pjz/2020.52.1.369.372>

Zhang, L., Luo, W., Xiong, R., Li, H., Yao, Z., Zhuo, W., Zou, G., Huang, Q., & Zhou, R. (2022). A Combinatorial Vaccine Containing Inactivated Bacterin and Subunits Provides Protection Against *Actinobacillus pleuropneumoniae* Infection in Mice and Pigs. *Frontiers in Veterinary Science*, 9, 902497.

<https://doi.org/10.3389/fvets.2022.902497>

Zhang, M.-Y., Wang, Y., Mankowski, M. K., Ptak, R. G., & Dimitrov, D. S. (2009). Cross-reactive HIV-1-neutralizing activity of serum IgG from a rabbit immunized with gp41 fused to IgG1 Fc: Possible role of the prolonged half-life of the immunogen. *Vaccine*, 27(6), 857–863.

<https://doi.org/https://doi.org/10.1016/j.vaccine.2008.11.083>

Zhang, M., Ge, J., Wen, Z., Chen, W., Wang, X., Liu, R., & Bu, Z. (2017).

Characterization of a recombinant Newcastle disease virus expressing the glycoprotein of bovine ephemeral fever virus. *Archives of Virology*, 162(2), 359–367. <https://doi.org/10.1007/s00705-016-3078-2>

Zhang, X., Calvert, R. A., Sutton, B. J., & Doré, K. A. (2017). IgY: a key isotype in antibody evolution. *Biological Reviews of the Cambridge Philosophical Society*, 92(4), 2144–2156. <https://doi.org/10.1111/brv.12325>

Zhang, Z., Chen, W., Ma, C., Zhao, P., Duan, L., Zhang, F., Sun, A., Li, Y., Su, H.,

- Li, S., Cui, H., & Cui, Z. (2014). Construction of recombinant Marek's disease virus (MDV) lacking the meq oncogene and co-expressing AIV-H9N2 HA and NA genes under control of exogenous promoters. *Journal of Biotechnology*, *181*, 45–54. <https://doi.org/10.1016/j.jbiotec.2014.03.032>
- Zhao, B., Zhang, X., Krummenacher, C., Song, S., Gao, L., Zhang, H., Xu, M., Feng, L., Feng, Q., Zeng, M., Xu, Y., & Zeng, Y. (2018). Immunization with Fc-based recombinant Epstein-Barr virus gp350 elicits potent neutralizing humoral immune response in a BALB/c mice model. *Frontiers in Immunology*, *9*(MAY). <https://doi.org/10.3389/fimmu.2018.00932>
- Zhao, R., Sun, J., Qi, T., Zhao, W., Han, Z., Yang, X., & Liu, S. (2017). Recombinant Newcastle disease virus expressing the infectious bronchitis virus S1 gene protects chickens against Newcastle disease virus and infectious bronchitis virus challenge. *Vaccine*, *35*(18), 2435–2442. <https://doi.org/10.1016/j.vaccine.2017.03.045>
- Zhao, W., Spatz, S., Zhang, Z., Wen, G., Garcia, M., Zsak, L., & Yu, Q. (2014). Newcastle Disease Virus (NDV) Recombinants Expressing Infectious Laryngotracheitis Virus (ILTV) Glycoproteins gB and gD Protect Chickens against ILTV and NDV Challenges. *Journal of Virology*, *88*(15), 8397 LP – 8406. <https://doi.org/10.1128/JVI.01321-14>
- Zhao, Y., Wang, L.-Q., Zheng, H.-H., Yang, Y.-R., Liu, F., Zheng, L.-L., Jin, Y., & Chen, H.-Y. (2020). Construction and immunogenicity of a gE/gI/TK-deleted PRV based on porcine pseudorabies virus variant. *Molecular and Cellular Probes*, *53*, 101605. <https://doi.org/10.1016/j.mcp.2020.101605>
- Zhen, S., Hua, L., Liu, Y.-H., Gao, L.-C., Fu, J., Wan, D.-Y., Dong, L.-H., Song, H.-F., & Gao, X. (2015). Harnessing the clustered regularly interspaced short

palindromic repeat (CRISPR)/CRISPR-associated Cas9 system to disrupt the hepatitis B virus. *Gene Therapy*, 22(5), 404–412.

<https://doi.org/10.1038/gt.2015.2>

Zhen, Shuai, Hua, L., Takahashi, Y., Narita, S., Liu, Y.-H., & Li, Y. (2014). In vitro and in vivo growth suppression of human papillomavirus 16-positive cervical cancer cells by CRISPR/Cas9. *Biochemical and Biophysical Research Communications*, 450(4), 1422–1426. <https://doi.org/10.1016/j.bbrc.2014.07.014>

Zheng, L., Guo, X., Zhu, Q., Chao, A., Fu, P., Wei, Z., Wang, S., Chen, H., & Cui, B. (2015). Construction and immunogenicity of a recombinant pseudorabies virus co-expressing porcine circovirus type 2 capsid protein and interleukin 18. *Virus Research*, 201, 8–15.

<https://doi.org/https://doi.org/10.1016/j.virusres.2015.02.010>

Zou, Z., Huang, K., Wei, Y., Chen, H., Liu, Z., & Jin, M. (2017). Construction of a highly efficient CRISPR/Cas9-mediated duck enteritis virus-based vaccine against H5N1 avian influenza virus and duck Tembusu virus infection. *Scientific Reports*, 7(1), 1–12. <https://doi.org/10.1038/s41598-017-01554-1>